INFORMATION TO USERS

This manuscript has been reproduced from the microfilm master. UMI films the text directly from the original or copy submitted. Thus, some thesis and dissertation copies are in typewriter face, while others may be from any type of computer printer.

The quality of this reproduction is dependent upon the quality of the copy submitted. Broken or indistinct print, colored or poor quality illustrations and photographs, print bleedthrough, substandard margins, and improper alignment can adversely affect reproduction.

In the unlikely event that the author did not send UMI a complete manuscript and there are missing pages, these will be noted. Also, if unauthorized copyright material had to be removed, a note will indicate the deletion.

Oversize materials (e.g., maps, drawings, charts) are reproduced by sectioning the original, beginning at the upper left-hand corner and continuing from left to right in equal sections with small overlaps.

Photographs included in the original manuscript have been reproduced xerographically in this copy. Higher quality 6" x 9" black and white photographic prints are available for any photographs or illustrations appearing in this copy for an additional charge. Contact UMI directly to order.

Bell & Howell Information and Learning
300 North Zeeb Road, Ann Arbor, MI 48106-1346 USA
800-521-0600

UNIVERSITY OF OKLAHOMA

GRADUATE COLLEGE

AN INVESTIGATION INTO THE PROPERTIES AND BEHAVIORS OF ALKYLDIPHENYL OXIDE DISULFONATE SURFACTANTS

A Dissertation

SUBMITTED TO THE GRADUATE FACULTY

in partial fulfillment of the requirements for the

degree of

Doctor of Philosophy

By

Laura Lei Wesson
Norman, Oklahoma
2001

UMI Number: 3004872

UMI Microform 3004872

Bell & Howell Information and Learning Company
300 North Zeeb Road
P.O. Box 1346
Ann Arbor, MI 48106-1346

AN INVESTIGATION INTO THE PROPERTIES AND BEHAVIORS OF SELECT ALKYLDIPHENYL OXIDE DISULFONATE SURFACTANTS

A dissertation APPROVED FOR THE
SCHOOL OF CHEMICAL ENGINEERING AND MATERIALS SCIENCE

BY

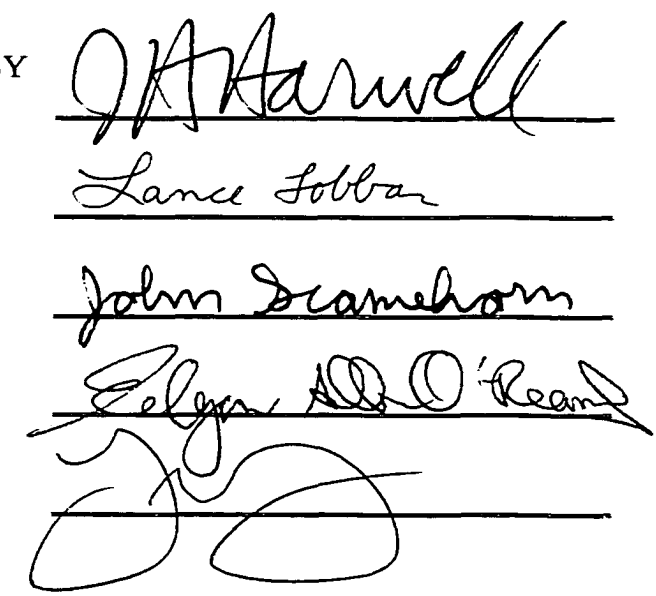

ACKNOWLEDGMENTS

I would like to acknowledge the many people who have contributed to the completion of my degree. First, I would like to thank my committee members who have contributed much to this dissertation. I have appreciated their input during my years at the University of Oklahoma. I have received help on many occasions from the office staff in the Chemical Engineering and Material Science office. They have included Rick Wheeler, Sherry Childress, Susan Cates, Donna King, Terri Colliver, and Carolyn Seratte. I must also acknowledge the input from my fellow graduate students who have included John O'Haver, Cheryl Haskins Rodriguez, Bita Phillipi, Karolina Ho, Russell Hooper, Phillip Howard and Greg Davis. Of course, none of this would have been possible without the support of my husband, Neal, and the tolerance of my children: David, Rachel, Matthew and Nathan. I only wish my son Kristopher were here to celebrate the completion of this journey. Finally, and most importantly I am thankful for the many mercies and abundant grace God has bestowed upon my family and myself during my studies.

Table of Contents

PROLOGUE

P.1 Overview of Surfactants 1
P.2 Overview of Alkyldiphenyl Oxide Sulfonates 6
P.3 References 17
P.4 Figures 19

CHAPTER 1 Determination of Critical Micelle Concentrations for Several Alkyldiphenyl Oxide Disulfonate Surfactants

1.1 Abstract 23
1.2 Introduction 24
1.3 Materials 25
1.4 Experimental 25
1.5 Results and Discussion 27
1.5.1 Critical Micelle Concentrations 27
1.5.2 Surface Tensions at the CMC 31
1.5.3 Surface Excess Concentration 31
1.5.4 Area per Molecule at the Air/Water Interface 32
1.5.5 Timed Surface Tension Values 33
1.6 Conclusions 34
1.7 References 35
1.8 Figures 36
1A Appendix: Surface Tension Data 43

CHAPTER 2 Preparation of Microemulsions Using Salinity and Modified Lipophilic Scans with Alkyldiphenyl Oxide Disulfonate Surfactants

2.1 Abstract 48
2.2 Introduction 49
2.2.1 Microemulsion 49
2.2.2 Solubilization 53
2.3 Materials 56
2.3.1 Salinity Scans 56
2.3.2 Modified Lipophilic Scans 56
2.4 Experimental 57
2.4.1 Salinity Scans 57
2.4.2 Modified Lipophilic Scans 57
2.5 Results and Discussion 58
2.5.1 Traditional Salinity Scans 58
2.5.1.1 Alkanes 59
2.5.1.2 Chlorinated Hydrocarbons 60

2.5.2 Modified Lipophilic Scans 60
2.5.2.1 Modified Lipophilic Scan: Salinity Scans 60
2.5.2.2 Modified Lipophilic Scans: Temperature Studies 62
2.5.2.3 Modified Lipophilic Scans: Solubilization 64
2.6 Conclusions 66
2.7 References 68
2.8 Figures 69
2A Appendix: Equations used for Preparing Systems for Salinity Scans 77
2B Appendix: Range of Component Concentrations and Visual Descriptions for Traditional Salinity Scans 82
2B.1 Alkane Scans 83
2B.2 Chlorinated Hydrocarbon Scans 86
2C Appendix: Summary of Traditional Salinity Scan Observations 88
2C.1 DADS 89
2C.2 MADS 89
2C.3 MAMS 89
2C.4 DAMS 89
2D Appendix: Data and Corrected Calculations From the Thesis of Sangaroon Aowiriyakul 90

CHAPTER 3 Surfactant Adsorption in Porous Media

3.1 Abstract 113
3.2 Introduction 114
3.3 Solid Surface Chemistry 117
3.3.1 Types of Solids 118
3.3.2 Electrical Characteristics and the Electrical Double Layer 120
3.3.3 Electrical Double Layer 121
3.4 Mechanisms of Surfactant Adsorption 125
3.4.1 Single Surfactant Systems 125
3.4.2 Mixed Surfactant Systems 131
3.5 Experimental Studies 133
3.5.1 Fundamental Adsorption Studies 133
3.5.1.1 Cationic Surfactant onto Quartz 134
3.5.1.2 Cationic Surfactants onto Silica 135
3.5.1.3 Anionic Surfactant onto Alumina and Kaolinite 136
3.5.1.4 Mixture of Anionic Surfactants onto Alumina 137
3.5.1.5 Cationic Surfactants onto Porous Silicas 138
3.5.2 Applied Adsorption Studies 139
3.5.2.1 Anionic Surfactants onto Kaolinite and Illite 140
3.5.2.2 Anionic Surfactant onto Kaolinite 140
3.5.2.3 Anionic Blends onto Sand and Clay 141
3.5.2.4 Cationic and Anionic Surfactants onto Carbonates 143
3.5.2.5 Ethoxylated Sulfate Surfactants onto Mineral Oxides and Sandstone Cores 145

3.5.2.6 Mixed Anionic Surfactants onto East Vacuum Grayburg-San Andres Unit (EVGSAU) and Baker Dolomite Cores 147
3.5.3 Adsorption of Alkyldiphenyl Oxide Mono and Disulfonate Surfactants 150
3.5.3.1 Anionic Surfactant Blend and Amphoteric Surfactants onto Berea Sandstone, Indiana Limestone, Baker Dolomite, and Quartz. 150
3.5.3.2 Anionic Surfactants onto Canadian River Alluvium (CRA) and Alumina 153
3.5.3.3 Adsorption onto Canadian River Alluvium (CRA) 154
3.5.3.4 Adsorption onto Alumina 156
3.6 Summary 161
3.7 Acknowledgment 162
3.8 References 163
3.9 Figures 169

CHAPTER 4 Adsolubilization and Solubilization of 2-Naphthol by Alkyldiphenyl Oxide Disulfonate Surfactants

4.1 Abstract 181
4.2 Introduction 182
4.3 Materials 183
4.4 Experimental 184
4.4.1 Adsolubilization 184
4.4.2 Solubilization 185
4.5 Results and Discussion 187
4.5.1 Behavior of Naphthol in the Absence of Surfactant 187
4.5.2 Adsorption of surfactants in the presence of naphthol 189
4.5.3 Adsolubilization 190
4.5.4 Solubilization 196
4.5.4.1 Comparison of Adsolubilization and Solubilization Parameters of Alkyldiphenyl Oxide Disulfonate Surfactants to Other Surfactants 197
4.5.4.2 Comparison of Adsolubilization and Solubilization Parameters of Alkyldiphenyl Oxide Disulfonate Surfactants 199
4.5.5 Two-Site Adsolubilization Model 202
4.6 Conclusions 204
4.7 References 207
4.8 Figures 209
4A Appendix: Data for Adsolubilization and SED 220
4B Appendix: Comparison of K_m Values Based on Initial Naphthol Concentrations 229

List of Figures

Figure P-1 Micelle shapes....20
Figure P-2 Changes in select physical properties upon micelle formation (adapted from Rosen, 1989)....21
Figure P-3 General structure of alkyl diphenyl ether sulfonates....22
Figure 1-1 Surface Tension Curve for C10 MADS / 0 M NaCl....37
Figure 1-2 Surface Tension Curve for C10 MADS / 0.15 M NaCl....37
Figure 1-3 Surface Tension Curve for C12 MADS / 0 M NaCl....38
Figure 1-4 Surface Tension Curve for C12 MADS / 0.15 M NaCl....38
Figure 1-5 Surface Tension Curve for C10 DADS / 0 M NaCl....39
Figure 1-6 Surface Tension Curve for C10 DADS / 0.9 M NaCl....39
Figure 1-7 Surface Tension Curve for C16 MADS / 0 M NaCl....40
Figure 1-8 Surface Tension Curve for C16 MADS / 0.15 M NaCl....40
Figure 1-9 Time Studies for 1.82×10^{-6} M C16 MADS/0.15 M NaCl using KRÜSS tensiometer....41
Figure 1-10 Time Studies for 1.82×10^{-6} M C16 MADS/0.15 M NaCl using rod tensiometer....42
Figure 2-1 Relationships between phase behavior, interfacial tension, and solubilization parameter (Wu et al, 2000)....70
Figure 2-2 Orientation of molecules located at the oil-water interface due to the presence of lipophilic linker molecules....71
Figure 2-3 Schematic of salting out of ionic amphiphiles: T-ε for ionic amphiphiles (Kahlweit, 1995)....72
Figure 2-4 Phase behavior seen in traditional salinity scan of C10 DADS + sec-butanol/ heptane, R=0.67, 24°C....73
Figure 2-5 Phase diagram of alkyldiphenyl oxide disulfonate/octanoic acid/PCE for R=0.86 at 24 °C....74
Figure 2-6 Phase diagram of alkyldiphenyl oxide disulfonate/octanoic acid/PCE for R=0.86 at 24, 35 and 45 °C....75
Figure 2-7 Schematic of salting out of alkyldiphenyl oxide mono- disulfonate + octanoic acid systems....76
Figure 3-1 Guoy-Chapman model of the electrical double layer and the potential distribution....170
Figure 3-2 Typical four-region adsorption isotherm for a monoisomeric surfactant....171
Figure 3-3 Two-region adsorption isotherm of dodecylamine on quartz....172
Figure 3-4 Adsorption isotherm of DPC onto Aerosil OX50. (Goulob et al., 1997)....173
Figure 3-5 Mixed adsorption isotherms of C_8SO_4 and $C_{12}S0_4$ onto α-alumina (Lopata et al., 1988)....174
Figure 3-6 Structure of the alkyldiphenyl oxide sulfonate surfactant where R are alkyl chains of C6, C10, C12, or C16....175
Figure 3-7 Alkyldiphenyl oxide sulfonate adsorption onto CRA, all components....176
Figure 3-8 Alkyldiphenyl oxide sulfonate adsorption onto CRA, C10 components....177
Figure 3-9 Alkyldiphenyl oxide sulfonate adsorption onto CRA, MADS components.178
Figure 3-10 Alkyldiphenyl oxide sulfonate adsorption onto alumina, all components. 179
Figure 3-11 Alkyldiphenyl oxide sulfonate adsorption onto alumina, all components. 180

Figure 4-1 Semiequilibrium dialysis cell description and terminology. 210
Figure 4-2 Adsorption of 2-naphthol onto porous alumina in the absence of surfactant. 211
Figure 4-3 Adsolubilization of 2-naphthol by C10 DADS. Values in the legends indicate the initial surfactant concentrations ($x10^{-3}M$). 212
Figure 4-4 Adsolubilization of 2-naphthol by C10 MADS. Values in the legends indicate the initial surfactant concentrations ($x10^{-4}M$). 213
Figure 4-5 Adsolubilization and solubilization of 2-naphthol by C12 MADS. 214
Figure 4-6 Adsolubilization and solubilization of 2-naphthol by C16 MADS. 215
Figure 4-7 Solubilization of 2-naphthol by C12 MADS and C16 MADS. 216
Figure 4-8 Change in K_{adm} with initial 2-naphthol concentration. 217
Figure 4-9 Adsolubilization and solubilization of 2-naphthol by C12 MADS and C16 MADS. 218
Figure 4-10 Aggregation numbers for the C12 MADS/naphthol adsolubilization. 219

PROLOGUE

This section is included to introduce the reader to the class of chemicals known as surfactants and to alkyldiphenyl oxide sulfonate surfactants in particular. This Prologue was included to avoid repeating introductory information in the chapters that follow.

P.1 Overview of Surfactants

Surface active agents or surfactants are characterized by several unique chemical and physical properties. Structurally, surfactant molecules are composed of at least two chemical groups: one group being lyophobic (solvent-hating), and the second lyophilic (solvent-loving). If water is the solvent these groups are referred to as hydrophobic and hydrophilic and are commonly referred to as the tail group and head group, respectively.

Structures suitable for lyophobic and lyophilic groups depend on the solvent of interest. In polar solvents such as water the lyophilic group may be ionic or highly polar in nature; whereas, suitable lyophobic groups may include branched or straight-chain hydrocarbon, fluorocarbon, or siloxane residues. In less polar solvents the opposite is generally true. The ionic or polar groups may act as the lyophobe, and the lypophile may be hydrocarbon, fluorocarbon, or siloxane residues.

Surfactants are commonly divided into classes according to differences in the charge on the hydrophilic group as shown in Table P-1

Table P-1 Classes of Surfactants

Class	Charge on Surface-Active Portion	Example
Anionic	Negative	$CH_3(CH_2)_{11}SO_3^-Na^+$ Sodium dodecylsulfonate
Cationic	Positive	$CH_3(CH_2)_{15}N^+(CH_3)_3Br^-$ Cetyltrimethyl ammonium bromide
Zwitterionic	Positive and Negative	$RN^+(CH_3)_2CH_2C00^-$ N-Alkylbetaines
Nonionic	None	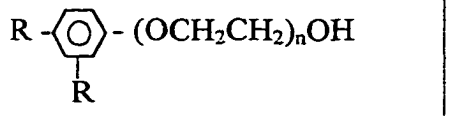

The favoring of one solvent medium over another by the groups composing the surfactant molecule leads to the surface activity exhibited by these chemical compounds. In order to lower the energy in a system, the disfavored moiety is removed to whatever extent possible from the solvent. This is exhibited by the concentration of surfactant molecules at surfaces and interfaces. The tendency to concentrate in these areas gives rise to several of the surfactant characteristics commonly utilized everyday in household, industrial, and laboratory applications. The most common household applications include the cleaning of hard and soft surfaces such as dishwashing, laundry, and personal care. Common industry applications include drilling muds used in the petroleum industry, ore flotation, subsurface remediation, electronic printing, drug delivery, and biotechnology. Research continues to look for answers to fundamental questions concerning surfactant behavior as well as practical and/or possible industrial applications.

The concentration of surfactant monomers at a surface or interface is not the only interesting behavior exhibited by surfactants. They also self-aggregate within the bulk solution, which is another means of removing the disfavored moiety from close contact

with the solvent. At low concentrations the surfactant molecules exist in the bulk solution as individual surfactant molecules or monomers, but at a given concentration designated as the critical micelle concentration (CMC), the monomers self-aggregate into structures known as micelles.

The value of the CMC is controlled by the structure of the surfactant, temperature, electrolyte concentration, concentration of other organic compounds, and the presence of a second liquid phase. Micelle formation is driven by the hydrophobic effect. This effect is due to the strong interaction between individual water molecules. The free energy of the system is reduced when the hydrophobic portions of the surfactants are removed from intimate contact with the solvent and there is a reduction in the number of water molecules with limited rotational orientations.

In general, as the hydrophobicity of the surfactant increases the value of the CMC decreases. Ionic surfactants have higher CMC's than nonionic surfactants with identical hydrophobic groups. This can be viewed as a result of having to overcome the electrical repulsion between the like-charged head groups. The addition of an electrolyte to a solution containing an ionic surfactant results in a lower CMC value as compared to an ionic surfactant solution with no electrolyte present. The electrolyte lowers the repulsion between the head groups by compressing the electrical double layer around these groups. With less repulsion between the like-charged head groups, the formation of micelles is facilitated. The presence of an electrolyte also affects other aspects of surfactant chemistry including surfactant precipitation, Krafft points and hardness tolerance. While the CMC decreases with increasing electrolyte concentration, the Krafft point increases. The Krafft point is the temperature at which the solubility of an ionic surfactant becomes

equal to the CMC. Hardness tolerance may increase with added electrolyte, since the additional electrolyte may decrease the surfactant monomer concentration.

In aqueous systems the surfactant monomers are arranged with the hydrophilic portion on the exterior of the micelle, in close contact with surrounding water molecules. The hydrophobic portion of the surfactant monomers lies in the interior of the micelle, creating a pseudo-oil phase. In referring to the different regions within a micelle the following terms have been introduced: the surface which is the area surrounding the exterior of the head groups, the core which is comprised of the tail groups, and the palisade layer which is the region where the head groups and the tail groups join. In this region a small section of the tail group is in contact with the surrounding solvent.

Much research has focused on the specific shape of the micelle. The shapes include spherical, elongated cylindrical, rod-like micelles with hemispherical ends (prolate ellipsoids), and vesicles. Vesicles are spherical structures consisting of lamellar micelles arranged in one or more concentric spheres (Rosen, 1989). These common micelle shapes are shown in Figure P-1. In non-polar solvents reverse micelles form. As their name implies, these micelles are formed with the polar head groups facing the interior of the micelle and the nonpolar tail groups extending into the bulk solution. Any water in the solution tends to locate in the interior of the reverse micelles i.e. in the vicinity of the polar head groups. Reverse micelles tend to be more loosely organized than their micelle counterparts.

The onset of micelle formation is reflected by dramatic changes in several physical properties of the surfactant solution. These include equivalent conductivity, detergency, osmotic pressure, and surface and interfacial tensions. A classic example of

these changes is shown in Figure P-2 (Rosen, 1989). The most common properties measured in order to determine the onset of micellization are conductivity, surface tension, light scattering, and refractive index.

Of all the properties which exhibit dramatic changes upon micelle formation, the changes in surface and interfacial tensions and the changes in solubilization which are directly related to detergency are of particular interest to the research results presented in the following chapters.

As shown in Figure P-2, the surface and interfacial tensions show a rapid decrease then plateau as the surfactant concentration increases. The rapid decrease is due to surfactant monomers exchanging with solvent molecules at the air-liquid interface. System equilibrium involves this single exchange. At the CMC and higher surfactant concentrations equilibrium involves the exchange of monomers at the interface and monomer-micelle exchange. Any surfactant added to the system beyond the CMC is involved in micelle formation and does not contribute to the interfacial exchanges.

The ability to form micelles has several practical applications. Solutes that are not very soluble in polar solvents, such as water, show a marked increase in solubility or solubilization when an appropriate surfactant is added to the solution. An appropriate surfactant must consist of a hydrophobe capable of forming a micelle of sufficient size to solubilize the solute.

The ability of nonionic surfactant micelles to form aggregates large enough to phase separate forms the basis of a separation technique. The phase separation is associated with the cloud point temperature. As a solution of nonionic surfactant is heated, the micelles grow in aggregation number until the phase separation is possible.

P.2 Overview of Alkyldiphenyl Oxide Sulfonates

The research presented in the following chapters focuses on the alkyldiphenyl oxide sulfonate surfactant series manufactured by Dow Chemical Company. The alkyl chains can be linear or branched alkyl chains and range in lengths of 6 to 24 carbons. The most common lengths are 10, 12, and 16 carbons. These surfactant molecules can be comprised of one or two alkyl chains and one or two sulfonate groups with the following designations: monoalkyl disulfonates (MADS), dialkyl disulfonates (DADS), monoalkyl monosulfonate (MAMS), and dialkyl monosulfonate (DAMS). The general structure of these surfactants is shown in Figure P-3. A literature search revealed several designations for these surfactants: DOWFAX disulfonated alkyldiphenyloxide, DPOS (Dawe and Oswald, 1989); alkyl diphenyl disulfonates, DPDS (Rouse et al., 1993 and 1995); alkyldiphenyl oxide disulfonates (Quencer and Loughney, 2001); and alkylated diphenyloxide disulfonates, ADPOD (Quencer, 1992). The Chemical Abstracts designation and their CAS# are shown in Table P-2.

Table P-2 Chemical Abstracts Designations

Surfactant	CAS#	Designation
C10 MADS	036445-71-3	Decyl (sulfophenoxy) benzene sulfonic acid, disodium salt
C10 DADS	070146-13-3	Oxybis (decylbenzenesulfonic acid), disodium salt
C12 MADS	114673-92-6	Dodecane, (phenoxy phenyl)-, ar, ar disulfo deriv., disodium salt
C16 MADS	065143-89-7	Hexadecyl (sulfophenoxy) benzene sulfonic acid, disodium salt

These surfactants have received attention, in part, due to their very low CMC's and lack of precipitation or slow rate of precipitation by several common electrolytes (Dawe and Oswald, 1989; Yin, 1994; Quencer and Loughney, 2001). The properties of the individual surfactant components and the commercially available mixtures continue

to be examined. Characterization of these surfactants is complicated by the lack of monoisomeric samples. All of the surfactants in this series are mixtures of isomers. Commercial mixtures are usually comprised of the mono- and dialkyl disulfonate components. Two of the most common commercial mixtures are designated as 3B2 and 8390 that are mixtures of C10 and C16 components, respectively. Pertinent physical properties of select individual components and commercial mixtures are given in Table P-3.

Table P-3 Properties of the Dowfax™ surfactants.

Surfactant	Molecular Weight (avg.)	CMC (M)
8390	636	2.20×10^{-5}*
3B2	542	2.21×10^{-4}*
C10 DADS	617*	1.33×10^{-4}**
C10 MADS	523*	1.40×10^{-4}**
C12 MADS	551*	1.30×10^{-4}**
C16 MADS	600*	2.53×10^{-4}**

* Dowfax™ product literature. Values determined in 0.1 N NaCl

** The values of the CMC shown in this table are values obtained by DOW with no additional electrolyte at room temperature during the early development of these surfactants. Later research indicated these values were not entirely accurate and more current values are reported in the first chapter of this work.

Alkyldiphenyl oxide sulfonates were first identified in 1937, but a commercially viable synthesis process was not developed until 1958 (Quencer and Loughney, 2001). Traditional uses of these surfactants that were listed by Quencer and Loughney (2001) included:

1. Emulsion polymerization to yield faster run times with less reactor waste and smaller particle size,
2. Acid dying of nylon carpet fiber as leveling agents to promote an even distribution of dye,
3. Crystal habit modification to alter crystal shape and size,
4. Cleaning formulations to provide solubilization in strongly acidic, caustic and bleach environments.

The results of several studies involving these surfactants conducted since the early 1990's are summarized in the paragraphs that follow and are meant to illustrate some of the fundamental properties of the alkyldiphenyl oxide sulfonate surfactants and their effectiveness in specific applications.

Perhaps the most well known fundamental study characterized several of the C10 components (Rosen et al., 1992). This study investigated several properties (including surface tensions, CMC values, areas per molecule at the interface, wetting time, foaming, solubilization, and hydrotropy) of purified samples of C10 MADS, DADS, MAMS, DAMS, and TrAMS. The CMC values that were reported for the MADS, MAMS, and DADS components were $3.7x10^{-4}$, $3.2x10^{-5}$, and $1.0x10^{-5}$ M, respectively. The surface tension measurements were conducted at 25°C, in 0.1 N NaCl for the MAMS and DADS and 1 N NaCl for the MADS, all using the Wilhelmy plate method.

The MADS and DADS components were found to be readily soluble in water while the MAMS and DAMS components were soluble in hexane. Wetting times increased in the order MAMS < DADS < MADS, and initial foams heights decreased in the order MAMS > DADS > MADS. Solubilization for three water insoluble surfactants, a silicon-based surfactant, an alcohol ethoxylate, and an alkylphenol ethoxylate were found to decrease in the order DADS > MAMS > MADS.

The solubilities of octanol in the linear C16, C10, and C6 disulfonate components; and in the branched C12 disulfonate component were reported by Quencer (1992). The results were presented relative to results obtained with sodium lauryl sulfate. The solubility of the octanol was reported to increase with decreasing alkyl chain length: C6 > C10 > C16. A simultaneous decrease in liquid crystal formation was also reported. For

the branched C12 component, the octanol solubility was lower than that seen with the three linear components, and high water concentrations were needed to achieve higher octanol solubilities relative to the lauryl sulfate.

There have been several studies published examining the suitability of the alkyldiphenyl oxide sulfonate surfactants in specific applications, primarily for detergency and environmental uses. A detailed discussion of the detergency properties of these surfactants has been reported by Quencer and Loughney (2001). This discussion includes most aspects of detergency applications as well as environmental and safety concerns. Only a few highlights are presented here. On dust-sebum swatches a linear C16 alkyldiphenyl oxide disulfonates yielded a higher detergency score than a C12 linear alkylbenzenesulfonate over a broad concentration range. This was true even for varying hardness levels.

The disulfonated surfactants were reported to show a lack of precipitation by divalent counterions, while the monosulfonated components readily precipitated. In relation to foaming, the disulfonates are considered moderate foamers. The foam profile of the C16 disulfonate was lower than that of the C12 linear alkylbenzenesulfonate over the range of test conditions.

In tests conducted to establish the stability of sodium hypochlorite (bleach) in the presence of several types of surfactants, the alkyldiphenyl oxide disulfonates systems remained stable after 319 days. Of the surfactants tested, only 2-ethyl hexyl sulfate exhibited similar stability.

The work by Quencer and Loughney concluded with a discussion of the environmental and safety concerns. The C16 alkyldiphenyl oxide disulfonate produced

no dermal irritation during the 3 days that the test rabbits were dosed. Degradation in activated sludge led to the classification of the C10 and C16 alkyldiphenyl oxide disulfonates as biodegradable and a commercial C12 branched and C6 alkyldiphenyl oxide disulfonates as non-biodegradable.

Several studies have examined various aspects of the alkyldiphenyl oxide sulfonate surfactants in order to determine the potential for their use in surfactant-enhanced environmental remediation, an application having its origin in the enhanced oil recovery (EOR) field. In relation to the use of the these surfactants in EOR, two patents have been granted for the use of these surfactants blended with other surfactants for mobility control in gas flooding or miscible gas flooding operations (Dawe et al., 1993; Oswald and Robson, 1989).

Research focusing on the suitability of the alkyldiphenyl oxide sulfonate surfactants for remediation has examined the effectiveness of these surfactants in solubilization and mobilization. If the study is application specific surfactant adsorption is usually done in conjunction with solubilization and mobilization. In order to be cost effective and competitive with other technologies, the loss of surfactant to adsorption must be minimized.

Early work tended to examine the performance of these surfactants for ideal contaminants and real soils. For example, the adsorption of C12 MADS onto Canadian River alluvium was reported to be significantly lower than that seen for sodium dodecylbenzene sulfonate (SDBS), and C12 MADS was not precipitated by the calcium that had been added to the system to provide a common background matrix. To avoid precipitation, the adsorption of the SDBS was carried out with no calcium added to the

system, but the adsorption of the SDBS was still significantly higher than the C12 MADS adsorption (Rouse et al., 1993). In the same study solubilization results for naphthalene in SDBS, C10, C12, and C16 MADS were also reported and indicated that the C12 and C16 components had a higher solubilization of naphthalene than the SDBS, while the solubilization by the C10 MADS was approximately equal to that observed for the SDBS.

In an attempt to more accurately reflect the dynamic conditions encountered in subsurface applications, solubilization studies were conducted using semiequilibrium dialysis cells (Rouse et al., 1995). Three unsaturated hydrocarbons with varying degrees of polarity, naphthalene, 1-naphthol, and naphthane (decalin), were solubilized in Dowfax 8390. It was reported that as the mole fraction of the hydrocarbon increased, the micelle-water partition coefficient, K_m, increased for naphthane, decreased for naphthol, and remained relatively constant for naphthalene. K_m is the ratio of the mole fraction of hydrocarbon in the micellar pseudo-phase versus the mole fraction of hydrocarbon in the aqueous phase.

Also reported were the results using sodium dodecyl benzenesulfonate (SDBS). For naphthol and naphthalene the mole fractions of the hydrocarbons in the SDBS' micellar phases were lower that that achieved with the Dowfax 8390.

The adsorption of the C10 MADS, C12 MADS, C10 DADS, and C16 MADS components onto Canadian River alluvium and the solubilization of phenanthrene by these same surfactants were examined by Sabatini et al. (2000). As expected, the solubilization of the phenanthrene increased with increasing alkyl chain length. While for a constant alkyl chain length (C10) and varying the number of alkyl and sulfonate groups, the degree of solubilization increased in the order MADS< MAMS < DADS.

Adsorption isotherms indicated generally Langmurian adsorptions with the disulfonates sorbing less than monosulfonates and less sorption for the shorter alkyl chain lengths.

Dowfax 8390 was used in a field demonstration in the solubilization and removal of non-aqueous phase liquids (NAPL) at Hill Air Force Base, Utah (Knox et al., 1999). The demonstration was conducted in a 3-D cell consisting of steel sheetpiling driven into an underlying impermeable layer. Despite problems with the cell (excessive leakage through the sheetpiling) contaminant extraction was as high as 58% with ten pore volumes of surfactant flushing. It was stated that although more efficient solubilization systems exist, the Dowfax 8390 system was very user-friendly and that the degree of solubilization was still significantly greater than that seen with water alone (less than 1% in the same number of pore volumes)

The next several studies involved examining the behavior of the alkyldiphenyl oxide sulfonate surfactants in what are known as Winsor Type microemulsion systems. A basic system consists of an aqueous phase (w), oil phase (o), an electrolyte, and a surfactant. The Type designation is determined by the phase in which the surfactant is located. In Winsor Type I systems (o/w) the surfactant is located in the aqueous phase. In Winsor Type II systems (w/o) the surfactant is located in the oil phase, and in Winsor Type III systems the surfactant has formed a separate or third phase situated between the oil and aqueous phases, i.e. a middle phase microemulsion. Bourrel and Schecter (1988) provide a comprehensive discussion concerning the Winsor formulations and how they can be achieved.

Based on observations made for the Dowfax 8390 performance at Hill Air Force Base, a study aimed at increasing the solubility enhancement of the Dowfax™

components was undertaken (Carter et al., 1998). Several methods including using a cosurfactant, adding an electrolyte, and forming middle-phase microemulsions were evaluated. The contaminants used were phenanthrene and tetrachloroethylene; while the surfactants were C10 MAMS, C10 MADS, C12 MAMS, C12 MADS, C16 MADS, and C20-24 MADS. The results indicated that the formation of the middle-phase microemulsion produced the greatest enhancement. The middle-phase microemulsions were produced using an electrolyte (NaCl), isobutanol, a cosurfactant (octylphenylethoxylate or nonylphenylethoxylate Igepal surfactants) and one of the alkyldiphenyl oxide sulfonate surfactants.

Although the study by Carter et al. demonstrated the effectiveness of the alkyldiphenyl oxide sulfonate middle-phase microemulsion systems, the use of an alcohol is generally not desirable for use in remediation applications. There are several areas of concern associated with the use of alcohols in remediation. There are the precautions and special equipment required for the handling of flammable substances, and the difficulties in separating the alcohol from the contaminant in order to recycle the alcohol. Recycling is usually required in order to keep the surfactant remediation process economically feasible. The desired use of the alkyldiphenyl oxide sulfonate surfactants in remediation necessitated the development of alcohol-free microemulsions. This was accomplished by Aowiriyakul (1998) and extended by Wu et al. (2000). The results obtained by Aowiriyakul indicated that the formation of alcohol-free microemulsions was possible with Dowfax 8390, and details of this study are presented as part of Chapter 2 of this dissertation.

Wu et al. (2000) reported that several combinations of surfactants, C16 MADS and Dowfax 8390, and adjuncts were prepared in order to examine systems that enhanced the solubilization of tetrachloroethylene (PCE), and decane. For example, for PCE it was found that the amount of PCE that could be solubilized increased in the order: molar C16 MADS-AOT < C16 MADS-AOT super solubilization system < C16 MADS-AOT middle-phase microemulsion system. Super solubilization was described as systems as close as possible to the Winsor Type I-III boundary but still within the Type I area. The desirability of formulating a system in this region is being able to take advantage of the "swollen" micelles that have a larger capacity for oil solubilization than normal micelles while avoiding the ultra-low interfacial tensions (IFT) obtained in Winsor Type III systems. Ultra-low IFT's would be undesirable in remediation situations in which downward migration of the contaminant would be undesirable.

The final area of study to be presented concerns the C10 DADS component that qualifies as a gemini surfactant (Rosen et al., 1992, 1993b; Rosen and Tracy, 1998). Gemini surfactant molecules contain at least two identical head groups and two identical tail groups. A recent review discusses the various properties of gemini surfactants and the differences between them and their monologue counterparts (Rosen et al., 1998). Gemini surfactants are characterized by much lower CMC's than their monologue counterparts, closer packing of their hydrophobic groups, and stronger interaction with oppositely charged surfactants at the aqueous solution/air interface.

As stated at the beginning of this section, the C10 DADS was shown to solubilize water-insoluble nonionic surfactants of the alcohol ethoxylate, alkylphenol ethoxylate, and N-alkylpyrrolidone types more efficiently and more effectively than its monologue

counterparts (Rosen, 1992). This observation is repeated now in light of the significance now placed on the gemini structure. Draves skein wetting tests involving the same water-insoluble surfactants and C10 DADS found that the water-insoluble surfactants mixed with C10 DADS had significantly lower wetting times than either of the surfactants alone. For example, mixtures containing 20% C10 DADS and at an overall concentration of 1 g/L had wetting times of less than 15 s, and a mixture containing 50% C10 DADS had wetting times ranging from 10.0 to 17.5 s. This is in contrast to wetting times for solutions containing a single surfactant of approximately 120 s for the water-insoluble surfactants and 430 s for the C10 DADS (Rosen and Zhu, 1993a).

The interaction and synergism between several of the C10 components, DADS, MAMS, and MADS with a second surfactant containing a single hydrophilic and a single hydrophobic group were examined (Rosen et al., 1993b). The surfactants containing a single hydrophilic and a single hydrophobic group were: N-dodecyl-N-benzyl-N-methylglycine; N,N-dimethyl-1-tetradecanamine oxide; and a polyoxyethylenated n-dodecyl alcohol with a homogenous head group of seven oxyethylene units ($C_{12}H_{25}(OC_2H_4)_7OH$). The interaction of the two surfactants in each of the systems was determined by calculating the β parameters, which are a measure of these interactions. These parameters can be calculated for mixed monolayer formation at the air/solution interface (β^{σ}) and for mixed micelle formation (β^{m}). The conclusions presented were that for binary mixtures of the C10 components with the non-anionic surfactants the attractive interaction in mixed monolayers at the solution/air interface increased in the order: MAMS < MADS < DADS, but in mixed micelles of the same mixtures the DADS component showed weaker interaction. Based on the stronger interaction of the C10

DADS with the non-anionic surfactants at the solution/air interface and the weaker interaction in mixed micelle formation, the DADS has a greater probability of exhibiting synergism in surface tension reduction, but a lower probability of showing synergism in mixed micelle formation.

The following chapters present several of the physical properties and behaviors exhibited by individual alkyldiphenyl oxide sulfonate surfactants and the commercially available alkyldiphenyl oxide sulfonate mixture DOWFAX 8390 beginning with the most fundamental to surfactant research, values of the CMC. The reported results are meant to compliment the work that has already been accomplished with these surfactants.

P.3 References

Aowiriyakul, S. Thesis, Petroleum and Petrochemical College, Chulalongkorn, University, Bangkok, Thailand, 1998.

Bourrel, M.; Schecter, R. S. *Microemulsions and Related Systems*, Surfactant Science Series, Marcel Dekker: New York, 1988; Vol 30.

Carter, T. C.; Wu, B.; Sabatini, D. A.; Harwell, J. H. Increasing the Solubility Enhancement of Anionic Dowfax Surfactants. *Sep. Sci Tech.* **1998**, *33(15)*, pp 2363-2377.

Dawe, B.; Oswald, T. Reduced Adsorption and Separation of Blended Surfactants on Sand and Clay. Presented at the 40th Annual Technical Meeting of the Petroleum Society of CIM in Banff, May 1989.

Dawe, R. D.; Oswald, T.; Robson, I. A. Oil Recovery Process Using Mobility Control Fluid Comprising Alkylated Diphenyloxide Sulfonates and Foam Forming Amphoteric Surfactants, 5203411, April 20, 1993.

Knox R. C.; Shau, B-J; Sabatini, D. A.; Harwell, J. H. Field Demonstration Studies of Surfactant-Enhanced Solubilization and Mobilization at Hill Air Force Base, Utah. In *Innovative Subsurface Remediation field Testing of Physical, Chemical, and Characterization Technologies*, Brusseau, M. L., Sabatini, D. A., Gierke, J. S., Annable, M. D. Eds; ACS Symposium Series 725; American Chemical Society: Washington, DC, 1999, Chapter 5.

Oswald, T.; Robson, I. A. Gas Flooding Processing for the Recovery of Oil From Subterranean Formations, 4860828, August 29, 1989.

Quencer, L. B. The Phase and Hydrotropic Behavior of Alkylated Diphenyloxide Disulfonates, Octanol and Water. Presented at CESIO, London, June 1992.

Quencer, L. B. Loughney, T. J. Detergency Properties of Alkyldiphenyl Oxide Disulfonates Marcel Dekker, New York, 2001.

Rosen, M. J. *Surfactants and Interfacial Phenomena* 2nd ed.; John Wiley & Sons: New York, 1989, pp 110, 112.

Rosen, M. J.; Tracy, D. J. Gemini Surfactants. *JSD.* **1998**, *1(4)*, pp 547-554.

Rosen, M. J.; Zhu, Z. H. Enhancement of Wetting Properties of Water-Insoluble Surfactants via Solubilization. *JAOCS*, **1993a**, *70(1)*, pp 65-68.

Rosen, M. J.; Zhu, Z. H.; Gao, T. Synergism in Binary Mixtures of Surfactants. 11. Mixtures Containing Mono- and Disulfonated Alkyl- and Dialkyldiphenylethers. *J. Colloid Interface Sci.* **1993b** *157*, pp 254-259.

Rosen, M. J.; Zhu, Z. H.; Hua, X. Y. Relationship of Structure to Properties of Surfactants. 16. Linear Decyldiphenylether Sulfonates. *JAOCS*, **1992**, *69(1)*, pp 30-33.

Rouse, J. D.; Sabatini, D. A.; Deeds, N. E.; Brown, R. E. Micellar Solubilization of Unsaturated Hydrocarbon Concentrations as Evaluated by Semiequilibrium Dialysis. *Environ Sci & Technol.* **1995**, *29(10)*, pp 2484-2489.

Rouse, J. D.; Sabatini, D. A.; Harwell, J. H. Minimizing Surfactant Losses Using Twin-Head Anionic Surfactants in Subsurface Remediation. *Environ. Sci. Technol.* **1993**, *27(10)*, pp 2072-2078.

Sabatini, D. A.; Harwell, J. H.; Deshpande, S.; Wesson, L.; Wade, D. Dowfax Surfactant Components in Surfactant-Enhanced Soil Remediation. *Water Res.* **2000**, *34(3)*, pp 1030-1036.

Salager, J-L. Microemulsions. In *Handbook of Detergents Vol 82* U. Zoller Ed-in-Chief, Part A: Properties, G. Broze, Ed, Marcel Dekker: New York, 1999; Chapter 8.

Van Duine, J. Thesis, University of Oklahoma, Norman, OK, 1996.

Wesson, L.; Harwell, J. H. Adsorption in Porous Media, In *Surfactants, Fundamentals and Applications in the Petroleum Industry* L. L. Schramm, Ed, Cambridge University Press: New York, Chapter 4, 2000.

Wu, B.; Harwell, J. H.; Sabatini, D. A.; Bailey, J. D. Alcohol-Free Diphenyloxide Disulfonates (DPDS) Middle Phase Microemulsion Systems. *JSD*. **2000**, 3, pp 465-474.

Yin, Y. Thesis, University of Oklahoma, Norman, OK, 1994.

P.4 - Figures

Spherical

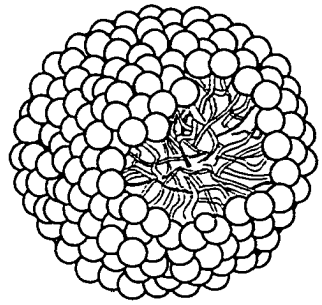

Cylindrical or rod-like with hemispherical ends

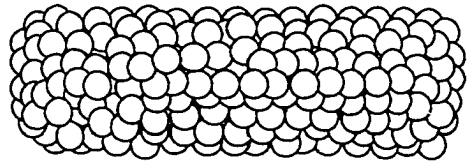

Vesicles

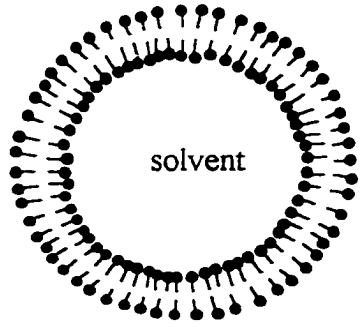

Figure P-1 Micelle shapes.

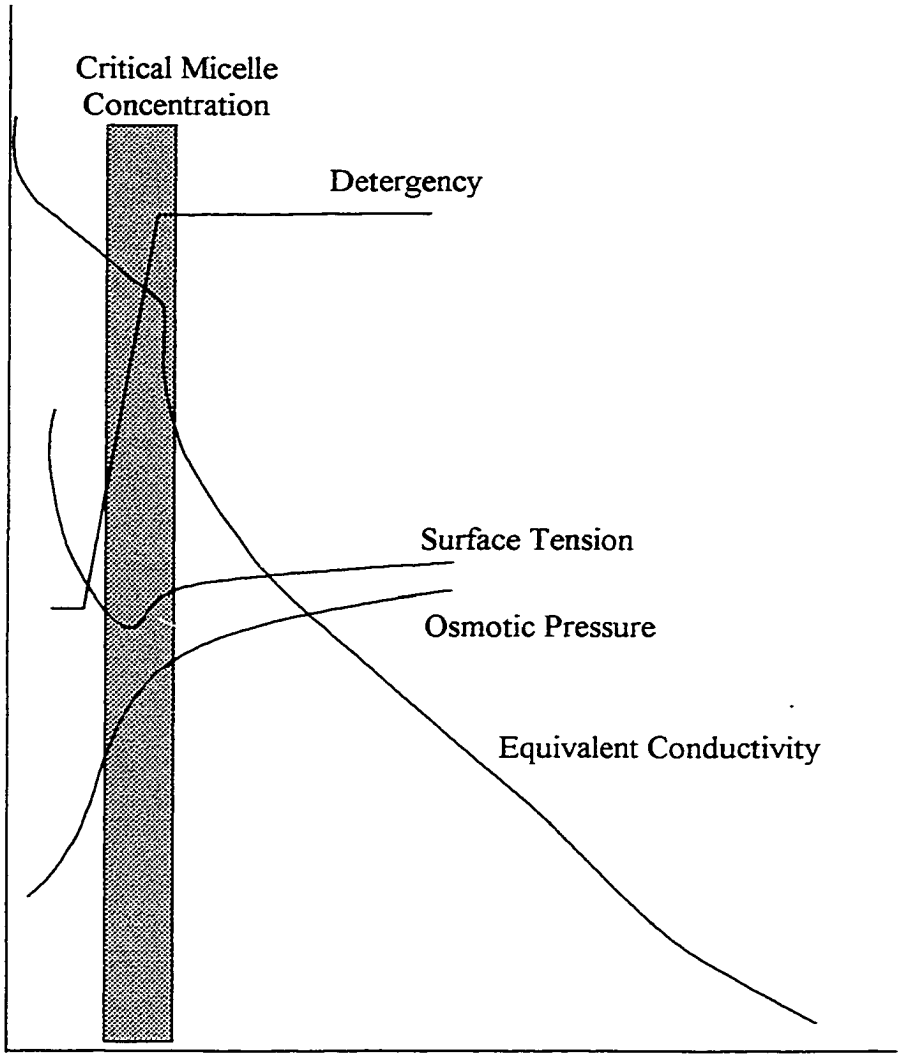

Figure P-2 Changes in select physical properties upon micelle formation (adapted from Rosen, 1989).

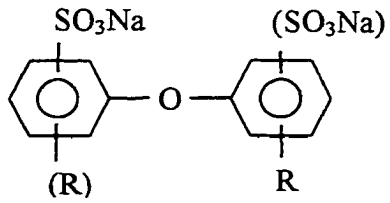

Figure P-3 General structure of alkyl diphenyl ether sulfonates.

Chapter 1

Determination of Critical Micelle Concentrations for Several Alkyldiphenyl Oxide Disulfonate Surfactants

1.1 Abstract

The critical micelle concentrations (CMC) for several alkyldiphenyl oxide disulfonate surfactants were determined in deionized water and in sodium chloride solutions. The CMC's ranged from 10^{-6} to 10^{-4} M with some values not following expected trends. Other values discussed are the surface tensions at the CMC, surface excess concentrations (molecule/m^2), and surface area per molecule at the air/water interface. The results are discussed in terms of the surfactants actually being mixed surfactant systems. The effect of adding the sodium chloride on the above values is also discussed.

1.2 Introduction

As discussed in the Prologue, surfactants exist in solution as individual molecules or monomers until a critical concentration is reached at which the monomers begin to self-aggregate. This concentration is designated as the critical micelle concentration (CMC) and is one of the most fundamental physical properties of surfactant solutions. Table 1-1 contains several CMC values reported and the conditions under which they were determined for various alkyldiphenyl oxide sulfonate surfactants.

Table 1-1 Reported CMC Values

Component	CMC (M)	Reported Conditions	Method
C10 MAMS[a]	3.2×10^{-5}	25° C; 0.1 N Na^+	Wilhelmy plate
C10 DADS[a]	1.0×10^{-5}	25° C; 0.1 N Na^+	Wilhelmy plate
C10 MADS[a]	3.7×10^{-4}	25° C; 1.0 N Na^+	Wilhelmy plate
3B2[b]	4.0×10^{-3}	RT	Capillary rise
C12 MADS[b]	5.0×10^{-3}	RT	Capillary rise
8390[b]	6.3×10^{-3}	RT	Capillary rise
8390[c]	3×10^{-3}	RT	Estimated from SED
C10 DADS[d]	1.54×10^{-3}	36° C; 0 M Na^+	Max. bubble tensiometer
C10 DADS[d]	1.26×10^{-3}	36° C; 8.6×10^{-4} M Na^+	Max. bubble tensiometer
C10 DADS[d]	5.89×10^{-4}	36° C; 3.4×10^{-3} M Na^+	Max. bubble tensiometer
C10 DADS[d]	2.88×10^{-4}	36° C; 0.01 M Na^+	Max. bubble tensiometer
C10 DADS[d]	2.33×10^{-4}	36° C; 0.025 M Na^+	Max. bubble tensiometer
C10 DADS[d]	1.80×10^{-4}	36° C; 0.05 M Na^+	Max. bubble tensiometer
C10 DADS[d]	1.43×10^{-4}	36° C; 0.1 M Na^+	Max. bubble tensiometer
C10 DADS[d]	1.14×10^{-4}	36° C; 0.2 M Na^+	Max. bubble tensiometer
C10 DADS[d]	5.37×10^{-3}	36° C, 0 M K^+	Max. bubble tensiometer
C10 DADS[d]	2.09×10^{-3}	36° C, 0.05 M K^+	Max. bubble tensiometer
C10 DADS[d]	1.48×10^{-4}	36° C, 0.1 M K^+	Max. bubble tensiometer
C10 DADS[d]	1.00×10^{-4}	36° C, 0.2 M K^+	Max. bubble tensiometer
C10 MADS[e]	1.40×10^{-4}	RT	Cahn tensiometer
C12 MAD[e]	1.30×10^{-4}	RT	Cahn tensiometer
C16 MADS[e]	2.53×10^{-4}	RT	Cahn tensiometer
C10 DADS[e]	1.33×10^{-4}	RT	Cahn tensiometer

[a]Rosen et al. 1992 [b]Rouse et al. 1993; 8390 is a commercial mixture of C16 components. Composition: 15-35% C16 MADS and 5-10% C16 DADS. 3B2 is a commercial mixture of C10 components containing 15-35% C10 MADS and 5-10% C16 DADS
[c]Rouse et al 1995 [d]Yin 1994 [e]Quencer, 1995

The purpose of the current research was to determine the CMC's of C10 MADS, C12 MADS, C16 MADS and C10 DADS components in order to attempt to resolve

differences between reported CMC values and to verify the adsorption behaviors observed for several of the components. The observed behavior of surfactant adsorption is such that an increase in adsorption is observed until the CMC is reached. At the CMC the surfactant adsorption remains constant or plateaus with any further increase in surfactant concentration. The results of the adsorption studies in relation to the CMC's are presented in Chapter 3, Section 3.5.3.4 (Table 3-3).

1.3 Materials

The CMC's were determined for C10 MADS, C10 DADS, C12 MADS and C16 MADS. These surfactants are part of the Dowfax™ suite of surfactants and were provided by DOW Chemical, Midland, MI at approximately 35% active by weight. They were used as received. Sodium chloride, ACS grade, was purchased from Fisher Scientific and also used as received. Deionized water was manufactured in-house.

1.4 Experimental

From the 35% active solutions, stock solutions of approximately 10% active were prepared using deionized water. Two series of solutions were prepared, one in DI water and the other in sodium chloride, with surfactant concentrations ranging from 10^{-8} M to 0.1 M. For the MADS surfactants the sodium chloride concentration was 0.15 M, and for the DADS surfactant the sodium chloride concentration was 0.09 M. Previous research had shown the DADS surfactant to be susceptible to "salt-shock" or complex phase behavior in the presence of higher concentrations of sodium chloride. The lower salt concentration avoided this undesirable behavior. These two sodium chloride concentrations were chosen to compliment the adsorption studies discussed in Chapter 3.

The surface tensions were measured on a KRÜSS digital tensiometer, Model K 10 T using a plate method based on the Wilhelmy method. Prior to each measurement, the sample vessels were cleaned using a No-Chromix acid solution, triple rinsed and oven dried. The plate was rinsed with DI water and flamed to remove any trace contamination.

A circulation bath was used to maintain a constant temperature of 22° C, although some fluctuation was unavoidable. Approximately 25 mL of the surfactant solution was poured into the sample vessel, and the temperature was allowed to equilibrate. Preparing the tensiometer for each measurement required a null adjustment. The tensiometer was placed in the "Zero" mode. In this mode the digital display was zeroed then the balance beam of the force measuring unit was brought to the zero position. Measuring the surface tension was accomplished by raising the sample vessel so that the solution surface was approximately 1 mm from the bottom edge of the plate, checking the null adjustment, placing the tensiometer in the "Run" mode and raising the vessel just until the plate contacted the solution. At this point the tensiometer begins measuring the surface tension. The plate is torn out of the solution by a dial motor until the lower edge of the plate again exactly reaches the level of the solution surface. As the surface tension changes, either due to changes in temperature or enrichment of the surfactants at the surface, the display was capable of indicating the actual surface tension. This feature proved very useful due to the long equilibration times exhibited by the MADS and DADS surfactants.

The change in the surface tension with time was observed during timed studies using the inverted vertical pull surface tension method (Christian et al., 1998) for the following solutions: C16 MADS at 0.1925, 3.07×10^{-4}, 4.56×10^{-5}, and 1.82×10^{-6} M each in

0.15 M NaCl. For comparison, a timed study was also performed with 1.82×10^{-6} M C16 MADS in 0.15 M NaCl.

The surface tension measurements using the inverted vertical pull surface tension method were performed in two different ways: by leaving the sample on the balance until equilibrium was reached and by removing the sample from the balance and taking a "fresh" reading at each time interval. The time intervals for each method were such that measurements were taken at short durations initially, and as the amount of change in the surface tension decreased the time intervals were lengthened. Measurements on the KRÜSS were conducted by leaving the plate in the solution until equilibrium was established. The change in the time intervals was adjusted in the same manner as the inverted vertical pull method.

1.5 Results and Discussion

1.5.1 Critical Micelle Concentrations

Plots of surface tension (γ) versus log concentration (C) were prepared for each surfactant, and linear regressions were performed on the data points comprising the two linear sections of these plots. The CMC's were then determined from the intersection of these two regression lines. These plots are shown in Figure 1-1 through Figure 1-8, and complete lists of data points for each surfactant are provided in Appendix 1A.

Table 1-2 contains the CMC values determined by DOW Chemical and the values determined in this study.

Table 1-2 CMC Values (M)

Surfactant	CMC*	CMC**	CMC***
C10 MADS	1.40×10^{-4}	8.24×10^{-5}	2.58×10^{-5}
C12 MADS	1.30×10^{-4}	3.05×10^{-5}	1.26×10^{-5}
C16 MADS	2.53×10^{-4}	1.08×10^{-5}	8.12×10^{-6}
C10 DADS	1.33×10^{-4}	1.69×10^{-5}	4.96×10^{-6}

* Values obtained by DOW Chemical with no additional electrolyte (Quencer, 1995).

** Values obtained in the current study with no additional electrolyte.

*** Values obtained in the current study in 0.15 M NaCl for the MADS components and 0.09 M NaCl for the DADS component.

The values determined in the current study tend to be lower than previous values reported. In addition to the differences in the temperatures used in the different studies, there are the differences in the times allowed for equilibration. Most of the previous studies employed methods that involve relatively short times for equilibration. The only study that mentioned equilibration times of several hours was that by Rosen et al. (1992), but there are several key differences between that study and this. These include temperature and salinity, but most notably the surfactants. Rosen et al. used purified surfactants while the current study did not.

The CMC's determined in this study can be explained, in a large part, based on the composition of each of the surfactants which were shown in the following table. This information was provided by DOW Chemical for samples received from 1992 to 2000 and is considered confidential and is therefore not present in the final version of this dissertation.

Table 1-3 Composition of Dowfax Surfactants (Weight Percent*)

CONFIDENTIAL INFORMATION

For solutions prepared in DI water and sodium chloride the behavior of the two C10 components is as expected. As the number of alkyl chains increases, the CMC decreases. Rosen et al. (1992) reported values of 3.7×10^{-4} M in 1 N NaCl for the C10 MADS and 1.0×10^{-5} M in 0.1 N NaCl for the C10 DADS which are an order of magnitude greater than the values obtained here for the electrolyte systems, but are close to the current values for the DI solutions. There are several differences between the Rosen study and the current study. First, surfactants used in the Rosen study were said to be purified and to have a 99.7 % disulfonate content while the surfactants in this study were mixtures of the MADS, DADS and, in some cases, DAMS components. Second, the equilibration times are significantly different. Rosen et al. commented that in some cases equilibration took several hours. Times for the current study averaged 10 hours. Third, the temperature used was 25°C while the current temperature was 22°C. Fourth, surfactant solutions used in the current study contained trace amounts of sodium sulfate, with concentrations on the order of 10^{-7} M for solutions at the CMC.

Assuming ideal mixing for the C10 components and also assuming the value of the C10 MADS / 0.0 M NaCl is accurate; the following equation for ideal mixing was used to calculate a CMC for the C10 DADS surfactant:

$$C_{12}^{m} = \frac{C_1^{m} C_2^{m}}{C_1^{m}(1-\alpha) + C_2^{m}\alpha} \qquad (1\text{-}1)$$

Where C_1 is C10 MADS; C_2 is C10 DADS and α is 0.217. Ignoring the 7% DAMS content, the CMC for the C10 DADS was calculated to be 1.38×10^{-5} M which is similar to the value determined experimentally.

It would be expected that for the three MADS surfactants, C10, C12, and C16, the value of the CMC would decrease due to the increasing alkyl chain length. This is true for those solutions prepared in 0.15 M NaCl but not for those in deionized water. For the solutions prepared in deionized water the observed behavior can be explained, in part, by the component breakdown for each of the surfactants. Assuming the general rule of thumb for CMC's halving with the addition of each methylene group, and using the values for the C16 MADS as a base; the expected values for the C10 and C12 MADS would be greater by one and two orders of magnitude, respectively. The estimated CMC for the C10 MADS is 6.9×10^{-2}M and for the C12 MADS, 1.7×10^{-2}M. These values are higher than expected and indicate that the CMC determined for the C16 MADS may be too high.

When sodium chloride is added to the MADS solutions, the CMC's for the C10, C12, and C16 surfactants are reduced by factors of 69, 59, and 99% relative to the deionized water systems. Relative to each other the CMC's of the MADS components in NaCl decrease with increasing chain length, as would be expected. Using the C16 MADS 0.15M NaCl as a basis, estimated CMC's for the C10- and C12 MADS without DADS would be 5.2×10^{-4} and 1.3×10^{-4} M, respectively. These estimations are based on the general rule of thumb that the CMC of an ionic surfactant is halved by the addition of one methylene group to a straight-chain hydrophobic group attached to a single terminal hydrophilic group (Rosen, 1989).

1.5.2 Surface Tensions at the CMC

Surface tensions at the CMC's (γ_{CMC}) were also determined from the intersection of the two lines comprising the surface tension curves. These values are provided in Table 1-4. In comparing the two systems, it can be seen that there is a small increase in γ_{CMC} upon the addition of NaCl for all of the surfactants.

Table 1-4 Surface Tensions at the CMC (mN/m)

Surfactant	γ_{CMC}*	γ_{CMC}**
C_{10} MADS	27.6	31.6
C_{12} MADS	35.1	37.2
C_{16} MADS	38.4	39.7
C_{10} DADS	28.6	31.1

* Values obtained in the current study with no additional electrolyte.
** Values obtained in the current study in 0.15 M NaCl for the MADS components and 0.09 M NaCl for the DADS component.

1.5.3 Surface Excess Concentration

Estimates of the surface excess concentrations (Γ_1) were calculated using the following equations provided in Rosen (1989). For 1:1 ionic surfactants in swamping amount of electrolytes the following applies:

$$\Gamma_1 = -\frac{1}{2.303\ RT}\left(\frac{\partial \gamma}{\partial \log C_1}\right)_T \qquad (1\text{-}2)$$

Where $\partial\gamma/\partial\log C_1$ is the slope of a plot of γ (in mN m^{-1}) versus log C_1, R is the gas constant (8.31 $Jmol^{-1}$ K^{-1}), T is the absolute temperature, and Γ is in mol/1000m^2.

For 1:1 ionic surfactants containing no other solutes the following applies:

$$\Gamma_1 = -\frac{1}{4.606\ RT}\left(\frac{\partial \gamma}{\partial \log C_1}\right)_T \qquad (1\text{-}3)$$

Using equations (1-2) and (1-3), the following adsorption densities were calculated for the surfactants at both salinities examined.

Table 1-5 Adsorption Densities (mol/1000m^2)*

Surfactant	mol/1000m^2**	mol/1000m^2***
C_{10} MADS	3.20×10^{-3}	6.92×10^{-3}
C_{12} MADS	2.97×10^{-3}	5.98×10^{-3}
C_{16} MADS	1.17×10^{-3}	3.22×10^{-3}
C_{10} DADS	2.77×10^{-3}	3.81×10^{-3}

* For mol/cm^2 x10^{-10}. **Values obtained in the current study with no additional electrolyte.
*** Values obtained in the current study in 0.15 M NaCl for the MADS components and 0.09 M NaCl for the DADS component.

When using equations (1-2) and (1-3), care must be taken to ensure that they are suitable for the surfactant systems in question. For the electrolyte systems in this study the concentration of the sodium chloride was 0.15 M and 0.09 M, several orders greater than the CMC's of the surfactants. Therefore, equation (1-2) is applicable.

Sodium sulfate is present in the surfactant solutions received from Dow Chemical, and the weight percents present in each surfactant are shown in Table 1-2. At the CMC the concentration of the sodium sulfate is only one or two orders below the CMC's. This being the case, the values of the densities calculated from equation (1-3) should be treated as estimates. Since the concentrations of Na_2SO_4 in each surfactant are on the same order, the direction of change seen in the adsorption densities for these systems is still valid.

1.5.4 Area per Molecule at the Air/Water Interface

Using the adsorption densities calculated above the surface areas were calculated from the following equation (Rosen, 1989) with the results shown in Table 1-6:

$$a_1^s = \frac{10^{23}}{N\Gamma_1} \tag{1-4}$$

Where a_1^s is in square angstroms, N is Avogadro's number, and Γ_1 is in mol/1000m^2.

Table 1-6 Area per molecule ($Å^2$)

Surfactant	Area per molecule* ($Å^2$)	Area per molecule** ($Å^2$)
C_{10} MADS	52.0	24.0
C_{12} MADS	55.9	27.8
C_{16} MADS	142.2	51.6
C_{10} DADS	60.0	43.5

* Values obtained in the current study with no additional electrolyte.

** Values obtained in the current study in 0.15 M NaCl for the MADS components and 0.09 M NaCl for the DADS component.

For both systems the areas increase with increasing chain length. The area for the C10 DADS would be greater except for the amount of MADS present in the system. The area for the C10 DADS in deionized water is only slightly greater than the area for the C10 MADS indicating the strong influence of the MADS on the equilibrium surface composition of the DADS surfactant. In the saline solutions the difference in the areas for the C10 components is greater than their areas in deionized water. It would be expected that the C10 MADS molecules would have less repulsion for each other and therefore compress to a smaller area in a saline environment relative to the DADS. Hence the larger area for the C10 DADS/ 0.09 M NaCl.

1.5.5 Timed Surface Tension Values

Unfortunately, the timed studies using the inverted vertical pull surface tension method did not provide the information sought. Measurements conducted by removing the sample vial from the balance and taking a "fresh" reading at each time interval indicated essentially no change in the surface tension with time. Measurements taken by leaving the sample on the balance for the duration indicated that the surface tension decreased and then began to increase, but at the point of increase the rod broke free of the solution surface.

Timed surface tension measurements were taken on the KRÜSS to examine the change in the surface tension with time as the surface came to equilibrium. As seen in Figure 1-9 the time needed to reach equilibrium was just over 20 hours for the $1.82x10^{-6}$ M C16 MADS. While this time was on the upper end of the range of times needed to reach equilibrium for the different surfactant solutions, it was not atypical of the changes that had been observed for different surfactant solution. Plots of γ versus time for $1.82x10^{-6}$ M C16 MADS for the two different methods are shown in Figure 1-9 and Figure 1-10 and are shown for comparison.

1.6 Conclusions

It was interesting to note in Table 1-1 that the more dynamic methods used in the determination of CMC's, i.e. those that allow for only short equilibration times, tended to have much higher CMC's. So the question arises as to the surfactant composition at the surface at any given time as equilibrium is approached. Since diffusion coefficients are inversely proportional to the molecular volumes, components with larger molecular volumes would be expected to have smaller diffusion coefficients. This of course has implications for the applications in which these surfactants are used.

The CMC values determined for the C10, C12 and C16 MADS and for the C10 DADS can be explained on the basis of their compositions and follow expected trends. As the alkyl chain length increases, the CMC decreases. The values determined for the areas per molecule for the MADS components were smaller than expected but did show increasing surface area as the alkyl chain length increased from 10 to 16.

1.7 References

Christian, S. D.; Slagle, A. R.; Tucker, E. E.; Scamehorn, S. F. Inverted Vertical Pull Surface Tension Method. *Langmuir* **1998**, 14(11), pp 3126-3128.

Rosen, M. J.; Zhu, Z. H.; Hua, X. Y. Relationship of Structure to Properties of Surfactants. 16. Linear Decyldiphenylether Sulfonates. *JAOCS* **1992**, 69, 30.

Rosen, M. J. Surfactant and Interfacial Phenomena, 2nd Ed., John Wiley & Sons, New York, N. Y., 1989.

Rouse, J. D.; Sabatini, D. A.; Harwell, J. H. Minimizing Surfactant Losses Using Twin-Head Anionic Surfactants in Subsurface Remediation. *Environ. Sci. Technol.* **1993**, *27(10)*, pp 2072-2078.

Rouse, J. D.; Sabatini, D. A.; Deeds, N. E.; Brown, R. E. Micellar Solubilization of Unsaturated Hydrocarbon Concentrations as Evaluated by Semiequilibrium Dialysis. *Environ Sci & Technol.* **1995**, *29(10)*, pp 2484-2489.

Quencer, L. B., Dow Chemical, Midland. MI, Personal communication, 1995.

Yin, Y. Thesis, University of Oklahoma, Norman, OK, 1994.

1.8 - Figures

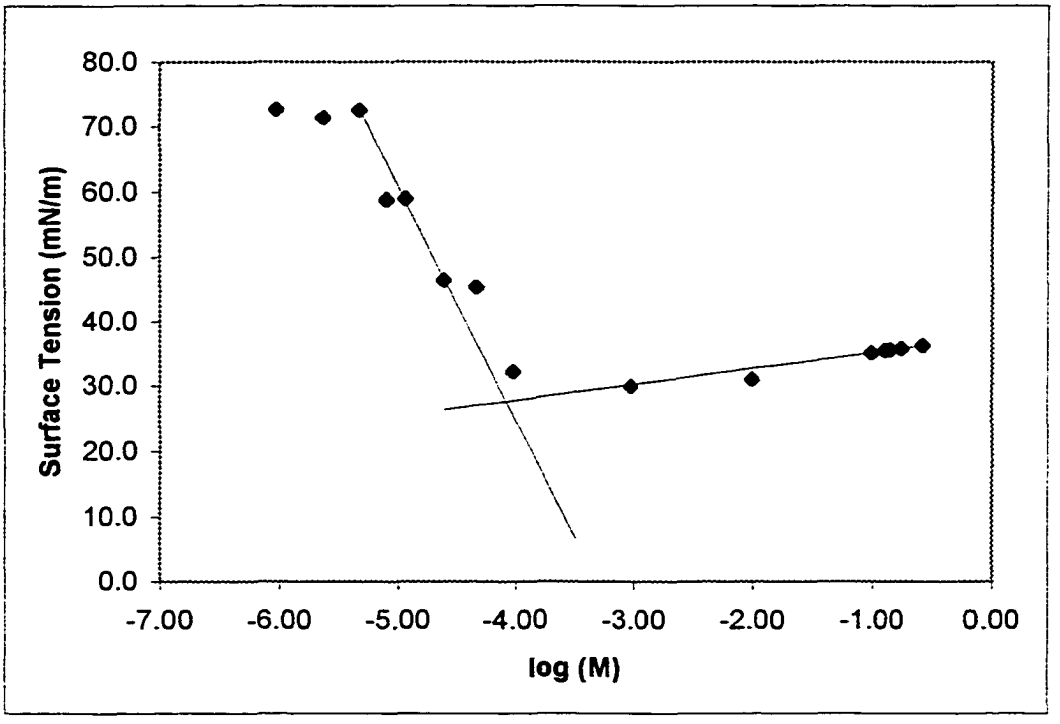

Figure 1-1 Surface Tension Curve for C10 MADS / 0 M NaCl

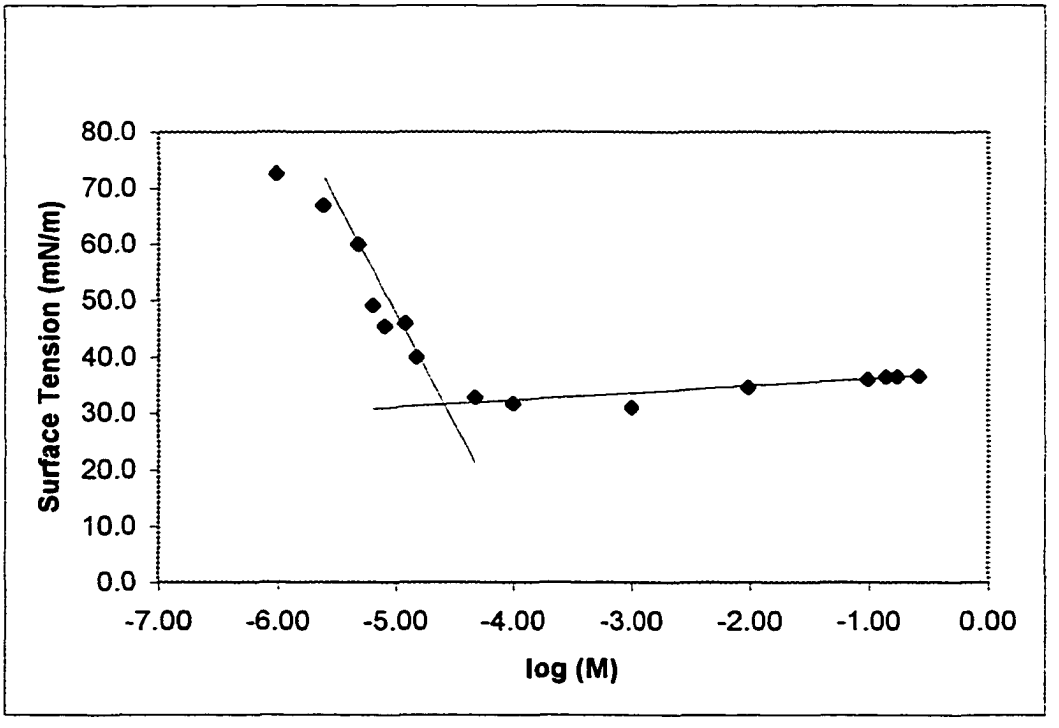

Figure 1-2 Surface Tension Curve for C10 MADS / 0.15 M NaCl

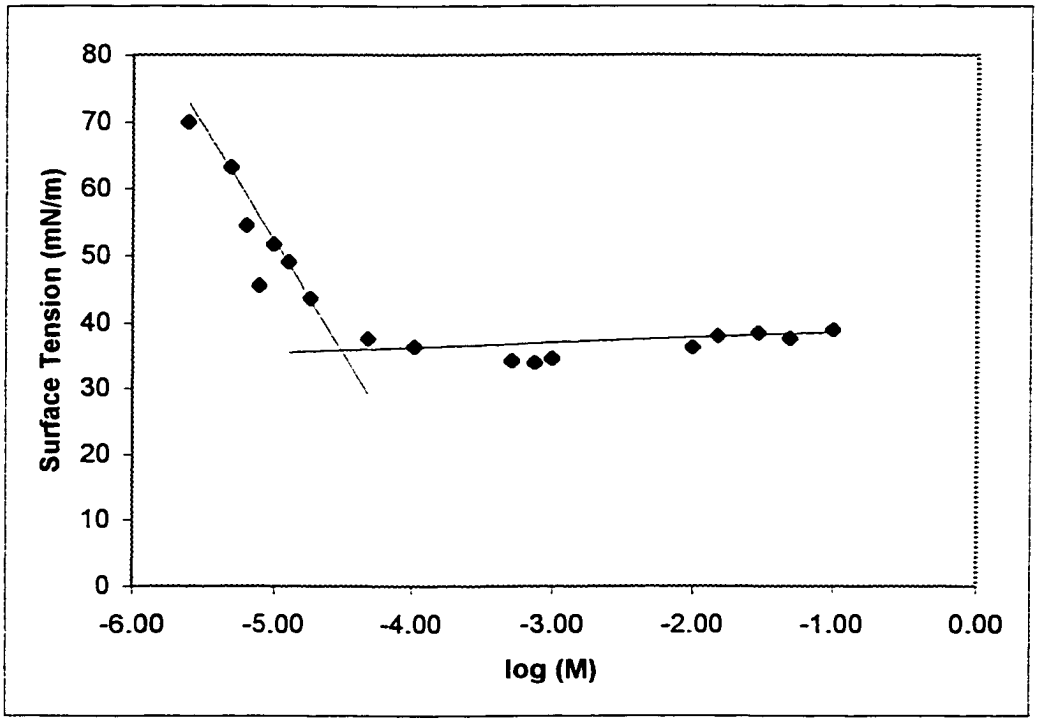

Figure 1-3 Surface Tension Curve for C12 MADS / 0 M NaCl

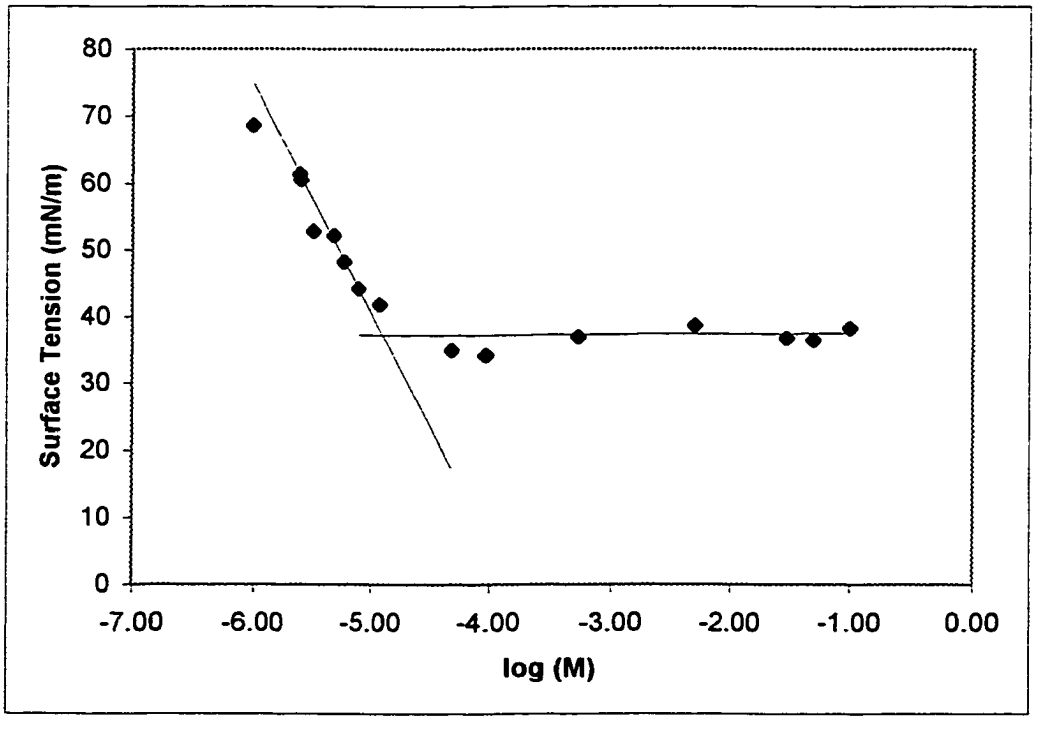

Figure 1-4 Surface Tension Curve for C12 MADS / 0.15 M NaCl

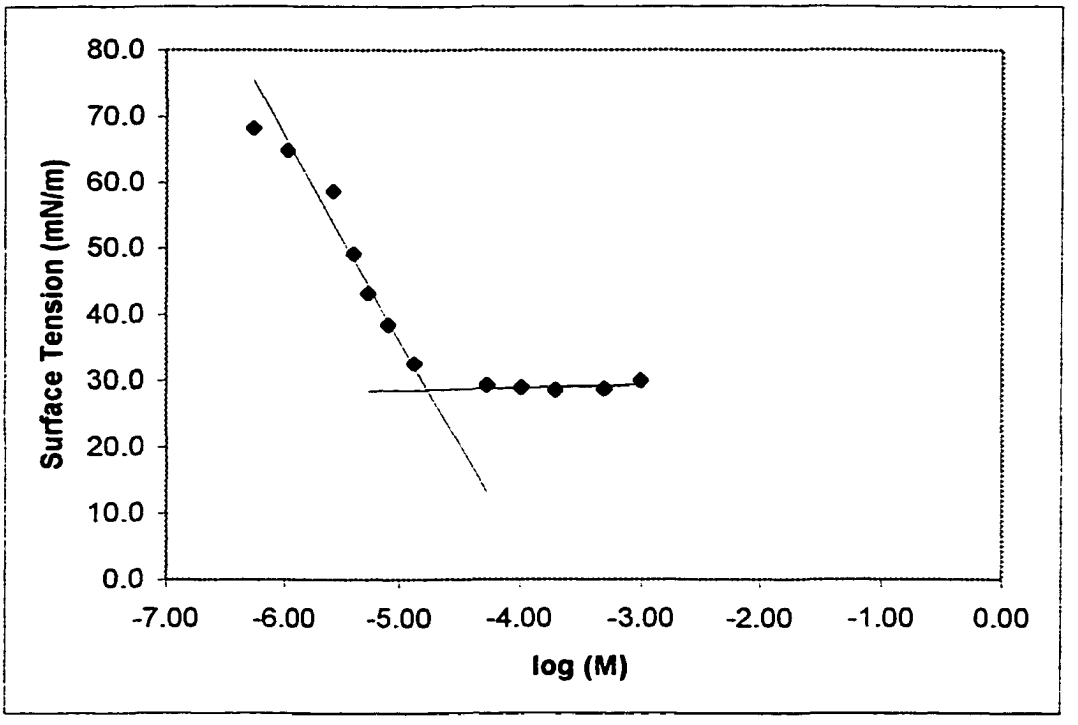

Figure 1-5 Surface Tension Curve for C10 DADS / 0 M NaCl

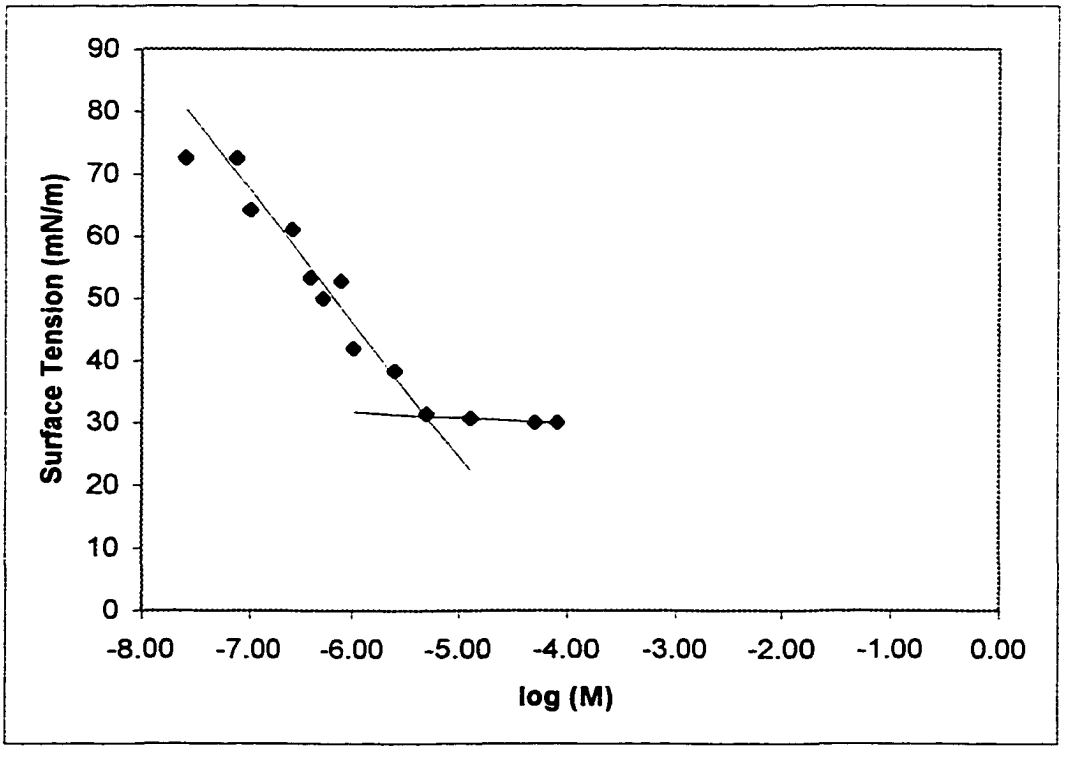

Figure 1-6 Surface Tension Curve for C10 DADS / 0.9 M NaCl

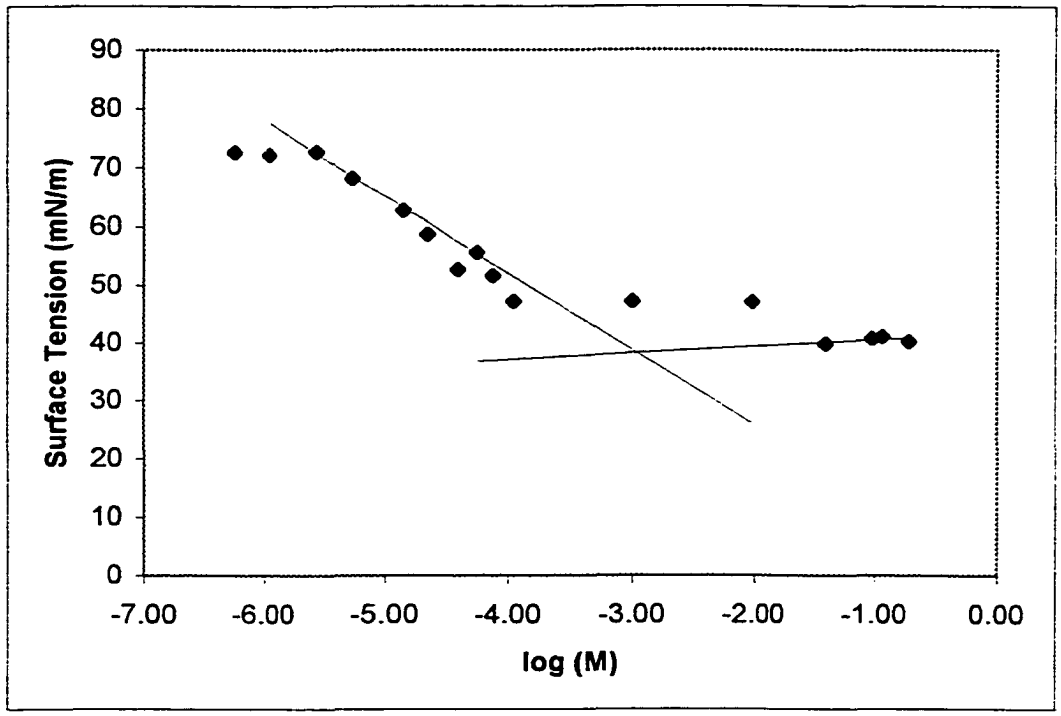

Figure 1-7 Surface Tension Curve for C16 MADS / 0 M NaCl

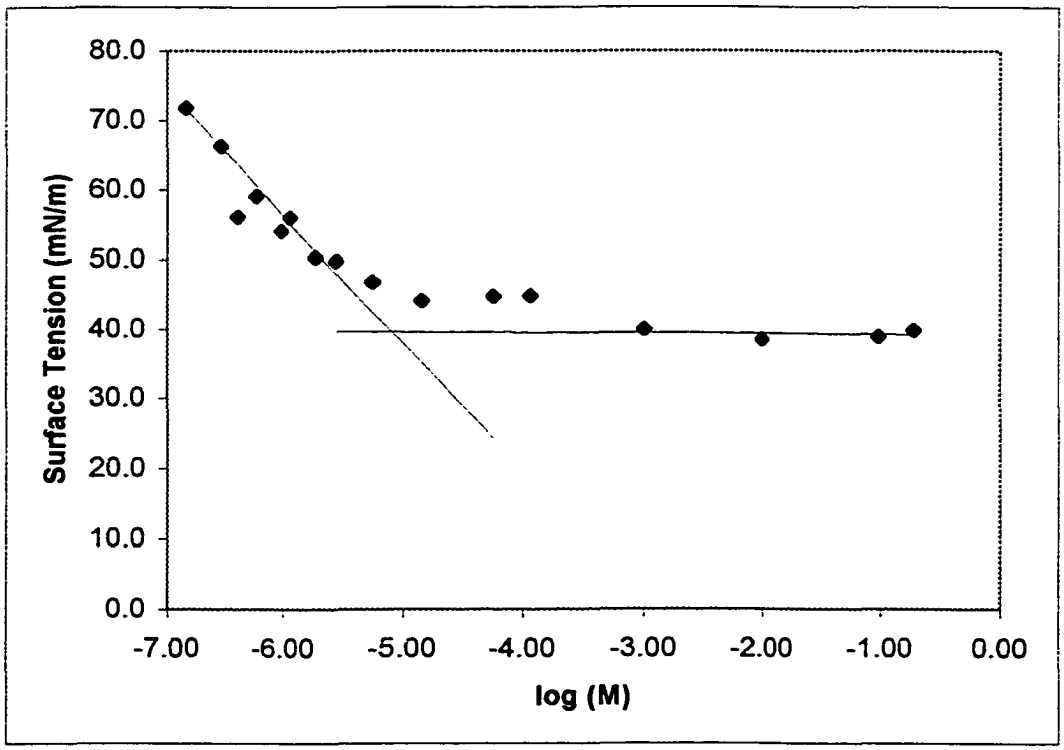

Figure 1-8 Surface Tension Curve for C16 MADS / 0.15 M NaCl

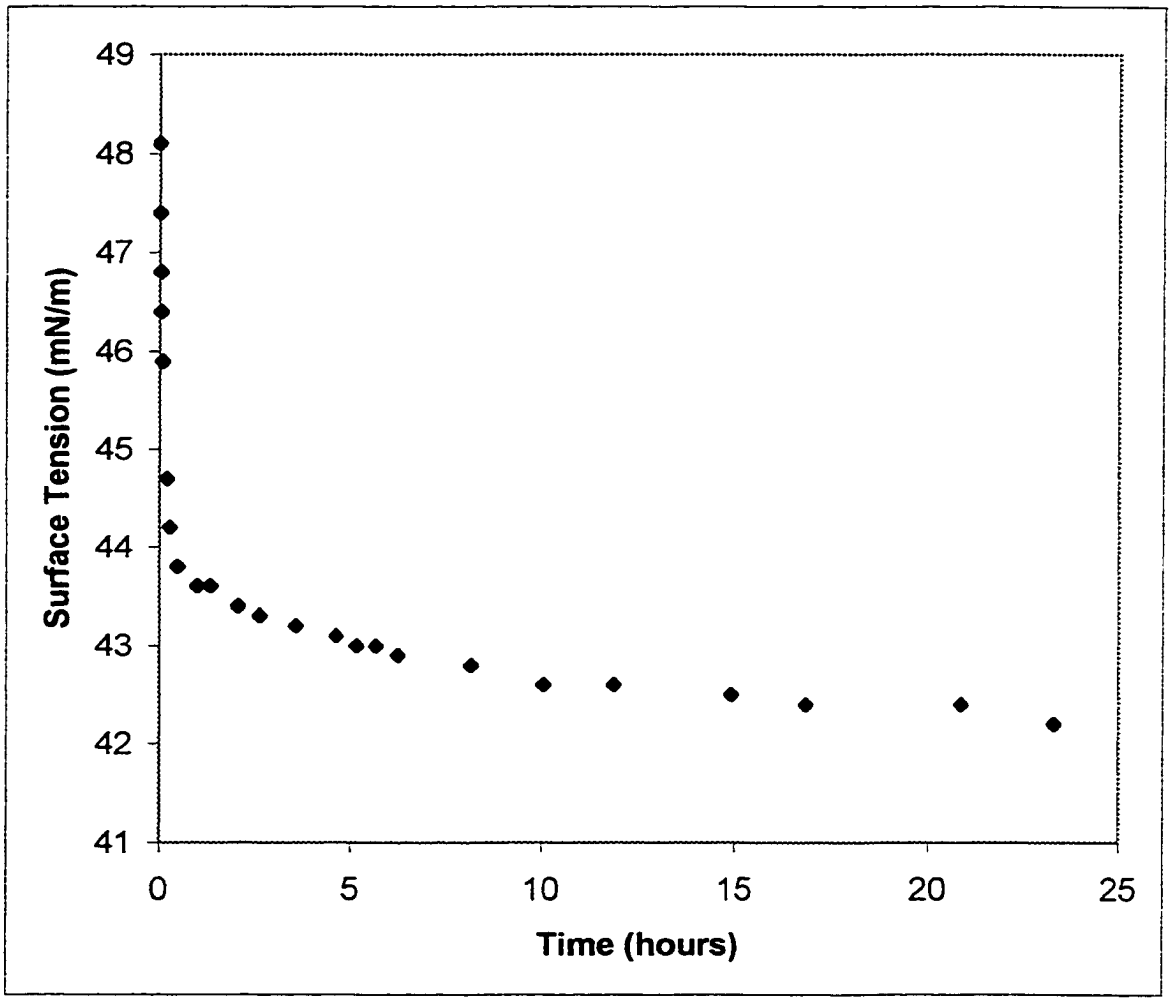

Figure 1-9 Time Studies for 1.82×10^{-6} M C16 MADS/0.15 M NaCl using KRÜSS tensiometer.

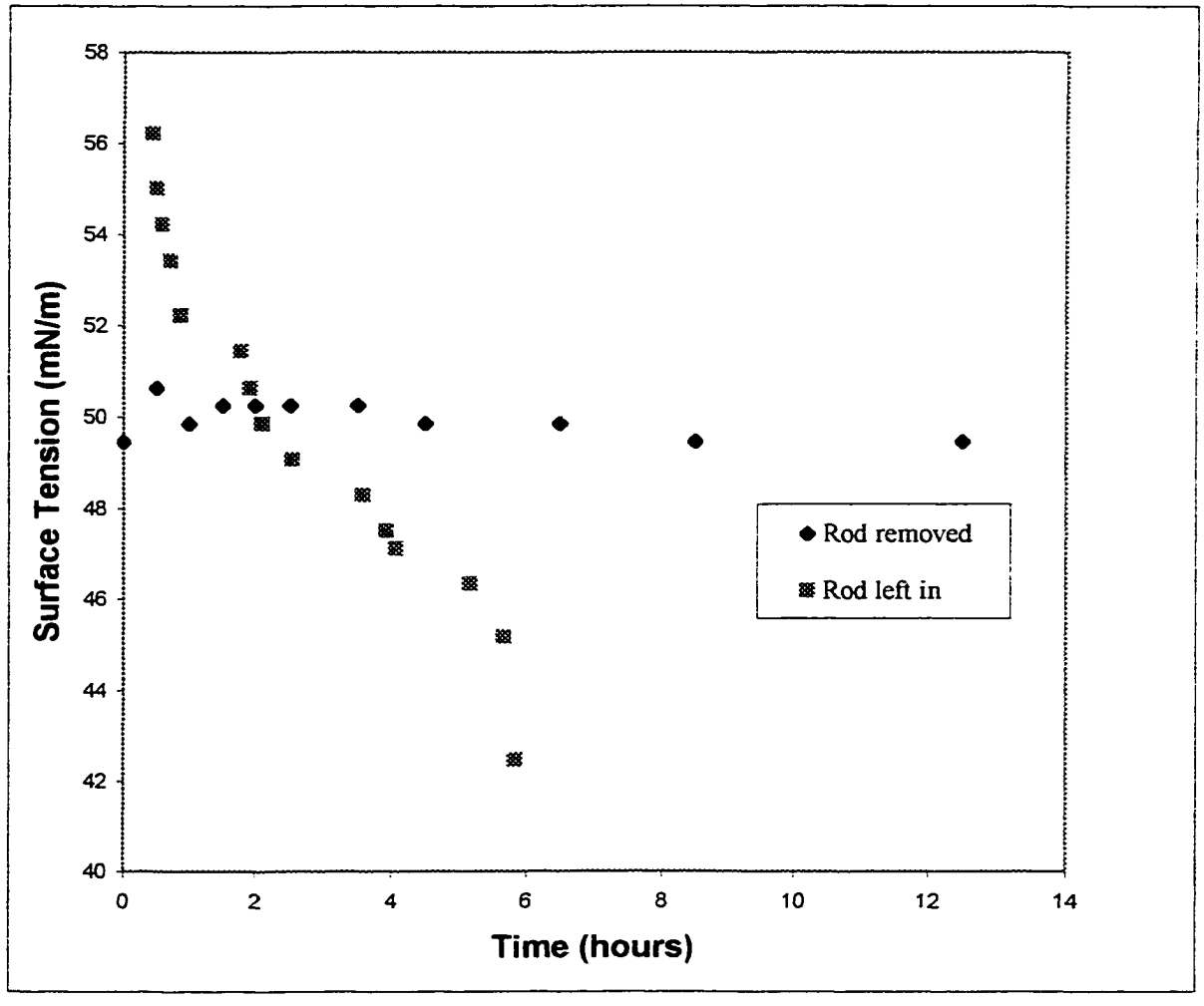

Figure 1-10 Time Studies for 1.82×10^{-6} M C16 MADS/0.15 M NaCl using rod tensiometer.

1A Appendix: Surface Tension Data

C10 MADS Surface Tension Data

Table 1A.1-1 Data for 0.0 M NaCl

Surfactant Concentration (M)	Log (M)	Surface Tension (mN/m)
$9.30x10^{-7}$	-6.03	72.6
$2.33x10^{-6}$	-5.63	71.4
$4.65x10^{-6}$	-5.33	72.5
$7.95x10^{-6}$	-5.10	58.8
$1.16x10^{-5}$	-4.94	59.0
$2.48x10^{-5}$	-4.61	46.4
$4.65x10^{-5}$	-4.33	45.3
$9.45x10^{-5}$	-4.02	32.2
$9.58x10^{-4}$	-3.02	29.9
$9.85x10^{-3}$	-2.01	31.0
$9.85x10^{-2}$	-1.01	35.2
$1.28x10^{-1}$	-0.89	35.2
$1.42x10^{-1}$	-0.85	35.6
$1.78x10^{-1}$	-0.75	35.8
$2.67x10^{-1}$	-0.57	36.3

Table 1A.1-2 Data for 0.15 M NaCl

Surfactant concentration (M)	Log (M)	Surface Tension (mN/m)
$9.58x10^{-7}$	-6.01	72.6
$2.40x10^{-6}$	-5.62	67.0
$4.79x10^{-6}$	-5.32	60.0
$6.31x10^{-6}$	-5.20	49.1
$7.95x10^{-6}$	-5.10	45.4
$1.20x10^{-5}$	-4.92	46.0
$1.49x10^{-5}$	-4.83	39.9
$4.79x10^{-5}$	-4.32	32.8
$9.93x10^{-5}$	-4.00	31.6
$1.02x10^{-3}$	-2.99	31.0
$9.83x10^{-3}$	-2.01	34.6
$9.83x10^{-2}$	-1.01	36.0
$1.42x10^{-1}$	-0.85	36.5
$1.78x10^{-1}$	-0.75	36.5
$2.67x10^{-1}$	-0.57	36.6

C12 MADS Surface Tension Data

Table 1A.2-1 Data for 0.0 M NaCl

Surfactant Concentration (M)	Log (M)	Surface Tension (mN/m)
$2.42x10^{-6}$	-5.62	70.0
$4.84x10^{-6}$	-5.32	63.2
$6.27x10^{-6}$	-5.20	54.5
$7.84x10^{-6}$	-5.11	45.5
$9.81x10^{-6}$	-5.01	51.7
$1.26x10^{-5}$	-4.90	49.0
$1.83x10^{-5}$	-4.74	43.6
$4.84x10^{-5}$	-4.32	37.6
$1.05x10^{-4}$	-3.98	36.4
$5.11x10^{-4}$	-3.29	34.2
$7.50x10^{-4}$	-3.12	33.9
$9.90x10^{-4}$	-3.00	34.6
$9.85x10^{-3}$	-2.01	36.3
$3.00x10^{-2}$	-1.52	38.4
$5.00x10^{-2}$	-1.30	37.6
$1.00x10^{-1}$	-1.00	38.9

Table 1A.2-2 Data for 0.15 M NaCl

Surfactant Concentration (M)	Log (M)	Surface Tension (mN/m)
$9.72x10^{-7}$	-6.01	68.6
$2.43x10^{-6}$	-5.61	61.4
$2.50x10^{-6}$	-5.60	60.5
$3.19x10^{-6}$	-5.50	52.8
$4.78x10^{-6}$	-5.32	52.2
$5.82x10^{-6}$	-5.24	48.2
$7.84x10^{-6}$	-5.11	44.2
$1.20x10^{-5}$	-4.92	41.8
$4.86x10^{-5}$	-4.31	35.0
$9.29x10^{-5}$	-4.03	34.2
$5.35x10^{-4}$	-3.27	36.9
$4.97x10^{-3}$	-2.30	38.6
$3.00x10^{-2}$	-1.52	36.8
$5.00x10^{-2}$	-1.30	36.5
$1.00x10^{-1}$	-1.00	38.3

C16 MADS Surface Tension Data

Table 1A.3-1 Data for 0.0 M NaCl

Surfactant Concentration (M)	Log (M)	Surface Tension (mN/m)
$5.59x10^{-7}$	-6.25	72.6
$1.12x10^{-6}$	-5.95	72.1
$2.80x10^{-6}$	-5.55	72.7
$5.59x10^{-6}$	-5.25	68.1
$1.40x10^{-5}$	-4.85	62.7
$2.16x10^{-5}$	-4.67	58.7
$3.89x10^{-5}$	-4.41	52.6
$5.59x10^{-5}$	-4.25	55.5
$7.58x10^{-5}$	-4.12	51.6
$1.10x10^{-4}$	-3.96	47.2
$1.00x10^{-3}$	-3.00	47.2
$9.54x10^{-3}$	-2.02	47.0
$4.00x10^{-2}$	-1.40	39.8
$9.58x10^{-2}$	-1.02	40.8
$1.16x10^{-1}$	-0.94	41.1
$1.93x10^{-1}$	-0.72	40.3

Table 1A.3-2 Data for 0.15 M NaCl

Surfactant Concentration (M)	Log (M)	Surface Tension (mN/m)
$1.43x10^{-7}$	-6.84	71.8
$2.86x10^{-7}$	-6.54	66.3
$3.94x10^{-7}$	-6.40	56.1
$5.72x10^{-7}$	-6.24	59.1
$9.57x10^{-7}$	-6.02	54.1
$1.14x10^{-6}$	-5.94	56.0
$1.91x10^{-6}$	-5.72	50.3
$2.86x10^{-6}$	-5.54	49.8
$5.72x10^{-6}$	-5.24	46.8
$1.43x10^{-5}$	-4.84	44.1
$5.72x10^{-5}$	-4.24	44.7
$1.16x10^{-4}$	-3.94	44.8
$1.01x10^{-3}$	-3.00	40.0
$9.81x10^{-3}$	-2.01	38.5
$9.61x10^{-2}$	-1.02	39.0
$1.93x10^{-1}$	-0.72	39.9

C10 DADS Surface Tension Data

Table 1A.4-1 Data for 0.0 M NaCl

Surfactant Concentration (M)	Log (M)	Surface Tension (mN/m)
$5.32x10^{-7}$	-6.27	68.3
$1.06x10^{-6}$	-5.97	64.9
$2.66x10^{-6}$	-5.58	58.7
$3.99x10^{-6}$	-5.40	49.2
$5.32x10^{-6}$	-5.27	44.2
$7.98x10^{-6}$	-5.10	38.4
$1.33x10^{-5}$	-4.88	32.5
$5.32x10^{-5}$	-4.27	29.3
$1.03x10^{-4}$	-3.99	28.9
$1.96x10^{-4}$	-3.71	28.5
$4.89x10^{-4}$	-3.31	28.7
$9.79x10^{-4}$	-3.01	30.0

Table 1A.4-2 Data for 0.09 M NaCl

Surfactant Concentration (M)	Log (M)	Surface Tension (mN/m)
$2.56x10^{-8}$	-7.59	72.5
$7.68x10^{-8}$	-7.11	72.5
$1.02x10^{-7}$	-6.99	64.2
$2.56x10^{-7}$	-6.59	61.1
$3.84x10^{-7}$	-6.42	53.3
$5.12x10^{-7}$	-6.29	50.0
$7.68x10^{-7}$	-6.11	52.8
$1.02x10^{-6}$	-5.99	42.0
$2.56x10^{-6}$	-5.59	38.4
$5.12x10^{-6}$	-5.29	31.4
$1.28x10^{-5}$	-4.89	30.7
$5.12x10^{-5}$	-4.29	30.0
$8.11x10^{-5}$	-4.09	30.0

Chapter 2

Preparation of Microemulsions Using Salinity and Modified Lipophilic Scans with Alkyldiphenyl Oxide Disulfonate Surfactants

2.1 Abstract

Traditional salinity scans were conducted in an attempt to force select mono- and dialkyldiphenyl oxide mono and disulfonate surfactants into undergoing the I-III-II and I-IV-II phase transitions. They were not entirely successful. A few surfactant systems underwent the I/III transition, but even when saturated with electrolyte, the type III microemulsions formed were under optimum and the formation of gels and precipitates was also observed. Modified lipophilic scans were conducted based on the concept of lipophilic linkers. The linker chosen was octanoic acid. In the presence of the linker the surfactants were able to undergo I-III-II and I-IV-II phase transitions, but gels were still present in many systems. The gels tended to occur at lower surfactant concentrations. For the systems containing $CaCl_2$, the optimum solubilization potentials averaged 2.93 mL/g at 24°C, 2.87 mL/g at 35°C, and 2.75 mL/g at 45°C. For the systems containing $MgCl_2.6H_2O$+$CaCl_2$, the optimum solubilization potentials averaged 3.03 mL/g at 24°C, 2.86 mL/g at 35°C and 45°C.

The material contained in this chapter is a compilation of research conducted by the author and Ms Sangaroon Aowiriyakul.

2.2 Introduction

2.2.1 Microemulsion

In systems containing electrolyte, hydrocarbon, water, and a water soluble amphiphilic compound (usually a surfactant) there exists the possibility of inducing the amphiphile to transition from the water-rich phase into the hydrocarbon or oil-rich phase. This transition has traditionally been described in terms of the Winsor nomenclature. The designation "Winsor type I" is used to describe a microemulsion system consisting of two phases, one water-rich and the other oil-rich, with the bulk of the surfactant located in the water-rich phase. Any oil located within the water-rich phase exists as an oil in water (o/w) microemulsion, regardless of the diameter of the oil "drops". Under certain conditions the surfactant will form a third phase which is an amphiphilic-rich phase containing emulsified water and oil in equilibrium with excess oil and water phases. This system is designated as a Winsor type III microemulsion. Upon formation of the type III, the surfactant-rich phase (also called the middle phase) contains primarily water, but as the transition continues the middle phase takes up increasing amounts of oil. The system is said to be at its optimum when equal amounts of water and oil are solubilized within the middle phase region. As more oil is solubilized, a second two-phase system (type II) is formed. In this second two-phase system the surfactant is located primarily in the oil-rich phase with any water within the oil phase existing as a water in oil (w/o) microemulsion. At sufficiently high surfactant concentrations the type I system may transition directly into a single-phase system designated as a Winsor type IV and then to a type II. The Winsor type IV system is single surfactant phase with no excess phases.

The transition of a hydrocarbon/water/electrolyte/surfactant system from type I to type II can be brought about by several means. A detailed description for promoting these transitions is provided by Bourrel and Schecter (1988). Included in this description are two of the most common methods that involve changing the salinity in so-called salinity scans or the changing of the temperature. Figure 2-1 is an illustration of the changes in interfacial tension and solubilization with increasing salinity and the corresponding changes in the appearances of the microemulsions.

Fundamental microemulsion research typically used alkanes as the hydrocarbon. From the many studies using alkanes of various carbon lengths, it was observed that the behavior of the microemulsion system was strongly dependent on the number of carbon atoms of the alkane. Many results were presented on the basis of the alkane carbon number (ACN). The concept of the ACN became such a standard that as microemulsion research expanded to include other types of oils, the term equivalent alkane number (EACN) was coined. Originally, EACN values were based on matching interfacial tension minima. An oil is said to be equivalent to an alkane that produces an interfacial tension minimum under the same conditions as the oil. However, equivalent does not mean that the oil of interest and its equivalent alkane behave identically. The EACN is used to provide a point of reference and has proven to be very useful.

In many hydrocarbon/water/surfactant/electrolyte systems examined, additives were often required to prevent the precipitation of the surfactant or the formation of gels. The most common additives were alcohols and secondary surfactants. The role of the alcohol was traditionally discussed in terms of its distribution within the regions of the microemulsion systems. Alcohols are known to be amphiphilic in nature, and because of

this amphiphilic nature a portion of the alcohol molecules will be located at the interface between the oil-rich phase and the surfactant-rich phase. The alcohol molecules will be oriented with their polar groups located between the ionic groups of the surfactant molecules and nearby water molecules and with their hydrocarbon groups located among the hydrocarbon groups of the surfactant. The remaining portion of the alcohol is distributed between the oil- and water-rich phases with the distribution into each phase depending on the hydrophilic/amphiphilic and lipophilic characters of the alcohol (Bourrel and Schecter 1988).

Kahlweit et al. (1991) proposed that alcohols should be considered as cosolvents rather than cosurfactants. It was stated that as cosurfactants alcohols were considered to act mainly on the properties of the interfacial layer, but viewing alcohols as cosolvents that distribute between the water- and oil-rich bulk phases serves to emphasize the role of the alcohol in decreasing the effective hydrophilicity of the amphiphile and the effective hydrophobicity of the oil. The distribution of the alcohol depends heavily on the carbon number of the alcohol and on the carbon number of the oil. Alcohols that are heavily concentrated in the water-rich phase serve to make the components in that phase more hydrophilic; while alcohols that tend to concentrate in the oil-rich phase produce an oil/alcohol mixture that is less hydrophobic than the pure oil. Because the alcohol is partially miscible with water, the alcohol also serves to make the water phase components less hydrophilic.

Kahlweit et al. (1995) reported the results of creating microemulsions of an anionic surfactant at fixed temperature, oil, and brine using alkyl poly (glycol ethers). The microemulsion formulation with ionic surfactants was accomplished using so-called

lipophilic scans. This procedure involves using a sufficiently lipophilic ionic surfactant and varying its effective lipophilicity by mixing it with either a less lipophilic or more lipophilic medium chain alcohol in order to affect the hydrophobicity of the system.

The concept of changing the hydrophobicity of the oil has also been addressed with the concept of lipophilic linkers (Graciaa et al, 1993a). A lipophilic linker was defined as an amphiphilic substance with a small hydrophilic group and a large hydrophobic group; such a substance would have an overall hydrophilic-lipophilic balance (HLB) that is very low. The HLB method was developed to relate the balance between the hydrophilic and lipophilic portions of the surfactant to the emulsification behavior of the surfactant. The HLB-value has served as one basis of comparison between surfactants.

Lipophilic linkers are located in the oil phase near the oil/water interface rendering the oil phase at the interface more polar than the bulk oil phase and are oriented perpendicular to the oil/water interface with their hydrophilic groups directed toward the interface. This perpendicular positioning of the linker molecules forces the neighboring oil molecules to be more ordered which results in enhanced interactions between neighboring oil molecules and between the surfactant and oil molecules. This orientation is shown in Figure 2-2. The examination of alcohols (Graciaa et al, 1993b) as lipophilic linkers led to the conclusion that long chain alcohols (above C8) do act as lipophilic linkers while shorter chain alcohols act as cosurfactants. It was also pointed out that an increase in either the lipophilic linker concentration or the lipophilicity of the linker would result in an increase in the orientation in the oil layer next to the interface with a resultant increase in solubilization.

2.2.2 Solubilization

The formulation of microemulsion systems has had as its focus the improved solubilization of compounds by a surfactant system. Compounds that show very low solubilities in aqueous solutions are known to have greater solubilities in solutions containing surfactants. In developing a suitable microemulsion system the solubilization capacity of the system must be considered. Reed and Healy (1977) defined the solubilization parameters as:

$$SP_O = V_O/V_S \tag{2-1}$$

$$SP_W = V_W/V_S \tag{2-2}$$

Where SP_O and SP_W are solubilization parameters for oil and water, respectively; V_O and V_W are volumes of oil and water, respectively, solubilized in the micellar solution; and V_S is the volume of surfactant in the micellar solution, excluding the alcohol volume (if an alcohol is present). This definition makes sense for nonionic surfactants that are liquid at room temperature but is awkward to apply to many ionic surfactants.

A modified solubilization parameter was used in this study. The solubilization parameter is defined per unit mass of surfactant rather than per unit volume, as follows:

$$SP_O = V_O/M_S \tag{2-3}$$

$$SP_W = V_W/M_S \tag{2-4}$$

Where M_S is the total mass (grams) of surfactant(s) present. In this definition the mass of any alcohol present is excluded in the calculation of M_S. However, the masses of any co-surfactants are included (Wu, 1996).

As the system undergoes the I-III-II transition there is a corresponding change in the solubilization parameters, SP_O and SP_W. Curves of these parameters intersect inside

the three-phase domain at a point where equal amounts of oil and water are solubilized i.e. $SP_O=SP_W$. The corresponding solubilization parameter is denoted as the optimum solubilization parameter, SP*, and the salinity at this point as the optimum salinity, s*.

Since the alkyldiphenyl oxide disulfonates used in this study were known to be mixtures of isomers, the initial premise for this research was that the presence of the dialkyl monosulfonate components might make these mixtures lipophilic enough to undergo the I-III-II transition without the addition of alcohol or other additives. The ability to formulate microemulsions without additives would make such a surfactant system a more viable candidate for use in subsurface remediation. The interest in these surfactants arose from their high hardness tolerances and low adsorptions that make them suitable for subsurface remediation. Based on this premise, the initial microemulsion research evaluated the phase behavior of many systems containing alkyldiphenyl oxide disulfonate surfactants with several types of oils. The final part of this research was based on the concepts proposed by Salager and Kahlweit with a focus on the development of alcohol-free microemulsions by varying the hydrophilicity of the oil phase through the addition of a long chain organic acid.

Kahlweit (1995) summarized procedures for systematically searching for appropriate amphiphiles to form microemulsions based on a distribution coefficient K_C. Where $K_C=c_B/c_A$, and the terms c_A and c_B are the amounts of amphiphile in the oil and water phases, respectively. The alkyldiphenyl oxide disulfonates used in the current study are more soluble in water than in oil, i.e. $K_C \ll 1$. In an attempt to shift this ratio such that $K_C \gg 1$, a long-chain organic acid was chosen. Selection of the specific acid used was based on the HLB values of the surfactant and of the acid.

Although the emphasis of the Kahlweit (1995) work was the preparation of microemulsions at fixed temperature, oil carbon number, and electrolyte concentration, relationships between temperature, electrolyte concentration, and K_C for ionic surfactant systems were discussed. One such relationship was between temperature (T) and electrolyte concentration in the brine [$\varepsilon \equiv$ salt/(salt + H_2O)]. At fixed oil and amphiphile, the amount of salt required for traversing the three-phase interval ($\Delta\varepsilon$) increases with decreasing K_C. Hence, on a T-ε plot, $\Delta\varepsilon$ shapes a cusp that ascends and widens for ionic amphiphiles (Figure 2-3). For a given oil and temperature, the amount of salt required decreases with increasing lipophilicity of the amphiphile, which makes the cusp in Figure 2-3 move to the left.

Several of the alkyldiphenyl oxide sulfonate surfactants are known for their low surface sorption, low precipitation potential, and strong electrolyte resistance which are favorable characteristics for many applications including groundwater remediation. Their most notable drawback is the relatively low solubilization enhancement for hydrophobic non-aqueous phase liquids (Carter et al., 1998). Middle phase microemulsions formulated with these surfactants required the use of additives (cosurfactants and isobutanol) due to their highly hydrophilic nature (Carter et al., 1998 and Wu, 1996). In light of the concepts proposed by Salager and Kahlweit, it was felt that it was worthwhile to re-examine the formulation of alcohol-free microemulsions using the alkyldiphenyl oxide disulfonate surfactants. The use of alcohols in microemulsion formulations has long been a concern. In many applications such as environmental remediation the use of alcohols is undesirable. There are concerns about special precautions and equipment required for flammable substances and more importantly the inability of separating the alcohol from the

contaminant in order to recycle the alcohol. There are also difficulties that arise with not being allowed to discharge any alcohol into municipal waste systems. Therefore, the development of alcohol-free microemulsions would greatly enhance the scope of environmental applications for the alkyldiphenyl oxide disulfonate surfactants and offer insight into the microemulsion formulation of other highly water soluble surfactants.

2.3 Materials

2.3.1 Salinity Scans

Salinity scans were conducted with alkyldiphenyl oxide mono and disulfonate surfactants listed under the trade name of DOWFAX™ Surfactants provided by Dow Chemical Co., Midland, MI. The specific surfactants used for the salinity scans consisted of C10 MADS, C12 MADS, C16 MADS and C10 DADS, and C10 MAMS. Additives included dioctyl sulfosuccinates (Aerosol OT, AOT) and sec-butanol both purchased from Fisher Scientific. Sodium chloride (NaCl), ACS grade, was purchased from Fisher Scientific and used without further purification. The hydrocarbons used were pentane, heptane, hexane, octane, dodecane, orthodichlorobenzene (ODCB), and perchloroethylene (PCE). Each of the hydrocarbons was purchased from Sigma and used as is. Deionized water was manufactured in-house.

2.3.2 Modified Lipophilic Scans

Preparation of microemulsions using a modification of the lipophilic scanning technique described by Kahlweit (1995) used DOWFAX™ 8390, a commercial surfactant which is approximately 35% active. The surfactant is a mixture of 15-35 w/w% C16

MADS and 5-10 w/w% C16 DADS (Material Safety Data Sheet: 001177). Perchloroethylene (PCE), ACS grade, was purchased from Aldrich Chemical Company. Octanoic acid, ACS grade, was purchased from Aldrich Chemical Company. Anhydrous calcium chloride ($CaCl_2$), desiccant grade, was purchased from Fisher Scientific. Magnesium chloride, hexa-hydrate ($MgCl_2 \cdot 6H_2O$), ACS grade, was purchased from J.T. Baker Inc.

2.4 Experimental

2.4.1 Salinity Scans

Salinity scans were conducted at room temperature. The systems were prepared in 15 ml test tubes by weighing in each component. When all components had been added, the test tubes were closed with screw-top caps and gently inverted several times to insure thorough mixing then allowed to equilibrate. Visual examination was used to determine the type of system formed. The desired mass of each component was determined by spreadsheet calculations that were based on designating a weight percent of surfactant plus co-surfactant (if a co-surfactant was used) and calculating the needed amount of the other components for a given range of electrolyte weight percents. Calculations were based on a water-to-oil ratio (WOR) of 1, and the equations used for several of the systems are provided in Appendix 2A.

2.4.2 Modified Lipophilic Scans

The modified lipophilic systems were prepared in 15 ml graduated test tubes using a WOR=1. The water phase consisted of water and the commercial mixture of C16

MADS and C16 DADS, and the oil phase contained PCE and octanoic acid. Octanoic acid was weighed-in relative to the surfactant into the tubes. PCE was added to make the oil volume 5 ml and then 5ml of the aqueous surfactant solution was added. Solid electrolyte was added to the system until the I-III-II or I-IV-II transition was complete or until a gel formed. The test tubes were shaken by hand until the solutions were homogeneous then allowed to equilibrate. The weight ratios of surfactant to octanoic acid were 0.86 or 1.15. The weight ratio of surfactant to additive is commonly referred to as the R-ratio, and this designation will be used in the following discussion. Systems were prepared with either calcium chloride alone or an equal molar ratio of magnesium chloride hexa-hydrate and calcium chloride. All systems prepared were observed at room temperature, 35°C and 45°C with the type of systems formed being determined by visual inspection.

Several computational errors were found in the in the original results reported by Ms Aowiriyakul. Appendix 2D contains the masses/volumes she had recorded in her thesis (Aowiriyakul, 1998) and corrected values for concentrations, overall weight percents, relative volumes, and solubilization parameters.

2.5 Results and Discussion

2.5.1 Traditional Salinity Scans

Traditional salinity scans were conducted using the individual mono and di-alkyldiphenyl oxide mono and disulfonate surfactants with alkanes and chlorinated hydrocarbons as the oil phases. The range of concentrations and details of the results of the visual examinations of the individual systems are provided in Appendices 2B and 2C.

2.5.1.1 Alkanes

Salinity scans were conducted using various alkanes as the oil phase. The MADS components remained Winsor type I even when the system was saturated with sodium chloride. The exceptions were a few of the systems made with some of the C16 MADS and a few of the systems containing sec-butanol.

The systems prepared with the DADS components and alkanes did produce type III's with two notable features. All of the type III's were below optimum (i.e. the middle phase contained more water than oil), and all of the systems exhibited complex phase behavior, primarily gels and precipitates. A typical phase diagram for these systems is shown in Figure 2-4.

The implication of the type III's below optimum is that the system is just above the I/III transition i.e. at a salt concentration below that needed to form an optimum type III in which equal parts of oil and water are solubilized within the type III layer. The position of the type III remained close to the I/III transition even in systems saturated with sodium chloride. This behavior of the DADS components lead to the conclusion that the DADS were too hydrophilic to form optimum systems with alkanes comprising the oil phase, and that they might perform better with chlorinated hydrocarbons as the oil phase since the chlorinated hydrocarbons would be better solvents. When the C10 DADS/octane systems were heated to 60°C for 24 hours, all of the precipitate dissolved; but there remained droplets of unknown composition clinging to the test tube wall near the octane layer. Upon cooling to room temperature, some precipitate reformed; but not to the degree originally present.

2.5.1.2 Chlorinated Hydrocarbons

After it became apparent that optimum formulations were not going to be possible using alkanes as the oil phase, the behavior of the components with chlorinated hydrocarbons was examined. The chlorocarbon research focused on the MADS and DADS components. The MAMS and DAMS were not studied because of their tendency to form gels and precipitates. As with the alkanes, the MADS/chlorocarbon systems resulted in only type I systems, but the DADS component, however, yielded some type III's. An important difference between the chlorocarbon and alkane scans for the DADS is the type III's exhibited significantly less complex behavior. Another notable difference in the DADS systems was the "cleaner" behavior of the C12 DADS versus either the C10 or C16 DADS, i.e. the C12 systems showed less complex phases than either the C10 or C16 systems.

2.5.2 Modified Lipophilic Scans

2.5.2.1 Modified Lipophilic Scan: Salinity Scans

As stated in Section 2.3.2, electrolyte was added until the I-III-II or the I-IV-II transition was complete or a gel had formed. Although the continuous addition of electrolyte changes the WOR, this change from WOR=1 was ignored. The maximum amount of electrolyte added resulted in a volume increase of 0.6 mL that resulted in a WOR increase to 1.12. For the following discussion surfactant refers to the commercial surfactant mixture (DOWFAX™ 8390) plus octanoic acid, all weight percents are reported as overall weight percents unless stated otherwise, and the WOR values are based on values determined before any electrolyte was added.

Initial studies were conducted at 24°C using $CaCl_2$ as the electrolyte and a surfactant to octanoic acid ratio of 0.86. Surfactant concentrations ranged from 4.33 to 38.47%. At the lower surfactant concentrations (4.33–25.82%) the systems underwent the I-III-II transition with gels present in the type II region. At surfactant concentrations above 25.82% the transitions were I-IV-II with no gel formation in the type II region. A plot of the phase boundaries for this system is shown in Figure 2-5. Also shown is the value of (S+A)* which is the minimum amount in weight percent of (surfactant+octanoic acid) required to produce a type IV microemulsion. The open circles lying in the center of the type III region of the phase diagram indicate an estimate for the optimum condition for each (S+A). These midpoints indicate the location at which equal volumes of PCE and water are solubilized in the middle phase region. The accuracy of these estimates will be discussed in Section 2.5.2.3.

Note also that the phase diagram has the same rotated appearance as is seen in systems containing alcohol. For systems containing alcohol the rotated appearance is due to the increase in the interfacial alcohol concentration arising from an increase in the surfactant+alcohol concentration while the surfactant to alcohol ratio is held constant. This increased alcohol concentration increases the surfactant-oil interaction at the expense of the surfactant-water interaction, a condition which favors the I/III transition (Bourrel and Schecter, 1988). This same situation arises in the current study: as the concentration of surfactant+octanoic acid is increased, while holding their ratio constant, the concentration of octanoic acid at the interface increases.

In an attempt to eliminate the gel formation seen in the system shown in Figure 2-5, the surfactant to octanoic acid ratio was increased to 1.15. This rendered the system

less hydrophobic, requiring a greater electrolyte concentration to force the surfactant to transition from one type to another. For example at R=0.86, the system containing 400 mM alkyldiphenyl oxide disulfonate required 4.83% $CaCl_2$ to transition from type I to type III while at R=1.15, 6.18% $CaCl_2$ was required. Similar increases were seen at the other surfactant concentrations. Unfortunately, the change in the alkyldiphenyl oxide disulfonate to octanoic acid ratio did not eliminate the gel formation. Gels were present in the type II region for surfactant concentrations less than 21%. Increasing R to 1.15 did lower the surfactant concentration required for type IV formation from 28.5 to 25.3%.

In a further attempt to avoid gel formation in the type II region, a mixed electrolyte was used. Equal molar amounts of $CaCl_2$ and magnesium chloride hexahydrate ($MgCl_2 \cdot 6H_2O$) were used. It was found that the amount of mixed electrolyte needed to force a transition from type I to type III for both R=0.86 and R=1.15 was much greater than the single electrolyte system. At 24% surfactant and R=0.86, only 4.83% $CaCl_2$ was required in the single electrolyte system, while at the same conditions 9.21% $CaCl_2$+$MgCl_2 \cdot 6H_2O$ was required to transition from type I to type III. On a water-free basis ($CaCl_2$+$MgCl_2$) the overall weight percent was 6.05% which is still greater than for the single electrolyte system.

2.5.2.2 Modified Lipophilic Scans: Temperature Studies

The same systems that were prepared and examined at 24°C were examined at 35° and 45°C. The relative volumes of the middle phases decreased slightly upon heating to 35°C. Upon heating to 45°C there was either a small decrease or no change seen in the relative volume of the middle phase compared to the volumes seen at 35°C. The increase

in temperature extended the surfactant concentrations at which the systems existed as type III's; i.e. type IV's did not form until higher surfactant concentrations were attained. For example, for the R=0.86, $CaCl_2$ system, a type IV formed at 28.5% surfactant at 24°C while at 35 and 45°C the type IV did not form until the surfactant concentration was 38.4%. The affect of temperature on the position of the phase boundaries is shown in Figure 2-6.

The amount of electrolyte required to produce a type III was reduced by about 10% in all systems while the amount of $CaCl_2$ required to produce a type IV increased slightly at the higher temperatures. This is not in complete agreement with the conclusions reached by Kahlweit (1995). According to Kahlweit at fixed oil and amphiphile concentrations the amount of electrolyte required to traverse the three-phase region increases with increasing temperature as shown in Figure 2-3. It can also be seen from this figure that the amount of salt needed to produce the I-III transition increases and that the width of the type III region increases slightly with increasing temperature for ionic surfactants. As seen in Figure 2-6, the alkyldiphenyl oxide disulfonate-octanoic acid systems do not completely follow this behavior. While the width of the type III region does increase with increasing temperature, it does so with a decreasing electrolyte concentration. This relationship is shown schematically in Figure 2-7. For a given surfactant concentration, ε (the fraction of electrolyte in the brine required to form a type III) decreases with increasing temperature. The boundaries shown in Figure 2-6 are merely suggestive. As will be discussed in the following section, there is the distinct possibility that the exact locations of the I/III and III/II boundaries were not accurately determined. This is even more of a possibility at the elevated temperatures since no

additional systems were prepared at electrolyte concentrations other than those for the 24°C study. Since the locations of these borders are the basis of this discussion, the accuracy in knowing these locations is imperative.

Another point that must be considered is the effect of the octanoic acid on the phase behavior of this system. Studies to determine the role of the octanoic acid would include creating systems of the same compositions with careful attention paid to accurately locating the phase transitions. Creating systems using carboxylic acids of different carbon lengths would be suggested.

2.5.2.3 Modified Lipophilic Scans: Solubilization

The preparation of the middle phase microemulsions without the use of an alcohol was very promising, but the usefulness of such systems is determined by the degree of increased solubilization over other micellar systems if any such increase exists. After the microemulsion systems were prepared, the solubilization parameters were determined when possible. In many solutions the presence of gels and other complex phase behavior prevented the solubilization parameters from being calculated. The following discussion is based on the results for all surfactant concentrations from the $CaCl_2$, R=0.86 at 24, 35, and 45°C data; and for alkyldiphenyl oxide disulfonate concentrations 440 mM and greater at all temperatures for $CaCl_2$, R=1.15; and $MgCl_2 \cdot 6H_2O + CaCl_2$, R=0.86 and R=1.15. The data and calculated values for this discussion are shown in Appendix 2D-VII through 2D-XXII.

Using the definitions of optimum as presented in Section 2.1.2, it was found for the $CaCl_2$ at R=0.86, 24°C that as the surfactant concentration increased, the optimum

salinity (s*) decreased. This would be expected from the rotation apparent in the phase diagram shown in Figure 2-5. For this same system at 24°C the optimum solubilization parameter (SP*) decreased from 3.09 mL/g at 440 mM alkyldiphenyl oxide disulfonate to 2.25 mL/g at 220 mM and then increased to 3.08 mL/g at 80 mM. This trend was not seen at 35°C, but was seen to a lesser extent at 45°C. For the electrolyte systems studied there was a small, but noticeable, decrease in SP* with increasing temperature. This behavior can be attributed to the affect of increasing temperature on ionic surfactants. As the temperature increases, the interaction per unit area of interface decreases because the area occupied per surfactant molecule increases. This is due primarily to a decrease in restriction of the movement of water molecules in the presence of a hydrocarbon or any apolar compound (hydrophobic effect) that reduces the adsorption driving force and the solvency in correspondingly reduced. As a consequence, the solubilization at optimum is expected to decrease, (Bourrel and Schecter, 1988).

Changing the electrolyte to $MgCl_2 \cdot 6H_2O + CaCl_2$ had little affect on the values of SP* when compared to those seen in the $CaCl_2$ systems. Although there are only a few data points to compare, it is interesting to note that the values of s* (grams) for the $CaCl_2$ systems are approximately half of the values of s* seen for the $MgCl_2 \cdot 6H_2O + CaCl_2$ systems at R=1.15. Basing the comparison on the normalities of s* for the mixed electrolyte systems on a water-free basis and for the $CaCl_2$ systems does not greatly change this relationship. See the data in Appendix 2D.

For the $CaCl_2$, R=0.86, 24°C, the optimum value of s* at each surfactant concentration estimated from the phase boundary diagram shown in Figure 2-5 are

compared to those calculated based on the solubilization parameters. The values are shown in Table 2-1.

Table 2-1 Comparison of values determined for s*.

Concentration of (S+A) weight %	Estimate of s* from phase boundary (gram/liter)	Estimate of s* from solubilization parameters
3.89	1.38	1.45
5.9	1.36	1.40
11.2	1.19	1.12
14.7	1.09	0.974
18.3	0.993	0.80
24.4	0.684	0.748

The different values of s* obtained from the phase boundary diagram indicate that the exact locations of the I/III, I/IV, III/II and IV/II boundaries were not seen at the electrolyte concentrations used in this study. The gap between successive electrolyte concentrations is not so large as to affect the preceding discussion on the results of modified lipophilic scan portion of this study.

2.6 Conclusions

From the traditional salinity scan studies several conclusions could be reached about the alkyldiphenyl oxide disulfonate surfactants studied. In order to form a type III, the alkane chain length must be shorter than the surfactant chain length. This is true for the systems studied using the traditional salinity scans, but is not necessarily true for all microemulsion systems. Refer to the discussion of alkane carbon numbers in Bourrel and Schecter (1988, Chapter 6). Based on the number of times gels and precipitates were observed, it was determined that the presence of the low water soluble impurities such as DAMS and to some extent DADS led to the undesirable phase behavior. Cleaner systems were observed in those systems containing higher concentrations of highly water soluble

impurities such as the MADS. The inability of completing the I/III/II transition indicated the necessity of lowering either the hydrophilicity of the surfactant or lowering the hydrophobicity of the oil.

Lowering the hydrophobicity of the oil was accomplished by the addition of the oil soluble octanoic acid. The addition of this lipophilic linker facilitated the ability of the commercial mixture of C16 MADS and C16 DADS to undergo the I-III-II transition. The formation of Type IV systems was also accomplished. This had not been achieved in previous research with these surfactants. Unfortunately, the gels seen in the traditional salinity scans were not eliminated by the addition of octanoic acid. It is possible that the solubility of the DADS component of the surfactant was exceeded. No separate study was performed examining the solubility of the octanoic acid alone under the same conditions of the surfactant/octanoic acid systems. Perhaps using a lipophilic linker with a different HLB would prevent the gel formation. Using other surfactants from this suite would also shed light on the exact component responsible for the gel formation. The C10 and C12 MADS are known to more water soluble than the C16, and it may be possible to use octanoic acid with either of these to further investigate the gel formation in mono and di-alkyldiphenyl oxide mono and di-sulfonate surfactants. The concept of lipophilic linkers should allow for microemulsion formulations using compounds that to date have not been able to form such systems.

2.7 References

Aowiriyakul, S., Thesis, Chulalongkorn University, Bangkok, Thailand, 1998.

Bourrel, M. and Schecter, R. S. Microemulsions and Related Systems Formulation, Solvency and Physical Properties, Marcel Dekker, New York, N. Y., 1988.

Carter, T.; Wu, B.; Sabatini, D. A.; Harwell, J. H. Increasing the Solubility Enhancement of Anionic DOWFAX Surfactants. *Sep Sci Tech.* **1998**, 33(15), pp 2363-2377.

Graciaa, A.; Lachaise, J.; Cucuphat, C.; Bourrel, M.; Salager, J. L. Improving Solubilization in Microemulsions with Additives. 1. The Lipophilic Linker Role. *Langmuir*, **1993a**, 9(3), pp 669-672.

Graciaa, A.; Lachaise, J.; Cucuphat, C.; Bourrel, M.; Salager, J. L. Improving Solubilization in Microemulsions with Additives. 2. Long Chain alcohols as Lipophilic Linkers. *Langmuir*, **1993b**, 9(12), pp 3371-3374.

Kahlweit, M. How To Prepare Microemulsions at Prescribed Temperature, Oil and Brine. *J Phys Chem.* **1995**, 99(4), pp 1281-1284.

Kahlweit, M.; Strey, R.; Busse, G. Effect of Alcohols on the Phase Behavior of Microemulsions. *J. Phys. Chem.* 1991, 95(13), pp 5344-5352.

Kahlweit, M.; Strey, R. Phase Behavior of Ternary Systems of the Type H_2O – Oil – Nonionic Amphiphile (Microemulsions). *Angew Chem Int Ed Engl.* **1985**, 24, pp 654-668.

Material Safety Data Sheet: 001177, effective date: 10/02/92, Dow Chemical U.S.A., Midland, MI 48674.

Reed, R. L.; Healy, R. N. In Improved Oil Recovery by Surfactant and Polymer Flooding, D. O. Shah; R. S. Schecter eds., Academic Press, New York, 1977.

Wu, B.; Harwell, J. H.; Sabatini, D. A.; Bailey, J. D. Alcohol-Free Diphenyloxide Disulfonate (DPDS) Middle Phase Microemulsion Systems. *JSD*, **2000**, 3, pp 465-474.

Wu, B. Thesis, University of Oklahoma, Norman, OK, 1996.

2.8 - Figures

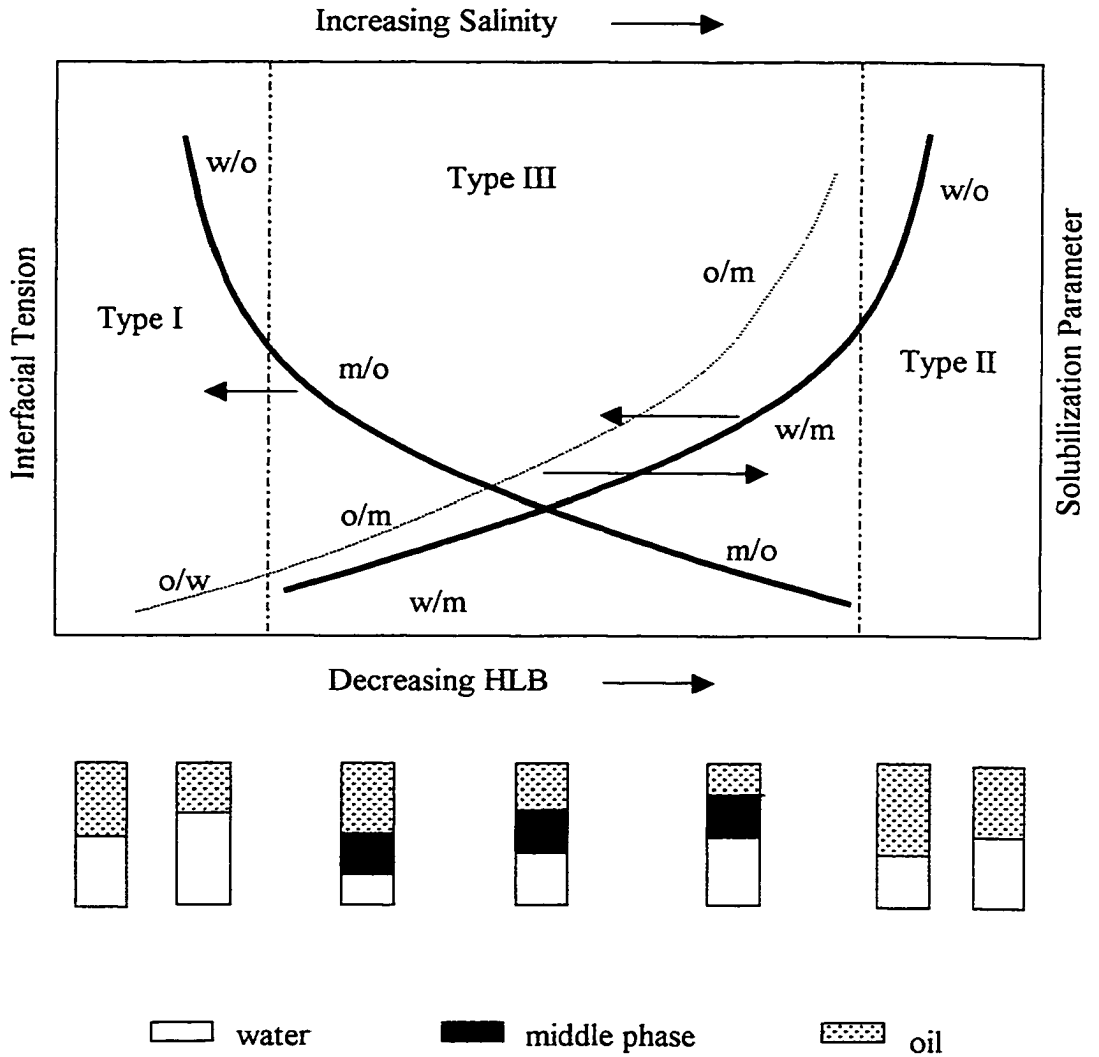

Figure 2-1 Relationships between phase behavior, interfacial tension, and solubilization parameter (Wu et al, 2000).

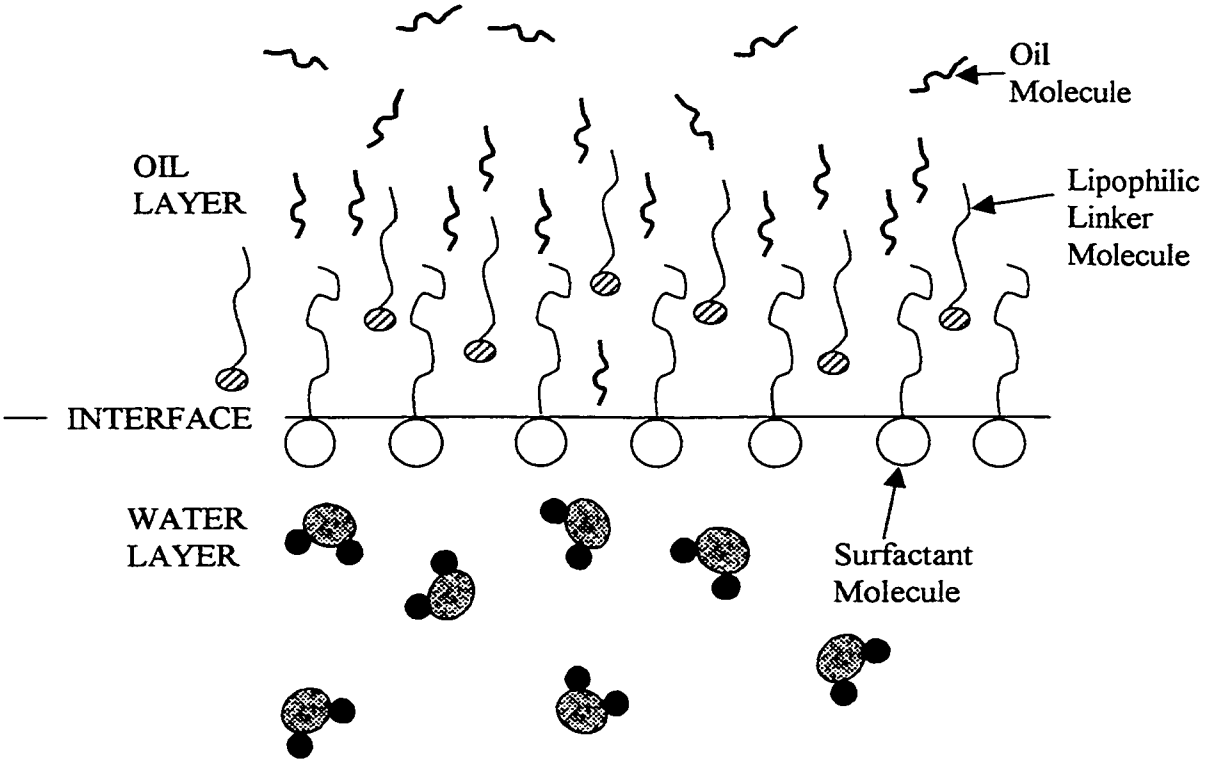

Figure 2-2 Orientation of molecules located at the oil-water interface due to the presence of lipophilic linker molecules.

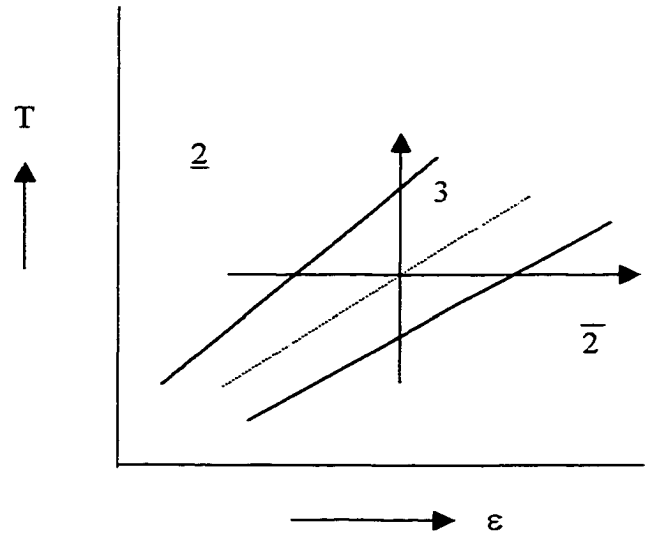

Figure 2-3 Schematic of salting out of ionic amphiphiles: T-ε for ionic amphiphiles (Kahlweit, 1995).
The numerals indicate the number of phases present with 2 indicating an oil-in-water emulsion and the line overhead indicating an water-oil-emulsion

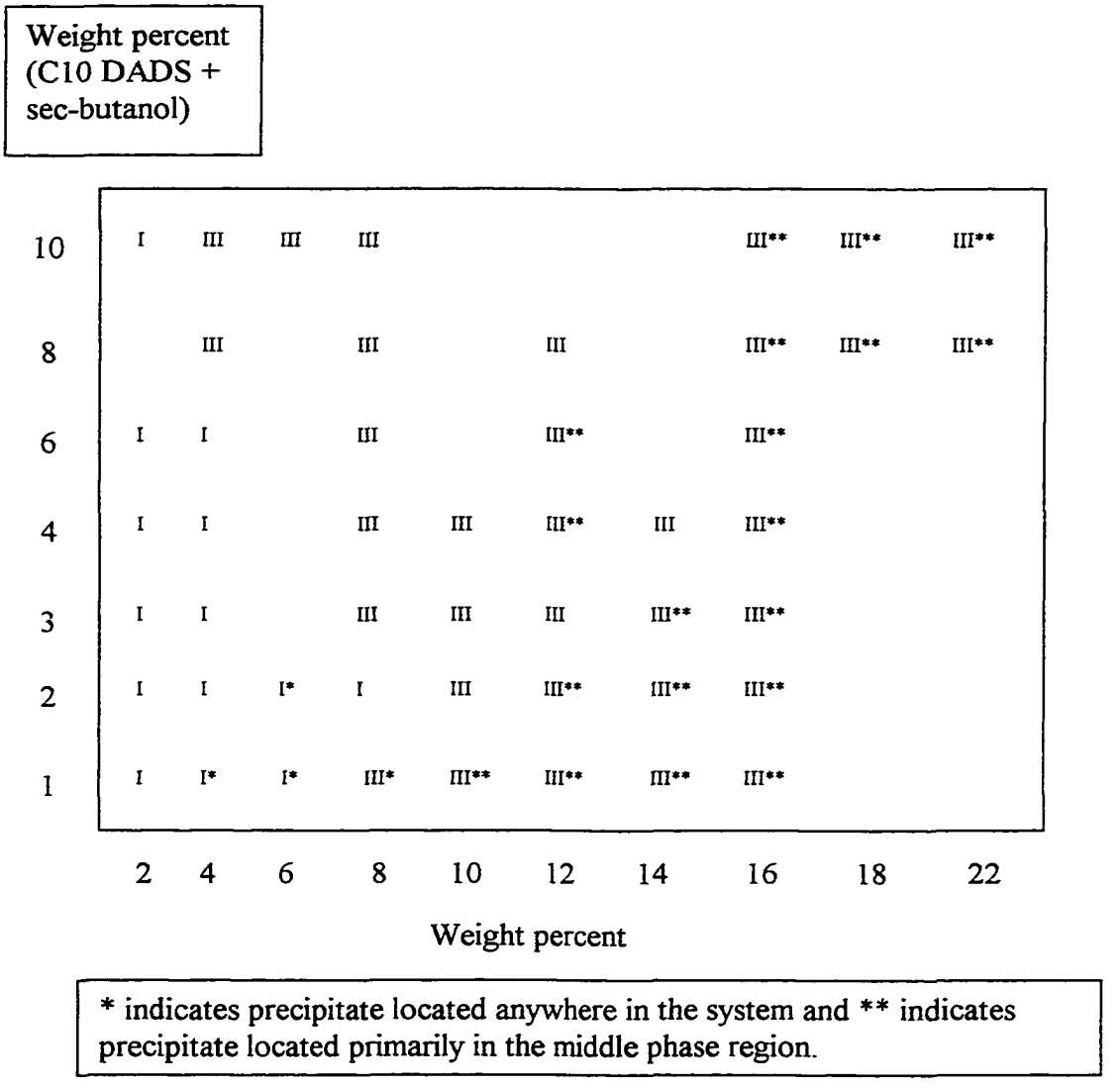

Figure 2-4 Phase behavior seen in traditional salinity scan of C10 DADS + sec-butanol/ heptane, R=0.67, 24°C.

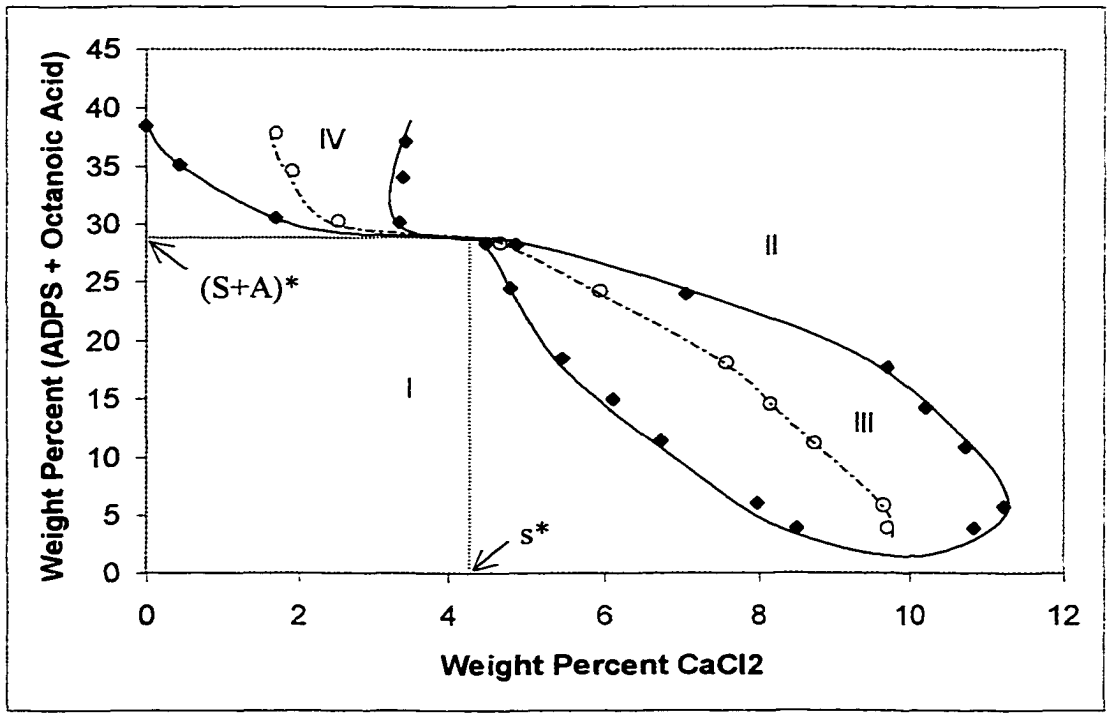

Figure 2-5 Phase diagram of alkyldiphenyl oxide disulfonate/octanoic acid/PCE for R=0.86 at 24 °C.

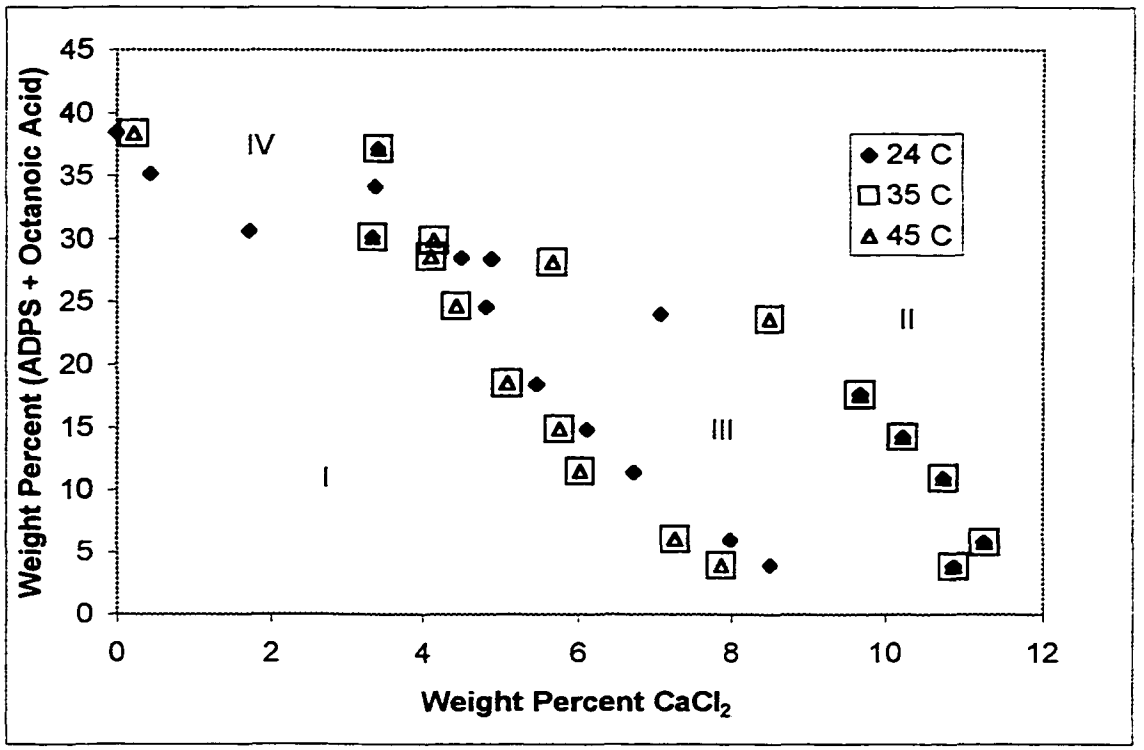

Figure 2-6 Phase diagram of alkyldiphenyl oxide disulfonate/octanoic acid/PCE for R=0.86 at 24, 35 and 45 °C.

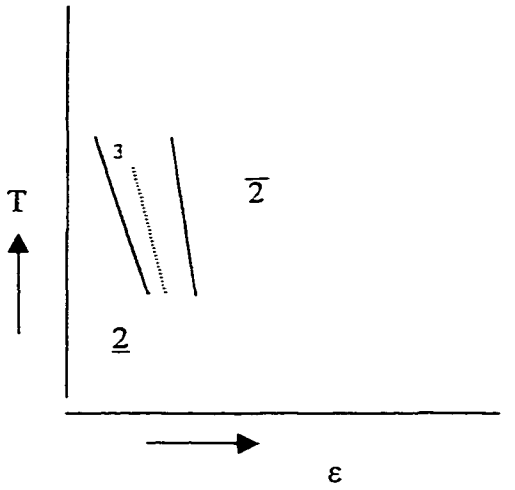

Figure 2-7 Schematic of salting out of alkyldiphenyl oxide mono- disulfonate + octanoic acid systems.

2A Appendix: Equations used for Preparing Systems for Salinity Scans

Note: The equations in the following appendices were solved for the masses needed to prepare the systems for salinity scans. The equations are based on the solubility of each component, physical state (i.e. solid or liquid), and the presence or absence of a co-surfactant. A sample spreadsheet is included to illustrate the recipes that were generated for these scans. The spreadsheets were arranged such that the surfactant to co-surfactant ratio and the range of weight percents of electrolyte were specified and the amounts (mass) of each component were calculated. The limit on how many systems could be created for a given set of conditions was indicated when one of the variable masses became negative.

The variables used in the following equations are defined as follows:

M_T = total mass of the system
W = mass of the electrolyte
V = mass of the oil
Y = mass of the surfactant
H = mass of the cosurfactant
Z = mass of water
FS = weight fraction of the surfactant
FN = weight fraction of the electrolyte
SSR = surfactant to co-surfactant ratio
ρ = density

2A.1 System: Solid electrolyte - water soluble liquid surfactant

The following set of equations was solved for Y and W for systems formulated with a total of 6 ml (3 ml of the water phase and 3 ml of the oil phase).

$$M_T = V\rho_{oil} + W + Y\rho_{surf} + Z\rho_{H2O}$$

$$FS = Y\rho_{surf} * \frac{gr.surf}{gr.sltn} / M_T$$

$$FN = {}^{W}\!/_{M_T}$$

$$3 = Y + {}^{W}\!/_{\rho_{NaCl}} + Z$$

Solving these equations for Y and W produces the following solutions:

$$Y = \frac{\left(V\rho_{oil} + 3\rho_{H2O} + W\left(1 - \frac{\rho_{h2O}}{\rho_{NaCl}}\right)\right)}{\left(\frac{1}{FS}\rho_{surf} * \frac{gr.surf}{gr.sltn} + \rho_{H2O} - \rho_{surf}\right)}$$

$$W = \frac{V\rho_{oil} + 3\rho_{H2O} + \left(\rho_{surf} - \rho_{H2O}\right)\left[\frac{V\rho_{oil} + 3\rho_{H2O}}{\frac{1}{FS}\rho_{surf} * \frac{gr.surf}{gr.sltn} + \rho_{H2O} - \rho_{surf}}\right]}{\frac{1}{FN} - \left(1 - \frac{\rho_{H2O}}{\rho_{NaCl}}\right) - \left(\frac{\left(\rho_{surf} - \rho_{H2O}\right)\left(1 - \frac{\rho_{H2O}}{\rho_{NaCl}}\right)}{\frac{1}{FS}\rho_{surf} * \frac{gr.surf}{gr.sltn} + \rho_{H2O} - \rho_{surf}}\right)}$$

2A.2 System: Liquid electrolyte – water soluble liquid surfactant

The following equations were solved for Y and W. Assuming 10 ml systems with 5 ml each for the oil and water phases.

$$M_T = V\rho_{oil} + W\rho_{NaCl} + Y\rho_{surf} + Z\rho_{H2O}$$

$$FS = \frac{Y\rho_{surf} * \frac{gr.surf}{gr.sltn}}{M_T}$$

$$FN = \frac{W\rho_{NaCl}\frac{gr.NaCl}{gr.sltn}}{M_T}$$

$$5 = Y + W + Z$$

Solving these for Y and W results in the following:

$$Y = \frac{V\rho_{oil} + \left(\rho_{NaCl} - \rho_{H2O}\right)W + 5\rho_{H2O}}{\frac{1}{FS}\rho_{surf} * \frac{gr.surf}{gr.sltn} - \rho_{surf} + \rho_{H2O}}$$

$$W = \frac{V\rho_{oil} + \left(\rho_{surf} - \rho_{H2O}\right)\left[\frac{V\rho_{oil} + 5\rho_{H2O}}{\frac{1}{FS}\rho_{surf}\frac{gr.surf}{gr.sltn} - \rho_{surf} + \rho_{H2O}}\right] + 5\rho_{H2O}}{\frac{1}{FN}\rho_{NaCl}\frac{gr.NaCl}{gr.sltn} - \rho_{NaCl} + \rho_{H2O} - \frac{\left(\rho_{surf} - \rho_{H2O}\right)\left(\rho_{NaCl} - \rho_{H2O}\right)}{\frac{1}{FS}\rho_{surf}\frac{gr.surf}{gr.sltn} - \rho_{surf} + \rho_{H2O}}}$$

2A.3 System: liquid electrolyte - water soluble liquid surfactant - water soluble liquid co-surfactant

The following equations were solved for Y, W and H. Assuming 6 ml systems with 3 ml each for the oil and water phases.

$$M_T = 3\rho_{oil} + Y\rho_{surf} + W\rho_{NaCl} + H\rho_{cosurf} + Z\rho_{H2O}$$

$$FS = \frac{\left(Y\rho_{surf} * \frac{gr.surf}{gr.sltn} + H\rho_{cosurf}\right)}{M_T}$$

$$FN = \frac{W\rho_{NaCl} * \frac{gr.NaCl}{gr.sltn}}{M_T}$$

$$3 = Y + W + H + Z$$

$$SSR = \frac{Y\rho_{surf} * \frac{gr.surf}{gr.sltn}}{H\rho_{cosurf}}$$

Solving for Y, W and H results in the following:

$$Y = \frac{3\rho_{oil} + W\rho_{NaCl} + 3\rho_{H2O} - W\rho_{H2O}}{\frac{1}{FS}\left(\rho_{surf} * \frac{gr.surf}{gr.sltn} + \frac{\rho_{surf} * \frac{gr.surf}{gr.sltn}}{SSR}\right) - \rho_{surf} - \frac{\rho_{surf} * \frac{gr.surf}{gr.sltn}}{SSR} + \rho_{H2O} + \frac{\rho_{surf}\rho_{H2O}\frac{gr.surf}{gr.sltn}}{SSR * \rho_{cosurf}}}$$

$$W = \frac{\left(3\rho_{oil} + 3\rho_{H2O} + \left(3\rho_{oil} + 3\rho_{H2O}\right) * X\right)}{\frac{\rho_{NaCl}\dfrac{gr.NaCl}{gr.sltn}}{FN} - \rho_{NaCl} + \rho_{H2O} + \left(\rho_{H2O} - \rho_{NaCl}\right) * X}$$

Where X is defined as shown below:

$$X = \frac{\rho_{surf} + \rho_{surf} * \dfrac{gr.surf}{gr.sltn} * \dfrac{1}{SSR} - \rho_{H2O} - \rho_{surf}\rho_{H2O} * \dfrac{gr.surf}{gr.sltn} * \dfrac{1}{SSR * \rho_{cosurf}}}{\dfrac{1}{FS}\left(\rho_{surf} * \dfrac{gr.surf}{gr.sltn} + \dfrac{\rho_{surf}}{SSR} * \dfrac{gr.surf}{gr.sltn}\right) - \rho_{surf} - \dfrac{\rho_{surf}}{SSR} * \dfrac{gr.surf}{gr.sltn} + \rho_{H2O} + \dfrac{\rho_{surf}\rho_{H2O}}{SSR * \rho_{cosurf}} * \dfrac{gr.surf}{gr.sltn}}$$

$$H = \frac{Y\rho_{surf}\dfrac{gr.surf}{gr.sltn}}{SSR\ \rho_{cosurf}}$$

2B Appendix: Range of Component Concentrations and Visual Descriptions for Traditional Salinity Scans

2B.1 Alkane Scans

C16 MADS

Octane	2-12% MADS	3-15% NaCl
Decane	2-12% MADS	3-15% NaCl
Dodecane	2-12% MADS	1-15% NaCl

No middle phases, all type I's, but the aqueous/oil interface flattened dramatically with increasing NaCl.

C10 DADS

Heptane	1-3% DADS	2-18% NaCl
Hexane	0.5-3% DADS	2-14% NaCl
Octane	1-3% DADS	2-14% NaCl

Precipitation present in all tubes; formation of gels; precipitates with middle phases. The octane scans were heated to 60° C, and all the precipitates and gels dissolved. Upon cooling to room temperature some of the precipitates reformed, but the gels did not.

C10 DADS/sec-Butanol

Hexane	0.2-3% (S+B)	2-18% NaCl
Heptane	1-4% (S+B)	2-16% NaCl

No gel formation, cleaner middle phases than those in the C10 DADS scans, if precipitate present it tended to form on the top of the middle phase. Heptane for ≥2% (S+B) no precipitate formed.

NOTE: The C10 DADS/sec-butanol results are for a C10 DADS:sec-butanol ratio of 4:6.

C10 DADS/AOT

Heptane	1-7% (S+S)	2-20% NaCl
Hexane	1-7% (S+S)	0-20% NaCl
Octane	3% (S+S)	0-17% NaCl

Middle phase formation at all percentages of (S+S); no gel formation, but precipitate tended to occur within the middle phase not at the two interfaces; precipitation worse at >14% NaCl; Precipitation with hexane worse than with heptane.

NOTE: The C10 DADS/AOT results are for a C10 DADS:AOT ratio of 1:1. Preliminary scans were performed using ratios of 3:1 and 1:2. The 3:1 ratio did not lessen the complex phase behavior exhibited by the C10 DADS scans while the 1:2 ratio did not contain enough of the DADS in order to distinguish the Winsor type.

C10 DADS/sec-Butanol

Heptane	6-10% (S+A)	2-22% NaCl

Tended to from clean type III's at low percentages of NaCl and 10% (S+A); high percentages of NaCl of the 6 and 8% (S+A) formed some precipitates.

C16 MADS

Octane	3% MADS	0-18% NaCl

No middle phases. Clean type I systems.

C12 MADS

Octane	3% MADS	0-18% NaCl

No middle phases. Clean type I systems.

C10 MADS

Octane	3% MADS	0-18% NaCl

No middle phases. Clean type I systems.

C16 MADS/sec-Butanol

Octane	3-8% (S+A)	2-16% NaCl
Decane	3-8% (S+A)	2-16% NaCl

Clean type I systems except 8% (S+A) and 16% NaCl that formed very weak type III's in both alkane scans.

C6 MAMS

Pentane	3 and 5% MAMS	2-16% NaCl
Hexane	3 and 5% MAMS	2-16% NaCl

No middle phases. Type I systems with precipitates and gels in systems containing more than 2% NaCl.

C10 MAMS

Octane	3 and 4% MAMS	2-16% NaCl
Hexane	3 and 5% MAMS	2-16% NaCl

No middle phases. Type I systems with precipitates in all systems.

C10 MAMS/C10 MAMS

Heptane	3 and 4% (S+S)	2-16% NaCl
Octane	3 and 4% (S+S)	2-16% NaCl

Types I and III systems. In all scans precipitates were present and located at the interfaces.

C16 DADS

Octane	4 and 9% DADS	2-14% NaCl
Decane	3 and 4% DADS	2-14% NaCl

Types I and III systems. The type III system formed at 4 and 9% DADS with 2 and 3% NaCl in octane, and for 7% DADS with 3% NaCl in decane. All of the systems exhibited extreme complex phase behavior.

C10 DADS + C10 DAMS

Heptane	1 and 3% (S+S)	2, 8, and 14% NaCl

Types 1 and III and possible a very weak type II. There is some yellow coloration in the heptane as well as the aqueous layer. Gels and/or precipitates in most systems.

C10 DADS

Hexane	0.58 and 1.15% DADS	0.09% DAMS
Heptane	0.58 and 1.07% DADS	0.07 – 0.08% DAMS
Octane	0.57 and 1.09% DADS	0.07 – 0.08% DAMS

No middle phases. Type I systems with organic layers that tended to remain clear while the aqueous layer was either clear or slightly cloudy. In all systems gels were present at the aqueous/oil interface.

2B.2 Chlorinated Hydrocarbon Scans

C10 MADS

ODCB	3% MADS	4-12% NaCl

No middle phases. Type I systems fairly clean, no gels or precipitates.

C12 MADS

ODCB	1 and 3% MADS	0-12% NaCl

No middle phases. Type I systems fairly clean, no gels or precipitates.

C16 MADS

ODCB	1 - 13% MADS	2 - 14% NaCl

No middle phases. Type I systems fairly clean, no gels or precipitates except in the 13% MADS with 10 and 14% NaCl.

C10 DADS

ODCB	0.5 - 3% MADS	0 – 12% NaCl
PCE	0.5 – 1% DADS	0 – 12% NaCl

Precipitation present in all tubes, and gels were present in several. Type III's at most percentages of NaCl.

C12 DADS

ODCB	0.5 - 3% MADS	4 – 12% NaCl
PCE	0.5 – 1% DADS	0 – 12% NaCl

In the ODCB scans, type III's were formed in all systems. At 0.5% DADS the systems were clean, but there was cloudiness and complex behavior in the 1 and 3% DADS scans. For the PCE systems, type III's were also formed in all tubes except for the systems containing 0% NaCl. There was some precipitate in the 1% DADS scans but overall these systems were cleaner than the C10 DADS'

C16 DADS

ODCB	0.5% MADS	0 – 12% NaCl
PCE	0.5% DADS	4 – 12% NaCl

For the ODCB systems there were no middle phases. The type I systems tended to have precipitates or gels present at the aqueous/oil interface. With PCE the systems were all type I except for those containing 8 and 12% NaCl. In the type I system at 4% NaCl there was a large amount of precipitate/gel.

C10 MAMS

ODCB	1 and 3% DADS	0-12% NaCl

No middle phases. The type I systems tended to from precipitate/gels.

2C Appendix: Summary of Traditional Salinity Scan Observations

2C.1 DADS

Alkane systems: Formed type I and type III systems. Gels and/or precipitates in all systems that did not contain a co-surfactant. The addition of a co-surfactant such as sec-butanol or Aerosol OT lessened the undesired phase behavior but did not eliminate it. The DADS were also susceptible to "salt shock".

Chlorocarbon systems: Formed Type I and Type III systems. Gels and/or precipitates in all systems. No co-surfactant scans were performed. The C12 systems were considerably cleaner than either the C10 or the C16 systems.

2C.2 MADS

Alkane systems: Formed Type I systems in systems with no co-surfactant, with the exception of the first shipment of C16 MADS. Neither the C12 nor the C10 formed Type III systems. The interfaces of all of the MADS' systems flattened dramatically with increasing NaCl concentration. In a few of the systems the interface was almost nonexistent. Addition of sec-butanol produced Type I systems except in systems of 8% MADS and 16% NaCl. These two systems were very weak Type III's. No complex phase behavior was seen.

Chlorocarbon systems: Formed Type I systems. Most of the systems contained no gels or precipitates with the exception of the high percentage C16 system.

2C.3 MAMS

Alkane systems: Formed Type I systems with gel and/or precipitated in most systems. In low percentage (2%) NaCl systems Type III systems were formed with gels present. Use as a co-surfactant lessened the complex phase behavior exhibited by the C10 DADS.

Chlorocarbon systems: Formed Type I systems with gels and/or precipitates present. No co-surfactant scans were performed.

2C.4 DAMS

Alkane systems: Attempts to achieve optimum systems without NaCl resulted in Type I systems with gels at the interfaces but no precipitates.

Chlorocarbon systems: No scans were performed.

2D Appendix: Data and Corrected Calculations From the Thesis of Sangaroon Aowiriyakul

Note: Equations used in the following pages:

Preparation of Systems:

g, DFX= mM DFX *mole/1000mmole * 643 g/mole * 5 mL / 1000 mL/L
R = g DFX / g octanoic acid
mL octanoic acid = g octanoic acid / 0.91 g/mL
Total g before salt = 5 g aqueous phase + g octanoic acid + g PCE
Assuming the density of the aqueous phase is 1 mL/cc

Overall weight percents:

Wt% $CaCl_2$ = g $CaCl_2$ / (5 + g PCE + g octanoic acid + g PCE)
Wt% (DFX+octanoic acid) = (g DFX + g octanoic acid) / (5 + g PCE + g octanoic acid + g $CaCl_2$)

Relative Volumes:

Relative lower = lower/upper
Relative middle = (middle – lower) / upper
Relative upper = (upper – next lower interface) / upper

Solubilization Parameters:

Vo = 5 – lower (if lower > 5 left blank)
Vw = Middle – 5 (if middle < 5 left blank) OR
Vw = Lower – 5 (if lower > 5)

Appendices 2D-VIII to 2D-XVIII are arranged by concentration of surfactant.
For concentrations of 80 – 340 mM surfactant, there is data for Part I at 24, 35, 45 °C
For concentrations of 440 – 625 mM surfactant there is data for Parts I, II, III, and IV at 24, 35, 45 °C.

Appendix 2D-I Original data and corrected values for sample preparation for single electrolyte systems

Part I: $CaCl_2$ Scan, R = 0.86

mM DFX	g DFX	g octanoic acid	R	mL octanoic acid	g PCE	total mass before salt
40	0.13	0.15	0.86	0.16	7.85	2.14
80	0.26	0.30	0.86	0.33	7.58	4.33
120	0.39	0.45	0.86	0.49	7.32	6.55
160	0.51	0.60	0.86	0.66	7.05	8.81
220	0.71	0.82	0.86	0.90	6.65	12.25
280	0.90	1.05	0.86	1.15	6.25	15.86
340	1.09	1.27	0.86	1.40	5.85	19.50
440	1.41	1.64	0.86	1.80	5.19	25.82
500	1.61	1.87	0.86	2.05	4.79	29.82
520	1.67	1.94	0.86	2.13	4.65	31.16
580	1.86	2.17	0.86	2.38	4.25	35.33
625	2.01	2.33	0.86	2.56	3.95	38.47

Part II: $CaCl_2$ Scan, R = 1.15

mM DFX	g DFX	g octanoic acid	R	mL octanoic acid	g PCE	total mass before salt
80	0.26	0.22	1.17	0.24	7.72	12.94
120	0.39	0.34	1.13	0.37	7.52	12.86
220	0.71	0.62	1.14	0.68	7.02	12.64
280	0.90	0.78	1.15	0.86	6.72	12.50
340	1.09	0.95	1.15	1.04	6.42	12.37
440	1.41	1.23	1.15	1.35	5.92	12.15
500	1.61	1.40	1.15	1.54	5.62	12.02
520	1.67	1.46	1.15	1.60	5.52	11.98
580	1.86	1.62	1.15	1.78	5.22	11.84
625	2.01	1.75	1.15	1.92	4.99	11.74

Appendix 2D-II Original data and corrected values for sample preparation for mixed electrolyte systems

Part III: $MgCl_2 \cdot 6H_2O$ + $CaCl_2$ Scan, R = 0.86

mM DFX	g DFX	g octanoic acid	R	mL octanoic acid	g PCE	total mass before salt
80	0.26	0.30	0.86	0.33	7.58	12.88
120	0.39	0.45	0.86	0.50	7.32	12.77
220	0.71	0.82	0.86	0.91	6.65	12.47
280	0.90	1.05	0.86	1.17	6.25	12.30
340	1.09	1.27	0.86	1.41	5.85	12.12
440	1.41	1.64	0.86	1.82	5.19	11.83
500	1.61	1.87	0.86	2.08	4.79	11.66
520	1.67	1.94	0.86	2.16	4.65	11.59
580	1.86	2.17	0.86	2.41	4.25	11.42
625	2.01	2.33	0.86	2.59	3.95	11.28

Part IV: $MgCl_2 \cdot 6H_2O$ + $CaCl_2$ Scan, R = 1.15

mM DFX	g DFX	g octanoic acid	R	mL octanoic acid	g PCE	total mass before salt
80	0.26	0.22	1.17	0.24	7.72	12.94
120	0.39	0.34	1.13	0.38	7.52	12.86
220	0.71	0.62	1.14	0.69	7.02	12.64
280	0.90	0.78	1.15	0.87	6.72	12.50
340	1.09	0.95	1.15	1.06	6.42	12.37
440	1.41	1.23	1.15	1.37	5.92	12.15
500	1.61	1.40	1.15	1.56	5.62	12.02
520	1.67	1.46	1.15	1.62	5.52	11.98
580	1.86	1.62	1.15	1.80	5.22	11.84
625	2.01	1.75	1.15	1.94	4.99	11.74

Appendix 2D-III Original data and corrected values for overall weight percents, Part I, $CaCl_2$ scan, R = 0.86

80 mM DFX

g $CaCl_2$	wt% $CaCl_2$	wt% (DFX+octanoic acid)
1.1	7.87	3.99
1.2	8.52	3.96
1.25	8.85	3.94
1.3	9.17	3.93
1.4	9.80	3.90
1.45	10.12	3.89
1.5	10.43	3.87
1.57	10.87	3.86
1.6	11.05	3.85

120 mM DFX

g $CaCl_2$	wt% $CaCl_2$	wt% (DFX+octanoic acid)
1	7.26	6.07
1.1	7.99	6.03
1.2	8.71	5.98
1.25	9.08	5.96
1.3	9.44	5.94
1.4	10.17	5.90
1.5	10.98	5.86
1.55	11.26	5.84
1.6	11.62	5.82

220 mM DFX

g $CaCl_2$	wt% $CaCl_2$	wt% (DFX+octanoic acid)
0.8	6.03	11.51
0.9	6.73	11.42
1	7.42	11.34
1.11	8.11	11.25
1.25	9.11	11.13
1.4	10.09	11.01
1.5	10.74	10.93
1.6	11.37	10.86

280 mM DFX

g $CaCl_2$	wt% $CaCl_2$	wt% (DFX+octanoic acid)
0.75	5.75	14.94
0.8	6.11	14.86
0.9	6.82	14.77
1.1	8.21	14.55
1.3	9.56	14.34
1.4	10.22	14.24
1.5	10.87	14.13

340 mM DFX

g $CaCl_2$	wt% $CaCl_2$	wt% (DFX+octanoic acid)
0.65	5.09	18.51
0.7	5.46	18.43
0.8	6.19	18.29
0.9	6.91	18.15
1.1	8.32	17.88
1.2	9.01	17.74
1.3	9.69	17.61
1.4	10.36	17.48

440 mM DFX

g $CaCl_2$	wt% $CaCl_2$	wt% (DFX+octanoic acid)
0.55	4.44	24.67
0.6	4.83	24.57
0.9	7.07	24.00
1.1	8.51	23.62

500 mM DFX

g $CaCl_2$	wt% $CaCl_2$	wt% (DFX+octanoic acid)
0.5	4.11	28.6
0.55	4.50	28.48
0.6	4.89	28.36
0.7	5.66	28.14

520 mM DFX

g $CaCl_2$	wt% $CaCl_2$	wt% (DFX+octanoic acid)
0.1	0.86	30.9
0.2	1.70	30.63
0.3	2.52	30.38
0.4	3.34	30.12
0.5	4.14	29.87

580 mM DFX

g $CaCl_2$	wt% $CaCl_2$	wt% (DFX+octanoic acid)
0.025	0.22	35.25
0.05	0.44	35.18
0.4	3.38	34.13
0.5	4.19	33.85

625 mM DFX

g $CaCl_2$	wt% $CaCl_2$	wt% (DFX+octanoic acid)
0	0	38.47
0.025	0.22	38.38
0.4	3.42	37.15
0.5	4.24	36.84

Appendix 2D-IV Original data and corrected values for overall weight percents, Part II, $CaCl_2$ scan, R = 1.15

80 mM DFX

g $CaCl_2$	wt% $CaCl_2$	wt% (DFX+octanoic acid)
1.1	7.83	3.40
1.2	8.49	3.37
1.3	9.13	3.35
1.4	9.76	3.33
1.5	10.39	3.30
1.6	11.00	3.28

120 mM DFX

g $CaCl_2$	wt% $CaCl_2$	wt% (DFX+octanoic acid)
1	7.22	5.24
1.1	7.88	5.20
1.2	8.53	5.16
1.3	9.18	5.13
1.4	9.82	5.09
1.5	10.45	5.05
1.6	11.07	5.02

220 mM DFX

g $CaCl_2$	wt% $CaCl_2$	wt% (DFX+octanoic acid)
0.9	6.03	11.51
1	6.73	11.42
1.15	7.42	11.34
1.6	8.11	11.25
1.7	9.11	11.13

280 mM DFX

g $CaCl_2$	wt% $CaCl_2$	wt% (DFX+octanoic acid)
0.9	6.72	12.54
1	7.41	12.45
1.3	9.42	12.18
1.4	10.07	12.09
1.5	10.71	12.00

340 mM DFX

g $CaCl_2$	wt% $CaCl_2$	wt% (DFX+octanoic acid)
0.7	5.36	15.63
0.8	6.07	15.51
1.1	8.17	15.17
1.3	9.51	14.95
1.5	10.81	14.73
1.6	11.45	14.62

440 mM DFX

g $CaCl_2$	wt% $CaCl_2$	wt% (DFX+octanoic acid)
0.7	5.45	20.58
0.8	6.18	20.42
0.9	6.90	20.27
1	7.60	20.11

500 mM DFX

g $CaCl_2$	wt% $CaCl_2$	wt% (DFX+octanoic acid)
0.7	5.5	23.64
0.788	6.15	23.48
0.802	6.25	23.46
0.9	6.97	23.28

520 mM DFX

g $CaCl_2$	wt% $CaCl_2$	wt% (DFX+octanoic acid)
0.3	2.44	25.50
0.4	3.23	25.30
0.7	5.52	24.70
0.8	6.26	24.51

580 mM DFX

g $CaCl_2$	wt% $CaCl_2$	wt% (DFX+octanoic acid)
0.1	0.84	29.19
0.2	1.66	28.94
0.6	4.82	28.01
0.7	5.58	27.79

625 mM DFX

g $CaCl_2$	wt% $CaCl_2$	wt% (DFX+octanoic acid)
0.038	0.32	31.92
0.05	0.42	31.89
0.6	4.86	30.46
0.7	5.63	30.22

Appendix 2D-V Original data and corrected values for overall weight percents, Part III, $MgCl_2 \cdot 6H_2O + CaCl_2$ scan, R = 0.86

80 mM

$MgCl_2 \cdot 6H_2O+CaCl_2$			DFX+
	hydrated	water-free	octanoic acid
g	wt%	wt%	wt%
2.0	13.44	8.82	3.74
2.1	14.02	9.20	3.72
2.2	14.59	9.58	3.69
2.3	15.15	9.95	3.67
2.4	15.71	10.31	3.65
2.5	16.25	10.67	3.62
2.6	16.80	11.03	3.60
2.7	17.33	11.38	3.58
2.8	17.86	11.72	3.55

120 mM

$MgCl_2 \cdot 6H_2O+CaCl_2$			DFX+
	hydrated	water-free	octanoic acid
g	wt%	wt%	wt%
2.0	13.54	8.89	5.66
2.1	14.12	9.27	5.62
2.3	15.26	10.02	5.55
2.5	16.37	10.75	5.47
2.7	17.45	11.46	5.40
2.8	17.98	11.81	5.37

220 mM

$MgCl_2 \cdot 6H_2O+CaCl_2$			DFX+
	hydrated	water-free	octanoic acid
g	wt%	wt%	wt%
1.3	9.44	6.20	11.09
1.4	10.09	6.63	11.01
1.5	10.74	7.05	10.93
1.7	12.00	7.88	10.78
1.9	13.22	8.68	10.63
2.5	16.70	10.96	10.20
2.7	17.80	11.68	10.07
2.8	18.34	12.04	10.00

280 mM

$MgCl_2 \cdot 6H_2O+CaCl_2$			DFX+
	hydrated	water-free	octanoic acid
g	wt%	wt%	wt%
1.2	8.89	5.84	14.45
1.4	10.22	6.71	14.24
1.5	10.87	7.14	14.13
1.8	12.77	8.38	13.83
2.4	16.33	10.72	13.27
2.5	16.89	11.09	13.18
2.6	17.45	11.46	13.09
2.8	18.54	12.17	12.92
3.0	19.61	12.87	12.75

340 mM

$MgCl_2 \cdot 6H_2O+CaCl_2$			DFX+
	hydrated	water-free	octanoic acid
g	wt%	wt%	wt%
1.1	8.32	5.46	17.88
1.2	9.01	5.91	17.74
1.3	9.69	6.36	17.61
1.7	12.30	8.08	17.10
2.5	17.10	11.23	16.16
2.6	17.66	11.60	16.05

440 mM

$MgCl_2 \cdot 6H_2O+CaCl_2$			DFX+
	hydrated	water-free	octanoic acid
g	wt%	wt%	wt%
1.1	8.51	5.58	23.62
1.2	9.21	6.05	23.44
2.3	16.28	10.69	21.62
2.4	16.87	11.07	21.47

500 mM

$MgCl_2 \cdot 6H_2O+CaCl_2$			DFX+
	hydrated	water-free	octanoic acid
g	wt%	wt%	wt%
1.0	7.90	5.19	27.47
1.1	8.62	5.66	27.25
1.7	12.72	8.35	26.03
1.8	13.37	8.78	25.84

520 mM

$MgCl_2 \cdot 6H_2O+CaCl_2$			DFX+
	hydrated	water-free	octanoic acid
g	wt%	wt%	wt%
1.0	7.94	5.21	28.69
1.1	8.67	5.69	28.46
1.4	10.78	7.08	27.80
1.5	11.46	7.52	27.59

580 mM

$MgCl_2 \cdot 6H_2O+CaCl_2$			DFX+
	hydrated	water-free	octanoic acid
g	wt%	wt%	wt%
0.075	0.65	0.43	35.10
0.1	0.87	0.57	35.02
0.9	7.31	4.80	32.75
1.0	8.05	5.29	32.49

625 mM

$MgCl_2 \cdot 6H_2O+CaCl_2$			DFX+
	hydrated	water-free	octanoic acid
g	wt%	wt%	wt%
0.0	0.00	0.00	38.47
0.05	0.44	0.29	38.30
0.1	0.88	0.58	38.13
0.8	6.62	4.35	35.92
0.9	7.39	4.85	35.63

Appendix 2D-VI Original data and corrected values for overall weight percents, Part III, $MgCl_2 \cdot 6H_2O + CaCl_2$ scan, R = 1.15

80 mM

$MgCl_2 \cdot 6H_2O+CaCl_2$			DFX+
	hydrated	water-free	octanoic acid
g	wt%	wt%	wt%
2.1	13.96	9.17	3.17
2.3	15.09	9.91	3.13
2.4	15.65	10.27	3.11
2.5	16.19	10.63	3.09
2.6	16.73	10.98	3.07
2.8	17.79	11.68	3.03
2.9	18.31	12.02	3.01

120 mM

$MgCl_2 \cdot 6H_2O+CaCl_2$			DFX+
	hydrated	water-free	octanoic acid
g	wt%	wt%	wt%
1.9	12.87	8.45	4.92
2.0	13.46	8.84	4.88
2.1	14.04	9.22	4.85
2.3	15.17	9.96	4.79
2.5	16.28	10.68	4.73
2.6	16.82	11.04	4.69
2.7	17.35	11.39	4.66

220 mM

$MgCl_2 \cdot 6H_2O+CaCl_2$			DFX+
	hydrated	water-free	octanoic acid
g	wt%	wt%	wt%
1.5	10.61	6.96	9.39
1.6	11.24	7.38	9.32
1.7	11.85	7.78	9.26
1.9	13.07	8.58	9.13
2.0	13.66	8.97	9.07
2.1	14.25	9.35	9.00
2.7	17.60	11.55	8.65
2.8	18.13	11.91	8.60
2.9	18.66	12.25	8.54
3.0	19.18	12.59	8.49

280 mM

$MgCl_2 \cdot 6H_2O+CaCl_2$			DFX+
	hydrated	water-free	octanoic acid
g	wt%	wt%	wt%
1.5	10.71	7.03	12.00
1.6	11.35	7.45	11.92
1.7	11.97	7.86	11.83
1.8	12.59	8.26	11.75
2.1	14.38	9.44	11.51
2.6	17.22	11.30	11.13
2.7	17.76	11.66	11.05

340 mM

$MgCl_2 \cdot 6H_2O+CaCl_2$			DFX+
	hydrated	water-free	octanoic acid
g	wt%	wt%	wt%
1.4	10.17	6.67	14.84
1.5	10.81	7.10	14.73
1.7	12.08	7.93	14.52
2.6	17.37	11.40	13.65
2.8	18.46	12.12	13.47
2.9	18.99	12.47	13.38

440 mM

$MgCl_2 \cdot 6H_2O+CaCl_2$			DFX+
	hydrated	water-free	octanoic acid
g	wt%	wt%	wt%
1.4	10.33	6.78	19.52
1.5	10.99	7.21	19.37
2.3	15.92	10.45	18.30
2.4	16.49	10.83	18.18

500 mM

$MgCl_2 \cdot 6H_2O+CaCl_2$			DFX+
	hydrated	water-free	octanoic acid
g	wt%	wt%	wt%
1.3	9.76	6.41	22.58
1.4	10.43	6.85	22.41
1.7	12.39	8.13	21.92
1.8	13.02	8.55	21.76

520 mM

$MgCl_2 \cdot 6H_2O+CaCl_2$			DFX+
	hydrated	water-free	octanoic acid
g	wt%	wt%	wt%
1.3	9.79	6.43	23.58
1.325	9.96	6.54	23.54
1.35	10.13	6.65	23.49

580 mM

$MgCl_2 \cdot 6H_2O+CaCl_2$			DFX+
	hydrated	water-free	octanoic acid
g	wt%	wt%	wt%
0.3	2.47	1.62	28.70
0.4	3.27	2.15	28.47
1.2	9.20	6.04	26.72
1.3	9.89	6.49	26.52

625 mM

$MgCl_2 \cdot 6H_2O+CaCl_2$			DFX+
	hydrated	water-free	octanoic acid
g	wt%	wt%	wt%
0.05	0.42	0.28	31.89
0.1	0.84	0.55	31.75
1.1	8.57	5.92	29.28
1.2	9.27	6.09	29.05

Appendix 2D-VII Original data and corrected values for excess volumes and solubilization parameters: Part I (R = 0.86), $CaCl_2$ scan, 80 mM DFX

At T = 24 °C				Relative	Relative	Relative				
g, $CaCl_2$	Lower	Middle	Upper	Lower	Middle	Upper	Vo	Vw	SPo	SPw
1.1	4.5		10.3	0.44		0.56	0.50		1.92	
1.2	4.4	4.7	10.5	0.42	0.03	0.55	0.60		2.31	
1.25	4.4	6.7	10.3	0.43	0.22	0.35	0.60	1.70	2.31	6.54
1.3	4.4	6.5	10.4	0.42	0.20	0.38	0.60	1.50	2.31	5.77
1.4	4.4	6	10.4	0.42	0.15	0.42	0.60	1.00	2.31	3.85
1.45	4.2	5.8	10.3	0.41	0.16	0.44	0.80	0.80	3.08	3.08
1.5	4.7	5.9	10.3	0.46	0.12	0.43	0.30	0.90	1.15	3.46
1.57	5.2	5.9	10.4	0.50	0.07	0.43		0.90		3.46
1.6	7.5		10.4	0.72		0.28		2.50		9.62

At T = 35 °C				Relative	Relative	Relative				
g, $CaCl_2$	Lower	Middle	Upper	Lower	Middle	Upper	Vo	Vw	SPo	SPw
1.1	4.5	7.5	10.3	0.437	0.291	0.272	0.50	2.50	1.92	9.62
1.2	4.4	6.1	10.4	0.423	0.163	0.413	0.60	1.10	2.31	4.23
1.25	4.5	6.2	10.4	0.433	0.163	0.404	0.50	1.20	1.92	4.62
1.3	4.4	6.1	10.4	0.423	0.163	0.413	0.60	1.10	2.31	4.23
1.4	4.4	5.9	10.4	0.423	0.144	0.433	0.60	0.90	2.31	3.46
1.45	4.3	5.8	10.4	0.413	0.144	0.442	0.70	0.80	2.69	3.08
1.5	4.7	5.9	10.3	0.456	0.117	0.427	0.30	0.90	1.15	3.46
1.57	5.2	6	10.4	0.500	0.077	0.423		1.00		3.85
1.6	7.5		10.4	0.721		0.279		2.50		9.62

At T = 45 °C				Relative	Relative	Relative				
g, $CaCl_2$	Lower	Middle	Upper	Lower	Middle	Upper	Vo	Vw	SPo	SPw
1.1	4.5	6.6	10.4	0.433	0.202	0.365	0.50	1.60	1.92	6.15
1.2	4.4	6.1	10.4	0.423	0.163	0.413	0.60	1.10	2.31	4.23
1.25	4.5	6.1	10.4	0.433	0.154	0.413	0.50	1.10	1.92	4.23
1.3	4.4	5.9	10.4	0.423	0.144	0.433	0.60	0.90	2.31	3.46
1.4	4.4	5.8	10.4	0.423	0.135	0.442	0.60	0.80	2.31	3.08
1.45	4.3	5.7	10.4	0.413	0.135	0.452	0.70	0.70	2.69	2.69
1.5	4.7	5.8	10.4	0.452	0.106	0.442	0.30	0.80	1.15	3.08
1.57	5.3	6	10.4	0.510	0.067	0.423		1.00		3.85
1.6	7.6		10.4	0.731		0.269		2.60		10.00

Appendix 2D-VIII Original data and corrected values for excess volumes and solubilization parameters: Part I (R = 0.86), $CaCl_2$ scan, 120 mM DFX

At T = 24 °C				Relative	Relative	Relative				
g, $CaCl_2$	Lower	Middle	Upper	Lower	Middle	Upper	Vo	Vw	SPo	SPw
1	4.1		10.2	0.40		0.60	0.90		2.31	
1.1	3.8	8.3	10.3	0.37	0.44	0.19	1.20	3.30	3.08	8.46
1.2	3.9	7	10.3	0.38	0.30	0.32	1.10	2.00	2.82	5.13
1.25	3.9	6.7	10.3	0.38	0.27	0.35	1.10	1.70	2.82	4.36
1.3	4	6.5	10.2	0.39	0.25	0.36	1.00	1.50	2.56	3.85
1.4	3.8	6.2	10.2	0.37	0.24	0.39	1.20	1.20	3.08	3.08
1.5	3.8	6.1	10.4	0.37	0.22	0.41	1.20	1.10	3.08	2.82
1.55	4.1	6.2	10.4	0.39	0.20	0.40	0.90	1.20	2.31	3.08
1.6	0.05		10.5	0.0048		0.9952	4.95		12.69	

At T = 35 °C				Relative	Relative	Relative				
g, $CaCl_2$	Lower	Middle	Upper	Lower	Middle	Upper	Vo	Vw	SPo	SPw
1	4.1	8.1	10.3	0.40	0.39	0.21	0.90	3.10	2.31	7.95
1.1	4	7.1	10.4	0.38	0.30	0.32	1.00	2.10	2.56	5.38
1.2	3.9	6.5	10.3	0.38	0.25	0.37	1.10	1.50	2.82	3.85
1.25	4	5.9	10.4	0.38	0.18	0.43	1.00	0.90	2.56	2.31
1.3	4	6.3	10.3	0.39	0.22	0.39	1.00	1.30	2.56	3.33
1.4	3.9	6.1	10.3	0.38	0.21	0.41	1.10	1.10	2.82	2.82
1.5	3.8	6	10.5	0.36	0.21	0.43	1.20	1.00	3.08	2.56
1.55	4.1	6.2	10.4	0.39	0.20	0.40	0.90	1.20	2.31	3.08
1.6	0.05		10.5	0.0048		0.9952	4.95		12.69	

At T = 45 °C				Relative	Relative	Relative				
g, $CaCl_2$	Lower	Middle	Upper	Lower	Middle	Upper	Vo	Vw	SPo	SPw
1	4.1	7.3	10.4	0.39	0.31	0.30	0.90	2.30	2.31	5.90
1.1	4	6.9	10.4	0.38	0.28	0.34	1.00	1.90	2.56	4.87
1.2	4	6.4	10.4	0.38	0.23	0.38	1.00	1.40	2.56	3.59
1.25	4.5	6.3	10.4	0.43	0.17	0.39	0.50	1.30	1.28	3.33
1.3	4	6.2	10.3	0.39	0.21	0.40	1.00	1.20	2.56	3.08
1.4	4	6	10.3	0.39	0.19	0.42	1.00	1.00	2.56	2.56
1.5	3.8	5.9	10.5	0.36	0.20	0.44	1.20	0.90	3.08	2.31
1.55	4.1	6.1	10.4	0.39	0.19	0.41	0.90	1.10	2.31	2.82
1.6	0.08		10.5	0.0076		0.9924	4.92		12.62	

Appendix 2D-IX Original data and corrected values for excess volumes and solubilization parameters: Part I (R = 0.86), $CaCl_2$ scan, 220 mM DFX

At T = 24 °C				Relative	Relative	Relative				
g, $CaCl_2$	Lower	Middle	Upper	Lower	Middle	Upper	Vo	Vw	SPo	SPw
0.8	3.2		10.3	0.31		0.69	1.80		2.54	
0.9	3.1	9.7	10.3	0.30	0.64	0.06	1.90	4.70	2.68	6.62
1	3.1	8.4	10.3	0.30	0.51	0.18	1.90	3.40	2.68	4.79
1.1	3	7.6	10.3	0.29	0.45	0.26	2.00	2.60	2.82	3.66
1.25	3.4	6.6	10.4	0.33	0.31	0.37	1.60	1.60	2.25	2.25
1.4	2.7	6.1	10.3	0.26	0.33	0.41	2.30	1.10	3.24	1.55
1.5	2.8	6.5	10.4	0.27	0.36	0.38	2.20	1.50	3.10	2.11
1.6	3.5		10.5	0.33		0.67	1.50		2.11	

At T = 35 °C				Relative	Relative	Relative				
g, $CaCl_2$	Lower	Middle	Upper	Lower	Middle	Upper	Vo	Vw	SPo	SPw
0.8	3.2	9.1	10.2	0.31	0.58	0.11	1.80	4.10	2.54	5.77
0.9	3.1	8.6	10.3	0.30	0.53	0.17	1.90	3.60	2.68	5.07
1	3.1	7.8	10.3	0.30	0.46	0.24	1.90	2.80	2.68	3.94
1.1	3	7.2	10.3	0.29	0.41	0.30	2.00	2.20	2.82	3.10
1.25	2.9	6.9	10.4	0.28	0.38	0.34	2.10	1.90	2.96	2.68
1.4	2.2	6.5	10.4	0.21	0.41	0.38	2.80	1.50	3.94	2.11
1.5	2.9	6.4	10.4	0.28	0.34	0.38	2.10	1.40	2.96	1.97
1.6	3.6		10.7	0.34		0.66	1.40		1.97	

At T = 45 °C				Relative	Relative	Relative				
g, $CaCl_2$	Lower	Middle	Upper	Lower	Middle	Upper	Vo	Vw	SPo	SPw
0.8	3.3	8.1	10.2	0.32	0.47	0.21	1.70	3.10	2.39	4.37
0.9	3.2	7.8	10.3	0.31	0.45	0.24	1.80	2.80	2.54	3.94
1	3.1	7.3	10.4	0.30	0.40	0.30	1.90	2.30	2.68	3.24
1.1	3.1	7	10.4	0.30	0.38	0.33	1.90	2.00	2.68	2.82
1.25	3	6.3	10.5	0.29	0.31	0.40	2.00	1.30	2.82	1.83
1.4	2.8	6.4	10.4	0.27	0.35	0.38	2.20	1.40	3.10	1.97
1.5	3	6.1	10.5	0.29	0.30	0.42	2.00	1.10	2.82	1.55
1.6	4.3		10.5	0.41		0.59	0.70		0.99	

Appendix 2D-X Original data and corrected values for excess volumes and solubilization parameters: Part I (R = 0.86), $CaCl_2$ scan, 280 mM DFX

At T = 24 °C				Relative	Relative	Relative				
g, $CaCl_2$	Lower	Middle	Upper	Lower	Middle	Upper	Vo	Vw	SPo	SPw
0.75	2.7		10.3	0.26		0.74	2.30		2.56	
0.8	2.6	9.7	10.2	0.25	0.70	0.05	2.40	4.70	2.67	5.22
0.9	2.6	8.7	10.2	0.25	0.60	0.15	2.40	3.70	2.67	4.11
1.1	2.4	7.6	10.3	0.23	0.50	0.26	2.60	2.60	2.89	2.89
1.3	2.1	7	10.4	0.20	0.47	0.33	2.90	2.00	3.22	2.22
1.4	1.9	6.3	10.4	0.18	0.42	0.39	3.10	1.30	3.44	1.44
1.5	4.7		10.5	0.45		0.55	0.30		0.33	

At T = 35 °C				Relative	Relative	Relative				
g, $CaCl_2$	Lower	Middle	Upper	Lower	Middle	Upper	Vo	Vw	SPo	SPw
0.75	2.7	9.4	10.3	0.26	0.65	0.09	2.30	4.40	2.56	4.89
0.8	2.6	8.9	10.3	0.25	0.61	0.14	2.40	3.90	2.67	4.33
0.9	2.6	8.2	10.3	0.25	0.54	0.20	2.40	3.20	2.67	3.56
1.1	2.4	7.3	10.3	0.23	0.48	0.29	2.60	2.30	2.89	2.56
1.3	2.1	6.9	10.4	0.20	0.46	0.34	2.90	1.90	3.22	2.11
1.4	1.9	6.2	10.4	0.18	0.41	0.40	3.10	1.20	3.44	1.33
1.5	4.9		10.4	0.47		0.53	0.10		0.11	

At T = 45 °C				Relative	Relative	Relative				
g, $CaCl_2$	Lower	Middle	Upper	Lower	Middle	Upper	Vo	Vw	SPo	SPw
0.75	2.8	8.5	10.3	0.27	0.55	0.17	2.20	3.50	2.44	3.89
0.8	2.6	8.2	10.3	0.25	0.54	0.20	2.40	3.20	2.67	3.56
0.9	2.6	7.7	10.3	0.25	0.50	0.25	2.40	2.70	2.67	3.00
1.1	2.4	7.1	10.3	0.23	0.46	0.31	2.60	2.10	2.89	2.33
1.3	2.1	6.8	10.4	0.20	0.45	0.35	2.90	1.80	3.22	2.00
1.4	1.9	6.6	10.4	0.18	0.45	0.37	3.10	1.60	3.44	1.78
1.5	5.5		10.4	0.53		0.47		0.50		0.56

Appendix 2D-XI Original data and corrected values for excess volumes and solubilization parameters: Part I (R = 0.86), $CaCl_2$ scan, 340 mM DFX

At T = 24 °C				Relative	Relative	Relative				
g, $CaCl_2$	Lower	Middle	Upper	Lower	Middle	Upper	Vo	Vw	SPo	SPw
0.65	2		10.2	0.20		0.80	3.00		2.75	
0.7	2	10	10.2	0.20	0.78	0.02	3.00	5.00	2.75	4.59
0.8	1.9	9.1	10.2	0.19	0.71	0.11	3.10	4.10	2.84	3.76
0.9	1.8	8.4	10.2	0.18	0.65	0.18	3.20	3.40	2.94	3.12
1.1	1.5	7.5	10.3	0.15	0.58	0.27	3.50	2.50	3.21	2.29
1.2	1.4	7.4	10.4	0.13	0.58	0.29	3.60	2.40	3.30	2.20
1.3	1.3	7.1	10.4	0.13	0.56	0.32	3.70	2.10	3.39	1.93
1.4	8.7		10.4	0.84		0.16		3.7		3.39

At T = 35 °C				Relative	Relative	Relative				
g, $CaCl_2$	Lower	Middle	Upper	Lower	Middle	Upper	Vo	Vw	SPo	SPw
0.65	3.1	9.7	10.2	0.30	0.65	0.05	1.90	4.70	1.74	4.31
0.7	2.1	9.3	10.2	0.21	0.71	0.09	2.90	4.30	2.66	3.94
0.8	1.9	8.6	10.2	0.19	0.66	0.16	3.10	3.60	2.84	3.30
0.9	1.8	8.1	10.3	0.17	0.61	0.21	3.20	3.10	2.94	2.84
1.1	1.5	7.4	10.3	0.15	0.57	0.28	3.50	2.40	3.21	2.20
1.2	1.4	7.3	10.4	0.13	0.57	0.30	3.60	2.30	3.30	2.11
1.3	1.3	7	10.4	0.13	0.55	0.33	3.70	2.00	3.39	1.83
1.4	7.7		10.4	0.74		0.26		2.7		2.48

At T = 45 °C				Relative	Relative	Relative				
g, $CaCl_2$	Lower	Middle	Upper	Lower	Middle	Upper	Vo	Vw	SPo	SPw
0.65	2.1	8.9	10.3	0.20	0.66	0.14	2.90	3.90	2.66	3.58
0.7	2.1	8.6	10.3	0.20	0.63	0.17	2.90	3.60	2.66	3.30
0.8	1.9	8.1	10.3	0.18	0.60	0.21	3.10	3.10	2.84	2.84
0.9	1.8	7.8	10.4	0.17	0.58	0.25	3.20	2.80	2.94	2.57
1.1	1.5	7.3	10.4	0.14	0.56	0.30	3.50	2.30	3.21	2.11
1.2	1.4	7.2	10.4	0.13	0.56	0.31	3.60	2.20	3.30	2.02
1.3	1.3	6.5	10.5	0.12	0.50	0.38	3.70	1.50	3.39	1.38
1.4	7.1		10.5	0.68		0.32		2.1		1.93

Appendix 2D-XII Original data and corrected values for excess volumes and solubilization parameters: 440 mM DFX, Parts I (R = 0.86) and II (R = 1.15), $CaCl_2$ scan

R = 0.86

At T = 24 °C				Relative	Relative	Relative				
g, $CaCl_2$	Lower	Middle	Upper	Lower	Middle	Upper	Vo	Vw	SPo	SPw
0.55	0.65		10.1	0.06		0.94	4.35		3.09	
0.6	0.8	9.8	10.1	0.08	0.89	0.03	4.20	4.80	2.98	3.40
0.9	0.25	8.2	10.3	0.02	0.77	0.20	4.75	3.20	3.37	2.27
1.1	7.7		10.3	0.75		0.25		2.70		1.91

At T = 35 °C				Relative	Relative	Relative				
g, $CaCl_2$	Lower	Middle	Upper	Lower	Middle	Upper	Vo	Vw	SPo	SPw
0.55	0.6	9.3	10.2	0.06	0.85	0.09	4.40	4.30	3.12	3.05
0.6	0.9	9	10.2	0.09	0.79	0.12	4.10	4.00	2.91	2.84
0.9	0.7	7.8	10.3	0.07	0.69	0.24	4.30	2.80	3.05	1.99
1.1	0.4	7.4	10.4	0.04	0.67	0.96	4.60	2.40	3.26	1.70

At T = 45 °C				Relative	Relative	Relative				
g, $CaCl_2$	Lower	Middle	Upper	Lower	Middle	Upper	Vo	Vw	SPo	SPw
0.55	0.6	9.2	10.3	0.06	0.83	0.11	4.40	4.20	3.12	2.98
0.6	0.9	8.9	10.2	0.09	0.78	0.13	4.10	3.90	2.91	2.77
0.9	0.7	7.8	10.3	0.07	0.69	0.24	4.30	2.80	3.05	1.99
1.1	0.4	7.4	10.4	0.04		0.96	4.60	2.40	3.26	1.70

R = 1.15

At T = 24 °C				Relative	Relative	Relative				
g, $CaCl_2$	Lower	Middle	Upper	Lower	Middle	Upper	Vo	Vw	SPo	SPw
0.7	0.9		10.1	0.09		0.91	4.10		2.91	
0.8	0.5	9.8	10.2	0.05	0.91	0.04	4.50	4.80	3.19	3.40
0.9	0.7	9.3	10.2	0.07	0.84	0.09	4.30	4.30	3.05	3.05
1	8.4		10.2	0.82		0.18		3.40		2.41

At T = 35 °C				Relative	Relative	Relative				
g, $CaCl_2$	Lower	Middle	Upper	Lower	Middle	Upper	Vo	Vw	SPo	SPw
0.7	0.9	9.2	10.2	0.09	0.81	0.91	4.10	4.20	2.91	2.98
0.8	0.5	8.9	10.2	0.05	0.82	0.13	4.50	3.90	3.19	2.77
0.9	0.7	8.7	10.2	0.07	0.78	0.15	4.30	3.70	3.05	2.62
1	7.9		10.4	0.76		0.24		2.90		2.06

At T = 45 °C				Relative	Relative	Relative				
g, $CaCl_2$	Lower	Middle	Upper	Lower	Middle	Upper	Vo	Vw	SPo	SPw
0.7	0.9	9.1	10.2	0.09	0.80	0.91	4.10	4.10	2.91	2.91
0.8	0.5	8.8	10.3	0.05	0.81	0.15	4.50	3.80	3.19	2.70
0.9	0.95	8.6	10.3	0.09	0.74	0.17	4.05	3.60	2.87	2.55
1	8		10.4	0.77		0.23		3.00		2.13

Appendix 2D-XIII Original data and corrected values for excess volumes and solubilization parameters: 440 mM DFX, Parts III (R = 0.86) and IV (R = 1.15), $MgCl_2 \cdot 6H_2O + CaCl_2$ scan

R = 0.86

At T = 24 °C				Relative	Relative	Relative				
g, Mg+Ca	Lower	Middle	Upper	Lower	Middle	Upper	Vo	Vw	SPo	SPw
1.1	1.3		10.5	0.12		0.88	3.70		2.62	
1.2	1.1	10.3	10.6	0.10	0.87	0.03	3.90	5.30	2.77	3.76
2.3	0.3	7.4	11.1	0.03	0.64	0.33	4.70	2.40	3.33	1.70
2.4	7.7		11.2	0.69		0.31		2.70		1.91

At T = 35 °C				Relative	Relative	Relative				
g, Mg+Ca	Lower	Middle	Upper	Lower	Middle	Upper	Vo	Vw	SPo	SPw
1.1	1.3	9.9	10.5	0.12	0.82	0.06	3.70	4.90	2.62	3.48
1.2	1.2	9.6	10.6	0.11	0.79	0.09	3.80	4.60	2.70	3.26
2.3	0.4	7.4	11.1	0.04	0.63	0.33	4.60	2.40	3.26	1.70
2.4	7.7		11.3	0.68		0.32		2.70		1.91

At T = 45 °C				Relative	Relative	Relative				
g, Mg+Ca	Lower	Middle	Upper	Lower	Middle	Upper	Vo	Vw	SPo	SPw
1.1	1.3	9.7	10.6	0.12	0.79	0.08	3.70	4.70	2.62	
1.2	1.2	9.5	10.7	0.11	0.78	0.11	3.80	4.50	2.70	3.19
2.3	0.45	7.4	11.2	0.04	0.62	0.34	4.55	2.40	3.23	1.70
2.4	7.8		11.4	0.68		0.32		2.80		1.99

R = 1.15

At T = 24 °C				Relative	Relative	Relative				
g, Mg+Ca	Lower	Middle	Upper	Lower	Middle	Upper	Vo	Vw	SPo	SPw
1.4	1		10.7	0.09		0.91	4.00		2.84	
1.5	1	10.4	10.7	0.09	0.88	0.03	4.00	5.40	2.84	3.83
2.3	0.64	7.9	11.1	0.06	0.65	0.29	4.36	2.90	3.09	2.06
2.4	8.1		11.3	0.72		0.28		3.10		2.20

At T = 35 °C				Relative	Relative	Relative				
g, Mg+Ca	Lower	Middle	Upper	Lower	Middle	Upper	Vo	Vw	SPo	SPw
1.4	1.1	9.9	10.7	0.10	0.82	0.07	3.90	4.90	2.77	3.48
1.5	1.1	9.5	10.8	0.10	0.78	0.12	3.90	4.50	2.77	3.19
2.3	0.8	7.7	11.2	0.07	0.62	0.31	4.20	2.70	2.98	1.91
2.4	7.8		11.3	0.69		0.31		2.80		1.99

At T = 45 °C				Relative	Relative	Relative				
g, Mg+Ca	Lower	Middle	Upper	Lower	Middle	Upper	Vo	Vw	SPo	SPw
1.4	1.1	9.7	10.8	0.10	0.80	0.10	3.90	4.70	2.77	3.33
1.5	1.1	9.3	10.9	0.10	0.75	0.15	3.90	4.30	2.77	3.05
2.3	0.8	7.7	11.3	0.07	0.61	0.32	4.20	2.70	2.98	1.91
2.4	7.8		11.4	0.68		0.32		2.80		1.99

Appendix 2D-XIV Original data and corrected values for excess volumes and solubilization parameters: 500 mM DFX, Parts I (R = 0.86) and II (R = 1.15), $CaCl_2$ scan

R = 0.86

At T = 24 °C				Relative	Relative	Relative				
g, $CaCl_2$	Lower	Middle	Upper	Lower	Middle	Upper	Vo	Vw	SPo	SPw
0.5	0.05		10.1	0.0050		0.9950	4.95		3.07	
0.55	10.2		10.2	1.0000		0.0000		5.20		3.23
0.6	9.6		10.2	0.9412		0.0588		4.60		2.86
0.7	8.9		10.1	0.8812		0.1188		3.90		2.42

At T = 35 °C				Relative	Relative	Relative				
g, $CaCl_2$	Lower	Middle	Upper	Lower	Middle	Upper	Vo	Vw	SPo	SPw
0.5	0.18	9.4	10.1	0.0178	0.9129	0.0693	4.82	4.40	2.99	2.73
0.55	0.1	9.2	10.2	0.0098	0.8922	0.0980	4.90	4.20	3.04	2.61
0.6	0.3	8.8	10.2	0.0294	0.8333	0.1373	4.70	3.80	2.92	2.36
0.7	0.24	8.4	10.2	0.0235	0.8000	0.1765	4.76	3.40	2.96	2.11

At T = 45 °C				Relative	Relative	Relative				
g, $CaCl_2$	Lower	Middle	Upper	Lower	Middle	Upper	Vo	Vw	SPo	SPw
0.5	0.18	9.4	10.2	0.0176	0.9039	0.0784	4.82	4.40	2.99	2.73
0.55	0.1	9.2	10.2	0.0098	0.8922	0.0980	4.90	4.20	3.04	2.61
0.6	0.32	8.8	10.3	0.0311	0.8233	0.1456	4.68	3.80	2.91	2.36
0.7	0.24	8.4	10.3	0.0233	0.7922	0.1845	4.76	3.40	2.96	2.11

R = 1.15

At T = 24 °C				Relative	Relative	Relative				
g, $CaCl_2$	Lower	Middle	Upper	Lower	Middle	Upper	Vo	Vw	SPo	SPw
0.7	0.2		10.1	0.0198		0.9802	4.80		2.98	
0.788	0.3	9.9	10.2	0.0294	0.9412	0.0294	4.70	4.90	2.92	3.04
0.802	0.1	9.8	10.2	0.0098	0.9510	0.0392	4.90	4.80	3.04	2.98
0.9	9.5		10.2	0.9314		0.0686		4.50		2.80

At T = 35 °C				Relative	Relative	Relative				
g, $CaCl_2$	Lower	Middle	Upper	Lower	Middle	Upper	Vo	Vw	SPo	SPw
0.7	0.2	9.2	10.1	0.0198	0.8911	0.0891	4.80	4.20	2.98	2.61
0.788	0.35	9.2	10.2	0.0343	0.8676	0.0980	4.65	4.20	2.89	2.61
0.802	0.22	9	10.2	0.0216	0.8608	0.1176	4.78	4.00	2.97	2.48
0.9	0.22	8.7	10.3	0.0214	0.8233	0.1553	4.78	3.70	2.97	2.30

At T = 45 °C				Relative	Relative	Relative				
g, $CaCl_2$	Lower	Middle	Upper	Lower	Middle	Upper	Vo	Vw	SPo	SPw
0.7	0.22	9.1	10.1	0.0218	0.8792	0.0990	4.78	4.10	2.97	2.55
0.788	0.51	9.1	10.3	0.0495	0.8340	0.1165	4.49	4.10	2.79	2.55
0.802	0.24	9	10.3	0.0233	0.8505	0.1262	4.76	4.00	2.96	2.48
0.9	0.24	8.7	10.3	0.0233	0.8214	0.1553	4.76	3.70	2.96	2.30

Appendix 2D-XV Original data and corrected values for excess volumes and solubilization parameters: 500 mM DFX, Parts III (R = 0.86) and IV (R = 1.15), $MgCl_2 \cdot 6H_2O$+$CaCl_2$ scan

R = 0.86

At T = 24 °C				Relative	Relative	Relative				
g, Mg+Ca	Lower	Middle	Upper	Lower	Middle	Upper	Vo	Vw	SPo	SPw
1	0.3		10.4	0.0288		0.9712	4.70		2.92	
1.1	0.33	9.9	10.5	0.0314	0.9114	0.0571	4.67	4.90	2.90	3.04
1.7	0.3	8.5	10.9	0.0275	0.7523	0.2202	4.70	3.50	2.92	2.17
1.8	8.3		10.9	0.7615		0.2385		3.30		2.05

At T = 35 °C				Relative	Relative	Relative				
g, Mg+Ca	Lower	Middle	Upper	Lower	Middle	Upper	Vo	Vw	SPo	SPw
1	0.3	9.9	10.5	0.0286	0.9143	0.0571	4.70	4.90	2.92	3.04
1.1	0.37	9.4	10.5	0.0352	0.8600	0.1048	4.63	4.40	2.88	2.73
1.7	0.4	8.4	10.9	0.0367	0.7339	0.2294	4.60	3.40	2.86	2.11
1.8	0.32	8.2	10.9	0.0294	0.7229	0.2477	4.68	3.20	2.91	1.99

At T = 45 °C				Relative	Relative	Relative				
g, Mg+Ca	Lower	Middle	Upper	Lower	Middle	Upper	Vo	Vw	SPo	SPw
1	0.3	9.8	10.5	0.0286	0.9048	0.0667	4.70	4.80	2.92	2.98
1.1	0.38	9.35	10.6	0.0358	0.8462	0.1179	4.62	4.35	2.87	2.70
1.7	0.47	8.2	11	0.0427	0.7027	0.2545	4.53	3.20	2.81	1.99
1.8	0.32	8.1	11	0.0291	0.7073	0.2636	4.68	3.10	2.91	1.93

R = 1.15

At T = 24 °C				Relative	Relative	Relative				
g, Mg+Ca	Lower	Middle	Upper	Lower	Middle	Upper	Vo	Vw	SPo	SPw
1.3	0.5		10.6	0.0472		0.9528	4.50		2.80	
1.4	0.15	10.4	10.7	0.0140	0.9579	0.0280	4.85	5.40	3.01	3.35
1.7	0.14	9.1	10.9	0.0128	0.8220	0.1651	4.86	4.10	3.02	2.55
1.8	8.8		10.9	0.8073		0.1927		3.80		2.36

At T = 35 °C				Relative	Relative	Relative				
g, Mg+Ca	Lower	Middle	Upper	Lower	Middle	Upper	Vo	Vw	SPo	SPw
1.3	0.5	10	10.6	0.0472	0.8962	0.0566	4.50	5.00	2.80	3.11
1.4	0.37	9.5	10.7	0.0346	0.8533	0.1121	4.63	4.50	2.88	2.80
1.7	0.4	8.6	10.9	0.0367	0.7523	0.2110	4.60	3.60	2.86	2.24
1.8	0.2	8.3	10.9	0.0183	0.7431	0.2385	4.80	3.30	2.98	2.05

At T = 45 °C				Relative	Relative	Relative				
g, Mg+Ca	Lower	Middle	Upper	Lower	Middle	Upper	Vo	Vw	SPo	SPw
1.3	0.55	9.8	10.7	0.0514	0.8645	0.0841	4.45	4.80	2.76	2.98
1.4	0.37	9.4	10.8	0.0343	0.8361	0.1296	4.63	4.40	2.88	2.73
1.7	0.4	8.6	11	0.0364	0.7455	0.2182	4.60	3.60	2.86	2.24
1.8	0.2	8.3	11	0.0182	0.7364	0.2455	4.80	3.30	2.98	2.05

Appendix 2D-XVI Original data and corrected values for excess volumes and solubilization parameters: 520 mM DFX, Parts I (R = 0.86) and II (R = 1.15), $CaCl_2$ scan

R = 0.86

At T = 24 °C				Relative	Relative	Relative				
g, $CaCl_2$	Lower	Middle	Upper	Lower	Middle	Upper	Vo	Vw	SPo	SPw
0.1	0.75		10	0.0750		0.9250	4.25		2.54	
0.2	10		10	1.0000		0.0000		5.00		2.99
0.4	10.2		10.2	1.0000		0.0000		5.20		3.11
0.5	10		10.2	0.9804		0.0196		5.00		2.99

At T = 35 °C				Relative	Relative	Relative				
g, $CaCl_2$	Lower	Middle	Upper	Lower	Middle	Upper	Vo	Vw	SPo	SPw
0.1	1.8		10.1	0.1782		0.8218	3.20		1.92	
0.2	1.25		10	0.1250		0.8750	3.75			
0.4	0.02	10	10.2	0.0020	0.9784	0.0196	4.98	5.00		2.99
0.5	9.2		10.2	0.9020		0.0980		4.20		2.51

At T = 45 °C				Relative	Relative	Relative				
g, $CaCl_2$	Lower	Middle	Upper	Lower	Middle	Upper	Vo	Vw	SPo	SPw
0.1	1.85		10.2	0.1814		0.8186	3.15		1.89	
0.2	1.3		10.1	0.1287		0.8713	3.70		2.22	
0.4	0.02	10	10.3	0.0019	0.9689	0.0291	4.98	5.00		2.99
0.5	9.3		10.2	0.9118		0.0882		4.30		2.57

R = 1.15

At T = 24 °C				Relative	Relative	Relative				
g, $CaCl_2$	Lower	Middle	Upper	Lower	Middle	Upper	Vo	Vw	SPo	SPw
0.3	0.06		10	0.0060		0.9940	4.94		2.96	
0.4	10.1		10.1	1.0000		0.0000		5.10		3.05
0.7	10.1		10.1	1.0000		0.0000		5.10		3.05
0.8	9.7		10.2	0.9510		0.0490		4.70		2.81

At T = 35 °C				Relative	Relative	Relative				
g, $CaCl_2$	Lower	Middle	Upper	Lower	Middle	Upper	Vo	Vw	SPo	SPw
0.3	0.3	9.7	10	0.0300	0.9400	0.0300	4.70	4.70	2.81	2.81
0.4	0.75	10.2	10.4	0.0721	0.9087	0.0192	4.25	5.20	2.54	3.11
0.7	9.4		10.1	0.9307		0.0693		4.40		2.63
0.8	9.5		10.2	0.9314		0.0686		4.50		2.69

At T = 45 °C				Relative	Relative	Relative				
g, $CaCl_2$	Lower	Middle	Upper	Lower	Middle	Upper	Vo	Vw	SPo	SPw
0.3	0.3	9.6	10	0.0300	0.9300	0.0400	4.70	4.60	2.81	2.75
0.4	0.8	10.2	10.4	0.0769	0.9038	0.0192	4.20	5.20	2.51	3.11
0.7	9.3		10.2	0.9118		0.0882		4.30		2.57
0.8	9.5		10.3	0.9223		0.0777		4.50		2.69

Appendix 2D-XVII Original data and corrected values for excess volumes and solubilization parameters: 520 mM DFX, Parts III (R = 0.86) and IV (R = 1.15), $MgCl_2 \cdot 6H_2O + CaCl_2$ scan

R = 0.86

At T = 24 °C				Relative	Relative	Relative				
g, Mg+Ca	Lower	Middle	Upper	Lower	Middle	Upper	Vo	Vw	SPo	SPw
1	0.1		10.5	0.0095		0.9905	4.90		2.93	
1.1	0.04	10.2	10.6	0.0038	0.9585	0.0377	4.96	5.20	2.97	3.11
1.4	0.08	9	10.6	0.0075	0.8415	0.1509	4.92	4.00	2.95	2.40
1.5	8.8		10.6	0.8302		0.1698		3.80		2.28

At T = 35 °C				Relative	Relative	Relative				
g, Mg+Ca	Lower	Middle	Upper	Lower	Middle	Upper	Vo	Vw	SPo	SPw
1	0.15	9.8	10.5	0.0143	0.9190	0.0667	4.85	4.80	2.90	2.87
1.1	0.2	9.5	10.6	0.0189	0.8774	0.1038	4.80	4.50	2.87	2.69
1.4	0.2	8.7	10.7	0.0187	0.7944	0.1869	4.80	3.70	2.87	2.22
1.5	0.4	8.3	10.6	0.0377	0.7453	0.2170	4.60	3.30	2.75	1.98

At T = 45 °C				Relative	Relative	Relative				
g, Mg+Ca	Lower	Middle	Upper	Lower	Middle	Upper	Vo	Vw	SPo	SPw
1	0.15	9.7	10.6	0.0142	0.9009	0.0849	4.85	4.70	2.90	2.81
1.1	0.2	9.4	10.6	0.0189	0.8679	0.1132	4.80	4.40	2.87	2.63
1.4	0.2	8.7	10.8	0.0185	0.7870	0.1944	4.80	3.70	2.87	2.22
1.5	0.4	8.3	10.7	0.0374	0.7383	0.2243	4.60	3.30	2.75	1.98

R = 1.15

At T = 24 °C				Relative	Relative	Relative				
g, Mg+Ca	Lower	Middle	Upper	Lower	Middle	Upper	Vo	Vw	SPo	SPw
1.3	0.35		10.7	0.0327		0.9673	4.65		2.78	
1.325	0.001	10.75	10.8	0.0001	0.9953	0.0046	5.00	5.75	2.99	3.44
1.35	10.6		10.8	0.9815		0.0185		5.60		3.35

At T = 35 °C				Relative	Relative	Relative				
g, Mg+Ca	Lower	Middle	Upper	Lower	Middle	Upper	Vo	Vw	SPo	SPw
1.3	0.4	10.7	10.7	0.0374	0.9626	0.0000	4.60	5.70	2.75	3.41
1.325	0.3	9.7	10.7	0.0280	0.8785	0.0935	4.70	4.70	2.81	2.81
1.35	0.18	9.5	10.8	0.0167	0.8630	0.1204	4.82	4.50	2.89	2.69

At T = 45 °C				Relative	Relative	Relative				
g, Mg+Ca	Lower	Middle	Upper	Lower	Middle	Upper	Vo	Vw	SPo	SPw
1.3	0.42	9.8	10.7	0.0393	0.8766	0.0841	4.58	4.80	2.74	2.87
1.325	0.3	9.5	10.7	0.0280	0.8598	0.1121	4.70	4.50	2.81	2.69
1.35	0.18	9.5	10.8	0.0167	0.8630	0.1204	4.82	4.50	2.89	2.69

Appendix 2D-XVIII Original data and corrected values for excess volumes and solubilization parameters: 580 mM DFX, Parts I (R = 0.86) and II (R = 1.15), $CaCl_2$ scan

R = 0.86

At T = 24 °C				Relative	Relative	Relative				
g, $CaCl_2$	Lower	Middle	Upper	Lower	Middle	Upper	Vo	Vw	SPo	SPw
0.025	0.18		10	0.0180		0.9820	4.82		2.59	
0.05	9.8		9.8	1.0000		0.0000		4.80		2.58
0.1	9.9		9.9	1.0000		0.0000		4.90		2.63
0.4	10		10	1.0000		0.0000		5.00		
0.5	9.8		10.2	0.9608		0.0392		4.80		

At T = 35 °C				Relative	Relative	Relative				
g, $CaCl_2$	Lower	Middle	Upper	Lower	Middle	Upper	Vo	Vw	SPo	SPw
0.025	0.6		10	0.0600		0.9400	4.40		2.37	
0.05	0.5		10	0.0500		0.9500	4.50		2.42	
0.1	0.5		10	0.0500		0.9500	4.50		2.42	
0.4	10		10.2	0.9804		0.0196		5.00		2.69
0.5	9.3		10.2	0.9118		0.0882		4.30		2.31

At T = 45 °C				Relative	Relative	Relative				
g, $CaCl_2$	Lower	Middle	Upper	Lower	Middle	Upper	Vo	Vw	SPo	SPw
0.025	0.6		10.1	0.0594		0.9406	4.40		2.37	
0.05	0.5		10.1	0.0495		0.9505	4.50		2.42	
0.1	0.5		10.1	0.0495		0.9505	4.50		2.42	
0.4	9.9		10.2	0.9706		0.0294		4.90		2.63
0.5	9.3		10.3	0.9029		0.0971		4.30		2.31

R = 1.15

At T = 24 °C				Relative	Relative	Relative				
g, $CaCl_2$	Lower	Middle	Upper	Lower	Middle	Upper	Vo	Vw	SPo	SPw
0.1	0.7		10	0.0700		0.9300	4.30		2.31	
0.2	10		10	1.0000		0.0000		5.00		2.69
0.6	10.1		10.1	1.0000		0.0000		5.10		2.74
0.7	10.1		10.1	1.0000		0.0000		5.10		2.74

At T = 35 °C				Relative	Relative	Relative				
g, $CaCl_2$	Lower	Middle	Upper	Lower	Middle	Upper	Vo	Vw	SPo	SPw
0.1	1		10.1	0.0990		0.9010	4.00		2.15	
0.2	0.08	9.8	9.9	0.0081	0.9818	0.0101	4.92	4.80	2.65	2.58
0.6	9.8		10.1	0.9703		0.0297		4.80		2.58
0.7	9.4		10.3	0.9126		0.0874		4.40		2.37

At T = 45 °C				Relative	Relative	Relative				
g, $CaCl_2$	Lower	Middle	Upper	Lower	Middle	Upper	Vo	Vw	SPo	SPw
0.1	1.1		10.1	0.1089		0.8911	3.90		2.10	
0.2	0.08	10.1	10.2	0.0078	0.9824	0.0098	4.92	5.10	2.65	2.74
0.6	9.8		10.2	0.9608		0.0392		4.80		2.58
0.7	9.4		10.3	0.9126		0.0874		4.40		2.37

Appendix 2D-XIX Original data and corrected values for excess volumes and solubilization parameters: 580 mM DFX, Parts III (R = 0.86) and IV (R = 1.15), $MgCl_2 \cdot 6H_2O + CaCl_2$ scan

R = 0.86

At T = 24 °C				Relative	Relative	Relative				
g, Mg+Ca	Lower	Middle	Upper	Lower	Middle	Upper	Vo	Vw	SPo	SPw
0.075	0.7		10.1	0.0693		0.9307	4.30		2.31	
0.1	9.9		9.9	1.0000		0.0000		4.90		2.63
0.9	10.5		10.5	1.0000		0.0000		5.50		2.96
1	10.1		10.5	0.9619		0.0381		5.10		2.74

At T = 35 °C				Relative	Relative	Relative				
g, Mg+Ca	Lower	Middle	Upper	Lower	Middle	Upper	Vo	Vw	SPo	SPw
0.075	0.95		10.1	0.0941		0.9059	4.05		2.18	
0.1	0.4		10.2	0.0392		0.9608	4.60		2.47	
0.9	9.8		10.5	0.9333		0.0667		4.80		2.58
1	9.5		10.5	0.9048		0.0952		4.50		2.42

At T = 45 °C				Relative	Relative	Relative				
g, Mg+Ca	Lower	Middle	Upper	Lower	Middle	Upper	Vo	Vw	SPo	SPw
0.1	1		10.1	0.0990		0.9010	4.00		2.15	
0.2	0.4		10.2	0.0392		0.9608	4.60		2.47	
0.6	9.8		10.6	0.9245		0.0755		4.80		2.58
0.7	9.5		10.6	0.8962		0.1038		4.50		2.42

R = 1.15

At T = 24 °C				Relative	Relative	Relative				
g, Mg+Ca	Lower	Middle	Upper	Lower	Middle	Upper	Vo	Vw	SPo	SPw
0.3	0.22		10.2	0.0216		0.9784	4.78		2.57	
0.4	10.2		10.2	1.0000		0.0000		5.20		2.80
1.2	10.6		10.6	1.0000		0.0000		5.60		3.01
1.3	10.3		10.7	0.9626		0.0374		5.30		2.85

At T = 35 °C				Relative	Relative	Relative				
g, Mg+Ca	Lower	Middle	Upper	Lower	Middle	Upper	Vo	Vw	SPo	SPw
0.3	0.72		10.2	0.0706		0.9294	4.28		2.30	
0.4	0.6		10.3	0.0583		0.9417	4.40		2.37	
1.2	10		10.7	0.9346		0.0654		5.00		2.69
1.3	9.6		10.7	0.8972		0.1028		4.60		2.47

At T = 45 °C				Relative	Relative	Relative				
g, Mg+Ca	Lower	Middle	Upper	Lower	Middle	Upper	Vo	Vw	SPo	SPw
0.3	0.75		10.3	0.0728		0.9272	4.25		2.28	
0.4	0.64		10.4	0.0615		0.9385	4.36		2.34	
1.2	10		10.8	0.9259		0.0741		5.00		2.69
1.3	9.5		10.8	0.8796		0.1204		4.50		2.42

Appendix 2D-XX Original data and corrected values for excess volumes and solubilization parameters: 625 mM DFX, Parts I (R = 0.86) and II (R = 1.15), $CaCl_2$ scan

R = 0.86

At T = 24 °C				Relative	Relative	Relative				
g, $CaCl_2$	Lower	Middle	Upper	Lower	Middle	Upper	Vo	Vw	SPo	SPw
0	9.9		9.9	1.0000		0.0000				
0.025	9.8		9.8	1.0000		0.0000		4.80		2.39
0.4	10.1		10.1	1.0000		0.0000		5.10		2.54
0.5	9.6		10.1	0.9505		0.0495		4.60		2.29

At T = 35 °C				Relative	Relative	Relative				
g, $CaCl_2$	Lower	Middle	Upper	Lower	Middle	Upper	Vo	Vw	SPo	SPw
0	0.2		10	0.0200		0.9800	4.80		2.39	
0.025	9.8		9.8	1.0000		0.0000		4.80		2.39
0.4	9.9		10.2	0.9706		0.0294		4.90		2.44
0.5	9.4		10.1	0.9307		0.0693		4.40		2.19

At T = 45 °C				Relative	Relative	Relative				
g, $CaCl_2$	Lower	Middle	Upper	Lower	Middle	Upper	Vo	Vw	SPo	SPw
0	0.2		10.1	0.0198		0.9802	4.80		2.39	
0.025	9.8		9.8	1.0000		0.0000		4.80		2.39
0.4	9.9		10.2	0.9706		0.0294		4.90		2.44
0.5	9.3		10.2	0.9118		0.0882		4.30		2.14

R = 1.15

At T = 24 °C				Relative	Relative	Relative				
g, $CaCl_2$	Lower	Middle	Upper	Lower	Middle	Upper	Vo	Vw	SPo	SPw
0.038	0.0001		10.1	0.0000		1.0000				
0.05	10		10	1.0000		0.0000		5.00		2.49
0.6	10.1		10.1	1.0000		0.0000		5.10		2.54
0.7	9.9		10.2	0.9706		0.0294		4.90		2.44

At T = 35 °C				Relative	Relative	Relative				
g, $CaCl_2$	Lower	Middle	Upper	Lower	Middle	Upper	Vo	Vw	SPo	SPw
0.038	0.6		10.1	0.0594		0.9406	4.40		2.19	
0.05	0.01		10	0.0010		0.9990	4.99		2.48	
0.6	9.8		10.2	0.9608		0.0392		4.80		2.39
0.7	9.7		10.2	0.9510		0.0490		4.70		2.34

At T = 45 °C				Relative	Relative	Relative				
g, $CaCl_2$	Lower	Middle	Upper	Lower	Middle	Upper	Vo	Vw	SPo	SPw
0.038	0.6		10.2	0.0588		0.9412	4.40		2.19	
0.05	0.01		10	0.0010		0.9990	4.99		2.48	
0.6	9.8		10.2	0.9608		0.0392		4.80		2.39
0.7	9.3		10.3	0.9029		0.0971		4.30		2.14

Appendix 2D-XXI Original data and corrected values for excess volumes and solubilization parameters: 625 mM DFX, Parts III (R = 0.86) and IV (R = 1.15), $MgCl_2 \cdot 6H_2O$+$CaCl_2$ scan

R = 0.86

At T = 24 °C				Relative	Relative	Relative				
g,Mg+Ca	Lower	Middle	Upper	Lower	Middle	Upper	Vo	Vw	SPo	SPw
0	9.9		9.9	1.0000		0.0000		4.90		2.44
0.05	9.9		9.9	1.0000		0.0000		4.90		2.44
0.1	10		10	1.0000		0.0000		5.00		2.49
0.8	10		10	1.0000		0.0000		5.00		2.49
0.9	10.3		10.5	0.9810		0.0190		5.30		2.64

At T = 35 °C				Relative	Relative	Relative				
g,Mg+Ca	Lower	Middle	Upper	Lower	Middle	Upper	Vo	Vw	SPo	SPw
0	0.2		10	0.0200		0.9800	4.80		2.39	
0.05	0.14		10	0.0140		0.9860	4.86		2.42	
0.1	0.12		10.1	0.0119		0.9881	4.88		2.43	
0.8	10.2		10.4	0.9808		0.0192		5.20		2.59
0.9	9.8		10.5	0.9333		0.0667		4.80		2.39

At T = 45 °C				Relative	Relative	Relative				
g,Mg+Ca	Lower	Middle	Upper	Lower	Middle	Upper	Vo	Vw	SPo	SPw
0	0.2		10.1	0.0198		0.9802	4.80		2.39	
0.05	0.14		10.1	0.0139		0.9861	4.86		2.42	
0.1	0.13		10.2	0.0127		0.9873	4.87		2.42	
0.8	10.3		10.5	0.9810		0.0190		5.30		2.64
0.9	9.8		10.6	0.9245		0.0755		4.80		2.39

R = 1.15

At T = 24 °C				Relative	Relative	Relative				
g,Mg+Ca	Lower	Middle	Upper	Lower	Middle	Upper	Vo	Vw	SPo	SPw
0.05	0.0001		10	0.0000		1.0000	5.00		2.49	
0.1	10		10	1.0000		0.0000		5.00		2.49
1.1	10.6		10.6	1.0000		0.0000		5.60		2.79
1.2	10.75		10.8	0.9954		0.0046		5.75		2.86

At T = 35 °C				Relative	Relative	Relative				
g,Mg+Ca	Lower	Middle	Upper	Lower	Middle	Upper	Vo	Vw	SPo	SPw
0.05	0.4		10	0.0400		0.9600	4.60		2.29	
0.1	0.35		10	0.0350		0.9650	4.65		2.31	
1.1	10.1		10.6	0.9528		0.0472		5.10		2.54
1.2	10		10.7	0.9346		0.0654		5.00		2.49

At T = 45 °C				Relative	Relative	Relative				
g,Mg+Ca	Lower	Middle	Upper	Lower	Middle	Upper	Vo	Vw	SPo	SPw
0.05	0.4		10.1	0.0396		0.9604	4.60		2.29	
0.1	0.35		10.1	0.0347		0.9653	4.65		2.31	
1.1	10.1		10.7	0.9439		0.0561		5.10		2.54
1.2	10		10.8	0.9259		0.0741		5.00		2.49

Appendix 2D-XXII Corrected values for optimum solubilization parameters (SP*) and optimum salinities (s*)

mM DFX, Part	s* $CaCl_2$ or $MgCl_2.6H_2O+CaCl_2$ grams	s* $MgCl_2+CaCl_2$ grams	SP* 24 °C mL/g	SP* 35 °C mL/g	SP* 45 °C mL/g
440, I	0.68		3.09		
340, I	0.80				2.84
340, I	0.88			2.92	
340, I	0.93		2.98		
280, I	0.97				2.75
280, I	1.05			2.81	
280, I	1.10		2.89		
220, I	1.12				2.69
220, I	1.17			2.89	
220, I	1.25		2.25		
120, I	1.40				2.56
120, I	1.40			2.82	
120, I	1.40		3.08		
80, I	1.45				2.69
80, I	1.45		3.08		
440, II	0.90		3.05		
440, II	0.71			2.95	
440, II	0.70				2.91
500, II	0.80		3.00		
520, II	0.30			2.81	
520, II	0.31				2.79
440, III	1.62	1.06	2.98		
440, III	1.49	0.98		2.85	
440, III	1.47	0.97			2.83
500, III	1.20	0.79	2.90		
500, III	1.05	0.69		2.90	
500, III	1.03	0.67			2.91
520, III	1.16	0.76	2.96		
520, III	0.98	0.64		2.91	
520, III	0.94	0.62			2.92
440, IV	1.89	1.24	2.96		
440, IV	1.73	1.14		2.83	
440, IV	1.67	1.10			2.81
500, IV	1.53	1.00	3.02		
500, IV	1.38	0.91		2.86	
500, IV	1.36	0.89			2.83
520, IV	1.36	0.89	3.36		
520, IV	1.33	0.87		2.81	

Chapter 3
Surfactant Adsorption in Porous Media

3.1 Abstract

An overview of some of the significant findings of surfactant adsorption research is presented. Subjects include the importance of surfactant adsorption in petroleum applications, some history of surfactant adsorption research, the mechanisms that have been proposed to explain observed adsorption behavior, and a review of several significant surfactant adsorption studies. The emphasis of this review is on the understanding of the mechanisms of surfactant adsorption as they relate to applications of surfactants in petroleum processes.

Note: Portions of this chapter have been published in **Surfactant, Fundamentals and Applications in the Petroleum Industry**, Laurier L. Schramm, Editor. The current version has been formatted for this dissertation. Portions of section 3.5.3 have been edited to examine the adsorption behavior of the alkyldiphenyl oxide sulfonate surfactants onto positively and negatively charged surfaces and the adsorption mechanisms demonstrated by these surfactants in their adsorption onto alumina.

3.2 Introduction

Surfactants have a variety of applications in the petroleum industry, and surfactant adsorption is a consideration in any application where surfactants come in contact with a solid surface. In enhanced or improved oil recovery (EOR or IOR) surfactants can be used in classic micellar/polymer (surfactant) flooding, alkaline/surfactant/polymer (ASP) flooding or in foams for mobility control or blocking and diverting. Surfactants can act in several ways to enhance oil production: by reducing the interfacial tension between oil trapped in small capillary pores and the water surrounding those pores, thus allowing the oil to be mobilized; by solubilizing oil (some micellar systems); by forming emulsions of oil and water (alkaline methods); by changing the wettability of the oil reservoir (alkaline methods) or by simply enhancing the mobility of the oil (Taber et al., 1997). In selecting a suitable surfactant for any EOR application, one of the criteria for economic success is minimizing surfactant loss to adsorption. Factors affecting surfactant adsorption included temperature, pH, salinity, type of surfactant and types of solids found in the reservoir. Usually the only factor that can be manipulated for EOR is the type of surfactant to be used; the other factors being determined by reservoir conditions.

When an oil reservoir is first produced, forces such as overburden pressure and evolution of gases dissolved in the reservoir oil cause spontaneous production of oil because of the pressure gradient between the interior of the reservoir and the production well. This spontaneous production is commonly referred to as primary recovery. Following the completion of the primary recovery phase, 60 to 80% of the oil originally in the reservoir commonly remains in the formation. Production has ceased because a

pressure gradient no longer exists to mobilize the oil. Secondary recovery consists of water-flooding to displace the remaining oil from the injection to the production well.

Nevertheless, a point is soon reached where the amount of oil produced by water-flooding is insufficient to justify the operating costs of the project. At this time it is common for 30 to 60% of the original reservoir oil to remain in the formation. The oil is trapped in the pores of the rock by capillary forces arising from the high oil/water interfacial tension. Additional water injected into the formation simply bypasses the trapped oil droplets on its way to the production well, following the path of least resistance to the flow.

It has long been known that surfactants lower oil/water interfacial tensions, thus reducing capillary forces such as those trapping the remaining oil. This raises the possibility of releasing trapped oil droplets by injecting surfactants into the reservoir. Early demonstrations of the technical feasibility of enhanced oil recovery by surfactant flooding (sometimes referred to as micellar or chemical flooding) were done in the laboratory by Novosad et al. (1982) and in field tests by Lake and Pope (1979) and by Holm (1982). In addition to the technical feasibility, economic feasibility must also be determined; however, the economic feasibility depends on a complex of factors such as oil prices, international economies, and the cost of the surfactants. Generally, the cost of the surfactant is the single most expensive item in the cost of a chemical flood. These costs include both the initial investment in purchasing the surfactant, as well as the cost of replacing surfactant that has been lost to adsorption. It is frequently found that the amount of surfactant adsorbed accounts for most of the cost of the surfactant. Since these surfactants are synthesized from petroleum, their costs will rise at least as fast as that of

the oil they are used to produce. So simply waiting for oil prices to increase will not necessarily make EOR economically feasible. The oil produced by a chemical flood must then be sufficient to replace the oil used for the surfactant (unless some means of recovering the surfactant from the reservoir is feasible), to pay for the price of producing the surfactant from the oil, to pay for all the additional engineering, equipment and operating costs during the several years the flood is occurring, and to provide a reasonable return on investment. All of these demands must be satisfied in a volatile oil market in which oil prices may fluctuate between the beginning of a surfactant flood and the time the tertiary oil is finally produced. Producing more barrels of oil for each kilogram of surfactant injected into the reservoir is a technological problem that has direct bearing on the economics of the process. Understanding and controlling the amount of surfactant adsorbed directly affects project economics. The following is a sample calculation that illustrates just how substantial the costs associated with losing surfactant to adsorption can be.

An area one acre (4047 m^2) by 3 meters deep is to be swept with a surfactant solution. Core samples reveal that the subsurface is approximately 70% solid material having a density of 2.5 g/cc. Thus approximately $2.12x10^{10}$ grams of solid material are available for adsorption of the surfactant. If the specific area of this solid were 0.5 m^2/g then the surface area of the solid would be $1.06x10^{10}$ m^2. Assuming surfactant adsorption reaches bilayer coverage at a density of 1 molecule per 0.5 nm^2 of available surface area which is typical for an ionic surfactant, then approximately $3.5x10^4$ moles of surfactant would be adsorbed onto the solid. If the surfactant had an average molecular weight of 500 g/mol this would result in $1.76x10^4$ kilograms of surfactant being adsorbed.

Assuming a purchase price of $2/kg for this surfactant, then the resultant loss to adsorption would be $34,300. If this surfactant were being used to produce oil worth $18/bbl then 1960 barrels would have to be produced just to compensate for the adsorbed surfactant. Looking at this situation in terms of EOR, if there is 50% residual saturation and EOR is expected to remove 50% of the residual or 5727 barrels of oil, then the cost of the surfactant loss to adsorption would account for approximately one-third of the total value of the oil recovered by EOR. Obviously, it is critical to the economic success of an EOR project that adsorption be minimized in the design of the project; to do so requires an understanding of surfactant adsorption mechanisms.

In the first part of this chapter, reviews of the background research on surfactant adsorption and the mechanisms involved in surfactant adsorption are presented. In the second part of the chapter, several pertinent experimental studies are presented which illustrate the mechanisms of surfactant adsorption in various systems. As already stated, there are multiple factors that affect adsorption. These factors will now be presented, beginning with the characteristics of the solid materials commonly used in adsorption studies.

3.3 Solid Surface Chemistry

Many surfactants adsorb onto a solid due, in a large part, to the electrostatic interactions between charged sites on the solid surface and the charged head groups of the ionic surfactants. The adsorption of nonionic surfactants is discussed later in this chapter. The structures of several solids used in adsorption research and the electrical properties

associated with them are discussed in this section. Most mineral surfaces in reservoirs can assumed to be charged.

3.3.1 Types of Solids

There have been a variety of solids used in surfactant adsorption research. These solids have included "ideal" reservoir materials such as alumina (Al_2O_3) and silica (SiO_2); and "real" materials such as kaolinite clays, river alluvium, and sandstones.

There are several crystalline phases of alumina arising from the different configurations possible for the aluminum and oxygen ions. The surface charge on alumina in contact with a surfactant solution arises indirectly from the crystal structure of the alumina. The most commonly used alumina in adsorption studies has been α-alumina or corundum which has a rhombohedral crystal structure comprising a hexagonal close-packed array of oxygen ions with aluminum ions on two-thirds of the octahedral sites (Greenwood et al., 1997). The other two forms of alumina are the η-phase, which has a cubic structure, and the θ-phase, which has a monoclinic structure.

Crystalline silica can exist as quartz, cristobalite, and tridymite, with quartz being the form most commonly used in adsorption studies. Many studies also use amorphous silicon oxides. The quartz crystal consists of silica tetrahedra with the silicon ions located in the center and the oxygen ions located at the corners. The tetrahedra are arranged to form interlinked helical chains (Greenwood et al., 1997). The different forms of quartz are distinguished by the differences between the angles formed by the Si-O-Si bond, with the α-form being the most common.

Kaolinite is a clay mineral with the chemical formula: $Al_2(OH)_4Si_2O_5$ (Greenwood et al., 1997) or $(OH)_8Si_4Al_4O_{10}$ (Grim, 1968). The basic unit of kaolinite consists of a single silica tetrahedral sheet and a single alumina octahedral sheet such that the oxygen atoms at the tips of the silica tetrahedrons and one of the oxygen atoms of the alumina octahedral sheet form a common layer.

River alluvium from the Canadian River in Cleveland County, Oklahoma has been used in several recent adsorption studies (Palmer et al., 1992, Rouse et al., 1996; Sabatini et al., 2000). Palmer et al. (1992) profiled the alluvium and found that it consisted of 91% sand, 2% silt and 7% clay.

An adsorption medium often considered typical of reservoir solids is sandstone which is an agglomeration of individual minerals with quartz as the primary component. Other minerals comprising sandstone include chert, fieldspar, mica, illite, kaolinite and calcium carbonate. A common type of sandstone used in adsorption research is Berea sandstone (Novosad, 1982; Mannhardt et al., 1992).

Other solids used in surfactant adsorption research include rutile (TiO_2) (Böhmer et al., 1992b and 1992c; Koopal et al., 1995; Lee and Koopal, 1996), carbonates, and graphite (Zhu et al., 1990; Manne et al., 1994; Manne et al., 1995; Krishnakumar and Somasundaran, 1996). Studies with carbonates have included purified calcium and magnesium carbonate (Tabatabai et al., 1993) and Indiana limestone (Mannhardt et al., 1992) and Baker dolomite (Mannhardt et al., 1992 and Tsau et al., 1994).

With the exception of graphite, the common characteristic of the solids used in adsorption research is the capacity of the surface of these solids to have an electrical surface charge. This capacity arises from the interaction between the oxygen atoms in the

structure and water molecules. It is especially significant to note that under typical reservoir conditions carbonates and sandstones have opposite charges.

3.3.2 Electrical Characteristics and the Electrical Double Layer

Electrical surface charges arise from charge imbalances due to imperfections in the crystal structure and preferential adsorption of counter or potential determining ions (Fuerstenau, 1970; van Olphen, 1963). At low surfactant concentrations the surface charge largely determines the surfactant adsorption. However, as the surfactant concentration increases other factors such as the tendency of the surfactant to aggregate, become significant.

Imperfections in the crystal structure include isomorphous replacement of ions within the crystal lattice, broken bonds, dislocations, and lattice defects (Fernandez, 1978). Ion replacement leads to a charge imbalance within the lattice resulting in a charged surface. A common substitution is the replacement of silicon atoms in kaolinite by aluminum atoms.

When a surface is fractured, bonds between layers, such as the alumina-silica layers in kaolinite or the metal-oxygen bonds in alumina, can be broken, leaving ions with unsatisfied valance conditions. The resulting charge can be either negative or positive depending on the type of bond broken. A related source of surface charge is the partial dissolution of the solid surface by water. This also leaves surface ions with unsatisfied valences.

Lattice defects are holes within the lattice due to missing ions. The missing ions leave the lattice with unbalanced charges. Charge imbalances can also arise in crystal

structures due to dislocations. There are two types of dislocations. In the screw dislocation a section of a crystal is skewed one atom spacing. In the edge dislocation an extra plane of atoms has been inserted into a section of a crystal. The charge imbalances arise at the sites of the dislocations.

Charge imbalances and broken bonds are accommodated by chemical adsorption of water by the solid surface. The chemically adsorbed water molecule forms an amphoteric site on the surface. Deprotonation of the group leaves a negative charge on the surface. Protonation of the amphoteric group leads to a positive charge on the surface. This charging mechanism makes the surface charge highly dependent on the pH of the contacting solution.

3.3.3 Electrical Double Layer

One of the earliest theories proposed for explaining interactions of charged particles at the solid/liquid interface was the electrical double layer theory developed to describe the formation of a charge on a mercury electrode surface. In early studies of surfactant adsorption on minerals, the surfactant concentrations were low enough that there were no interactions between surfactant monomers on the solid surface. The simple electrical double layer model developed for mercury electrodes was adequate for describing the adsorption behavior. When the surfactant concentrations increased to levels where surfactants began to interact with one another at the surface, this theory could no longer describe the adsorption behavior. The addition of higher electrolyte concentrations also affected the ability of this theory to describe adsorption behavior. The equations shown on the following pages provide an introduction to the kinds of

interactions that must be considered in describing adsorption behavior. In addition this theory serves as a starting point for many of the more complex models of surfactant adsorption. Some discussion of current models is provided in the next section.

The adsorption of counterions or potential determining ions at relatively low concentrations can be described by the electrical double layer which develops in response to a charge on the mineral surface. An electrical potential exists across an interface when there is an unequal distribution of charges across that interface. This unequal distribution results in each side of the interface acquiring net charges of opposite sign.

The idea of the electrical double layer was proposed by Helmholtz in 1879, and modified by Stern in 1924 (Rosen, 1989). In the Stern modification the counterions in the solution, opposite in charge relative to the surface, were divided into two layers: [1] a layer of ions adsorbed close to the surface (generally referred to as the Stern layer) and [2] a diffuse layer of counterions sometimes referred to the Gouy layer. As shown in Figure 3-1, the potential decreases rapidly within the Stern layer (δ) and more gradually within the diffuse layer (d). The net charge in the Stern layer plus the Gouy layer is equal and opposite in sign to the surface charge. For minerals the surface charge is primarily controlled by the pH and the nature of the mineral.

The diffuse layer charge, σ_d, which extends out from the plane δ seen in Figure 3-1, can be described by the following:

$$\sigma_d = -\sqrt{\frac{2\varepsilon kT}{\pi}}\sqrt{n_0}\sinh\left(\frac{Ze\Psi_\delta}{2kT}\right) \tag{3-1}$$

Where **ε** is the dielectric constant of water, **k** is Boltzmann's constant, **T** is the absolute temperature, **Z** is the valence charge including the sign of the adsorbing ion, **e** is the elemental charge, Ψ_δ is the electrical potential at the plane a distance δ from the surface (the Stern plane) and $\mathbf{n_0}$ is the number of ions/cc in the bulk phase (where the electrical potential is zero).

The adsorption of counterions at the plane δ from the surface can be described by the Gouy-Chapman equation as:

$$\Gamma_\delta = 2rC\exp\left(\frac{-W_\delta}{kT}\right) \tag{3-2}$$

Where Γ_δ is the adsorption density, **r** is the radius of the adsorbed ion, **C** is the concentration of ions in the bulk, and $\mathbf{W_\delta}$ is the work required to bring ions from the bulk solution to the plane δ and is comprised of electrostatic and interaction terms:

$$W_\delta = Ze\Psi_\delta - \phi \tag{3-3}$$

In equation (3-3) $\mathbf{Ze\Psi_\delta}$ is the electrical work of bringing the ion into the Stern plane, and **ϕ** is the free energy change associated with the partial removal of the alkyl chain for a surfactant from the water phase. Assuming for an alkyl chain of **n** carbon atoms:

$$\frac{\phi}{k\,T} = \frac{n\,\phi'}{k\,T} \tag{3-4}$$

Where ϕ' is the interaction energy per CH_2 group between adjacent chains of adsorbed surfactant molecules. This interaction begins when the bulk surfactant concentration reaches the hemimicelle concentration which is the concentration at which the first surfactant aggregates form on the solid surface. Details of the concept of the hemimicelle are presented in the next section of this chapter.

In applying these equations to surfactant adsorption research for surfactant concentrations greater than the hemimicelle concentration, Somasundaran et al. (1964) put equation (3-2) into logarithmic form and differentiated to give:

$$\frac{d\ln\Gamma_{\delta}}{d\ln C} = 1 - \frac{d\left(Ze\Psi_{\delta}/kT\right)}{d\ln C} - \frac{\phi'}{kT}\frac{dn}{d\ln C} \tag{3-5}$$

Where **n** is the number of carbon atoms and **dn/d ln C** indicates that the effective number of carbon atoms that can be removed totally from the aqueous environment by chain-chain association increases as the surface coverage increases. (van Olphen, 1963)

The concept of the electrical double layer works well in describing the behavior of simple ions like Na^+ or Cl^- or single ions like surfactants when a non-electrostatic term is added to the adsorption potential. For potential determining ions such as H^+ and OH^- however, the "site-binding" model is frequently used. This model is used to describe the development of a surface charge at a mineral/solution interface. It requires knowing the reactions responsible for surface charge development and the potential-charge relationships at the interface. It also limits the concentration of the surface species to the

total number of sites available on the surface. These interactions are specific for individual systems (Davis et al., 1978; James et al., 1982; Hankins et al., 1996).

The adsorption of H^+ and OH^- at the surface affects the charge on the surface of the solid. The charge on the surface can be negative, positive or neutral. The neutral condition is referred to as the point of zero charge or pzc. The pzc is the pH at which the net charge on the surface is zero. At a pH value above or below the pzc the surface is negatively or positively charged, respectively. In the case of alumina with a pzc of approximately 9 (Fuerstenau, 1970), the surface is positively charged at a pH less than 9 and negatively charged for pH values greater than 9. For silica the pzc is 2-3 (Fuerstenau, 1970), so the surface is negative above pH 3. For kaolinite the pzc is approximately 4.5 (Fernandez, 1978). If adsorption is desirable then the surfactant and surface should have opposite charges. If adsorption in undesirable, which is the case for applications such as EOR, then it may be advantageous to have a surfactant with the same charge as the solid. Surfactants will still adsorb on like charged surfaces, however, especially at high concentrations (above the CMC) and in the presence of multivalent counterions.

3.4 Mechanisms of Surfactant Adsorption

3.4.1 Single Surfactant Systems

Surfactant adsorption at the solid-liquid interface has been studied for several decades. Much of the early work reported in the literature was based on selecting the most effective surfactant for purifying ores by flotation. These studies focused on determining the interactions that bring about adsorption and determining the structures of the surface aggregates formed. Currently there is general agreement on the interactions

that bring about adsorption, but there is still extensive discussion concerning the structure of the surfactant surface aggregates.

Some of the experimental techniques employed in these studies have included determining the change in surfactant concentration in the bulk solution upon adsorption, zeta potential measurements, and probe techniques (electron spin resonance and fluorescence). Attempts to describe the adsorption behavior exhibited in the adsorption isotherms has led to the development of several mathematical models. (Somasundaran et al., 1964; Scamehorn et al., 1982a; Harwell et al., 1985; Zhu et al., 1989; Böhmer et al., 1992). To date, none of the models are capable of fully accounting for all of the phenomena that affect surfactant adsorption without introducing ad hoc assumptions and adjustable parameters, but they have offered some interesting insights.

Most adsorption studies have employed the surfactant depletion method with the results being presented as isotherms which are simply plots of the amount of surfactant adsorbed per gram of solid or per surface area of solid versus the equilibrium surfactant concentration at a constant temperature. These plots can be constructed using log-log, linear-log or linear-linear scales with the most common choice being the log-log scale. Böhmer and Koopal (1992b) present a discussion of the advantages and disadvantages for the different scales. The log-log scale can be used to obtain information over wide ranges of adsorption and surfactant concentrations, and the plots generally have abrupt changes in slope with increasing surfactant concentration. A typical four-region isotherm constructed on a log-log scale for a monoisomeric anionic surfactant is shown in Figure 3-2. The reasons for the changes in slope are discussed below.

Not all log-log isotherms seen in the literature consist of four regions. Some of the earliest adsorption studies were conducted by de Bruyn in 1955, Shinoda in 1963, and Jaycock and Ottewill in 1963 using surfactant concentrations well below the CMC, and the reported isotherms consisted of only two regions (Somasundaran et al., 1964). Further studies showed that at higher surfactant concentrations log-log isotherms exhibited three distinct regions (Somasundaran et al., 1966) and at still higher concentrations four regions (Scamehorn et al., 1982b; Chandar et al., 1987). It is important to note that the exact shape of the isotherm will depend on several factors including the type of surfactant, the charge on the surface, and the presence or absence of additional compounds including electrolytes, co-surfactants, hydrotropes or alcohols.

The mechanisms driving surfactant adsorption are generally discussed in terms of the four-region isotherms. At low surfactant concentrations, designated as region I (see Figure 3-2), the adsorption behavior can usually be described by Henry's Law, i.e. linear with a slope of one. This is also the region where the simple Stern/Gouy double-layer model is appropriate. Early work by de Bruyn (1955) and Gaudin and Morrow (1954), and Gaudin and Fuerstenau (1955) determined that in this region surfactant monomers adsorbed as individual ions with no interaction between the adsorbed molecules. This conclusion was based on the zeta potential measurements of quartz/dodecylammonium chloride systems at low surfactant concentrations being nearly identical to the zeta potential measurements of quartz/sodium chloride systems (Gaudin and Fuerstenau, 1955). Today, it is known that the surface-surfactant interaction depends on the type of surfactant. For nonionic surfactants the interactions involve hydrogen bonding between surface hydrogen atoms and proton acceptors in the head groups and hydrophobic

bonding between the hydrocarbon tails of surfactants and the surface. Scamehorn et al. (1982a) and Harwell et al. (1985) showed that a tail-surface interaction involving adsorbed monomers affects the value of the Henry's Law coefficient. For ionic surfactants there are electrostatic interactions between the head groups of the surfactants and charged sites on the surface. This electrostatic attraction is typically described in terms of the interaction of the charged surfactant ion with the electrical double layer of the solid.

The mechanism dominating adsorption in region II was described by Gaudin and Fuerstenau (1955) as being due to the association of the adsorbed surfactants into patches at the solid/liquid interface. These associations were attributed to tail-tail interactions, which are the same hydrophobic interactions by which micelle formation is described today.

The region I/region II break corresponds, therefore, to the surfactant concentration at which the first surfactant aggregates form on the surface. This concentration is referred to as the hemimicelle concentration (HMC) (Somasundaran and Fuerstenau, 1966) or as the critical admicelle concentration (CAC) (Harwell et al., 1985). This aggregate formation can be viewed as a two-dimensional phase transition occurring on the highest energy patches on the solid surface (Scamehorn et al., 1982a). The CAC/HMC varies with surfactant chain length and branching in the same manner as CMC varies with these parameters (Wakamatsu and Fuerstenau, 1968). If the system contains ionic surfactants, the addition of an electrolyte will decrease the CAC in the same manner that electrolytes reduce the critical micelle concentration (CMC) (Bitting and Harwell, 1987). A note of practical application: in systems with added electrolyte care must be

taken to avoid precipitation of the surfactant by the electrolyte (Amante et al., 1991). The presence of a precipitate is easily hidden by the solid material upon which adsorption is supposed to be occurring, and the decrease in surfactant concentration due to precipitation could be interpreted as greater surfactant adsorption than what is actually occurring. Familiarity with the precipitation phase boundaries of the surfactant for a given electrolyte or preliminary precipitation analyses using the surfactant and electrolyte concentrations of interest may eliminate this error.

In region III a decrease in the slope relative to the slope in region II is seen. There have been several theories proposed to explain this change. This change in slope was attributed to the surfactant ions having filled all of the surface sites by the end of region II with further adsorption being due to association between first and second layer hydrocarbon chains in region III (Somasundaran et al., 1964; Somasundaran and Fuerstenau, 1966). The observed change in slope was also attributed to a reversal in surface charge due to the adsorbed surfactant ions. Scamehorn et al. (1982a) proposed that bilayer formation began in region II and continued into region III but at a different rate. This can also be viewed as adsorption taking place on the least energetic patches on the surface in region III.

Region IV or plateau adsorption generally begins at or near the critical micelle concentration (CMC) and is characterized by little or no increase in adsorption with increasing surfactant concentration. In this region micelles exist in the bulk solution and act as a chemical potential sink for any additional surfactant added to the system. Most researchers agree that the surfactant aggregates have a bilayer structure when the solution concentration exceeds the CMC. The total adsorption above the CMC may still be

substantially less than complete a bilayer, however, and depends strongly on surface charge and, therefore, pH.

There have been several surfactant structures proposed in attempts to describe the adsorption isotherm. Two of them have been mentioned already, the hemimicelle and local bilayer or admicelle. Gaudin and Fuerstenau (1955) introduced the term hemimicelle to describe the adsorption behavior they had observed in region II. Hemimicelles can be described as aggregates of adsorbed surfactant molecules in which the surfactant monomers are arranged in a single layer with the head groups facing the solid surface. This structure was proposed to explain the increased adhesion of bubbles to the surface of minerals in region II of the adsorption isotherm. The bilayer structure consists of surfactant monomers arranged such that the head groups of the first layer are facing the surface and those of the second layer face the surrounding solution. The tail groups of the two layers interact in the same manner as they do in micelles. The bilayer structure was first proposed in the 1940's (Gaudin and Fuerstenau, 1955). In 1985 the term admicelle was introduced and was used to describe surfactant surface aggregates which were bilayer in structure and had formed without an intermediate hemimicelle structure existing at a lower surfactant concentration (Harwell et al., 1985). Such structures almost certainly dominate at the CMC when the total surface coverage is well below complete bilayer coverage.

Some additional structures that have been proposed are the surface micelles proposed by Gao et al. (1987), and the hemicylinders and cylinders proposed by Manne et al. (1994; 1995). Surface micelles are aggregates described as spheres with only one surfactant monomer adhering to the solid surface. The hemicylinder and cylinder

structures were based on atomic force microscopy (AFM) images of several surfactant systems involving adsorption of cetyltrimethylammonium bromide on pyrolitic graphite (Manne et al., 1994), tetradecyltrimethylammonium bromide (C_{14}TAB) on silica, C_{14}TAB and didocecyl dimethylammonium bromide on mica (Manne and Gaub, 1995), and C_{14}TAB, hexadecyltrimethylammonium hydroxide, and sodium dodecylsulfate on gold (Jaschke et al., 1997). These cylindrical structures are arranged such that the head groups of the surfactants are facing outward.

As the study of surfactant adsorption has evolved, the debate over the exact structure of the adsorbed surfactant aggregates has become more confused rather than becoming clarified. Until the recent advent of AFM studies most of the debate had focused on monolayer (hemimicelle) and bilayer (admicelle) structures. Current literature indicates that many researchers are beginning to believe that the structure of the adsorbed surfactant depends on the system being studied. Somasundaran and Kunjappu (1989) introduced the term solloid to describe any surfactant aggregates at the solid-liquid interface without attempting to define its morphology. Despite the uncertainty or at least the complexity of the structure of adsorbed surfactant aggregates, it is clear that micelle-like aggregates form spontaneously at concentrations well below the bulk CMC. Also, a complete bilayer is formed at the maximum adsorption of surfactants adsorbing onto surfaces of opposite charge.

3.4.2 Mixed Surfactant Systems

Most surfactant systems used in the petroleum industry are comprised of more than one surfactant. The similarities and differences between pure component and mixed

surfactant systems have been presented by Harwell and Scamehorn (1993). As adsorption behavior from single surfactant systems mirrors the behavior of micelle formation in solution, so too does adsorption from mixed surfactant systems mirror mixed micelle behavior. Since there is no interaction between surfactant molecules in region I, adsorption in this region for a mixed surfactant system is driven by the same interactions as for single surfactant systems, and the surfactants adsorbing from a mixture will behave as their pure components; but as the surfactant concentrations increase, the position of the region I/region II break may shift relative to the break in the single component adsorption isotherms. Adsorption from a mixture may fall in region II when the adsorption of either pure component would still be in region I. This behavior is exactly analogous to the lowering of the CMC in mixed surfactant systems.

The position of the remainder of the isotherm (regions II, III and IV) relative to the adsorption isotherms of the pure component will depend on the types and amounts of surfactants in the mixture. When surfactants of similar head groups are mixed, the adsorption of the mixture will vary monotonically between the adsorptions of the pure components. This is the same as the CMC of the mixture varying monotonically with the mole fraction of each component. If the mixture exhibits negative deviations from ideal mixing behavior such as when ionic and nonionic surfactants are mixed, then the CAC will also exhibit negative behavior. That is the mixture CAC will be lower than either of the CAC's of the pure components. If anionic and cationic surfactants are mixed then deviations more negative than those seen for ionic-nonionic systems will be seen. This results in CAC's that will again be lower than that of either of the pure components adsorptions. To summarize: mixtures exhibiting nonideal behavior can produce the same

surface coverage but with lower total surfactant concentrations relative to the pure component systems.

3.5 Experimental Studies

Surfactant adsorption research covers many disciplines. Theoretical studies include attempts to create models capable of accounting for every facet of surfactant adsorption including determining the structure of the adsorbed aggregates and determining the mechanisms driving the adsorption process. Practical studies focus on evaluating surfactant systems suitable for applications like ore flotation, improved oil recovery, in situ and ex-situ soil remediation (a field which has its origins in EOR), cleaning applications, surfactant based separation processes, and wetting. Often the results obtained from a study have both theoretical and practical applications.

The literature review in this section is intended as an introduction to the types of research that have been done; and is divided into the following sections: (3.5.1) general adsorption studies with an emphasis on those results which were significant in furthering the basic understanding of surfactant adsorption; (3.5.2) applied studies with an emphasis on EOR and related fields; and (3.5.3) recent studies involving alkyldiphenyl oxide sulfonate surfactants.

3.5.1 Fundamental Adsorption Studies

This section presents a few of the studies which were fundamental to understanding the mechanisms of surfactant adsorption and several recent studies which have served to expand our basic knowledge.

3.5.1.1 Cationic Surfactant onto Quartz

In the early 1950's attempts were made to move the ore flotation process from an art to a science. These attempts were driven by the more complex ores being mined and the recognized need for a systematic approach to selecting a suitable collector (surfactant) for a given ore. The purpose of the collector was to promote adhesion of ore fines to bubbles sparged into a slurry of ore. The early studies focused on quartz using dodecylammonium acetate concentrations which spanned what are now termed regions I and II adsorption.

Figure 3-3 is the isotherm which Gaudin and Bloecher (1950) obtained. They noted that the observed change in slope in the isotherm occurred slightly below the bulk critical micelle concentration (CMC), and that the adsorption was reversible. They also found that the amount adsorbed in a flotation process which resulted in almost complete recovery of the oxide was under 5% of the amount required for monolayer coverage.

Based on zeta potential measurements of dodecylammonium chloride adsorption onto quartz (Gaudin and Fuerstenau, 1955), it was proposed that the observed change in the adsorption behavior was due to the association of the adsorbed surfactants into patches at the solid/liquid interface. It was hypothesized that these aggregates of adsorbed surfactant formed for the same reasons surfactant monomers associate to form micelles in solution, and the term hemimicelle was introduced. The aggregates were proposed to be "half" micelles on the surface because the surface now spontaneously dewet to allow bubble attachment. Zeta potential measurements showed that the surface potential changed from negative to positive in systems containing multivalent ions. This change in potential was also observed in systems containing dodecylammonium ions. Based on

these observations it was proposed that the association of adsorbed ammonium ions acted as multivalent cations.

Continuing research led to the application of electrical double layer theory to describe surfactant adsorption. This theory was applied to sodium dodecyl sulfonate adsorption onto alumina (Somasundaran and Fuerstenau, 1966; Chandar et al., 1987). Region III adsorption was observed and attributed to the surfactant ions having filled all of the first layer sites by the end of region II with further adsorption being due to association between of the first layer hydrocarbon chains and second layer hydrocarbon chains. The region II/III transition was attributed to reversal of the surface charge leading to repulsion of the surfactant ions from the surface in region III thus reducing the electrical component of the adsorption potential. For a time after these studies, researchers tended to focus on the electrical interactions between the surfactant ions and the surface while other features, such as patchwise adsorption and the presence of bilayers, were overlooked.

3.5.1.2 Cationic Surfactants onto Silica

The effect of surfactant types on the adsorption mechanism was illustrated by a study of dodecylpyridinium chloride (DPC) and cetylpyridinium chloride (CPC) onto silica. (Goulob and Koopal, 1997) Due to the more hydrophobic nature of the silica surface relative to rutile and alumina, both the head and tail groups of DPC and CPC can interact with the solid surface. Adsorptions were conducted with various pH values and salt concentrations. The resulting isotherms, on a logarithmic scale, consisted of four regions, but the shape of the isotherms depended on the potassium chloride concentration and the pH. Figure 3-4 illustrates the differences in these isotherms relative to the typical

isotherm shown in Figure 3-2 for varying pH values. Adsorption of DPC onto the commercial silica Aerosil was also conducted at two salt concentrations (0.001M and 0.1M). For both salt concentrations used, the slopes of the region I adsorptions were approximately one, and the region IV plateau adsorption was only slightly higher for the higher salt system. For the low salt system region II appeared as a pseudoplateau. This behavior was attributed to both the head and tail groups adsorbing onto to the surface and thus inhibiting adsorption. For the high salt concentration there was no pseudo-plateau but a steep increase in the slope as is typically seen for surfactant adsorption on mineral oxides. This steep increase in the slope was attributed to the salt ions being able to screen the headgroup repulsion. As in micelle formation this screening allows the head groups to approach each other more closely and facilitate surfactant aggregation. Similar results were obtained for tetramethylammonium bromide (TMAB) and cetyltrimethylammonium bromide (CTAB) (Goulob et al., 1996).

3.5.1.3 Anionic Surfactant onto Alumina and Kaolinite

A study involving the adsorption behavior of isomerically pure alkylbenzene sulfonates onto alumina and kaolinite and the development of a predictive patchwise adsorption model to explain the observed isotherm examined the underlying forces causing surfactant adsorption and provided information which could aid in minimizing the loss of surfactant to adsorption in EOR (Scamehorn et al., 1982a). The resulting isotherms did not exhibit apparent adsorption maxima or minima that had been seen in previous studies. The presence of maxima and minima in earlier studies were attributed to using surfactants which were not monoisomerically pure and to the interactions which occur between the

isomers in mixed micelles during adsorption. This is analogous to the minima observed in surface tensions curves for mixed surfactant systems. The agreement between the theoretical calculations and experimental data was good for both mineral oxide systems except for the region just prior to the plateau region for the kaolinite isotherms. The structures predicted by the patchwise adsorption model were unassociated molecules in region I, hemimicelles then mixtures of hemimicelles and bilayers in region II, and bilayers in regions III and IV.

A second aspect of this work was comparing the plateau adsorption on alumina at varying pH values to bilayer values calculated from adsorption densities for monolayers. The monolayer values were estimated to range from 1.94 to 2.87 molecules/100 $Å^2$. These estimates were determined from surface tension data, film pressure studies on sodium dodecyl sulfonate, and sulfonate head group densities for cubic packing. When the plateau adsorption values were compared with adsorption densities for bilayer coverage calculated from the monolayer values it was observed that the plateau adsorption values fell in between the values calculated for bilayer coverage below pH 7 but fell below the bilayer range for adsorption above pH 7, thus indicating the formation of bilayers at pH values far below the pzc of approximately 9. As the pH approaches the pzc it is only natural that there would not be complete bilayer coverage since the charge on the surface is becoming less positive.

3.5.1.4 Mixture of Anionic Surfactants onto Alumina

Most EOR surfactants are mixtures of isomers, but these mixtures are too complex for application of basic theory. In contrast, the effectiveness of ideal solution theory in

explaining region II adsorption for binary mixtures of anionic surfactants has been demonstrated (Lopata et al., 1988). These controlled isomeric mixtures allow application of the ideal solution theory. The application of this theory utilized a reduced adsorption equation for mixtures of anionic surfactants (Scamehorn et al., 1983). The parameters for this reduced equation were obtained from the individual adsorption isotherms for sodium octyl sulfate (C_8SO_4), sodium decyl sulfate ($C_{10}SO_4$) and sodium dodecyl sulfate ($C_{12}SO_4$) onto α-alumina at 30°C. The alumina had a surface area of $160m^2/g$ and the pH was adjusted to produce an equilibrium pH of 8.4. This pH results in a positive charge to the alumina surface leading to high adsorption of the anionic surfactants. Figure 3-5 illustrates the agreement between ideal solution theory and experimental data for a binary mixture of $C_8SO_4/C_{12}SO_4$. Agreement was also demonstrated for a binary mixture of $C_{10}SO_4$ and $C_{12}SO_4$ on γ-alumina (Roberts et al., 1986). Regular solution theory has been shown to describe adsorption of mixtures of anionics and nonionics (Lopata, 1987). One important observation in these mixture studies is the reinforcement of the view that micelle formation and mixed micelle formation play a central role in the behavior of such systems, as proposed earlier by Trogus et al. (1979). Another important conclusion is that mixed admicelle and hemimicelle formation is very similar to that of mixed micelle formation.

3.5.1.5 Cationic Surfactants onto Porous Silicas

Remarkably, while many of the studies of surfactant adsorption have been on porous materials, little attention has been paid to the effect of pore size on the isotherms. Indeed, all of the models of surfactant adsorption that have been developed ignore the effect of pore structure on the electrical double layer, treating the surface as a plane.

Recently, the influence of pore size on the adsorption of cationic surfactants onto porous and nonporous silicas was examined in a study using the cationic surfactants hexadecylpyridinium chloride and dimethylbenzyltetradecylammonium chloride (TBzCl) (Treiner and Montocone, 1995). The porous silicas were Sorbsil C30 from Rhone-Poulenc with an average pore volume of 0.6 ml/g and Sipernat 50S from Degussa-France with a pore volume of 0.003 ml/g. The corresponding BET surface areas are 700 and 450 m^2/g, respectively. It might be expected that the higher surface area silica would have the highest plateau adsorption, but this was not the case. For TBzCl in 0.01 mol/L NaCl the maximum adsorption on the Sorbsil C30 was $5.5x10^{-6}$ mol/g and on Sipernat 50S it was $9x10^{-6}$ mol/g. This behavior was attributed to the Sipernat 50S having large pore diameters while the Sorbsil had small diameters. This behavior had been seen in a previous study (Giordano et al., 1993) using a nonionic surfactant, Triton X-100 adsorbed onto various silicas with well characterized pore radii. Again, as the BET surface areas increased, the pore radii decreased and the plateau adsorption decreased.

3.5.2 Applied Adsorption Studies

This section deals primarily with the application of surfactant adsorption to EOR processes and related fields. From early work involving the formation of optimum microemulsions (three phase or Winsor Type III systems) to the current use of surfactants in other tertiary processes such as foam, CO_2, steam, and alkaline floods, surfactant adsorption has always played a significant role in surfactant selection. The following are just a few of the many articles that have involved studies of surfactant adsorption. These

articles range from having surfactant adsorption as the primary topic to those in which adsorption is but one facet of the work being presented.

3.5.2.1 Anionic Surfactants onto Kaolinite and Illite

In the investigation of the adsorption of sodium dodecylbenzenesulphonate (SDBS) and sodium dodecyl sulphate (SDS) onto asphalt covered kaolinite and illite surfaces, Siffert et al. (1992) observed Langmuir type I isotherms for SDS adsorption onto Na^+ kaolinite and Na^- illite while the SDBS exhibited a maximum in adsorption with a decrease beginning near the CMC. Adsorption maxima were observed near the CMC for both surfactants in the Ca^{2+} kaolinite and Ca^{2+} illite systems. The adsorption behavior was explained as precipitation of the calcium salt of the surfactants (an idea supported by other studies), and the interaction of the aromatic ring in SDBS with the asphalt. This interaction favors desorption of the asphalt rather than adsorption of the SDBS. The amount of asphalt desorbed by SDBS was twice that desorbed by SDS. Other explanations for adsorption maxima include mixed micelle formation (Trogus et al., 1979) and electrostatic repulsion of micelles from the bilayer covered surface (Ananthapadmanabhan and Somasundaran, 1983).

3.5.2.2 Anionic Surfactant onto Kaolinite

The adsorption of a petroleum sulfonate surfactant, TRS 10-80, onto Na-kaolinite was conducted in batch experiments at low-to-medium salinity and under conditions in which liquid-crystal suspensions formed in alcohol containing brines (Bavière et al., 1991). TRS 10-80 was described as not being very brine-soluble. The adsorption studies were

conducted at 30°C with pH values ranging from 7 to 13. The alcohol used was 2-butanol and its concentration was held constant at 30g/l.

The adsorption of systems containing NaCl alone and NaCl-Na_2CO_3 were markedly different. For NaCl systems (26.2 and 21 g/l NaCl) the adsorption isotherms are marked by maxima of approximately 55 and 40 g/l, respectively. The maxima for both systems occurred at an equilibrium sulfonate concentration slightly below 5 g/l. In contrast the NaCl-Na_2CO_3 adsorption plateaued at approximately 10 mg/l.

Other findings presented in this study include 1) the observation that sodium hydroxide while producing a higher pH than sodium carbonate, (12.2 versus 11.3) did not decrease the adsorption as effectively as sodium carbonate; 2) the substitution of SO_4^- ions for Cl^- ions at constant ionic strength strongly diminishes sulfonate adsorption; 3) adding sodium silicates to the NaCl brines was said to give adsorption results similar to those with Na_2CO_3 (no data was presented) while systems containing phosphates gave adsorptions of less than 5 mg/g, and in some systems negative adsorption was observed.

Some of the conclusions presented were that for these systems, the pH dependent part of adsorption is small, the decrease in the adsorption was correlated with the lowering of the sulfonate activity, and sodium carbonate reduces sulfonate adsorption more than sodium hydroxide.

3.5.2.3 Anionic Blends onto Sand and Clay

Following a successful enhanced oil recovery demonstration using a surfactant blend in a foam flood, research was conducted to examine the fate of the blends in core studies (Dawe and Oswald, 1991). The surfactant blend was composed of alpha olefin

sulfonates (AOS's) and the DOWFAX® surfactant 3B2. This surfactant is a disulfonated alkyldiphenyloxide (DPOS). This line of surfactants is discussed in more detail in the Section 3.5 of this chapter.

It was pointed out that the use of AOS's was desirable for EOR applications due to their low cost, but that they tend to precipitate in the presence on such cations as calcium and magnesium. The DPOS surfactant, on the other hand, does not tend to precipitate in the presence of the cations because of the disulfonate anion.

Solubility experiments indicated that a 50:50 blend of the surfactants was soluble in 90, 000 ppm Ca^{++}; sufficient for most conditions encountered in oil reservoirs. Adsorption studies on sand indicated that the pure surfactants had maximum adsorptions of approximately 150 and 50 μgrams/gram for AOS and DPOS respectively; while the 50:50 blend had a maximum adsorption of about 75 μgrams/gram. This reduced adsorption for the disulfonate is consistent with the role of surface charge in surfactant adsorption mechanism.

In static studies using the clay monmorillonite, surfactant adsorption as a function of blend composition was examined. It was found that when the blend consisted of more than 30% DPOS, total adsorption was suppressed, again consistent with reduction of adsorption when charge repulsion between surface and surfactant is increased.

Column studies were conducted on sand using each of the pure surfactants, and a 50:50 blend of the surfactants in a 5% (weight to volume) sodium chloride solution. In each of the three cases the surfactant solution was injected in 1/4 pore volume slugs and the effluent continuously monitored. The DPOS was the least adsorbed, the AOS the

most adsorbed, and the degree of adsorption of the blend fell between the two pure surfactant adsorptions, but was still much less than the AOS adsorption.

Conclusions concerning the adsorption work presented were that the blend provided increased calcium tolerance and losses of surfactant due to precipitation by calcium and adsorption onto reservoir rocks can be reduced by the presence of the disulfonate.

3.5.2.4 Cationic and Anionic Surfactants onto Carbonates

The adsorption onto several carbonates of the cationic surfactants, cetylpyridinium chloride (CPC) and dodecyl pyridinium chloride (DPC) were compared to the adsorption of the anionic surfactant sodium dodecyl sulfate (SDS) (Tabatabai et al., 1993). It was expected that cationic surfactants would exhibit adsorption lower than anionic surfactants on carbonate minerals, which tend to be positively charged. The carbonate solids were a synthetic calcite ($CaCO_3$) and natural dolomite ($CaMgCO_3$).

The surface charges on these carbonate minerals was attributed to preferential dissolution of lattice ions, Mg^{2+}, Ca^{2+} and CO_3^{2-} and the adsorption of H^+ or OH^- which may act as potential determining ions for carbonates. Therefore, the adsorption was conducted using various concentrations of $MgCl_2$, $CaCl_2$, Na_2CO_3, but no attempt was made to regulate the pH, although the pH was measured. The average pH value of the $MgCl_2$ and $CaCl_2$ systems was approximately 8.0, and the average pH of the Na_2CO_3 systems was approximately 10.0. The pzc of the calcite was 9.2 and the pzc of the dolomite was 7.4 (Gonzalez, 1989).

The adsorption behaviors of the CPC and DPC on the two carbonates were markedly different. DPC exhibited region I (linear) adsorption over the entire range of surfactant concentrations examined, up to the CMC, with the exception of the DPC/calcite/ $MgCl_2$ system. For this system there was approximately zero adsorption until the equilibrium surfactant concentration reached approximately 4500 μmolar. At this concentration the adsorption was measured as a negative value. Negative adsorption was explained as the repelling of the like-charged surfactant from the surface and the subsequent concentration of surfactant in the region of the solution from which the analyte sample was collected.

CPC with no electrolyte present had nearly constant adsorption (0.05 - 0.1 μmole/gram) on calcite. Adsorptions from 0.05 M $MgCl_2$ onto calcite and from 0.05 M $CaCl_2$ onto calcite resulted in nearly constant adsorptions at approximately 0.05 μmole/gram until the equilibrium surfactant concentration approached 200 μmolar, then the adsorption became negative. In contrast, adsorption isotherms for the dolomite system were more like the traditional isotherm shown in Figure 3-2. For the system with no additional electrolyte the adsorption values ranged from approximately 0.01 - 2.0 μmole/gram. Adsorption values from 0.05 M $MgCl_2$ ranged from 0.02 - 0.35 μmole/gram. While the values from 0.05 $CaCl_2$ ranged from 0.2-0.4 μmole/gram.

The adsorption isotherms of anionic SDS on the carbonates indicated typical surfactant adsorption behavior with the plateau adsorption occurring at 9-10 μmole/gram for the system containing no additional electrolyte, and in the $MgCl_2$ solutions on both carbonates. The maximum adsorption for both carbonate systems containing Na_2CO_3 was approximately 4 μmole/gram while the $CaCl_2$ systems were approximately 5 μmole/gram.

The conclusions reached by the authors were that the addition of lattice ions from the solid enhances the adsorption of the anionic surfactant while reducing the adsorption of a cationic surfactant by directly affecting the surface charge. The enhancement of the anionic surfactant adsorption arises from the decrease in the electrostatic repulsion between the head groups of the adsorbed surfactant molecules due to the addition of the divalent cations. This effect would not, of course, be observed in the cationic surfactant systems.

Further, just as in micelle formation, the addition of counterions can reduce the repulsion between the head groups of the anionic surfactants by compressing the electrical double layer between them. This compression acts to increase the adsorption. This increase in adsorption was not observed for addition of divalent cations to the cationic surfactants systems, however.

The authors proposed that a reduction in surfactant losses for EOR in carbonate reservoirs would be possible by using a cationic surfactant with an appropriate concentration of added multivalent electrolyte where the cations were also lattice ions for the mineral. In addition to lower adsorption losses the cationic surfactant offer good corrosion inhibiting capabilities and antibacterial properties. Unfortunately, cationic surfactants are more expensive than anionic surfactants; however, to the author's knowledge the economics of the proposed application have never been examined.

3.5.2.5 Ethoxylated Sulfate Surfactants onto Mineral Oxides and Sandstone Cores

Various features of anionic surfactant systems in EOR have been illustrated in a series of studies using ethoxylated sulfates as the primary surfactants with additives that

included co-surfactants, alcohols, electrolytes, polyethylene oxide and polymers (Austad et al., 1991a, b, c, 1992a, b, 1994, and Fjelde et al., 1995). The solids included kaolinite, quartz, sandstone cores, Berea cores, and oil containing reservoir cores.

The initial study (Austad et al., 1991a) examined the adsorption of commercial mixtures of polyethylene oxide nonyl-phenolether sulfates, C_9-Ph-$(EO)_x$-SO_3Na and their corresponding nonionic surfactants, C_9-Ph-$(EO)_x$-OH with **x** = 2, 4, 5.5,6, and 9. The nonionic surfactant is present as unreacted feed in the production of the sulfated material. These studies also examined the adsorption behavior of an isomerically pure polyethylene oxide nonyl-phenolether sulfate, C_9-Ph-$(EO)_4$-SO_3Na. The adsorption isotherms for the commercial surfactant systems containing less than 30 mol % anionic surfactant indicated that the plateau adsorption decreases, on a mole basis, as the number of EO-groups increases. An additional observation was that as the amount of nonionic surfactant increases there is an increase in adsorption in regions II through IV, with the increase being greater for quartz than for kaolinite. When comparing the adsorption of the isomerically pure sulfate with sulfate/nonionic mixtures, it was observed that both anionic and nonionic surfactants adsorbed onto kaolinite and quartz, but adsorption of the nonionic was approximately 50% greater on both solids. Since the quartz is negatively charge, this is again consistent with our understanding of the central role of electrostatics in surfactant adsorption.

A later study (Austad et al., 1992a) focused on the nonequilibrium adsorption of C_9-Ph-$(EO)_6$-SO_3Na, 88 mol% sulfonate and 12 mol% unconverted nonionic surfactant, with a polymer, xanthan, onto oil-containing sandstone cores from the North Sea. Addition of the polymer reduced the surfactant adsorption by 80% relative to adsorption

without xanthan, yet there was no complex formation between the surfactant and the xanthan. This study reflects one of the current trends of using systems containing surfactant/polymer mixture and emphasizes the need for system specific adsorption studies in EOR applications.

A later study (Austad et al., 1997) examined the effects of the polymer on surfactant adsorption in a low tension polymer water flood (LTPWF). The surfactant was a alkylpropoxyethoxy sulfate, $C_{12\text{-}15}$-$(PO)_4$-$(EO)_2$-OSO_3^- Na^+, and the polymers were xanthan and a copolymer of acrylamide and sodium 2-acrylamido-2-methylpropane sulfonate (AN 125 from Floerger). The solid materials were sandstone cores from a North Sea oil reservoir, Berea, and Bentheim cores. For these systems the xanthan caused a 20% reduction in the adsorption of the surfactant. It was also observed that surfactant adsorption appeared to increase as the water wettability decreased under LTPWF conditions and also as the salinity of the brine increased. No mechanism was presented to explain the effect of wettability on surfactant adsorption; however, it was proposed that the polar components in the crude oil were adsorbed onto the solid surface and would not be displaced under the LTPWF conditions. The effect of the brine was explained as a reduction in lateral electrostatic repulsion among adsorbed surfactant ions which causes a closer packing of the adsorbed molecules, thus facilitating formation of admicelles.

3.5.2.6 Mixed Anionic Surfactants onto East Vacuum Grayburg-San Andres Unit (EVGSAU) and Baker Dolomite Cores

The surfactant CHASER™ CD1045 (Chevron Chemical Co.) described only as a mixed surfactant was adsorbed onto EVGSAU and Baker dolomite cores as part of a

study examining CO_2-foam in mobility control (Tsau et al., 1994). The adsorption portion of this study was conducted at room temperature and atmospheric conditions.

On Baker dolomite cores the results of four studies were reported. The differences between the studies were the presence or absence of additional electrolytes (4% brine) and the porosity of the cores. Comparing the adsorption of the surfactant from distilled water versus from the 4% brine solution for cores with similar porosity indicates that the adsorption from the distilled water was slightly less than the adsorption from the brine solution. For example, for cores with porosities averaging 18.8 % with equilibrium surfactant concentrations of approximately 2180 ppm, the adsorption was 3200 lb/acre-ft for the distilled water system and 3577 lb/acre-ft for the 4% brine system. The adsorption was described as "reasonably Langmurian," meaning that the slope decreased as adsorption increased. For the distilled water systems, the adsorption appears to be just beginning to plateau at the maximum of the surfactant concentration range studied. The brine systems exhibit an adsorption plateau of approximately 3500 lb/acre-ft. The differences in the adsorption behavior between the distilled water and brine systems were attributed to the brine shifting the surface charge of calcite towards less negative or even positive values. Any anionic surfactant would tend to adsorb to a greater extent under increased electrolyte concentrations.

The adsorption behavior of the CHASER^{TM} CD1045 onto EVGSAU cores was similar to the behavior seen for the dolomite cores. For the distilled water it appears that the adsorption is just beginning to plateau, but greater surfactant concentrations would have to be studied in order to confirm this. For the 4% brine system the adsorption

plateaus at slightly greater than 2000 lb/ acre-ft which is less than the adsorption seen on the dolomite cores.

In a similar study using Chaser™ CD-1045 for CO_2-foam applications, the adsorption of the surfactant onto Baker dolomite was determined (Contracts.., 1996). The dolomite used in this study was similar in porosity to the previous study discussed but the studies were conducted using synthetic South Camden Unit (SCU). The average surfactant adsorption was approximately 420 lb/acre-ft which is considerable lower than that reported for the East Vacuum Grayburg-San Andres Unit. The composition of the brine was not provided in this report, but it may be at least part of the reason for the great difference between the two adsorption studies conducted on Baker dolomite.

There are two additional types of chemical flooding systems that involve surfactants which are briefly mentioned here. One of these systems utilizes surfactant-polymer mixtures. One such study was presented by Osterloh et al. (1992) that examined anionic PO/EO surfactant microemulsions containing polyethylene glycol additives adsorbed onto clay. The second type of chemical flood involves the use of sodium bicarbonate. The aim of the research was to demonstrate that the effectiveness of sodium bicarbonate in oil recovery could be enhanced with the addition of surfactant. The surfactant adsorption was conducted in batch studies using kaolinite and Berea sandstone (Peru et al., 1990). It was determined that the presence of a low concentration of surfactant was effective in maintaining the alkalinity even after long exposures to reservoir minerals. Also, the presence of the sodium bicarbonate is capable of reducing surfactant adsorption.

3.5.3 Adsorption of Alkyldiphenyl Oxide Mono and Disulfonate Surfactants

This section examines the adsorption behavior of alkyldiphenyl oxide sulfonate surfactants on several different solid surfaces both negatively and positively charged. Several aspects of adsorption are discussed including surface charge and porosity.

3.5.3.1 Anionic Surfactant Blend and Amphoteric Surfactants onto Berea Sandstone, Indiana Limestone, Baker Dolomite, and Quartz.

The first study to be presented examined the adsorption behavior of two amphoteric surfactants, a betaine (Empigen BT) and a sulfobetaine (Varion CAS); and a 50:50 blend of a C_{10} diphenyl oxide disulfonate (DOWFAX® 3B2), and a $C_{14\text{-}16}$ α-olefin sulfonate (Mannhardt et al., 1992). The anionic surfactant blend was designated as DOW XS84321.05. As a reminder the C_{10} diphenyl ether disulfonate surfactant is one isomer in a suite of surfactants that differ in their degree of alkylation and sulfonation and in their alkyl chain lengths. This suite consists of monoalkyl disulfonates (MADS), dialkyl disulfonates (DADS), monoalkyl monosulfonates (MAMS), and dialkyl monosulfonates (DAMS). The C_{10} diphenyl oxide disulfonate is a mixture of C10 MADS and C10 DADS. The general structure of these surfactants is shown in Figure 3-6.

The adsorption studies were conducted on core samples of Berea sandstone, Indiana limestone, Baker dolomite, and quartz sand from three brines (a sodium chloride solution of 2.32% and two synthetic reservoir brines with total dissolved solids of 2.1 and 10.5%). Conclusions were based on the maximum or plateau adsorption values obtained, and these values are shown in Table 3-1.

Table 3-1 Plateau adsorption values (mg/g) from adsorption isotherms[a]

Rock Type	Brine	Surfactant Types[b]		
		Anionic	Betaine	Sulfobetaine
Sandstone	2.1% TDS	0.11	1.31	1.30
Sandstone	10.5% TDS	0.26	1.12	-
Sandstone	2.32% NaCl	0.03	0.94	1.29
AGSCO Quartz	2.1% TDS	0.15	0.23	-
AGSCO Quartz	10.5% TDS	0.15	0.09	-
Indiana Limestone	2.1% TDS	0.37	0.31	0.21
Indiana Limestone	10.5% TDS	0.30	0.33	-
Indiana Limestone	2.32% NaCl	0.21	0.12	0.19
Baker Dolomite	2.1% TDS	0.13	0.38	0.32
Baker Dolomite	2.32% NaCl	0.12	0.37	0.34

[a]Taken from Table 5 of Mannhardt et al. (1992).
[b]Anionic surfactant (DOW XS84321.05); betaine (Empigen BT); sulfobetaine (Varion CAS).

As shown in Table 3-1, the anionic surfactant blend gave the lowest adsorption onto sandstone and onto the dolomite for all three of the brine conditions examined. While onto quartz, the adsorption of the anionic surfactant remained constant for both of the synthetic reservoir brines tested with amounts in between those seen for the betaine surfactant. For limestone the adsorption of the anionic and the betaine were approximately the same in the two synthetic reservoir brines, but both were greater than the adsorption of the sulofbetaine. For adsorption onto limestone from the brine solution the anionic adsorption was greater than the betaine and slightly greater than that of the sulfobetaine.

Upon examining the adsorption data from the reservoir brines, there was no consistent pattern seen in the adsorption behavior. Based on this it was concluded that the tendency of surfactant adsorption to increase with increasing salt concentration is minor

and that the trends in adsorption can be explained solely on the basis of the interaction of the charge on the surfactant with the solid surface charges.

The surface charge on the solid depended, in part, on the brine solution surrounding the surface. Electrophoretic mobilities were determined in the 2.1% TDS and the 2.32% NaCl brines, and at pH 7 the following trend was observed:

Berea clays < quartz < dolomite < limestone
(most negative).....(least negative)

The Berea sandstone had been split into clay and quartz fractions, but the Berea whole rock was still more negative relative to the other core listed for this study. Even though the trend was the same for both brines, the divalent cations in the 2.1% TDS brine produced less negatively charged surfaces than did the NaCl brine. This behavior was attributed to adsorption of these ions into the Stern layer or, in the case of carbonates, to preferential dissolution of CO_3^{2-} over Ca^{2+} or Mg^{2+} in the presence of excess divalent cations in the aqueous phase. It was also noted that adsorption of metal hydroxide ions or mineral transformation reactions at the solid surface may play a role.

A detailed discussion was presented on the relationship between surfactant adsorption and the solid surface charge. For the anionic surfactant, as expected, as the surface became increasingly positive the adsorption increased. This increase in positive charge occurs either when the rock type was changed in the order shown above while keeping the brine fixed or when divalent cations are added to the brine for a fixed rock type.

Some of the conclusions presented were that the anionic surfactant blend exhibits low adsorption levels on sandstone, but adsorbs more strongly onto dolomite and

limestone. Divalent cations increase the adsorption of the anionic surfactant and the betaine on sandstone and limestone under constant ionic strength conditions, but the adsorption of the sulfobetaine was affected very little by the presence of the divalent cations. Increasing the total dissolved solids at constant ionic composition gave mixed results, increasing the adsorption for some surfactant/rock combinations, but decreasing it for others. See Table 3-1. In terms of adsorption levels, the anionic surfactant appears to be the best choice of the systems studied for applications in sandstone and dolomite reservoirs. In limestone reservoirs, the sulfobetaine would be best, particularly in the presence of hardness ions. Finally the trends in the adsorption of the anionic surfactant appear consistent with the electrostatic mechanisms.

3.5.3.2 Anionic Surfactants onto Canadian River Alluvium (CRA) and Alumina

The second study on alkyldiphenyl oxide sulfonate surfactants to be discussed was conducted in order to determine strategies for designing surfactants in order to minimize adsorption. The adsorption studies were conducted on Canadian River alluvium (CRA) (Sabatini et al., 2000) and on alumina at room temperature. CRA consists primarily of sand and is expected to behave similarly to sandstone cores. The anionic surfactants were supplied by DOW and used as received. The alkyl groups used in the CRA and alumina studies were linear and included alkyl chain lengths of C6, C10, C12, and C16. The DAMS components and the C12 and C16 DADS were not studied due to their low water solubilities.

3.5.3.3 Adsorption onto Canadian River Alluvium (CRA)

The adsorption studies done on CRA were part of a larger study focused on examining the behavior of the alkyldiphenyl oxide sulfonate surfactants in soil remediation processes (Sabatini et al., 2000). For the adsorption onto CRA, the surfactants studied consisted of C10, and C16 MADS; C10 DADS; and C10 MAMS.

Prior to use, the CRA was crushed and sieved. The BET (N_2) surface area was determined to be 4.63 m^2/g with an average pore diameter of 55.52 Å. Five grams of soil were used with 0.1 ml of a calcium chloride solution (0.005M) added and allowed to dry. Previous research had shown the calcium chloride to be necessary to get the soil fines to separate from the bulk solution. When the soil was dry, 25 mL of each surfactant solution (1/5 to 10 times the CMC) was added. The CMC values for the individual components are given in Table 3-2.

Table 3-2 Alkyldiphenyl Oxide Sulfonate Surfactants Properties

Surfactant	Avg. MW (g/mol)	CMC (M)*
C10-MAMS	423	$3.53x10^{-4}$
C10-MADS	523	$1.40x10^{-4}$
C10-DADS	617	$1.33x10^{-4}$
C12-MADS	551	$1.30x10^{-4}$
C16-MADS	600	$2.53x10^{-4}$

*Reported by Dow Chemical and determined at room temperature and native electrolyte conditions.

The samples were placed on a finger-tip shaker for 24 hours then centrifuged for 20 minutes. The amount of adsorption was determined by calculating the change in surfactant concentration in the bulk solution. The equilibrium surfactant concentrations were determined by HPLC with a UV detector set at 254 nm and methanol as the mobile

phase. Prior to analysis on the HPLC, all samples were passed through a 0.2 μm syringe filter to remove any suspended soil particles.

As shown in Figure 3-7, the greatest adsorption is shown by the C10 MAMS component (4.91 mg/g). The higher adsorption of the C10 MAMS is attributed to the monosulfonated component having less electrostatic and steric hindrances than the disulfonated components. The maximum adsorption of the C10 MADS was 0.6 mg/g, considerably lower than the 4.91 mg/g seen for the C10 MAMS. The more hydrophobic nature of the MAMS relative to the MADS component arises from the absence of the second sulfonate group. This greater degree of hydrophobicity is the source of the increase in adsorption.

Figure 3-8 depicts the adsorption isotherms of the three C10 components. For the reasons stated above, the monosulfonate had the greatest adsorption (4.91 mg/g). While between the two disulfonated components (MADS and DADS), the dialkyl component had the greatest amount of adsorption (2.25 versus 0.6 mg/g). This is due to the greater hydrophobicity of the dialkyl component. The difference seen in the maximum adsorption of the MAMS and DADS components, 4.91 and 2.25 mg/g, respectively, is due to both steric hindrances caused by the second alkyl group and the more ionic nature of the DADS component due to the second sulfonate group.

The adsorption isotherms of the C10 and C16 MADS components are shown in Figure 3-9. It can be seen that the adsorption increases at lower surfactant concentration with increasing chain length, from C10 to C16 (0.6 to 1.83 mg/g). This increase is attributed to increasing hydrophobicity with increasing chain length.

Adsorption studies have been conducted with other alkyldiphenyl oxide sulfonate surfactants on CRA. Rouse et al. (1996) studied the adsorption of DOWFAX® 8390, a commercially available C16 surfactant, and found a maximum adsorption of 4.3 mg/g while the maximum adsorption of the C16 MADS component was 1.8 mg/g. The commercial product contains approximately 35 wt% active component. The increase in the dialkylated component in the commercial mixture is responsible for its greater maximum adsorption compared to the C16 MADS.

The adsorption behavior of the C10 DADS relative to the C16 MADS is worth special note. Comparing initial concentrations, it is seen that at lower surfactant concentrations the C16 has the greatest amount of adsorption; however, as the plateau region is approached the C10 adsorption exceeds that of the C16. Since they are both disulfonates this behavior can be attributed to the difference in chain lengths and the degree of alkylation, both of which are directly related to the hydrophobicity of the surfactants. At the lower surfactant concentrations the longer chain length dominates the adsorption, but at higher concentrations the dialkylation dominates.

3.5.3.4 Adsorption onto Alumina

The goal of the adsorption studies on alumina was to study the adsorption of the alkyldiphenyl oxide sulfonate surfactants on a positively charged alumina substrate, leading to high adsorption and bilayer formation. The primary purpose for this study was to determine the initial surfactant concentrations that were to be used in adsolubilization studies that are discussed in Chapter 4. For the adsolubilization studies, the desired initial surfactant concentrations would be those that produced adsorptions that were less than

the plateau amounts, i.e. prior to region 4 adsorption. The adsorptions of the C10, C12, and C16 MADS and the C10 DADS components were studied.

The alumina used was manufactured by LaRoche and has a BET (N_2) surface area of 301.83 m^2/g and an average pore diameter of 105.08 Å. Due to the high surface area, only 0.05 grams of alumina and 30 ml of surfactant solution were used. These quantities allowed enough surfactant to remain in the bulk solution at equilibrium to be analyzed. The surfactant feed concentrations ranged from approximately 1/5 to 10 times the CMC with NaCl concentrations of 0.15 M for the MADS solutions and 0.09 M for the DADS solutions. The pH of the alumina/surfactant solutions was measured and adjusted to values ranging from 2.3 to 3.5 using sulfuric acid. The pH was allowed to equilibrate without further adjustment. The vials were placed on a table-top type shaker for 24 hours. The alumina in the adsorption solutions was allowed to settle prior to analysis. Centrifuging was found not to be effective in separating the alumina from the surfactant solutions. The equilibrium pH was then measured. The equilibrium surfactant concentrations were determined by HPLC using methanol as the mobile phase and a UV detector with the wavelength varying from 254 to 264 nm depending on the surfactant. Prior to injection into the HPLC the solutions were passed through a 0.2 μm syringe filter to remove any suspended alumina.

Of the MADS components the order of increasing adsorption was C10, C12, and C16. This is in agreement with adsorption studies of sodium alkylsulfonates onto alumina conducted by Wakamatsu and Fuerstenau (1968). From the isotherms shown in Figure 3-10, the behavior of the C16 and C12 MADS are very similar, noticeably the sharp increase in adsorption just prior to the plateau region. The C10 MADS component has a more

gradual increase with no sharp break before apparently plateauing. The third, fourth and eighth data points of the C10 MADS isotherm were at lower feed pH's than the remaining points on the curve. The effect of varying feed pH's on C12 and C16 MADS was not as noticeable as on the C10 MADS.

As discussed in Section 3.4.1 and shown graphically in Figure 3-2, log-log plots of adsorption results are often constructed in order to clearly observe regions of adsorption exhibited by a particular surfactant. The adsorption curves shown in Figure 3-11 of the same adsorption data discussed above indicate that region 1 adsorption was not seen for any of the components. For the C12 MADS and C10 DADS, regions 2, 3 and 4 were observed. For the C16 MADS: region 4 was clearly observed, but there were insufficient data points to determine if the other points were in region 2 or 3. The same can be said for the C10 MADS, but it could also be argued that the last of the data points lie within region 3 and that plateau adsorption was not observed.

In order to test the notion that region 4 adsorption began at or near the CMC, the CMC's for each of the surfactants were determined at the same salinities that the adsorption studies were conducted. From Figure 3-10 the CMC's were estimated to fall in the ranges shown in Table 3-3:

Table 3-3 Estimated Critical Micelle Concentrations

Surfactant	Critical Micelle Concentration (M)
C10 MADS	$2x10^{-4}$ to $3x10^{-4}$
C12 MADS	$8x10^{-5}$ to $1.6x10^{-4}$
C16 MADS	$6x10^{-5}$ to $1.4x10^{-4}$
C10 MADS	$1.4x10^{-4}$ to $2.4x10^{-4}$

The values shown in Table 3-3 are greater than the values shown in Table 1-2 of Chapter 1 by at least an order of magnitude. It was hoped that the CMC's determined

from the surface tension curves would correspond to the CMC's suggested in Figure 3-10, but they do not. As a matter of fact, they correspond more closely to the values shown in Table 1-1 of Chapter 1. There are several possible explanations. There were some differences between the temperatures of the surface tension measurements and the adsorption studies. Since these are mixtures, it is also possible that the more active species at the air/water interface is not the most active at the solid/water interface.

If the emphasis of this study had been on the theoretical aspects of surfactant adsorption, additional samples containing less than 1/10*CMC solutions or systems containing more surfactant solution and/or less alumina would have to have been prepared and analyzed for all of the surfactants. In the current study the lower concentrations were close to the experimental error limits of liquid chromatography analysis. For the C10 MADS systems containing greater than 10*CMC initial surfactant concentrations would have been required to adequately span the adsorption regions.

There were several observations made concerning the effect pH had on the adsorption on alumina. Adsorption of the DADS component onto alumina was very sensitive to variations in the feed pH that was exhibited by the several points that did not fit smoothly on the isotherm. See Figure 3-10. It was also noted that for any of the surfactants if the feed pH was at or below 2.5 or 2.6 the final pH was usually below 3.0, but if the feed pH approached 3.0 the final pH would approach 4.0.

In general the alkyldiphenyl oxide sulfonate components adsorbed as expected on the CRA and alumina surfaces. The oppositely charged alumina with the higher surface area had significantly greater adsorption than that on the CRA. See Table 3-4 for the actual values. The monosulfonates showed the greatest amount of adsorption due to the

lack of electrostatic and steric hindrances. In the series of MADS components there was increasing adsorption with increasing chain length due to increasing hydrophobicity.

Table 3-4 Maximum Adsorptions of Alkyldiphenyl Oxide Sulfonate Surfactants

Surfactant	CRA	Alumina
C10-MAMS	4.91 mg/g ($1.16x10^{-5}$ mol/g)	-
C10-MADS	0.6 ($1.15x10^{-6}$)	236.5 mg/g ($4.52x10^{-4}$ mol/g)
C10-DADS	2.25 ($3.66x10^{-6}$)	237.0 ($3.86x10^{-4}$)
C12-MADS	-	299.1 ($5.43x10^{-4}$)
C16-MADS	1.83 ($3.05x10^{-6}$)	527.5 ($8.79x10^{-4}$)

In comparing all of the adsorption studies involving the alkyldiphenyl oxide sulfonate surfactants discussed in this section it can be seen that adsorption onto negatively charge surfaces such as sandstone (Berea clays) result in adsorption amounts that are much less than adsorption onto positively charged surfaces such as limestone, CRA and alumina. Also, the studies on the CRA indicate that the purer components had significantly less soil adsorption than the commercially available C16 MADS surfactant mixture.

In EOR or soil remediation projects this smaller amount of surfactant loss to the soil could amount to significant cost savings, but as with all commercial applications the economics of the higher costs associated with producing purer products must be weighed against profit losses associated with losing surfactant to adsorption.

While the alkyldiphenyl oxide sulfonate surfactants discussed above have many properties favorable for EOR and remediation applications, like all surfactants their use will be determined by their behavior under conditions specific to the application. In general their adsorption values were lower than that exhibited by many other surfactants, and their salinity tolerance has been demonstrated. As discussed in the prologue there is a

lot of interest in the class of surfactants described as gemini surfactants. The C10 DADS surfactant used in the current study can be classified as a gemini, but is worth noting that for this particular suite of surfactants the components which are not "true gemini" surfactants tend to have the more favorable adsorption properties, monoalkyl versus dialkyl components.

3.6 Summary

Surfactants are used extensively in enhanced oil recovery. Applications include micellar floods or flooding in conjunction with polymers, alkalies, steam, or carbon dioxide. Another application is the generation of foams for mobility control or blocking and diverting. For each of these applications care must be taken in selecting the surfactants. Surfactants tend to be a major portion of the costs associated with EOR, and losing surfactant to adsorption leads to substantial economic losses.

Surfactant adsorption depends on many factors. Factors discussed in this chapter include the electrical nature of the solid surface, pH of the system, and the structure of the surfactant. For most of the solids in the various studies reviewed, the charge on the surface is determined in large part by the pH of the system. Adsorption is enhanced in those systems in which the solid surface and the surfactant have opposite charges, and the greater the surface charge the greater the surfactant adsorption. Higher surface area solids tend to have increased adsorption, but pore size can also affect the degree of adsorption. Care must be taken to avoid confusing precipitation of the surfactant for adsorption; hence, familiarity with the solubility of a surfactant in the presence of counterions is necessary.

The studies reviewed for this chapter are examples of the types of studies that have been done on surfactant adsorption. They included those upon which fundamental theories and models have been developed as well as those used to develop practical applications of surfactants in the field of enhanced oil recovery.

3.7 Acknowledgment

We would like to express our appreciation to Lisa Quencer of the DOW Chemical Company for all of her help in the alkyldiphenyl oxide sulfonate surfactant research conducted on Canadian River alluvium and alumina.

3.8 References

Amante, J. C.; Scamehorn, J. F.; Harwell, J. H. Precipitation of Mixtures of Anionic and Cationic Surfactants II: Effect of Surfactant Structure, Temperature and pH. *J. Coll. Interface Sci.* **1991**, 144, 243-253.

Ananthapadmanabhan, K. P.; Somasundaran, P. Mechanism for Adsorption Maximum and Hysteresis in a Sodium Dodecylbenzene Sulfonate/Kaolinite System. *Colloids Surfaces* **1983**, 7, 105-114.

Austad, T.; Bjørkum, P. A.; Rolfsvåg, T. A. Adsorption II. Nonequilibrium Adsorption of Surfactants onto Three Reservoir Cores from the Norwegian Continental Shelf. The Effects of Clay Minerals. *J. Petrol. Sci. Eng.* **1991**, 6, 125-135.

Austad, T.; Bjørkum, P. A.; Rolfsvåg, T. A.; Øysæd, K. B. Adsorption III. Nonequilibrium Adsorption of Surfactants onto Reservoir Cores from the North Sea. The Effects of Oil and Clay Minerals. *J. Petrol. Sci. Eng.* **1991**, 6, 137-148.

Austad, T.; Ekrann, S.; Fjelde, I.; Taugbøl, K. Chemical Flooding of Oil Reservoirs Part 9. Dynamic Adsorption of Surfactant onto Sandstone cores from Injection Water With and Without Polymer Present. *Colloids Surfaces* **1997**, 127, 69-82.

Austad, T.; Fjelde, I.; Rolfsvåg, T. A. Adsorption V. Nonequilibrium Competitive Adsorption of Polydisperse Ethoxylated Sulfonates onto Clay-Containing Cores and Kaolinite. *J. Petrol. Sci. Eng.* **1992**, 6, 277-287.

Austad, T.; Fjelde, I.; Veggeland, K. Adsorption VI. Nonequilibrium Adsorption of Ethoxylated Sulfonate onto Reservoir Cores in the Presence of Xanthan. *J. Petrol. Sci. Eng.* **1994**, 12, 1-8.

Austad, T.; Løvereide, T.; Olsvik, K.; Rolfsvåg, T. A.; Staurland, G. Adsorption I. Competitive Static Adsorption of Mixtures of Ethoxylated Surfactants onto Kaolinite and Quartz. *J. Petrol. Sci. Eng.* **1991**, 6, 107-124.

Austad, T.; Rørvik, O.; Rolfsvåg, T. A.; Øysæd, K. B. Adsorption IV. An Evaluation of Polyethylene Glycol as a Sacrificial Adsorbate Towards Ethoxylated Sulfonates in Chemical Flooding. *J. Petrol. Sci. Eng.* **1992**, 6, 265-276.

Bavière, M.; Ruaux, E.; Defives, D. Sulfonate Retention by Kaolinite at High pH: Effect of Inorganic Anions. *SPE International Symposium on Oilfield Chemistry*: Anaheim, CA, 1991, paper SPE 21031.

Bitting, D.; Harwell, J. H. Effects of Counterions on Surfactant Surface Aggregates at the Alumina/Aqueous Solution Interface. *Langmuir* **1987**, 3, 500-511.

Böhmer, M. R.; Koopal, L. K. Adsorption of Ionic Surfactants on Constant Charge Surfaces. Analysis Based on A Self-Consistent Field Lattice Model. *Langmuir* **1992a**, 8(6), 1594-1602.

Böhmer, M. R.; Koopal, L. K. Adsorption of Ionic Surfactants on Variable-Charge Surfaces. 1. Charge Effects and Structure of the Adsorbed Layer. *Langmuir* **1992b**, 8(11), 2649-2659.

Böhmer, M. R.; Koopal, L. K. Adsorption of Ionic Surfactants on Variable-Charge Surfaces. 2. Molecular Architecture and Structure of the Adsorbed Layer. *Langmuir* **1992c**, 8(11), 2660-2665.

Chandar, P.; Somasundaran, P.; Turro, N. J. Fluorescence Probe Studies on the Structure of the Adsorbed Layer of Dodecyl Sulfate at the Alumina-Water Interface. *J. Colloid Interface Sci.* **1987**, 117, 31-46.

Chimahusky, J. F. Design and Implementation of a CO_2 Flood Utilizing Advanced Reservoir Characterization and Horizontal Injection Wells in a Shallow-Shelf Carbonate Approaching Waterflood Depletion. In *Contracts for Field Projects and Supporting Research on Enhanced Oil Recovery*, U. S. Department of Energy, Progress Review No. 86, Contract No. DE-FG22-94BC14991, 1996.

Davis, J. A.; James, R. O.; Leckie, J. O. Surface Ionization and Complexation at the Oxide/Water Interface 1. Computation of Electrical Double Layer Properties in Simple Electrolytes *J. Coll. Interface Sci.* **1978**, 63, 480-499.

Dawe, B.; Oswald, T. Reduced Adsorption and Separation of Blended Surfactants on Sand and Clay. *J. Canadian Pet. Tech.* **1991**, 30, 133-137.

de Bruyn, P. L. Flotation of Quartz by Cationic Collectors. *Trans AIME* **1955**, 202, 291-296.

Deshpande, S.; Wesson, L.; Wade, D.; Sabatini, D. A.; Harwell, J. H.; Dowfax Surfactant Components for Enhancing Contaminant Solubilization. *Water Research*, 2000.

Fernandez, M. E. Master's Thesis, University of Texas at Austin, 1978.

Fjelde, I.; Austad, T.; Milter, J. Adsorption VII. Dynamic Adsorption of a Dual Surfactant System onto Reservoir Cores at Seawater Salinities. *J. Petrol. Sci. Eng.* **1995**, 13, 193-201.

Fuerstenau, D. W. Interfacial Processes in Mineral/Water Sytems. *Pure Appl. Chem.* **1970**, 24, 135-164.

Gao, Y.; Du, J.; Gu, T. Hemimicelle Formation of Cationic Surfactants at the Silica Gel-Water Interface. *J. Chem. Soc., Faraday Trans.* 1987, **83(8),** 2671.

Gaudin, A. M.; Bloecher, F. W. Concerning the Adsorption of Dodecylamine on Quartz. *Trans AIME* **1950**, 187, 499-505.

Gaudin, A. M.; Fuerstenau, D. W. Quartz Flotation with Cationic Collectors. *Trans. AIME* **1955**, 202, 958-962.

Gaudin, A. M.; Morrow, J. G. Adsorption of Dodecylammonium Acetate on Hematite and Its Flotation Effect. *Trans AIME* **1954**, 199, 1196-1202.

Giordano, F.; Desnoyel, R.; Rouquerol, J. Influence of Porosity on the Adsorption of a Nonionic Surfactant on Silica. *Colloids Surfaces A* **1993**, 71, 293-298.

Gonzalez, M. Master's Thesis, University of Oklahoma, Norman, Oklahoma, 1989.

Goulob, T. P.; Koopal, L. K. Adsorption of Cationic Surfactants on Silica. Comparison of Experiment and Theory. *Langmuir* **1997**, 13(4), 673-681.

Goulob, T. P.; Koopal, L. K.; Bijsterbosch, B. H.; Sidorova, M. P. Adsorption of Cationic Surfactants on Silica. Surface Charge Effects. *Langmuir* **1996**, 12(13), 3188-3194.

Greenwood, N. N.; Earnshaw. A. *Chemistry of the Elements, 2nd ed.*; Butterworth-Heineman, Boston, 1997, pp 242-4, 352.

Grim, R. *Clay Mineralogy*; McGraw-Hill: New York, 1968, p 59.

Hankins, N. P.; O'Haver, J. H.; Harwell, J. H. Modeling Effects of pH and Counterions on Surfactant Adsorption at the Oxide/Water Interface. *Ind. Eng. Chem. Res.* **1996**, 35, 2844-2855.

Harwell, J. H.; Hoskins, J. C.; Schecter, R. S.; Wade, W. H. Pseudophase Separation Model for Surfactant Adsorption: Isomerically Pure Surfactants. *Langmuir* **1985**, 1, 251-262.

Harwell, J. H.; Scamehorn, J. H. Adsorption from Mixed Surfactant Systems. In *Mixed Surfactant Systems;* Ogino, K.; Abe, M., Eds.; Marcel Dekker, New York, 1993, pp 263-281.

Holm, L. W. Design, Performance and Evaluation of the Uniflood Micellar-Polymer Process-Bell Creek Field. *Proceedings of the 57th Annual Fall Technical Conference of SPE*; Society of Petroleum Engineers: New Orleans, LA, 1982, paper SPE 11196.

James, R. O.' Parks, G. A. Characterization of Aqueous Colloids by Their Electrical Double-Layer and Intrinsic Surface Chemical Properties. In *Surface and Colloid Science*; Matijevic, E., Ed.; Plenum Press: New York, 1982, Vol. 12, pp 119-216.

Jaschke, M.; Butt, H.-J.; Gaub, H. E.; Manne, S. Surfactant Aggregates at a Metal Surface. *Langmuir* **1997**, 13, 1381-1384.

Koopal, L. K.; Lee, E. M.; Böhmer, M. R. Adsorption of Cationic and Anionic Surfactants on Charged Metal Oxide Surfaces. *J. Colloid Interface Sci.* **1995**, 170, 85-97.

Krishnakumar, S.; Somasundaran, P. Adsorption of Aerosol-OT on Graphite from Aqueous and Non-Aqueous Media. *Colloids Surfaces* **1996**, 117, 227-233.

Lake, L. W.; Pope, G. W. Status of Micellar-Polymer Field Tests. *Pet. Eng. Int.* **1979**, 51, 38.

Lee, E. M.; Koopal, L. K. Adsorption of Cationic and Ionic Surfactants on Metal Oxide Surfaces: Surface Charge Adjustment and Competition Effects. *J. Colloid Interface Sci.* **1996**,177, 478-89.

Lopata, J. J. Master's Thesis, University of Oklahoma, Norman, Oklahoma, 1987.

Lopata, J. J.; Harwell, J. H.; Scamehorn, J. F. Adsorption of Binary Anionic Surfactant Mixtures on α-Alumina. In *Surfactant-Based Mobility Control; Progress in Miscible-Flood Enhanced Oil Recovery*; Smith, D. H., Ed.; American Chemical Society: Washington, DC, 1988, pp 205-219.

Manne, S.; Cleveland, J. P.; Gaub, H. E.; Stucky, G. D.; Hansma, P. K. Direct Visualization of Surfactant Hemimicelles by Force Microscopy of the Electrical Double Layer. *Langmuir* **1994**, 10, 4409-4413.

Manne, S.; Gaub, H. Molecular Organization of Surfactants at Solid-Liquid Interfaces. *Science* **1995**, 270, 1480-1842.

Mannhardt, K.; Schramm, L. L.; Novosad, J. J. Adsorption of Anionic and Amphoteric Foam-Forming Surfactants on Different Rock Types. *Colloids Surfaces* **1992**, 68, 37-53.

Novosad, J.J. Surfactant Retention in Berea Sandstone-Effects of Phase Behavior and Temperature. *SPEJ* **Dec. 1982**, 962-970.

Novosad, J.; Maini, B.; Batycky, J. A Study of Surfactant Flooding at High Salinity and Hardness. *JAOCS* **1982**, 59, 833.

Osterloh, W. T.; Jante, M. J., Jr. Surfactant-Polymer Flooding with Anionic PO/EO Surfactant Microemulsions Containing Polyethylene Glycol Additives. *SPE/DOE Eighth Symposium on Enhanced Oil Recovery:* Tulsa, OK, 1992, paper SPE/DOE 24151.

Palmer, C.; Sabatini, D. A.; Harwell, J. H. Sorption of Hydrophobic Organic Compounds and Nonionic Surfactants with Subsurface Materials. In *Transport and Remediation of Subsurface Contaminant*, Sabatini, D. A.; Knox, R. C. Eds.; American Chemical Society: Washington DC, 1992; pp 169-181.

Peru, D. A.; Lorenz, P. B. Surfactant-Enhanced Low pH Alkaline Flooding. paper SPE 17117, 1990.

Roberts, B. L.; Scamehorn, J. F.; Harwell, J. H. In *Phenomena in Mixed Surfactant Systems;* Scamehorn, J. F., Ed; American Chemical Society: Washington, DC, 1986; p 200.

Rosen, M. J. *Surfactants and Interfacial Phenomena*; Wiley, New York, 1989, 2nd ed, pp 35-38.

Rosen, M. J.; Tracy, D. J. Gemini Surfactants. *J. Surf. Detergents* 1998, 1, 547-554.

Rouse, J. D.; Sabatini, D. A.; Brown, R. E.; Harwell, J. H. Evaluation of Ethoxylated Alkylsulfate Surfactants for Use in Subsurface Remediation. *Water Env. Res.* **1996**, 68, 162-168.

Scamehorn, J. F.; Schecter, R. S.; Wade, W. H. Adsorption of Surfactants on Mineral Oxide Surfaces from Aqueous Solutions I: Isomerically Pure Anionic Surfactants. *J. Colloid Interface Sci.* **1982a**, 85, 463-478.

Scamehorn, J. F.; Schecter, R. S.; Wade, W. H. Adsorption of Surfactants on Mineral Oxide Surfaces from Aqueous Solutions II: Binary Mixtures of Anionic Surfactants. *J. Colloid. Interface Sci.* **1982b**, 85, 479-493.

Scamehorn, J. F.; Schecter, R. S.; Wade, W. H. A Reduced Adsorption Isotherm for Surfactant Mixtures. *JAOCS* **1983**, 60, 1345-1349.

Siffert, B.; Jada, A.; Wersinger, E. Anionic Surfactant Adsorption on to Asphalt-Covered Clays. *Colloids Surfaces* **1992**, 69, 45-51.

Somasundaran, P.; Fuerstenau, D. W. Mechanisms of Alkyl Sulfonate Adsorption at the Alumina-Water Interface. *J. Phys. Chem.* **1966**, 70, 90-96.

Somasundaran, P.; Healy, T. W.; Fuerstenau, D. W. Surfactant Adsorption at the Solid-Liquid Interface – Dependence of Mechanism on Chain Length. *J. Phys. Chem.* **1964**, 68, 3562-3566.

Somasundaran, P.; Kunjappu, J. T. In-Situ Investigation of Adsorbed Surfactants and Polymers on Solids in Solution. *Colloids Surfaces* **1989**, 37, 245-268.

Tabatabai, A.; Gonzalez, M. V.; Harwell, J. H; Scamehorn, J. F. Reducing Surfactant Adsorption in Carbonate Reservoirs. *SPERE* **1993**, 117-122.

Taber, J. J.; Martin, F. D.; Seright, R. S. EOR Screening Criteria Revisited – Part 2: Applications and Impact of Oil Prices. *SPERE* Aug. **1997**, 199-205.

Treiner, C.; Montocone, V. Porosity Effects on the Adsorption of Cationic Surfactants and the Coadsorption of 2-Napththol at Various Silica-Water Interfaces. In *Surfactant Adsorption and Surface Solubilization*; Sharma, R., Ed.; American Chemical Society: Washington, DC, 1995, pp 36-48.

Trogus, F. J.; Schecter, R. S.; Wade, W. H. A New Interpretation of Adsorption Maxima and Minima *J. Coll. Interface Sci.* **1979**, 70, 293-305.

Tsau, J-S.; Heller, J. P.; Moradi-Araghi, A.; Zornes, D. R.; Kuehne, D. L. CO_2 Foam Field Verification Pilot Test at EVGSAU: Phase IIIA-Surfactant Performance Characterization and Quality Assurance. *SPE/DOE Ninth Symposium on Improved Oil Recovery*: Tulsa OK, 1994, paper SPE/DOE 27785.

van Olphen, H. *An Introduction to Clay Colloid Chemistry*; Interscience, New York, 1963, pp 17-20.

Wakamatsu, T.; Fuerstenau, D. W. The Effect of Hydrocarbon Chain Length on the Adsorption of Sulfonates at the Solid/Water Interface. In *Adsorption From Aqueous Solution*; Weber, W. J.; Matijevic E., Eds.; American Chemical Society: Washington, DC, 1968; pp 161-172.

Zhu, B-Y; Gu, T. Reverse Hemimicelle Formation of 1-Decanol from Heptane at the Solution/Graphite Interface. *Colloids Surfaces* **1990**, 46, 339-345.

Zhu, B-Y; Gu, T. General Isotherm Equation for Adsorption of Surfactants at Solid/Liquid Interface. *J. Chem. Soc., Faraday Trans.* **1989**, 85(11), 3813-3817.

3.9 – Figures

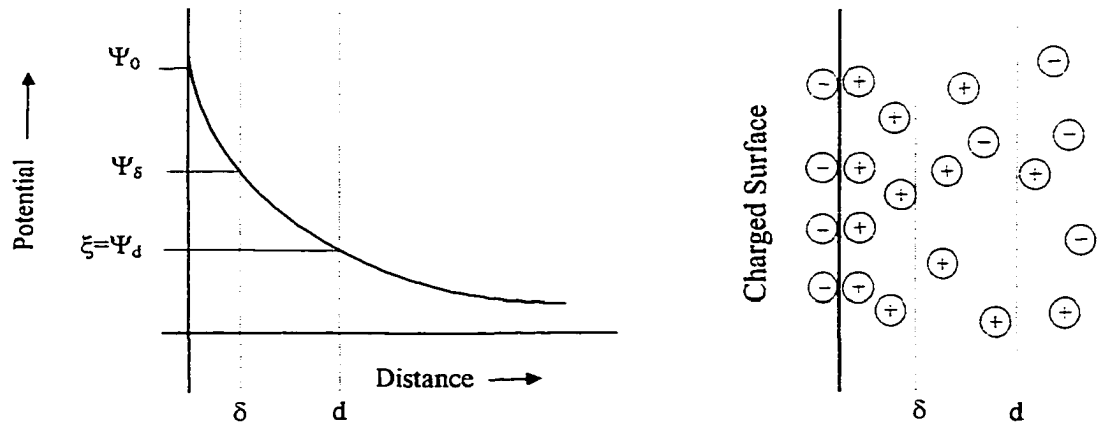

Figure 3-1 Guoy-Chapman model of the electrical double layer and the potential distribution.
Where δ is the Stern plane within which counterions are adsorbed close to the surface and d is the diffuse layer of counterions.

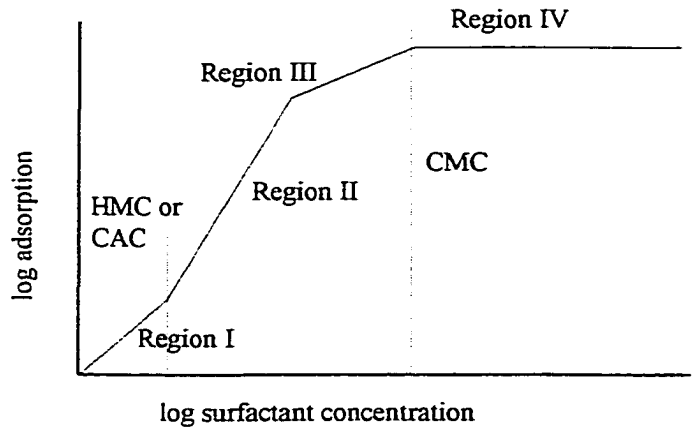

Figure 3-2 Typical four-region adsorption isotherm for a monoisomeric surfactant.

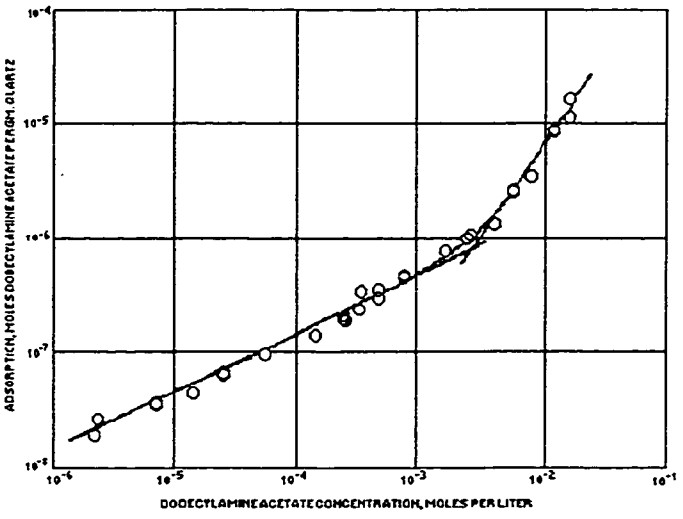

Figure 3-3 Two-region adsorption isotherm of dodecylamine on quartz (Gaudin et al., 1950).

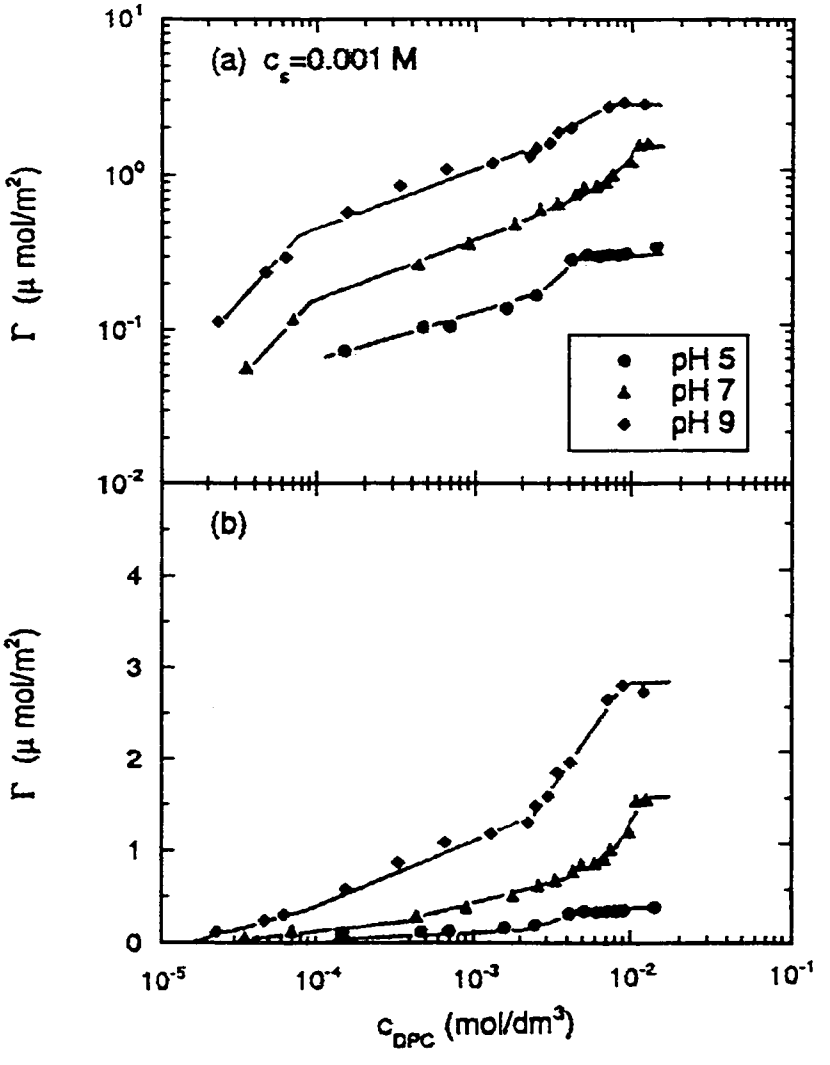

Figure 3-4 Adsorption isotherm of DPC onto Aerosil OX50. (Goulob et al., 1997)

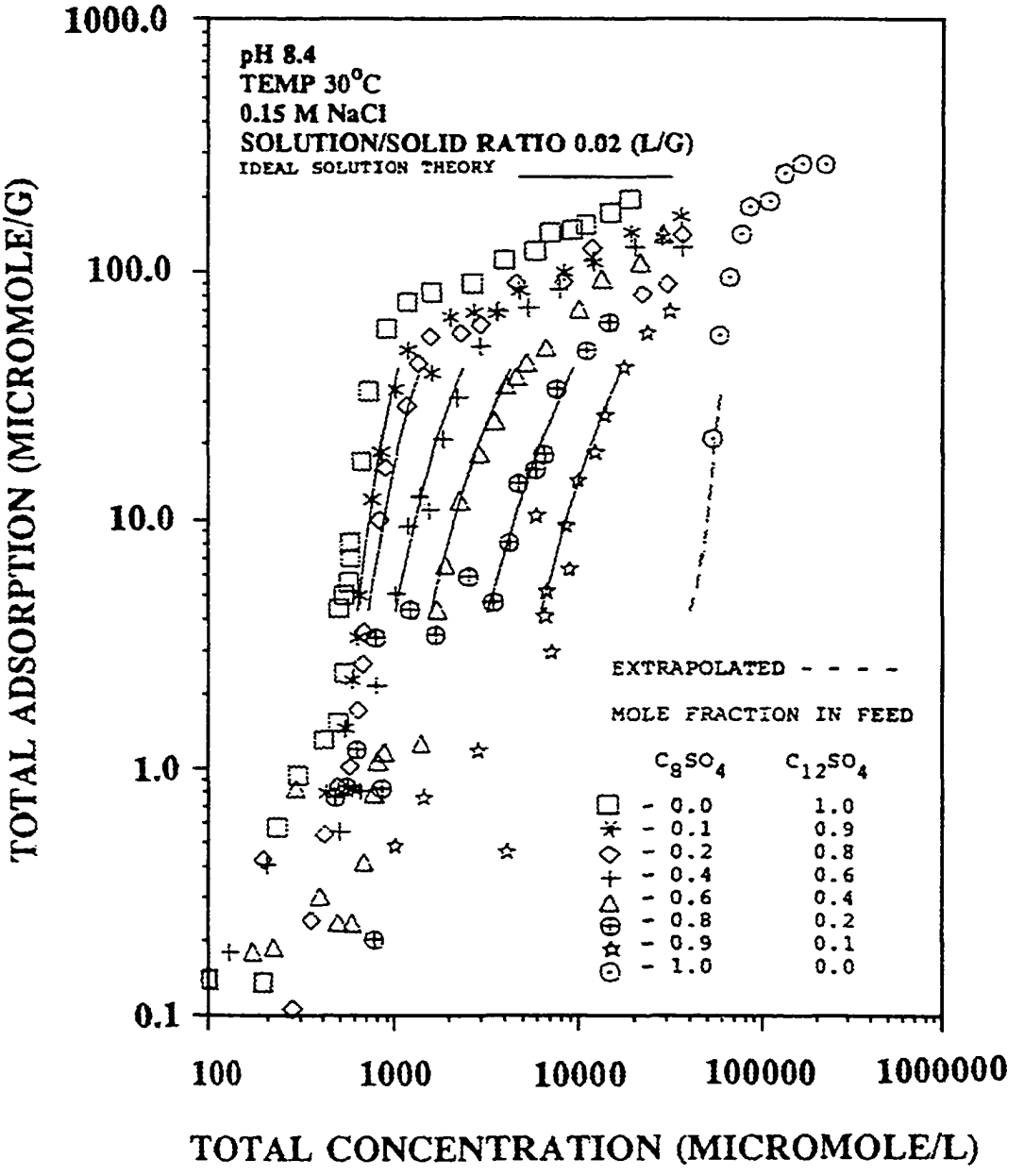

Figure 3-5 Mixed adsorption isotherms of C_8SO_4 and $C_{12}S0_4$ onto α-alumina (Lopata et al., 1988).

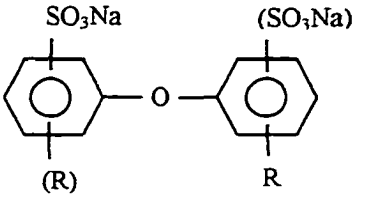

Figure 3-6 Structure of the alkyldiphenyl oxide sulfonate surfactant where R are alkyl chains of C6, C10, C12, or C16.

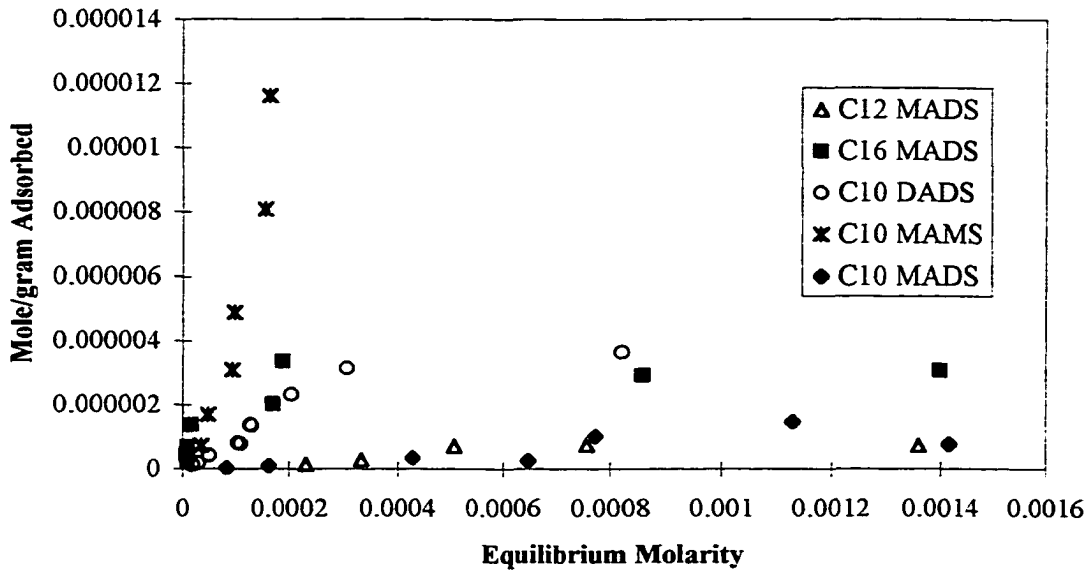

Figure 3-7 Alkyldiphenyl oxide sulfonate adsorption onto CRA, all components.

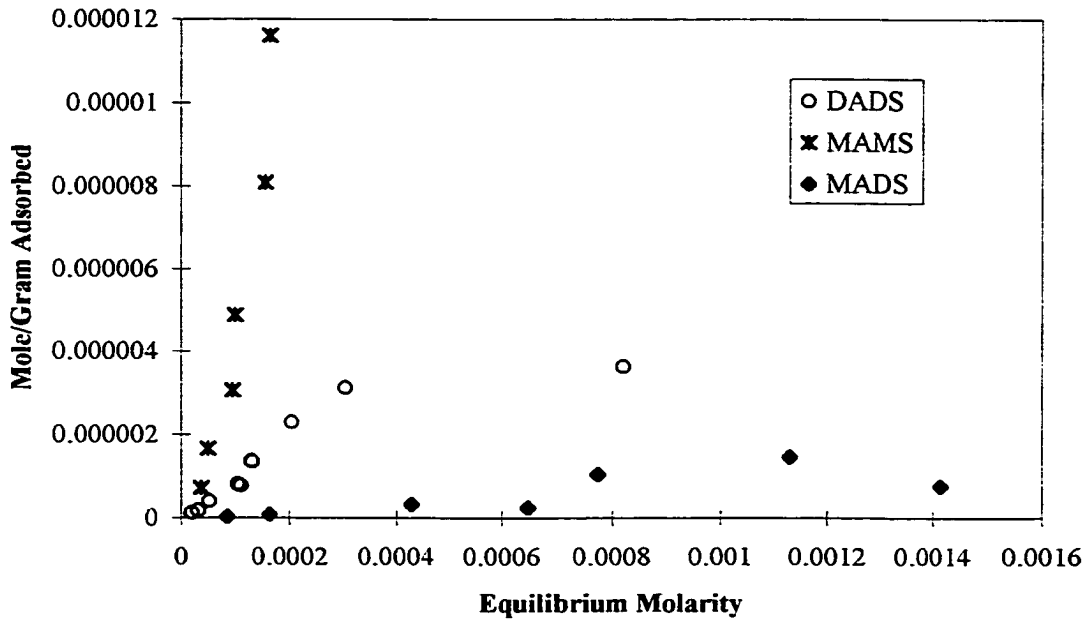

Figure 3-8 Alkyldiphenyl oxide sulfonate adsorption onto CRA, C10 components.

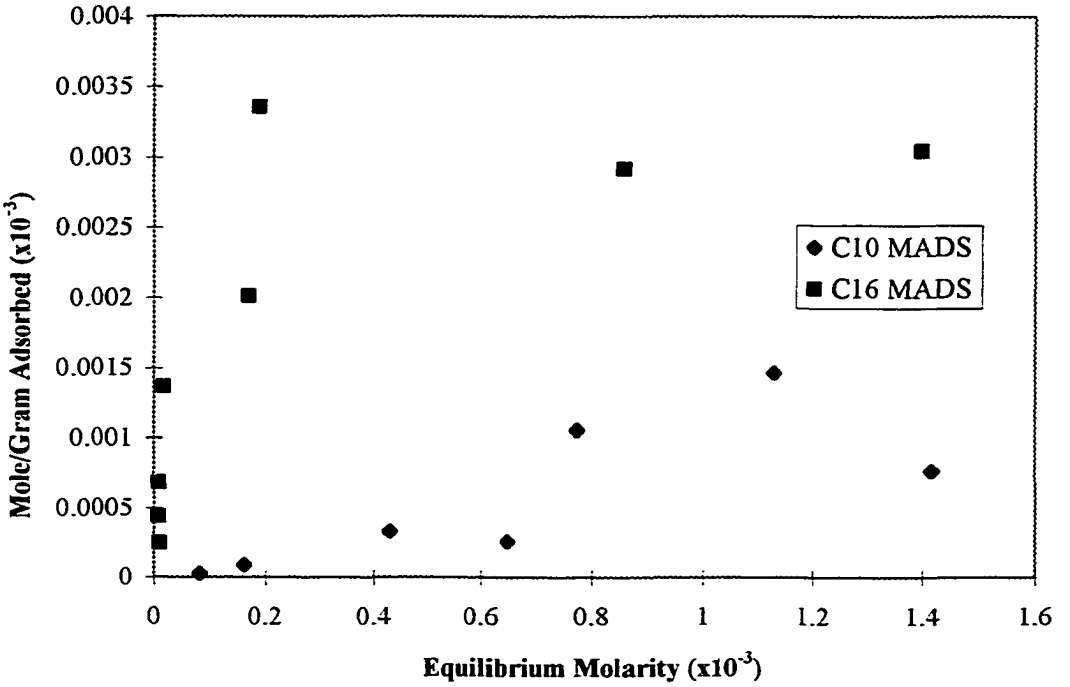

Figure 3-9 Alkyldiphenyl oxide sulfonate adsorption onto CRA, MADS components.

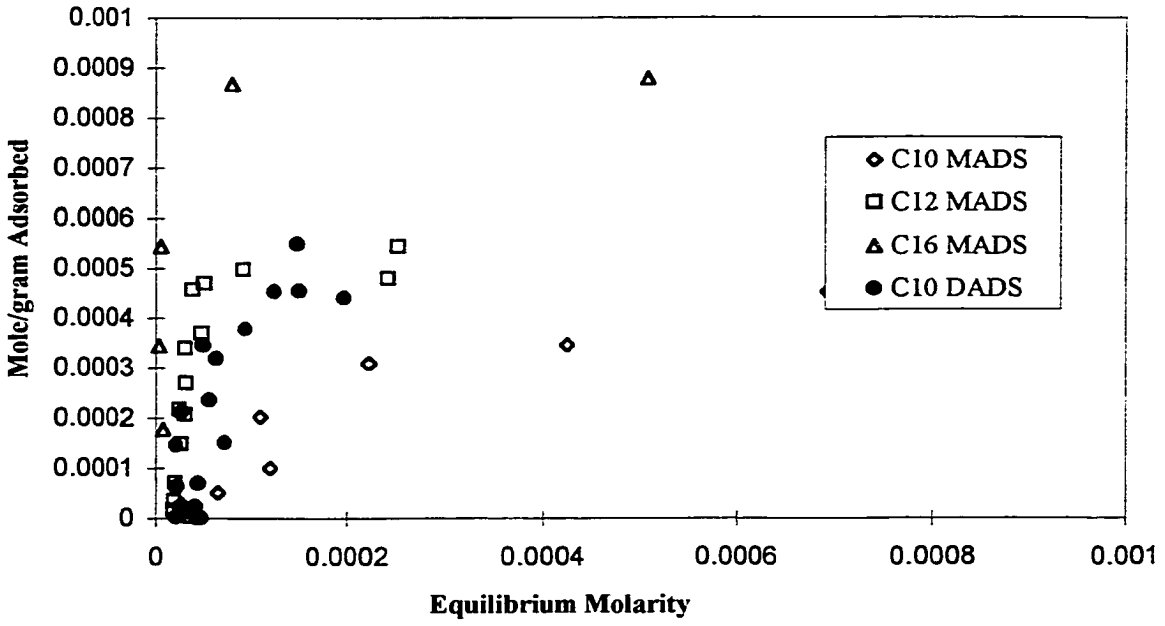

Figure 3-10 Alkyldiphenyl oxide sulfonate adsorption onto alumina, all components.

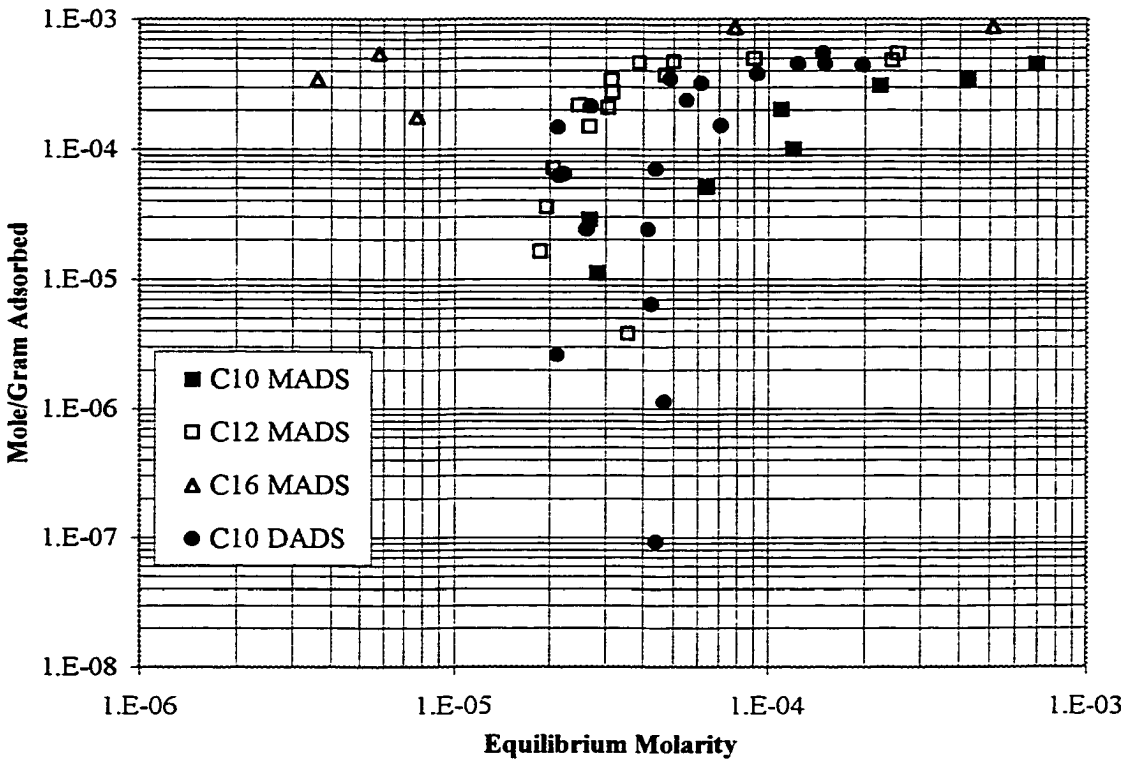

Figure 3-11 Alkyldiphenyl oxide sulfonate adsorption onto alumina, all components.

Chapter 4

Adsolubilization and Solubilization of 2-Naphthol by Alkyldiphenyl Oxide Disulfonate Surfactants

4.1 Abstract

The adsolubilization of 2-naphthol by alkyldiphenyl oxide disulfonate surfactants was conducted on porous alumina, and solubilization studies were conducted using semi-equilibrium dialysis cells. For the C12 MADS as the average feed concentrations of increased, the admicellar mole fractions of 2-naphthol decreased, while the partition coefficient decreased. The adsolubilization behavior and the admicellar aggregation numbers calculated for the C12 MADS surfactant suggest the possibility of perimeter adsorption. This was not the case for the C16 MADS surfactant in which the admicellar mole fractions of 2-naphthol for the two C16 MADS feed concentrations overlapped each other and also overlapped the micellar mole fractions of 2-naphthol over most of the values of the aqueous naphthol mole fractions. This indicates that the admicelles formed by the C16 MADS are more micelle-like in structure than the C12 MADS i.e. no edge-sites are available for naphthol adsorption in the C16 MADS. In the solubilization of 2-naphthol the C12 MADS and C16 MADS surfactants behaved almost identically. The surfactants used in the current study had admicellar or micellar partition coefficients for 2-naphthol that were greater or approximately equal to the partition coefficients as those for cetylpyridinium chloride on silica, sodium dodecyl sulfate, and sodium dodecylbenzene sulfonate on alumina.

4.2 Introduction

The presence of surfactant micelles in solution is known to enhance the apparent solubility of hydrophobic organic compounds by the process of solubilization. Solubilization is the dissolving of an organic solid by reversible interaction with the micelles of a surfactant in an aqueous solution. The amount of an organic compound that can be solubilized depends on the surfactant structure, aggregation number, micelle geometry, ionic strength and chemistry, temperature, solubilizate chemistry and solubilizate size. Those surfactants that produce larger micelles or have lower CMC's tend to have greater degrees of solubilization. For ionic surfactants, increased temperatures tend to promote solubilization, but the behavior of nonionic surfactants is more complex. Less polar solubilizates tend to solubilize better, but larger solubilizates may not solubilize as well as smaller compounds. This is especially true of those solubilizates that solubilize in the core or interior of the micelle.

Mukerjee (1979) proposed a two-state model for solubilization in which there is a distribution between a dissolved state in the nonpolar hydrocarbon pseudophase of the interior of the micelle and an adsorbed state at the micellar-water interface (commonly referred to as the palisade layer). Based on the polarity of the solubilizate it would be expected that nonpolar solubilizates would tend to locate in the core of the micelle while more polar or polarizable solubilizates would tend to locate in the palisade layer.

If solubilization occurs in conjunction with surfactant adsorption onto a solid the process is known as adsolubilization (Harwell, 1985). Lee et al. (1990) reported on the findings of Yeskie (1988) that the incorporation of alcohols into admicelles produced high ratios of alcohol to surfactant adsorption at lower surfactant coverages. Enhanced

surfactant adsorption below the CMC and a slight decrease in the plateau adsorption of the surfactant were also reported. Based on the observations of alkane and alcohol adsolubilizations, it was concluded that for the C12 anionic surfactants studied alcohols can be incorporated into the core and at the hydrophobic perimeter of the admicelle aggregates on the solid surface while alkanes are incorporated only into the core of the admicelles.

The objectives of the current research were to evaluate the adsolubilization behavior of a polar hydrocarbon at two different levels of surfactant surface coverage on a porous mineral oxide. Both of the surfactant surface coverages were below the plateau (region IV) of surfactant adsorption. The adsolubilization was then followed with solubilization studies using the same hydrocarbon. Finally, the various aspects of the adsolubilization and solubilization behaviors were compared.

4.3 Materials

The surfactants used were alkyldiphenyl oxide disulfonates that included C10 DADS, C10 MADS, C12 MADS and C16 MADS which are described in the Prologue. These surfactants were provided by DOW Chemical, Midland, MI and were approximately 35% active by weight. They were used as received. Sodium Chloride, ACS grade, was purchased from Fisher Scientific and also used as received. 2-Naphthol, 99%, was purchased from Aldrich and used as received. Alumina with a BET surface area of 301.83 m^2/g and an average pore diameter of 105.08 Å was provided by LaRoche, Baton Rouge, LA. Methanol, HPLC grade, was purchased from Fisher Scientific.

Semi-equilibrium dialysis (SED) cells (5 mL) and cellulose dialysis membrane filters with an average molecular weight cutoff of 6000 dalton were purchased from Fisher Scientific. A description of an SED cell is given in Section 4.4.2.

4.4 Experimental

4.4.1 Adsolubilization

Adsolubilization studies were conducted using 0.5 grams of alumina and 30 mL of surfactant/naphthol solutions in 40 mL vials. The surfactant/naphthol solutions were prepared in 0.15 M NaCl with a constant surfactant concentration and increasing naphthol concentrations. The naphthol concentrations ranged from 0.0 to 3.5×10^{-3} M. It was desired that the surfactant concentrations selected would produce equilibrium surfactant concentrations that were below the CMC, i.e. below bilayer coverage and with different degrees of coverage of the alumina surface. The initial surfactant concentrations were based on the adsorption isotherms shown in Figure 3-11, and the feed concentrations selected are shown in Table 4-1.

Table 4-1 Initial Surfactant Concentrations Used in Adsolubilization Studies.

Surfactant	C10 DADS	C10 MADS	C12 MADS	C16 MADS
Initial Concentrations (M)	1.92×10^{-4} 1.01×10^{-3}	4.35×10^{-4} 7.42×10^{-4} 7.26×10^{-4}	3.94×10^{-4} 5.99×10^{-4} 6.79×10^{-4}	8.60×10^{-4} 1.43×10^{-3}

After the surfactant/naphthol solutions were added onto the alumina, the pH was adjusted to approximately 3.3. After pH adjustment, the vials were placed on a tabletop shaker for a total of 24 hours. The C10 DADS, C10 MADS and C12 MADS systems were allowed to equilibrate without further pH adjustment, but for the C16 MADS

systems the pH was adjusted 3-4 times in order to force the final pH to be approximately 3.4. Maintaining tighter control of the pH resulted in no experiments having to be repeated for the C16 systems, which was not the case for the other surfactant systems.

At the end of the 24 hours, the vials were removed from the shaker, and the alumina was allowed to settle. When the supernatant was essentially clear of alumina, 3 mL was passed through a 0.2 μm syringe filter and discarded. A second 3 mL was passed through the same filter and collected for analysis. The feed solutions and the supernatant solutions were analyzed on a Shimadzu high performance liquid chromatograph (HPLC) with a Waters UV detector. The mobile phase was 55 % methanol and the UV wavelength was 254 nm. Data collection for the C10 DADS, C10 MADS and C12 MADS was done by a Hewlett-Packard integrator, Model HP 3396 Series III and for the C16 MADS using Varian's STAR chromatography software, Version 4.51.

4.4.2 Solubilization

Solubilization studies were conducted using SED cells with cellulose dialysis membranes. A SED cell (Figure 4-1) consists of Plexiglas halves each having a 5 mL void and a threaded access port. When assembled the two voids are separated by a cellulose dialysis membrane. This membrane allows the movement of surfactant monomers and solubilizate from the retentate to the permeate side. The key to this method is that the monomeric solubilizate concentrations are the same on both sides of the membrane. This allows for the assumption of equal activity coefficients of the solubilizate on both sides of the membrane. In an ideal dilute solution the solubilizate activity equals the concentration

of the solubilizate monomer. From this, solubilization constants can be determined from SED data (Christian et al., 1985).

Initial surfactant concentrations were chosen that were well above the CMC. The initial concentrations were 1.34×10^{-3} M for the C10 DADS, and 2.50×10^{-3} M for the C12 and C16 MADS. These concentrations were approximately 20 times the CMC reported by DOW for C12 MADS and 10 times the CMC reported by DOW for the C16 MADS and C10 DADS.

Naphthol concentrations ranged from 0.0 to 6×10^{-3} M. As with the adsolubilization surfactant/naphthol solutions, the solubilization solutions were prepared in 0.15 M NaCl for the MADS surfactants while the C10 DADS was prepared in 0.09 M NaCl. The retentate side of the cell was filled with surfactant/naphthol/NaCl solution and the permeate side was filled with a solution of NaCl. Due to the unavoidable flexing of the membrane, filling the two chambers was done in alternating 1 mL increments. This helped insure equal volumes in both chambers. The final 0.5 mL of each chamber was filled using a syringe. The narrower diameter of the needle allowed any air bubbles present in the chamber to move up and out of the chambers through the access ports. The chambers were sealed with stainless steel bolts covered with parafilm. The cells were allowed to sit at room temperature for 24 hours. Similar work (Rouse et al., 1995) had shown this to be an acceptable time frame for these types of surfactants and solute. At the end of the 24 hours, the solutions in the retentate and permeate chambers were extracted using a disposable pipette. The feed, permeate, and retentate solutions were then analyzed using the same HPLC procedure described in the previous section. Since these are closed systems, mass balances were performed on each of the samples.

4.5 Results and Discussion

4.5.1 Behavior of Naphthol in the Absence of Surfactant

The adsolubilization behavior of alumina/naphthol systems was analyzed at the same salinity and pH of the surfactant/naphthol/alumina systems. Initial naphthol concentrations ranged from $6.66x10^{-4}$ to $2.64x10^{-3}$ M. It should be pointed out that in the current study the naphthol/alumina systems were not studied in a systematic manner. The samples evaluated were prepared as naphthol blanks during individual surfactant analyses. While the results presented suggest a degree of interaction between naphthol and alumina, the following discussion is presented as the basis for not taking these results into account in the adsolubilization results. Table 4-2 lists the results of these analyses.

Table 4-2 Adsorption Results of Naphthol/Alumina Blanks

Equilibrium Concentration (M)	Mole naphthol adsorbed/ gram alumina	pH_{final}
$5.82x10^{-4}$	$5.06x10^{-5}$	5.15
$5.89x10^{-4}$	$5.37x10^{-5}$	4.65
$8.99x10^{-4}$	$2.13x10^{-4}$	NA
$9.42x10^{-4}$	$3.28x10^{-4}$	3.21
$1.84x10^{-3}$	$5.76x10^{-5}$	3.82
$2.52x10^{-3}$	$1.33x10^{-4}$	3.66

From Table 4-2 and the data in Tables 4A-2 through 4A-4 it can be seen that the apparent amount of naphthol adsorbed in the absence of surfactant is less than the amount of naphthol adsolubilized in the presence of surfactant for the same initial concentration of naphthol, but is still on the same order of magnitude. The pK_a of 2-naphthol is 9.51, and at the pH values used in the current study the naphthol would be expected to be undissociated, and interaction with the alumina would not be expected based on electrostatic interactions. Nor is this apparent relationship due to the final pH values. As

shown in Table 4-2, there was a sizable range of final pH values; but while the lowest pH value corresponded to the system with the greatest amount of "adsorption", there is no trend of decreasing adsorption with increasing pH. The error bars shown in Figure 4-2 are used to indicate errors of ±10% which are a common for HPLC analysis. As discussed in section 4.5.3 there was great concern about the HPLC analysis, in particular the calibration curves used to determine the equilibrium concentrations and the procedure used to assure the accuracy of the adsolubilization results. It appears that in order to assure the accuracy of the adsolubilization results that involve the concentrations of the surfactants and naphthol, the accuracy of the naphthol blank solution analyses is suspect.

While several adsolubilization studies have been conducted with 2-naphthol, the interaction of naphthol with the solid surface (porous and nonporous silicas) is not discussed in detail. Any interaction is presented as being very small or nil, but no numerical values are provided (Treiner and Monticone, 1994 and Esumi et al., 1996). In the study presented by Nayyar (1993) a naphthol/alumina system was analyzed. The alumina used had a reported surface area of 155 m^2/g and from the data provided the naphthol adsorption was calculated to be 7.74×10^{-6} mole/gram. Unfortunately, there was no adjustment of the pH to a lower value as was done in the current study and in the studies reported by Treiner and Monitcone (1994) and Esumi et al. (1996). Based on the concerns about the HPLC analysis and no apparent chemical explanation for any naphthol/alumina interaction, the "adsorption" values for the 2-naphthol were ignored for the analysis of the adsolubilization data.

4.5.2 Adsorption of surfactants in the presence of naphthol

The effect of naphthol on the surfactant adsorption was examined by determining the surfactant adsorptions that would have been seen in the absence of naphthol which were determined from the surfactant adsorption isotherms from Figure 3-11 and were based on the average initial surfactant concentrations used in the adsolubilization studies. The expected surfactant adsorptions from the adsorption isotherms and the actual surfactant adsorptions in the presence of naphthol are shown in Table 4-3.

Table 4-3 Surfactant Adsorption onto Alumina

Surfactant	Average initial concentration (M)	Mole/gram (expected)	Mole/gram (actual)
C10 MADS	4.25×10^{-4}	1.1×10^{-4}	1.68×10^{-4}
	7.40×10^{-4}	3.1×10^{-4}	2.83×10^{-4}
C12 MADS	3.94×10^{-4}	2.1×10^{-4}	2.04×10^{-4}
	5.99×10^{-4}	3.2×10^{-4}	3.27×10^{-4}
	6.80×10^{-4}	3.5×10^{-4}	3.36×10^{-4}
C16 MADS	8.60×10^{-4}	6.0×10^{-4}	4.04×10^{-4}
	1.43×10^{-4}	8.7×10^{-4}	6.93×10^{-4}
C10 DADS	1.92×10^{-4}	9.1×10^{-5}	1.06×10^{-4}
	1.01×10^{-3}	4.6×10^{-4}	5.23×10^{-4}

The expected and actual adsorption amounts were very similar with the exception for the C16 MADS where the actual adsorptions were 67% and 79% of their expected value. This difference is attributed to lower equilibrium pH values from the adsorption studies. For the other surfactants the similarity of the adsorption values in the presence of naphthol and those obtained without naphthol indicate that the presence of the naphthol has little effect on the adsorption of the surfactant.

4.5.3 Adsolubilization

In order to quantify the adsolubilization capabilities of the surfactants the partition coefficient, K_{adm}, will be used. K_{adm} is a ratio of the mole fraction of the adsolubilizate in the admicellar pseudophase, X_{adm}, to the mole fraction of adsolubilizate in the aqueous phase, X_a. K_{adm} was calculated using Equation 4-1:

$$K_{adm} = X_{adm} / X_a \tag{4-1}$$

Where X_{adm} is calculated from:

$$X_{adm} = (mole/gram)_{sol} / \left((mole/gram)_{sol} + (mole/gram)_{surf}\right) \tag{4-2}$$

and X_a from:

$$X_a = C_{equi}^{sol} * 0.01805 \tag{4-3}$$

Where C_{equi}^{sol} is the equilibrium concentration in Molarity, 0.01805 is the molar volume of water in L/mol at 25 °C, and the super- and subscripts *sol* and *surf* refer to solubilizate and surfactant, respectively. It should be noted that Equation 4-3 is applicable for dilute solutions. Alternate definitions reported in the literature include:

$$X_a = C_{eq} / (C_{eq} + 55.55) \qquad \text{(Nayyar et al., 1994)}$$

and,

$$X_a = C_{eq} / (C_{eq} + S_{eq} + 55.55) \qquad \text{(Esumi et al., 2000)}$$

Where C_{eq} and S_{eq} are the equilibrium adsolubilizate and surfactant concentrations, respectively and 55.55 is the inverse molar volume of water. Equation 4-3 was chosen to

compliment the calculations for the solubilization data which are presented in the next section, but the acceptability of the dilute solution assumption was checked by calculating X_a from all three equations for several systems and comparing the final values. Selected values are shown in Table 4-4. It can be seen that there is little or no difference between the values of X_a calculated from the three different equations, and the assumption of a dilute solution is acceptable.

Table 4-4 Comparison of X_a for C16 MADS (8.60×10^{-4} M initial concentration)

Sample	X_a (Eqn. 4-3)	X_a (Nayyar)	X_a (Esumi)
1	5.42×10^{-7}	5.41×10^{-7}	5.41×10^{-7}
3	1.48×10^{-5}	1.14×10^{-5}	1.14×10^{-5}
5	2.80×10^{-5}	2.79×10^{-5}	2.79×10^{-5}
7	4.75×10^{-5}	4.74×10^{-5}	4.74×10^{-5}

Plots of X_a versus X_{adm} and of X_{adm} versus K_{adm} were constructed and are shown in Figure 4-3 through 4-6. From the plots of X_{adm} versus K_{adm}, shown in Figure 4-5 and 4-6, a sharp increase in K_{adm} at the lowest values of X_{adm} was observed. For example, in the adsolubilization of 2-naphthol in C12 MADS (feed concentration 5.99×10^{-4} M) at a X_{adm} of 0.24 the K_{adm} was 109613 while at X_{adm} of 0.38 the K_{adm} was 44603. Similar decreases were seen for the other C12 MADS system and for the C16 MADS. This same trend had been observed in a solubilization study of a commercial mixture of C16 MADS and C16 DADS (Dowfax® 8390) and 1-naphthol (Rouse, 1994). He attributed this to the influence of the more hydrophobic components of the surfactant solution dominating micelle formation at lower surfactant concentrations (which would be expected to have greater solubilization potentials and thus higher K_m's), but in the current study the surfactant concentrations are held constant so further examination of this sharp increase in K_{adm} was warranted.

It was obvious that the value of K_{adm} was strongly affected by small changes in the value of either X_{adm} or X_a. At low values of X_{adm} and X_a, the value of K_{adm} is very sensitive to inaccuracies in the determination of X_a or X_{adm}. It was noted that the choice of calibration curves for naphthol had a great affect at the lowest values of C_{equi}^{sol} and thus X_a. To elaborate, from the HPLC data two calibration curves for naphthol could be and were constructed. One from chromatograms from standard solutions containing only naphthol and a second from the adsolubilization feed solutions. Theoretically, the two curves should overlap, but this was not always the case, particularly for the higher surfactant concentrations. In these systems the surfactant peak tended to have a trailing end which overlapped the beginning of the naphthol peak, and there was not the clean separation between the 2-naphthol and the surfactant except at the lower surfactant concentrations. Attempts were made to enhance the chromatographic separation of the two peaks by adjusting the ratio of the water and methanol composing the mobile phase, but lower methanol concentrations tended to only increase the broadening of the surfactant peak while higher methanol concentrations did not separate the two components.

When it was realized that this interaction could not be avoided, analysis of the HPLC data involved assuring consistency in the calculations. The calibration curve generated from the naphthol standard solutions was used to calculate the naphthol concentrations in the feed solutions whose concentrations were known. If the values calculated were within ±10% of the actual values then the calibration curve with the best linear fit was chosen to calculate the unknown naphthol concentrations. For many of the analyses the calculated values for the initial naphthol concentrations were greater than

±10%, and in these cases the calibration curve generated from the feed solutions was used to calculate the naphthol concentrations. Examination of the chromatograms indicated that the interaction of the naphthol and surfactant peaks for the initial solution and the adsolubilized solution for a given sample tended to be very similar in nature. This provided a more consistent base for the remaining calculations in the analysis of the data.

All of the HPLC data was reanalyzed in order to assure that consistency in analysis had been maintained throughout. This reanalysis of the C10 DADS was not possible since naphthol standards had not been used.

With the limitations of the data analysis in mind, it is realized that the actual values of K_{adm} at the lowest X_{adm} values may not be as high as shown for some of the samples, but that the trend of higher values of K_{adm} at the lower X_{adm} values is a real phenomena. This discussion is also applicable to the analysis of the SED data. The higher values of K_m at lower X_m values were also seen in the solubilization of 2-naphthol.

Adsolubilization was conducted for each surfactant at a minimum of two concentrations; both of which were located in the type II region of adsorption. For the C10 DADS, the average initial surfactant concentrations were 1.92×10^{-4} and 1.01×10^{-3}M, and the naphthol concentrations ranged from 2.77×10^{-4} to 3.75×10^{-3} M. Plots of X_{adm} versus K_{adm} are shown in Figure 4-3. The K_{adm} values for the 1.92×10^{-4} M system are greater than those of the 1.01×10^{-3} M feed over the same range of initial naphthol concentrations suggesting that the there are more available sites for naphthol adsolubilization in systems containing less surfactant. This is consistent with the findings of Yeskie (1988) for sodium dodecyl sulfate/alcohol systems.

Comparison of the partition coefficients for the C10 MADS and C12 MADS surfactants based on the initial surfactant concentrations is not as straightforward. For each surfactant, the results of the lower surfactant feed concentration systems were as expected, but the results of systems with higher initial surfactant concentrations were not. The C10 MADS, $4.35X10^{-4}$ M initial surfactant, behaved as expected with a smooth decrease in K_{adm} with increasing X_{adm}, but for the systems with $7.4x10^{-4}$ M initial surfactant K_{adm} tended to decrease but not as smoothly as in the $4.35x10^{-4}$ M system. In an attempt to confirm or refute this behavior a second experiment was conducted at the higher initial surfactant concentration. This time the average initial surfactant concentration was $7.26x10^{-4}$ M. The final results were even more complex. There was no smooth decrease in K_{adm} with increasing X_{adm} as seen in Figure 4-4.

Initially, it was felt that there was probably a significant amount of deviation in the final pH values between the solutions of $7.26x10^{-4}$ M C10 MADS that was responsible for the complex behavior of the naphthol, but this was not the case. The final pH values of the samples comprising this run do not deviate from each other any more than in the other systems. The final pH values are provided in Appendix 4A. Re-examination of the HPLC analysis did not indicate any problems with the HPLC analysis other that already discussed, and no definitive explanation of this complex behavior is readily apparent.

Comparing the results from the C10 MADS systems containing $4.35x10^{-4}$ and $7.4x10^{-4}$ M initial surfactant, it can be said that from Figure 4-4 that for a given X_a, the values of X_{adm} are very similar until $X_a > 2x10^{-5}$; at which point the mole fraction of naphthol in the admicelles formed in the $4.35x10^{-4}$ M surfactant continues to increase, but in the $7.4x10^{-4}$ M begins to decrease. But in relation to the partition coefficient, the values

of K_{adm} for both surfactant concentrations are similar above $X_{adm} = 0.1$. Below this, greater partitioning is seen in those solutions containing the higher concentration of surfactant.

For the C12 MADS systems containing 3.94×10^{-4} and 5.99×10^{-4} M initial surfactant concentrations, the partitioning coefficients for the 3.94×10^{-4} M systems tended to be greater than those of the 5.99×10^{-4} M systems.

C12 MADS systems prepared with 6.8×10^{-4} M initial surfactant concentration reflected a non-smooth change in K_{adm} with X_{adm}. Again there was no significant difference in the pH values between the different samples. In order to confirm this behavior, the HPLC analysis was performed twice with very similar results. The most significant difference between this situation and the behavior seen in the C10 MADS is that the partition coefficients for the 3.94×10^{-4} M C12 MADS systems are consistently greater than those of the 5.99×10^{-4} and 6.80×10^{-4} M systems. The lower partition coefficients for the 6.80×10^{-4} M surfactant system relative to the 5.99×10^{-4} M systems could not be readily explained until the SED data was analyzed. As shown in Figure 4-5, there is an overlap of the K_{adm} values of the 6.80×10^{-4} M adsolubilization system and the K_m for the 2.53×10^{-3} M SED system. This strongly suggests the presence of micelles in the adsolubilization solutions made with 6.80×10^{-4} M C12 MADS, although the presence of micelles does not readily explain the complex behavior seen.

Comparison of the two C16 MADS systems, average initial surfactant concentrations of 8.60×10^{-4} and 1.43×10^{-3} M, indicates very little difference between the partitioning coefficients for the two systems for all values of X_{adm}. See Figure 4-6. This suggests that the C16 MADS forms similar surface aggregates at both concentrations.

This behavior does not fit the behavior demonstrated by the C12 MADS surfactant in this study, in the alcohol/SDS study reported by Yeskie (1988) or that of naphthol adsolubilized by SDS (Nayyar et al., 1994). In these studies the surfactants were comprised of shorter alkyl chains. The similar adsolubilization behavior demonstrated by the two concentrations of C16 MADS is discussed in further detail in Section 4.4.5

4.5.4 Solubilization

Solubilization studies were conducted with the C10 DADS, C12 MADS, and C16 MADS surfactants using the procedure described in Section 4.3.2. Since the SED cells can be considered closed systems, it was possible to perform mass balances on the surfactants and naphthol in order to check the accuracy of the HPLC analysis. The mass balances on the surfactants were within ±10% for the C12 MADS and C16 MADS, while the error associated with the C10 DADS was slightly larger at ±16%. The balances on naphthol were generally within ±10% for the C12 MADS and C16 MADS with only a few samples outside of this range. For the C10 DADS the naphthol mass balances were within ±20%. It is felt that the larger errors and problems with the HPLC analysis in general with the C10 DADS prevent any definitive conclusion on its solubilization abilities and will not be discussed.

As with the adsolubilization, there are several values that are typically calculated in order to evaluate a surfactant's ability to solubilize a particular solubilizate. The equations used for solubilization are shown on the next page. The data for and the results from these calculations are in Appendix 4A, Tables 4A-5, 4A-6, and 4A-7.

For semi-equilibrium dialysis the following equations were applied:

$$X_a = C_{perm}^{sol} * 0.01805 \tag{4-4}$$

$$X_m = \left(C_{ret}^{sol} - C_{perm}^{sol}\right) \Big/ \left(C_{ret}^{sol} - C_{perm}^{sol} + C_{ret}^{surf} - C_{perm}^{surf}\right) \tag{4-5}$$

$$K_m = X_m / X_a \tag{4-6}$$

Where the definitions of X_a, X_m, and K_m are the same as in the previous section except X_m is the mole fraction of solubilizate in the micelle, the solubilization potential, K_m, is the ratio of the mole fraction of solubilizate in the micellar pseudophase to the mole fraction in the aqueous pseudophase. The subscripts *ret* and *perm* refer to retentate and permeate, respectively.

Comparing the solubilization parameters of the C12 and C16 MADS shown in Figure 4-7B, it can be seen that for all X_m, the values of K_m overlap. This indicates that for the same initial surfactant concentration, the C12 and C16 MADS surfactant micelles have nearly identical capabilities of solubilizing naphthol.

4.5.4.1 Comparison of Adsolubilization and Solubilization Parameters of Alkyldiphenyl Oxide Disulfonate Surfactants to Other Surfactants

Several studies have been conducted using 2-napthol as the solubilizate using both cationic and anionic surfactants on porous and nonporous silica and alumina. The maximum adsolubilization of naphthol at an equilibrium cetylpyridinium chloride concentration of 2.0×10^{-4} M on porous silica was approximately 2.5×10^{-4} mole/L of solution at a pH of 3.6 and a NaCl concentration of 0.01 M (Monticone and Treiner, 1995) compared to a maximum adsolubilization in the C16 MADS system, pH = 3.36 and

a NaCl concentration of 0.15 M just over 5.00×10^{-4} M. The equilibrium C16 MADS concentration was approximately 1.3×10^{-4} M.

Using the data provided by Esumi et al. (1995) for the adsolubilization of naphthol by SDS on nonporous alumina the value of K_{adm} was estimated to be 13000 for an initial naphthol concentration of 0.4 mmol/dm^3 and an equilibrium SDS concentration of 5 mmol/dm^3 at an initial pH of 3.5. This value is about one-fourth of the K_{adm} calculated for similar systems in the current C12 MADS adsolubilization study. A more realistic comparison would be to compare their results and the current results based on the initial surfactant concentrations, since several initial surfactant concentrations can produce the same amount of adsorption. Unfortunately, the initial surfactant concentrations were not provided.

Nayyar et al. (1994) reported a maximum X_{adm} of approximately 0.224 for a X_a of 9.7×10^{-5} in a titration study involving SDS and 2-naphthol. Alumina with a surface area of 155m^2/g was used for this study. The initial SDS concentration was not reported. For the C12 MADS surfactant used in the current study a similar value of X_{adm} (0.244) was seen at a X_a of 2.23×10^{-6}. Also, the values of X_a did not exceed 3.5×10^{-5}.

Rouse et al. (1995) reported on the solubilization of 1-naphthol by the surfactants sodium dodecyl benzenesulfonate (SDBS) and DPDS. DPDS is a commercially available mixture of C16 MADS and C16 DADS. They reported a maximum X_m of 0.31 at an equilibrium retentate concentration of 2.24×10^{-2} M DPDS and a maximum X_m of slightly greater than 0.20 at an equilibrium SDBS retentate concentration of 1.96×10^{-2} M. Assuming the behavior of 1-and 2- naphthol would be similar, the values of X_m reported by Rouse et al. compare to a X_m of 0.29 for an equilibrium C16 MADS retentate

concentration of 2.6×10^{-3} M and a X_m of 0.29 for an equilibrium C12 MADS retentate concentration of 2.2×10^{-3} M.

These comparisons suggest that the alkyldiphenyl oxide disulfonate surfactants used in the current study have greater solubilization potential for naphthol that SDS, SDBS, or cetylpyridinium chloride. From the solubilization studies involving the C16 alkyldiphenyl oxide disulfonate surfactants similar results were obtained for the commercially available mixture and the C16 MADS used in this study. This is not unexpected since the C16 used in this study is also a mixture. The component distributions are provided in Table 1-3 of Chapter 1.

4.5.4.2 Comparison of Adsolubilization and Solubilization Parameters of Alkyldiphenyl Oxide Disulfonate Surfactants

Comparisons between the alkyldiphenyl oxide disulfonate surfactants used in this study began by comparing the partition coefficients of all of the surfactants based on solutions containing initial naphthol concentrations within ±0.15 M of each other. It was found that no one surfactant tends to dominate with higher partition coefficients in the adsolubilization of 2-naphthol. This comparison is based on data summarized in Appendix 4B and Figure 4-8.

In comparing the values of X_m for the different surfactants, it can be seen that for the C12 MADS, the maximum value of X_m for solubilization is 0.29 which is slightly less than half of the maximum X_{adm} seen for the C12 MADS adsolubilization samples (X_{adm} = 0.73).

The maximum value of X_m for the C16 MADS solubilization was 0.44, although this particular data point appears out of place and the actual maximum X_m would be

expected to be closer to 0.30. The data in question is enclosed with a box in Figure 4-7a. The maximum value of X_{adm} for adsolubilization is 0.42. But it should be pointed out that for these two samples, the initial concentration of naphthol in the solubilization was almost twice the concentration used in the adsolubilization sample, $6.3x10^{-3}$ versus $3.3x10^{-3}$ M. As seen in Figure 4-6a, the values of X_m for the micelles are only slightly lower than those of the admicelles. However from Figure 4-6b, the K_m's for solubilization for values of $X_m < 0.17$ are lower than the K_{adm} values for adsolubilization for the same range of X_{adm} values. Indicating that for $X_{adm} < 0.17$ the admicelles are more capable of solubilizing naphthol, but beyond this the micelles and admicelles of C16 MADS have very similar capabilities.

Although there was some difference between the values of K_{adm} and K_m for the adsolubilization and solubilization of naphthol by C16 MADS, there was not the large difference as was seen for the C12 MADS. It was felt that either micelles were present in the C16 MADS adsolubilization samples or the C16 MADS behaved differently than the C12 MADS. Pinacyanol chloride (PCC) was used to determine whether or not micelles were present in the adsolubilization samples. PCC is known to exhibit different colors in aqueous and organic solutions and has been used to determine whether or not micelles are present. In the presence of water PCC is purple and in organic compounds, royal blue. The royal blue color appeared in solutions containing $1.4x10^{-3}$ M surfactant, but lower concentrations varied from bluish green to brown. Standard surfactant solutions of 0.25 to 5*CMC were prepared, and PCC was added to each. Table 4-5 contains the color variations produced by the PCC in various concentrations of these surfactant solutions.

Table 4-5 Colors of PCC in C16 MADS Solutions

Sample	$1.82x10^{-6}$ M	0.25*CMC	0.50*CMC	1*CMC	3*CMC	5*CMC
Color	Purple	Purplish-brown	Brown	Bluish-green	Greenish blue to blue	Royal blue

PCC was added to samples containing only surfactant, feed solutions, and adsolubilized solutions from each of the C16 MADS adsolubilization runs. The feed solution containing $7.39x10^{-4}$ M surfactant was greenish-blue to blue while its adsolubilized counterpart was brown. The feed solution containing $1.41x10^{-3}$ M surfactant was royal blue while its adsolubilized counterpart was brown. Since the brown coloration was present only in solutions below the CMC, it can be concluded that the C16 MADS adsolubilization solutions equilibrated below the CMC, and that the behavior of the C16 MADS is different than that of the C12 MADS. Figure 4-9 offers some further insight. As seen, the partition coefficients are far greater for the adsolubilization of naphthol at both initial surfactant concentrations than for the solubilization in C12 MADS. The partition coefficient for the C12 MADS adsolubilization is also greater than those of the adsolubilizations and solubilization for the C16 MADS. Error analysis for the C12 MADS adsolubilization and solubilization results indicate that the trends discussed for the partition coefficients (K_{adm} and K_m) are valid. The values for $\lambda^2(K_{adm})$ and $\lambda^2(K_m)$It is proposed that the longer chain lengths of the C16 MADS allows the formation of admicelles which are more micelle-like, i.e. with no edge-effects and that the presence of these "edges" allow for the greater adsolubilization by the C12 MADS. It is proposed the differences in the structures and compositions of the C12 MADS and C16 MADS are the sources of these differences. The exact nature of the structural differences is considered proprietary information and cannot be discussed in this writing (Quencer, 2001).

4.5.5 Two-Site Adsolubilization Model

In an attempt to verify the existence of the edge-affect for the C12 MADS the two-site adsolubilization model reported by Lee et al. (1990) was applied. This model was used to calculate the average aggregation number of the surfactant, and the reasonableness of the results was offered as proof of the existence of edges for the 2-naphthol solubilization. The equation used is shown below and the reader is referred to the reference for the derivation.

$$N_{AV} = \frac{8 l^2 A_S \pi}{A_A^2} \left(\frac{\Gamma_A}{\Gamma_S} - \frac{C_A K_{A,b}}{1 - C_A K_{A,b}} \right)^{-2} \tag{4-7}$$

Where the variables were defined as follows in Table 4-6. If the values are constant for all calculations, they are also indicated.

Table 4-6 Definitions and Numerical Values of Variables Used in Two-site Adsolubilization Model

Variable	Definition	Value	Source of value
N_{AV}	Average aggregation number		
l	Length of a surfactant hydrocarbon chain	1.6 nm	Theoretical length of fully extended hydrocarbon tail of surfactant
A_S	Area per headgroup for surfactants in the admicelle	0.278 nm^2	From the adsorption density of C12 MADS monolayer at the air/water interface
A_A	Area per headgroup for alcohol molecules adsorbed at the hydrocarbon band around the perimeter of the admicelles	0.20 nm^2	Adsorption density of an alcohol monolayer at an oil/water interface
Γ_A	Gibbs adsorption of alcohol	varies	Measured experimentally at each alcohol and surfactant concentration
Γ_S	Gibbs adsorption of surfactant	varies	Measured experimentally at each alcohol and surfactant concentration
C_A	Equilibrium concentration of alcohol in solution	varies	Measured experimentally at each alcohol and surfactant concentration
$K_{A,b}$	Partition of alcohol into the palisade layer of the admicelle	271	Estimated from the experimental partition coefficient measured nearest bilayer coverage: $K_{A,b} = (X_{A,C}/C_A)_{bilayer}$

Of the three adsolubilization studies, only the C12 MADS surfactant could be used to test the applicability of the two-site model due to the fact that this is the only surfactant

for which $K_{A,b}$ could be estimated. The relationships between the aggregation numbers calculated from Equation 4-7 and the surfactant adsorption density are shown in Figure 4-10. There is a decrease in the aggregation number with increasing initial naphthol concentration and at the highest naphthol concentrations a decrease in the surfactant adsorption density. The aggregation numbers are reasonable and combined with the fact that the solutions containing the lower concentration of surfactant had the greater adsolubilization; in agreement with the findings of Yeskie (1988), suggest the possibility of edge adsorption. Confirmation of the existence of edge-site adsorption would require a more in-depth study; particularly, adsolubilization studies conducted in which the naphthol concentrations were held constant and the surfactant concentrations were varied.

4.6 Conclusions

While the possibility of naphthol/alumina interaction is suggested in the current study, it could not be proven conclusively. In any future research involving naphthol and alumina or any other porous surface a systematic investigation into this interaction would be warranted.

The presence of the naphthol did not affect the degree of adsorption of the surfactants. The differences seen for the C16 MADS was attributed to the differences in the pH values used in the adsorption and adsolubilization studies.

Two methods for comparing the adsolubilization of naphthol were used. Based on the changes of K_{adm} with X_{adm} the C12 MADS demonstrated greater solubilizing capabilities relative to the C10 MADS, C16 MADS, and the higher concentration of C10 DADS, but about the same capability as the lower C10 DADS concentration.

Comparisons based on the changes of K_{adm} with increasing initial naphthol concentrations indicate that the alkyldiphenyl oxide disulfonate surfactants have about equal capabilities for the adsolubilization of 2-naphthol. Each of the methods used in the comparison offers insight into the behavior of these surfactants in the presence of naphthol.

For the C12 MADS the greater values of K_{adm} than of K_m for all X_m indicate the possibility of naphthol adsorption at the perimeter of the C12 MADS admicelles. Further evidence was offered by the aggregation number calculated from the Lee and Yeskie two-site adsolubilization model.

The C16 MADS did not exhibit the same type of behavior with the values of K_{adm} and K_m overlapping for all but the lowest values of X_m. This behavior indicates the structures of the admicelles are very similar to the structure of the micelles.

The alkyldiphenyl oxide disulfonate surfactants tended to have greater adsolubilization and partitioning of the 2-naphthol compared to the cationic surfactant cetylpyridinium chloride and the anionic surfactant SDS.

Comparing the solubilization of naphthol by C16 MADS with its commercially available counterpart, DPDS, the micellar mole fraction of naphthol in the C16 MADS was approximately the same as that in the DPDS although the retentate surfactant concentration of the C16 MADS was an order of magnitude less than the DPDS.

At the same initial concentration the C12 MADS and the C16 MADS micelles have nearly identical solubilizing capabilities for 2-naphthol. It would be interesting to conduct these solubilization studies using surfactant concentrations at identical factors of

the CMC where it would be expected that the C16 MADS would be able to solubilize a greater amount of naphthol.

4.7 References

Christian, S. D.; Smith, G. A.; Tucker, E. A.; Scamehorn, J. F. Semiequilibrium Dialysis: A New Method for Measuring the Solubilization of Organic Solutes by Aqueous Surfactant Solution. *Langmuir*, **1985**, 1(5), pp 564-567.

Edwards, D.A.; Luthy, R. G.; Liu, Z. Solubilization of Polycyclic Aromatic Hydrocarbons in Micellar Nonionic Surfactant Solutions. *Environ. Sci. Technol.* **1991**, 25(1) pp 127-133.

Esumi, K.; Goino, M.; Koide, Y. Adsorption and Adsolubilization by Monomeric, Dimeric or Trimeric Quaternary Ammonium Surfactant at Silica/Water Interface. *J. Colloid Interface Sci.*, **1996**, 183, pp 539-545.

Esumi, K.; Mizuno, K.; Yamanaka, Y. Adsolubilization Behavior of 2-Naphthol into Adsorbed Surfactant and Poly(vinylpyrrolidone) at an Alumina/Water Interface. *Langmuir*, **1995**, 11(5), pp 1571-1575.

Esumi, K.; Uda, S.; Suhara, T.; Fukui, H.; Koide, Y. Cationic Surfactant Adsolubilization of 2-Naphthol and Naphthalene with Titanium Dioxide Having Dodecyl Chain, *J. Colloid Interface Sci.*, **1997**, 193, pp 315-318.

Harwell, J. H.; Hoskins, J. C.; Schecter, R. S.; Wade, W. H. Pseudophase Separation Model for Surfactant Adsorption: Isomerically Pure Surfactants. *Langmuir*, **1985**, 1(2), pp 251-262.

Lee, C.; Yeskie, A.; Harwell, J. H.; O'Rear, E. A. Two-Site Adsolubilization Model of Incorporation of Alcohols into Adsorbed Surfactant Aggregates. *Langmuir*, **1990**, 6(12), pp 1758-1762.

Monticone, V.; Treiner, C. Coadsorption of Naphthalene Derivatives and Cationic Surfactants on Porous Silica in Aqueous Solutions. *Langmuir*, **1995**, 11(5), pp 1753-1759.

Mukerjee, P. Solubilization in Aqueous Micellar Systems. In *Solution Chemistry of Surfactants*, Vol. 1, Mittal, K. L. Ed; Plenum Press: New York, 1979.

Nayyar, S. P. Master Thesis, University of Oklahoma, Norman, OK, 1993.

Nayyar, S. P.; Sabatini, D. A.; Harwell, J. H. Surfactant Adsolubilization and Modified Admicellar Sorption of Nonpolar, Polar and Ionizable Organic Contaminants. *Environ Sci Technol.* **1994**, 28(1), pp 1874-1881.

Quencer, L. B. The Dow Chemical Company, Midland, MI, Personal communication, 2001.

Rouse, J. D. Ph.D. Thesis, University of Oklahoma, Norman, OK, 1994, Chapter 3 pp 75 and 77.

Rouse, J. D.; Sabatini, D. A.; Deeds, N. E.; Brown, R. E. Micellar Solubilization of Unsaturated Hydrocarbon Concentrations As Evaluated by Semiequilibrium Dialysis. *Environ. Sci. Technol.* **1995**, 29(10), pp2484-2489.

Rosen, M. J., *Surfactants and Interfacial Phenomena*, 2nd Ed. John Wiley & Sons, New York, 1989.

Treiner, C.; Monticone, V. Porosity Effects on the Adsorption of Cationic Surfactants and the Coadsorption of 2-Napthol at Various Silica-Water Interfaces. In *Surfactant Adsorption and Surface Solubilization*, Vol. 615, Sharma, R., Ed; American Chemical Society, Washington D. C., 1995.

Yeskie, M. Ph.D. Thesis, University of Oklahoma, Norman, OK, 1988.

4.8 - Figures

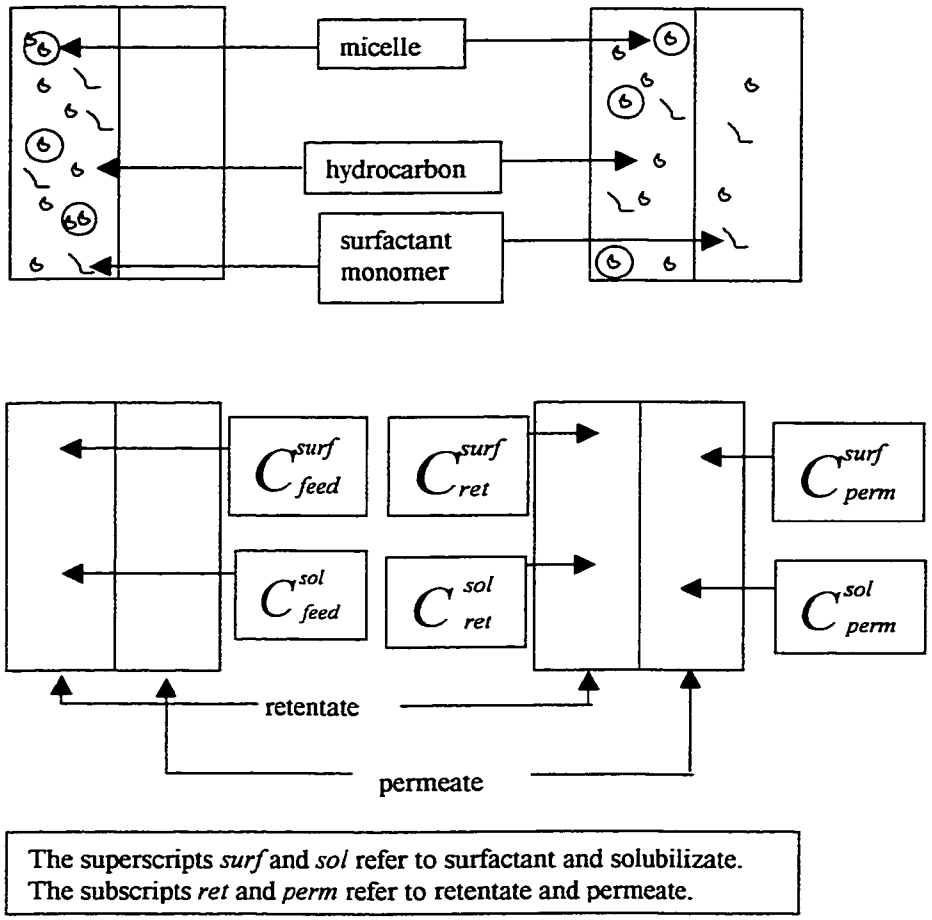

Figure 4-1 Semiequilibrium dialysis cell description and terminology.

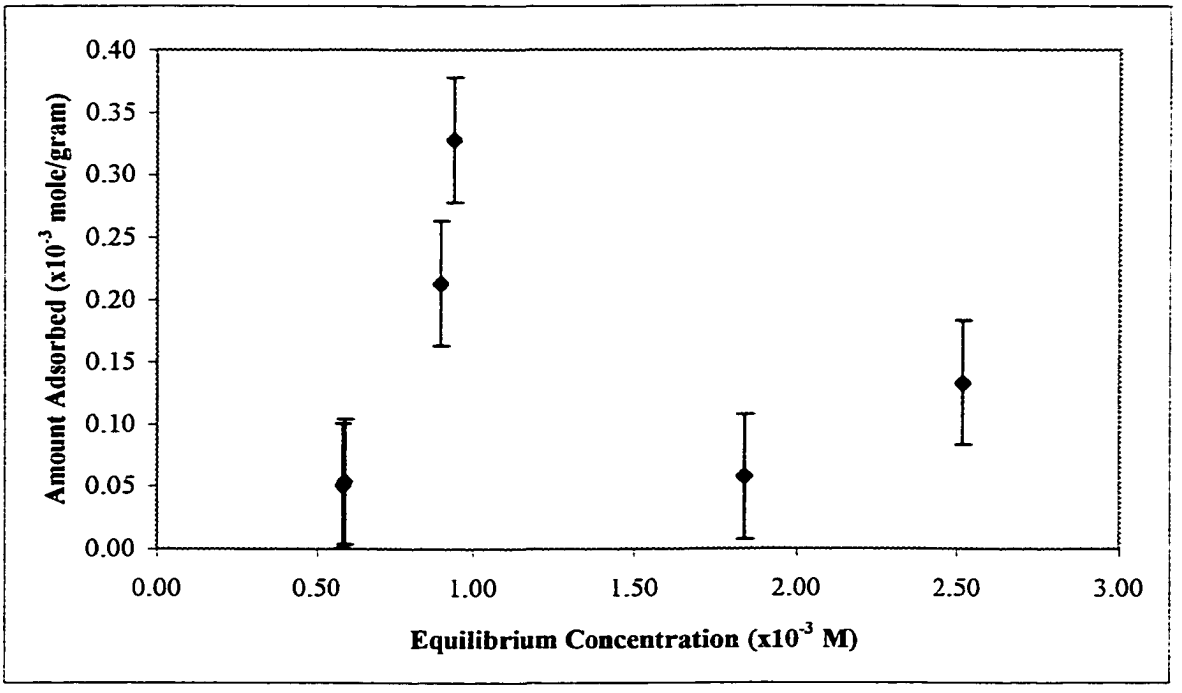

Figure 4-2 Adsorption of 2-naphthol onto porous alumina in the absence of surfactant.

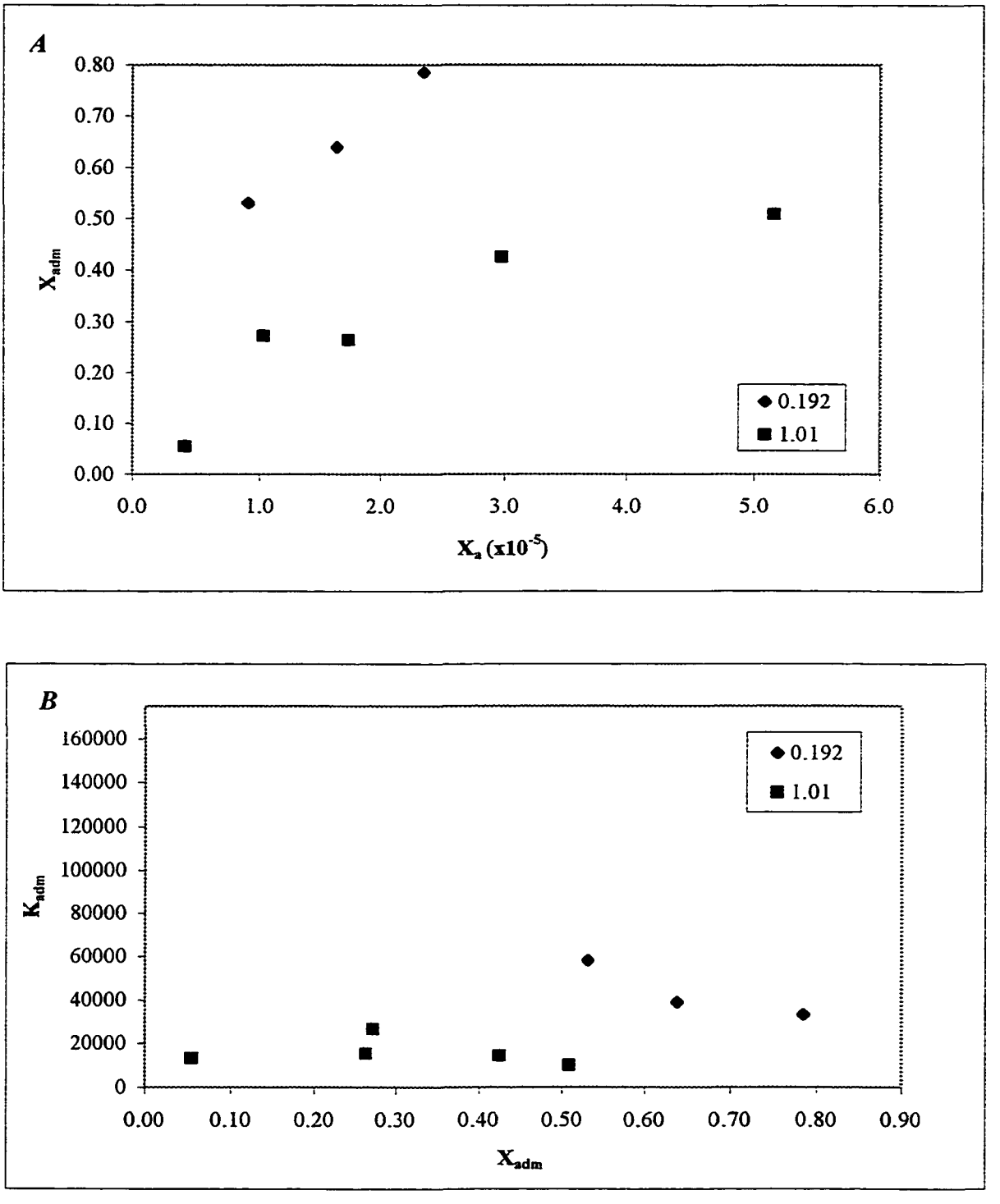

Figure 4-3 Adsolubilization of 2-naphthol by C10 DADS. Values in the legends indicate the initial surfactant concentrations (x10^{-3}M).

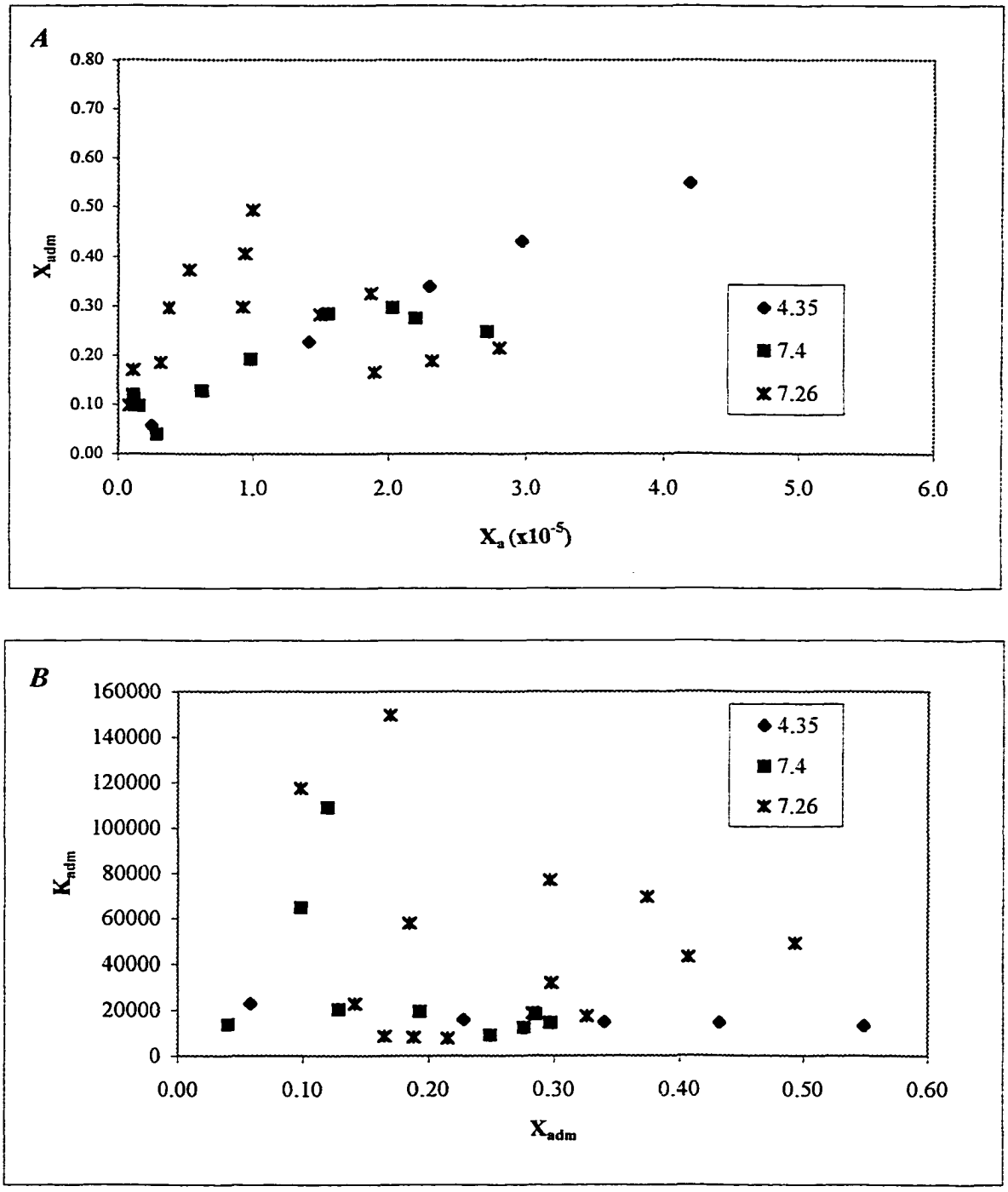

Figure 4-4 Adsolubilization of 2-naphthol by C10 MADS. Values in the legends indicate the initial surfactant concentrations (x10^{-4}M).

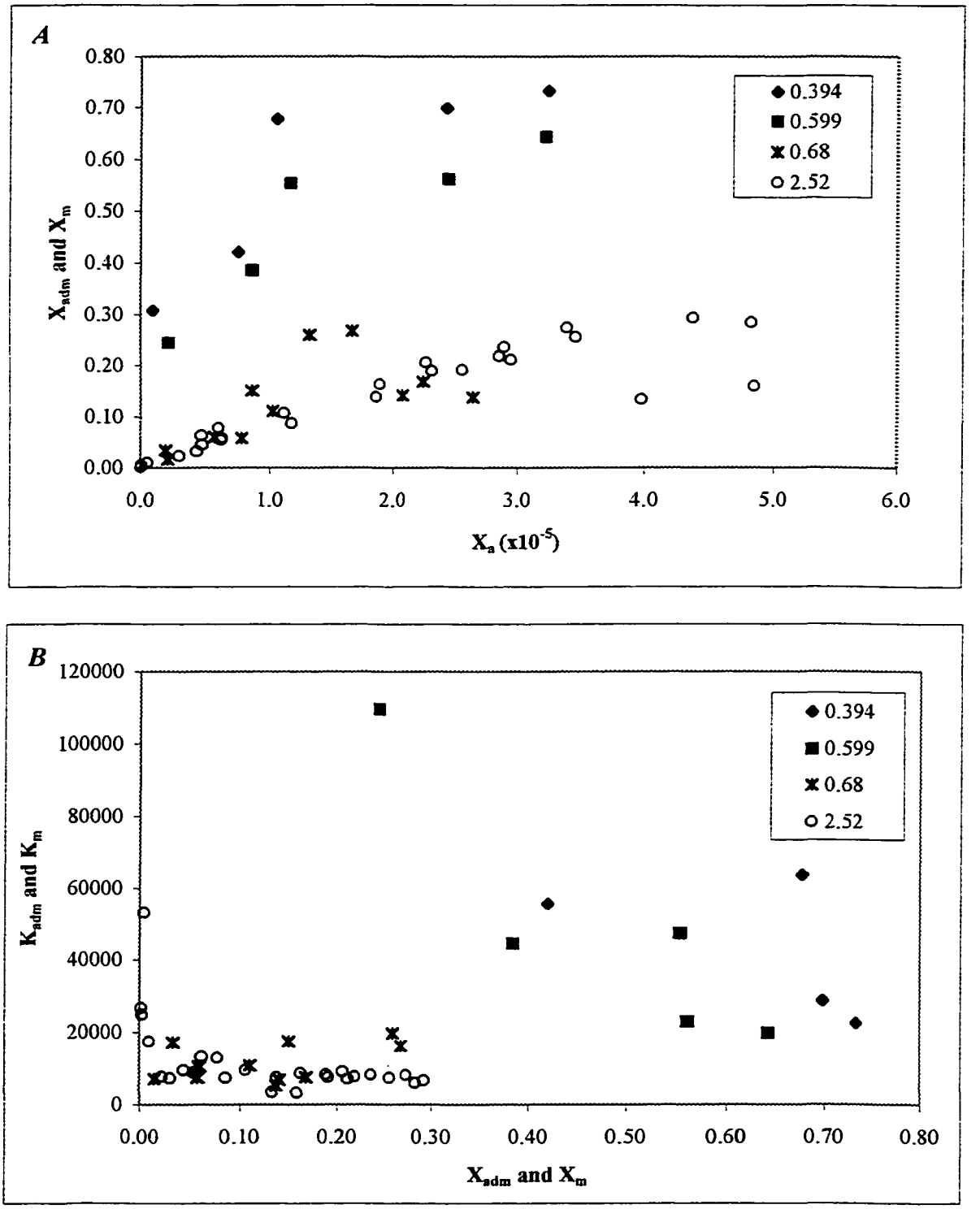

Figure 4-5 Adsolubilization and solubilization of 2-naphthol by C12 MADS. Where K_{adm} values are indicated by ♦,■, and ✳, and K_m values are represented by ○. Values in the legends indicate the initial surfactant concentrations ($x10^{-3}$M).

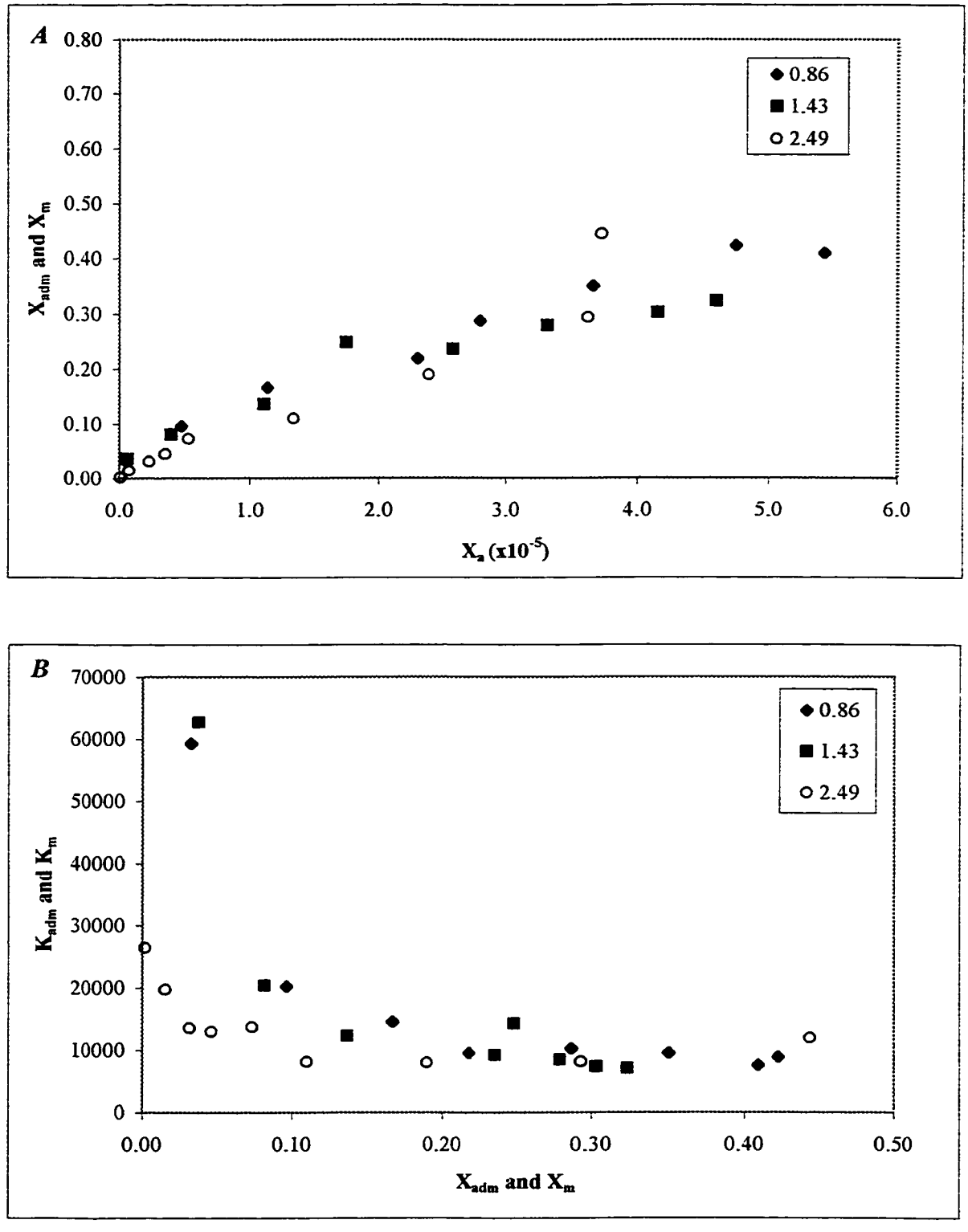

Figure 4-6 Adsolubilization and solubilization of 2-naphthol by C16 MADS. Where K_{adm} values are indicated by ◆ and ■, and K_m values are represented by ○. Values in the legends indicate the initial surfactant concentrations ($x10^{-3}$M).

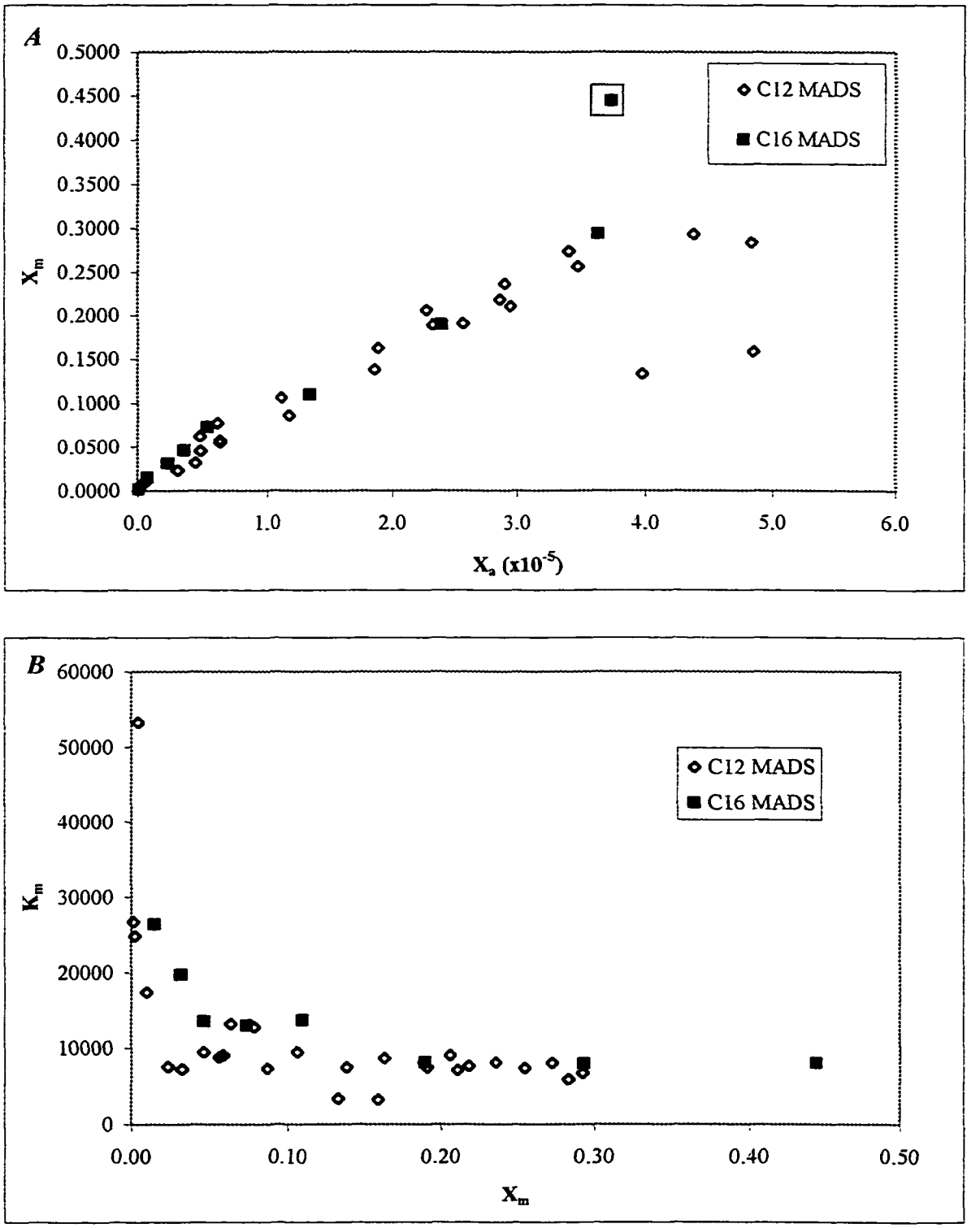

Figure 4-7 Solubilization of 2-naphthol by C12 MADS and C16 MADS.

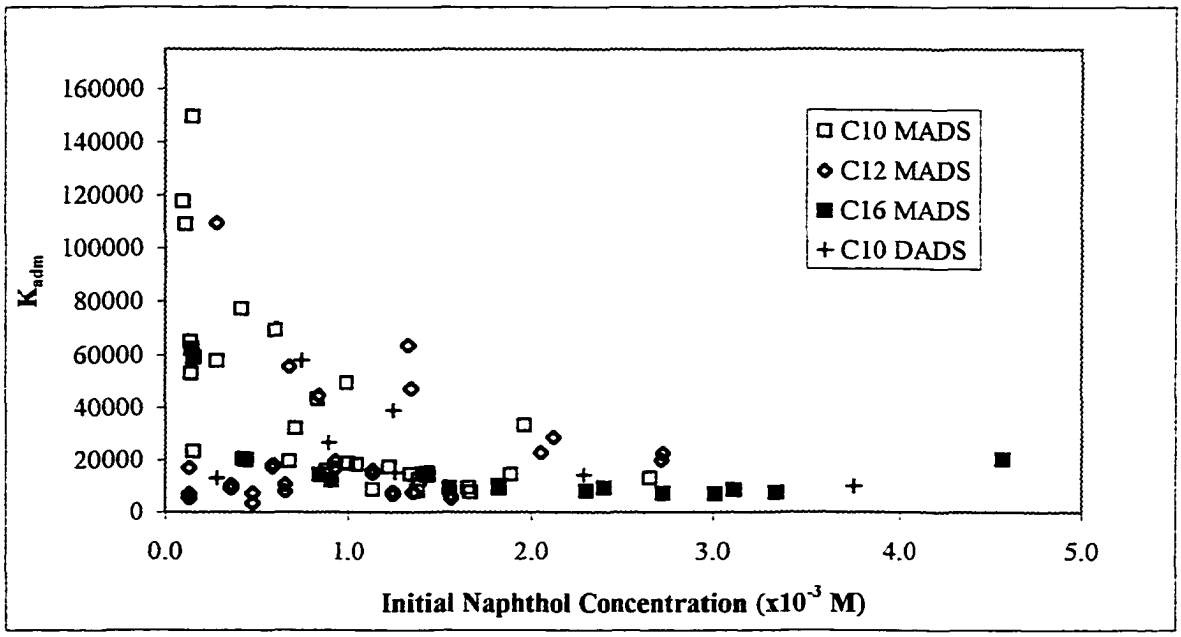

Figure 4-8 Change in K_{adm} with initial 2-naphthol concentration.

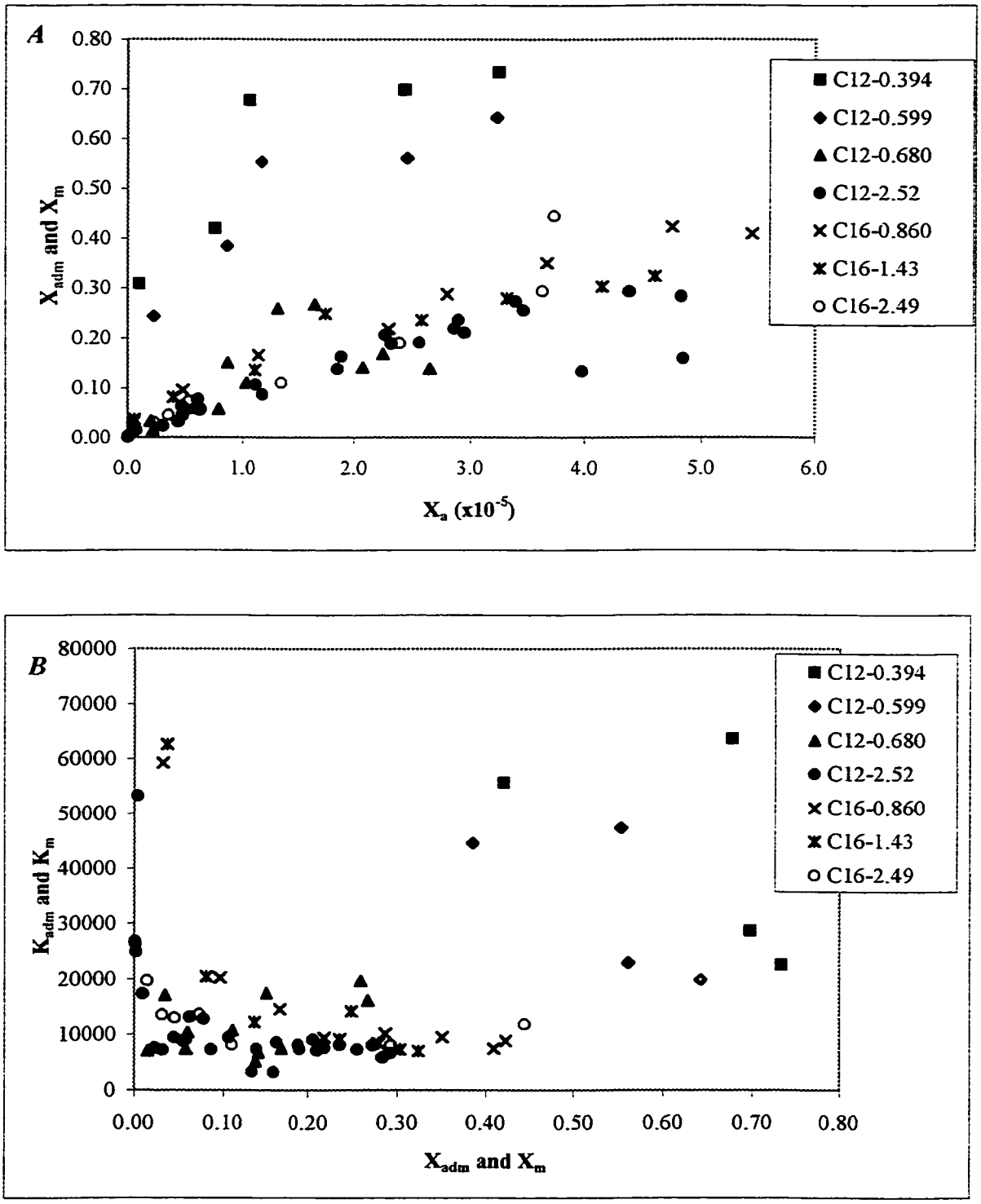

Figure 4-9 Adsolubilization and solubilization of 2-naphthol by C12 MADS and C16 MADS.
Values in the legend are the initial surfactant concentrations ($x10^{-3}$M). K_m is indicated by • and ○, and the remaining symbols represent K_{adm} values.

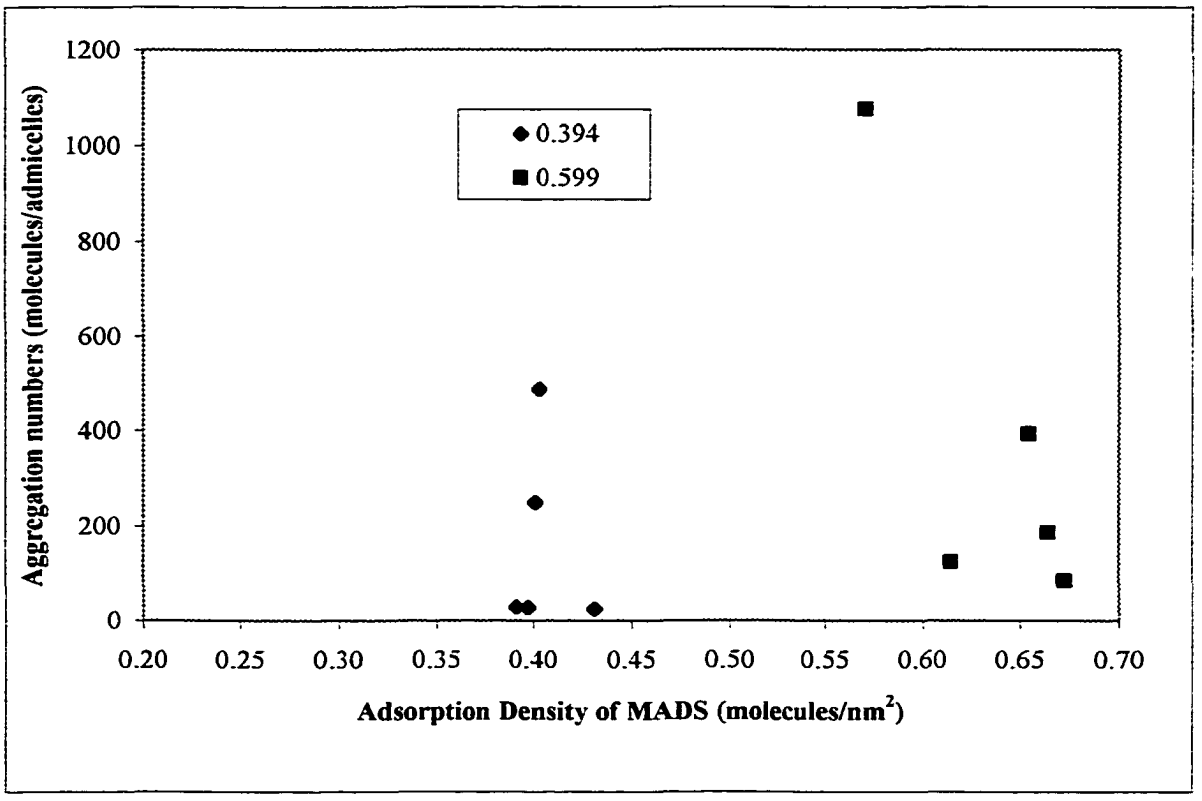

Figure 4-10 Aggregation numbers for the C12 MADS/naphthol adsolubilization. Values in the legend are the initial surfactant concentrations ($x10^{-3}M$)

4A Appendix: Data for Adsolubilization and SED

Data for C10 DADS Adsolubilization

Table 4A-1a 1.92×10^{-4} M Average Initial Surfactant Concentration

$DADS_{initial}$ $x10^{-4}$ M	$Naphthol_{initial}$ $x10^{-4}$ M	$pH_{,final}$	DADS, mole/gram $x10^{-4}$	Naphthol, mole/gram $x10^{-5}$	X_a, $x10^{-6}$	X_{adm}	K_{adm}
1.97	0.00	4.23	9.97	0.00			
2.06	7.35	3.84	1.15	1.62	8.19	0.1325	16185
1.99	12.50	3.82	1.02	1.78	17.20	0.1336	7770
1.85	19.60	4.19	1.06	3.66	23.70	0.2641	11122

Table 4A-1b 1.01×10^{-3} M Average Initial Surfactant Concentration

$DADS_{initial}$ $x10^{-4}$ M	$Naphthol_{initial}$ $x10^{-4}$ M	$pH_{,final}$	DADS, mole/gram $x10^{-4}$	Naphthol, mole/gram $x10^{-5}$	X_a, $x10^{-6}$	X_{adm}	K_{adm}
10.3	0.00	4.79	5.61	0.00			
10.0	2.77	2.45	5.13	0.416	4.16	0.0544	13075
10.1	8.88	4.70	4.56	1.03	10.27	0.2729	26565
10.1	12.63	4.45	5.43	1.74	17.40	0.2644	15195
10.1	22.89	4.54	5.63	2.98	29.81	0.4251	14258
10.0	37.46	4.69	5.02	5.15	51.49	0.5083	9872

Data for C10 MADS Adsolubilization

Table 4A-2a 4.35x10^{-4} M Average Initial Surfactant Concentration

$MADS_{initial}$ x10^{-4} M	$Naphthol_{initial}$ x10^{-4} M	$pH_{,final}$	MADS, mole/gram x10^{-4}	Naphthol, mole/gram x10^{-5}	X_a, x10^{-6}	X_{adm}	K_{adm}
4.15	1.53	5.37	1.51	0.921	2.47	0.0573	23202
4.27	8.74	4.45	1.73	5.10	14.24	0.2277	15992
4.67	14.29	4.63	1.88	9.68	22.85	0.3403	14892
4.58	18.87	4.06	1.89	14.39	29.72	0.4317	14526
4.04	26.64	4.20	1.68	20.45	41.88	0.5487	13102
4.37	0.00	3.00	1.40	0.00			
0.00	6.66	5.15	0.00	5.06			

Table 4A-2b 7.40x10-4 M Average Initial Surfactant Concentration

$MADS_{initial}$ x10^{-4} M	$Naphthol_{initial}$ x10^{-4} M	$pH_{,final}$	MADS, mole/gram x10^{-4}	Naphthol, mole/gram x10^{-5}	X_a, x10^{-6}	X_{adm}	K_{adm}
7.67	1.11	6.45	2.13	2.91	1.10	0.1200	109165
7.06	1.38	3.54	2.89	3.14	1.51	0.0981	65094
7.74	1.39	4.58	2.98	2.82	1.63	0.0866	52957
7.22	4.16	4.86	2.73	4.03	6.30	0.1285	20404
7.40	6.66	3.91	2.98	7.12	9.85	0.1929	19577
7.36	10.54	4.54	3.01	12.04	15.56	0.2855	18352
7.74	13.46	4.78	3.23	13.67	20.33	0.2972	14616
7.49	13.94	3.65	2.73	10.42	21.89	0.2759	12604
7.21	16.58	3.82	2.70	8.94	27.14	0.2488	9166
8.11	0.00	3.57	3.03	0.00			
0.00	6.80	4.65	0.00	5.37			

Table 4A-2c 7.26x10-4 Average Initial Surfactant Concentration

$MADS_{initial}$ x10^{-4} M	$Naphthol_{initial}$ x10^{-4} M	$pH_{,final}$	MADS, mole/gram x10^{-4}	Naphthol, mole/gram x10^{-5}	X_a, x10^{-6}	X_{adm}	K_{adm}
6.85	0.971	4.64	2.76	3.01	0.837	0.0982	117583
7.07	1.46	5.37	2.41	4.92	1.14	0.1697	149550
7.47	2.77	4.82	2.69	6.12	3.20	0.1851	57857
7.33	4.09	4.43	2.76	11.63	3.85	0.2965	76943
7.36	5.90	5.46	3.28	19.60	5.38	0.3738	69445
7.36	7.01	4.72	2.66	11.31	9.30	0.2981	32060
7.29	8.25	5.05	2.64	18.10	9.42	0.4067	43161
7.21	9.92	4.88	2.71	26.39	10.00	0.4933	49339
7.12	9.99	4.00	2.52	9.93	15.02	0.2829	18834
7.25	11.38	4.62	2.60	5.16	18.99	0.1657	8724
7.44	12.35	5.32	2.45	11.83	18.69	0.3259	17433
7.14	13.80	5.06	2.57	5.97	23.15	0.1883	8133
7.35	16.72	4.70	2.67	7.32	28.00	0.2152	7687

Data for C12-MADS Adsolubilization

Table 4A-3a 3.94x10^{-4} M Average Initial Surfactant Concentration

$MADS_{initial}$ x10^{-4} M	$Naphthol_{initial}$ x10^{-4} M	pH_{final}	MADS, mole/gram x10^{-4}	Naphthol, mole/gram x10^{-5}	X_a, x10^{-6}	X_{adm}	K_{adm}
4.00	2.08		2.02	8.96	1.01	0.3079	306187
3.92	6.66		2.01	14.59	7.55	0.4201	55643
4.00	13.32		2.16	45.27	10.64	0.6770	63631
3.82	21.23		1.96	45.39	24.28	0.6981	28753
3.76	27.33		1.99	54.72	32.54	0.7332	22532
4.12	0.00		2.11	0.00			
0.00	12.63		0.00	21.28			

Table 4A-3b 5.99x10^{-4} Average Initial Surfactant Concentration

$MADS_{initial}$ x10^{-4} M	$Naphthol_{initial}$ x10^{-4} M	pH_{final}	MADS, mole/gram x10^{-4}	Naphthol, mole/gram x10^{-5}	X_a, x10^{-6}	X_{adm}	K_{adm}
5.27	2.77	3.41	2.86	9.23	2.23	0.2441	109613
6.24	8.32	3.12	3.28	20.48	8.62	0.3843	44603
6.14	13.46	4.02	3.37	41.68	11.67	0.5531	47368
5.96	20.53	3.55	3.33	42.52	24.47	0.5611	22925
5.60	27.19	3.06	3.08	55.22	32.30	0.6422	19880
6.71	0.00	3.48	3.72	0.00			
0.00	14.85	3.21	0.00	32.81			

Table 4A-3c 6.80x10^{-4} M Average Initial Surfactant Concentration

$MADS_{initial}$ x10^{-4} M	$Naphthol_{initial}$ x10^{-4} M	pH_{final}	MADS, mole/gram x10^{-4}	Naphthol, mole/gram x10^{-5}	X_a, x10^{-6}	X_m	K_m
6.90	1.31	2.85	3.37	0.532	2.21	0.0155	7036
6.90	1.31	3.56	3.45	1.22	2.01	0.0343	17065
6.66	3.53	3.40	3.30	2.11	5.75	0.0600	10441
6.45	4.68	3.30	3.19	1.97	7.87	0.0582	7394
6.65	5.77	3.59	3.37	5.98	8.64	0.1507	17448
6.79	6.44	3.58	3.40	4.24	10.32	0.1108	10739
6.83	9.26	3.57	3.33	11.69	13.21	0.2597	19660
7.00	11.36	3.67	3.49	12.80	16.58	0.2681	16178
6.95	12.47	3.61	3.36	5.55	20.84	0.1416	6794
6.86	13.61	3.65	3.40	6.89	22.47	0.1685	7498
6.84	15.62	3.63	3.38	5.41	26.54	0.1378	5193

Data for C16 MADS Adsolubilization

Table 4A-4a 8.60×10^{-4} M Average Initial Surfactant Concentration

$MADS_{initial}$ $x10^{-4}$ M	$Naphthol_{initial}$ $x10^{-4}$ M	$pH_{,final}$	MADS, mole/gram $x10^{-4}$	Naphthol, mole/gram $x10^{-5}$	X_a, $x10^{-6}$	X_{adm}	K_{adm}
7.70	1.53	3.06	3.52	1.17	0.542	0.0321	59260
8.63	4.30	2.88	3.95	4.20	4.76	0.0961	20212
8.14	8.32	3.21	3.79	7.57	1.14	0.1664	14578
10.17	15.54	3.18	4.89	13.68	2.30	0.2185	9500
7.72	18.17	3.07	3.59	14.46	2.80	0.2873	10266
8.61	24.00	4.04	3.98	21.47	3.67	0.3505	9541
9.25	31.08	3.83	4.51	33.06	4.75	0.4229	8902
9.00	33.30	3.82	4.37	30.28	5.44	0.4095	7522
8.13	0.00	3.79	3.79	0.00			
0.00	19.01	3.82	0.00	5.76			

Table4A-4b 1.43×10^{-3} M Average Initial Surfactant Concentration

$MADS_{initial}$ $x10^{-4}$ M	$Naphthol_{initial}$ $x10^{-4}$ M	$pH_{,final}$	MADS, mole/gram $x10^{-4}$	Naphthol, mole/gram $x10^{-5}$	X_a, $x10^{-6}$	X_{adm}	K_{adm}
15.12	1.39	3.43	6.95	2.69	0.595	0.0372	62644
13.91	4.58	3.34	6.52	5.75	3.96	0.0810	20447
14.12	9.02	3.31	6.94	10.96	1.11	0.1364	12268
14.82	14.29	3.43	7.38	24.50	1.75	0.2492	14209
13.65	18.17	3.26	6.61	20.48	2.58	0.2364	9171
14.85	23.03	3.30	7.28	28.26	3.32	0.2796	8416
14.13	27.33	3.26	6.80	29.55	4.15	0.3030	7301
14.29	30.11	3.28	7.13	34.16	4.60	0.3238	7038
14.05	0.00	3.33	6.76	0.00			
0.00	26.36	3.66	0.00	13.33			

Data for C10 DADS SED

Table 4A-5 1.34×10^{-3} M Average Initial Surfactant Concentration.

Initial		Retentate		Permeate				
MADS, $\times 10^{-3}$ M	Naphthol, $\times 10^{-4}$ M	MADS, $\times 10^{-3}$ M	Naphthol, $\times 10^{-4}$ M	MADS, $\times 10^{-3}$ M	Naphthol, $\times 10^{-4}$ M	X_a, $\times 10^{-6}$	X_m	K_m
1.34	0.00	1.01	0	0.144	0			
1.34	6.58	1.04	3.31	0.137	2.48	4.48	0.0845	18880
1.34	11.00	1.07	5.62	0.157	4.15	7.49	0.1361	18165
1.34	21.90	0.977	9.85	0.150	8.24	14.87	0.1630	10957
1.34	32.90	1.02	15.50	0.109	11.40	20.58	0.3109	15112
1.34	43.90	1.08	21.50	0.112	17.50	31.59	0.2928	9268
1.34	54.90	1.08	28.00	0.126	24.50	44.22	0.2673	6045

Data for C12 MADS SED

Table 4A-6 2.52×10^{-3} M Average Initial Surfactant Concentration.

Initial		Retentate		Permeate				
MADS, $\times 10^{-3}$ M	Naphthol, $\times 10^{-4}$ M	MADS, $\times 10^{-3}$ M	Naphthol, $\times 10^{-4}$ M	MADS, $\times 10^{-3}$ M	Naphthol, $\times 10^{-4}$ M	X_a, $\times 10^{-6}$	X_m	K_m
2.50	0.0811	1.72	0.0483	0.587	0.0312	0.0564	0.0015	26727
2.42	0.162	1.62	0.0870	0.555	0.0589	0.106	0.0026	24881
2.42	0.162	1.65	0.0969	0.551	0.0470	0.0848	0.0045	53274
2.43	0.811	1.65	0.430	0.546	0.318	0.575	0.0100	17420
2.46	6.17	1.77	3.46	0.523	2.63	4.74	0.0625	13184
2.45	8.60	1.67	4.31	0.534	3.36	6.06	0.0777	12829
2.53	3.54	2.10	2.07	0.585	1.71	3.08	0.0234	7607
2.52	5.55	2.17	3.41	0.575	2.65	4.78	0.0452	9451
2.52	5.55	2.02	2.92	0.572	2.44	4.41	0.0318	7227
2.48	7.84	2.01	4.30	0.603	3.48	6.28	0.0553	8807
2.48	7.84	2.01	4.37	0.538	3.48	6.29	0.0578	9106
2.53	14.36	2.04	8.02	0.532	6.22	11.23	0.1064	9482
2.53	14.36	2.00	7.90	0.537	6.52	11.77	0.0863	7332
2.55	22.34	2.16	13.63	0.531	10.46	18.88	0.1631	8641
2.55	22.34	1.96	12.59	0.531	10.30	18.59	0.1386	7456
2.52	26.08	2.14	16.49	0.573	12.84	23.18	0.1889	8152
2.52	26.08	2.19	16.80	0.562	12.58	22.70	0.2059	9072
2.55	29.97	2.13	17.87	0.560	14.16	25.56	0.1910	7473
2.53	35.31	2.08	20.30	0.502	15.88	28.66	0.2185	7621
2.54	35.52	2.16	21.11	0.526	16.04	28.96	0.2362	8159
2.54	35.52	2.12	20.62	0.524	16.35	29.51	0.2108	7142
2.55	42.52	2.16	25.15	0.484	18.83	33.98	0.2737	8054
2.54	42.38	2.13	24.89	0.492	19.24	34.73	0.2559	7368
2.57	49.60	2.23	31.44	0.493	24.26	43.78	0.2926	6684
2.52	51.26	1.83	24.17	0.446	22.03	39.77	0.1335	3358
3.01	59.52	2.40	30.49	0.483	26.86	48.48	0.1591	3282
3.01	59.52	2.57	34.95	0.495	26.74	48.27	0.2837	5878

Data for C16 MADS SED

Table 4A-7 $2.49X10^{-3}$ M Average Initial Surfactant Concentration

Initial		Retentate		Permeate				
MADS, $x10^{-3}$ M	Naphthol, $x10^{-4}$ M	MADS, $x10^{-3}$ M	Naphthol, $x10^{-4}$ M	MADS, $x10^{-3}$ M	Naphthol, $x10^{-4}$ M	Xa, $x10^{-6}$	Xm	Km
2.53	0.114	2.61	0.0778	0.0542	0.0350	0.0632	0.0017	26425
2.47	1.18	2.56	0.802	0.0598	0.422	0.761	0.0150	19739
2.52	3.68	2.64	2.11	0.0570	1.28	2.31	0.0312	13556
2.48	4.86	2.59	3.16	0.0639	1.95	3.52	0.0457	12988
2.49	8.19	2.59	4.93	0.0567	2.95	5.32	0.0728	13701
2.45	21.99	2.51	10.53	0.0579	7.50	13.54	0.1101	8131
2.50	34.96	2.58	19.15	0.0623	13.26	23.93	0.1897	7929
2.48	49.53	2.58	30.56	0.0604	20.10	36.27	0.2934	8090
2.50	62.64	2.61	41.11	0.0534	20.66	37.29	0.4443	11914

Table 4A-8 Error Analysis for select C12 MADS Results.

$MADS_{initial}$ concentration $x10^{-4}M$	K_{adm} or K_m	$\lambda^2(K_{adm})$ or $\lambda^2(K_m)$	K_{max}	K_{min}
4.15	306187	$4.1x10^{10}$	508951	103422
4.27	55643	$5.12x10^{8}$	78268	33017
4.67	63631	$1.57x10^{8}$	76193	51070
4.58	28753	$2.24x10^{7}$	33486	24019
4.04	22532	$6.44x10^{6}$	25070	19995
5.27	109613	5.21x109	181820	37406
6.24	44603	$1.57x10^{8}$	57152	32053
6.14	47368	$4.58x10^{7}$	54133	40602
5.96	22925	$1.07x10^{7}$	26201	19648
5.60	19880	$4.55x10^{6}$	22012	17747
25.3	7607	$2.11x10^{6}$	9059	6156
25.2	9451	$2.36x10^{4}$	9605	9297
25.2	7227	$9.80x10^{4}$	7540	6914
24.8	8807	$1.22x10^{5}$	9157	8458
24.8	9106	$3.13x10^{5}$	9666	8546
25.3	9482	$1.17x10^{5}$	9824	9140
25.3	7332	$3.98x10^{4}$	7532	7033
25.5	8641	$2.81x10^{4}$	8809	8473
25.5	7456	$2.21x10^{4}$	7605	7307
25.2	8152	$1.49x10^{5}$	8539	7766
25.2	9072	$1.06x10^{5}$	9397	8747
25.5	7473	$1.68x10^{5}$	7883	7062
25.3	7621	$4.50x10^{4}$	7833	7409
25.4	8159	$1.35x10^{5}$	8527	7791
25.4	7142	$1.57x10^{5}$	7531	6753
25.5	8054	$2.25x10^{6}$	9555	6553
25.4	7368	$9.20x10^{6}$	10401	4335
25.7	6684	$1.40x10^{6}$	7866	5501
25.2	3358	$1.55x10^{6}$	4603	2113
30.1	3282	$6.42x10^{5}$	4083	2481
30.1	5878	$3.59x10^{5}$	6477	5279

4B Appendix: Comparison of K_m Values Based on Initial Naphthol Concentrations

Comparison of K_{adm} Values Based on Initial Naphthol Concentrations

Table 4B.1 Comparison of K_{adm} Values Based on Initial Naphthol Concentrations

Initial Naphthol, (M)	Surfactant – Initial Concentration ($x10^{-3}M$)	X_a	X_{adm}	K_{adm}
$1.38x10^{-4}$	C10 MADS-0.740	$1.51x10^{-6}$	0.0981	65094
$1.39x10^{-4}$	C10 MADS-0.740	$1.63x10^{-6}$	0.866	52957
$1.39x10^{-4}$	C16 MADS-1.43	$5.95x10^{-7}$	0.0372	62644
$1.53x10^{-4}$	C10 MADS-0.435	$2.47x10^{-6}$	0.0573	23202
$1.53x10^{-4}$	C16 MADS-0.860	$5.42x10^{-7}$	0.0321	59260
$2.77x10^{-4}$	C10 DADS-1.01	$4.16x10^{-6}$	0.0544	13075
$2.77x10^{-4}$	C12 MADS-0.680	$2.23x10^{-6}$	0.2441	109613
$4.30x10^{-4}$	C16 MADS-0.860	$4.76x10^{-6}$	0.0961	20212
$4.58x10^{-4}$	C16 MADS-1.43	$3.96x10^{-6}$	0.0810	20447
$4.68x10^{-4}$	C12 MADS-0.680	$7.87x10^{-6}$	0.0582	7394
$6.44x10^{-4}$	C12 MADS-0.680	$1.03x10^{-5}$	0.1108	10739
$6.66x10^{-4}$	C10 MADS-0.740	$9.85x10^{-6}$	0.1929	19577
$6.66x10^{-4}$	C12 MADS-0.394	$7.55x10^{-6}$	0.4201	55643
$8.25x10^{-4}$	C10 MADS-0.726	$9.42x10^{-6}$	0.4067	43161
$8.32x10^{-4}$	C12 MADS-0.599	$8.62x10^{-6}$	0.3843	44603
$8.32x10^{-4}$	C16 MADS-0.860	$1.14x0^{-5}$	0.1664	14578
$8.74x10^{-4}$	C10 MADS-0.435	$1.42x10^{-5}$	0.2277	15992
$8.88x10^{-4}$	C10 DADS-1.01	$1.03x10^{-5}$	0.2729	26565
$9.02x10^{-4}$	C16 MADS-1.43	$1.11x10^{-5}$	0.1364	12268
$1.14x10^{-3}$	C10 MADS-0.726	$1.90x10^{-5}$	0.1657	8724
$1.14x10^{-3}$	C12 MADS-0.680	$1.66x10^{-5}$	0.2681	16178
$1.23x10^{-3}$	C10 MADS-0.726	$1.87x10^{-5}$	0.3259	17433
$1.25x10^{-3}$	C12 MADS-5	$2.05x10^{-5}$	0.1624	7927
$1.25x10^{-3}$	C12 MADS-0.680	$2.08x10^{-5}$	0.1416	6794
$1.26x10^{-3}$	C10 DADS-1.01	$1.74x10^{-5}$	0.2644	15195

Table 4B.1 (cont'd) Comparison of K_{adm} Values Based on Initial Naphthol Concentrations

Naphthol, initial (M)	Surfactant – Initial Concentration ($x10^{-3}M$)	X_a	X_{adm}	K_{adm}
$1.33x10^{-3}$	C12 MADS-0.394	$1.06x10^{-5}$	0.6770	63631
$1.35x10^{-3}$	C10 MADS-0.740	$2.03x10^{-5}$	0.2972	14616
$1.35x10^{-3}$	C12 MADS-0.599	$1.17x10^{-5}$	0.5531	47368
$1.36x10^{-3}$	C12 MADS-0.680	$2.25x10^{-5}$	0.1685	7498
$1.38x10^{-3}$	C10 MADS-0.726	$2.31x10^{-5}$	0.1883	8133
$1.39x10^{-3}$	C10 MADS-0.740	$2.19x10^{-5}$	0.2759	12604
$1.43x10^{-3}$	C10 MADS-0.435	$2.29x10^{-5}$	0.3403	14892
$1.43x10^{-3}$	C16 MADS-1.43	$1.75x10^{-5}$	0.2492	14209
$1.55x10^{-3}$	C16 MADS-0.860	$2.30x10^{-5}$	0.2185	9500
$1.56x10^{-3}$	C12 MADS-0.680	$2.65x10^{-5}$	0.1378	5193
$1.66x10^{-3}$	C10 MADS-0.740	$2.71x10^{-5}$	0.2488	9166
$1.67x10^{-3}$	C10 MADS-0.726	$2.80x10^{-5}$	0.2150	7687
$1.82x10^{-3}$	C16 MADS-0.860	$2.80x10^{-5}$	0.2873	10266
$1.82x10^{-3}$	C16 MADS-1.43	$2.58x10^{-5}$	0.2364	9171
$1.89x10^{-3}$	C10 MADS-0.435	$2.97x10^{-5}$	0.4317	14526
$2.29x10^{-3}$	C10 DADS-1.01	$2.98x10^{-5}$	0.4251	14258
$2.30x10^{-3}$	C16 MADS-1.43	$3.32x10^{-5}$	0.2796	8416
$2.40x10^{-3}$	C16 MADS-0.860	$3.67x10^{-5}$	0.3505	9541
$2.72x10^{-3}$	C12 MADS-0.599	$3.23x10^{-5}$	0.6422	19880
$2.73x10^{-3}$	C12 MADS-0.394	$3.25x10^{-5}$	0.7332	22532
$2.73x10^{-3}$	C16 MADS-1.43	$4.15x10^{-5}$	0.3030	7301